Anoxic thermal degradation of kānuka and tobacco between 180^{o}C and 390^{o}C: a comparative study

A thesis presented in partial fulfilment of the requirements for the degree of

Masters of Engineering

In

Chemical and Bioprocess Engineering

At Massey University, Manawatu, New Zealand.

Rhiannon Wright

2021

Abstract

Heat-not-burn (HnB) devices are a recent innovation used to heat tobacco and other herbal material to temperatures up to 350°C, which are significantly below those typical of cigarettes. Similarly, wood smoke for food smoking is made at temperatures between 280-350°C in friction smokers, to far higher in smouldering combustion systems where local temperatures are similar to cigarettes. The drive towards lower temperature smoke generation is to allay concerns about harmful compounds that are produced at higher temperatures. The most well-known of these are polycyclic aromatic hydrocarbons (PAHs). Most research in tobacco smoking has naturally focussed on smouldering combustion up to 950°C. This research reported here is aimed at low temperatures, 180^{o}C to 390^{o}C, and in anoxic conditions. It compares two types of tobacco - loose leaf tobacco for roll-your-own cigarettes and HEETS which are a Phillip Morris cigarette used in the Philip Morris iQOS device - and kānuka wood, to understand the similarities and differences in energetics and compound formation.

The analytical techniques used were thermogravimetric analysis (TGA), simultaneous thermal analysis using thermogravimetry and differential scanning calorimetry (STA-TG/DSC), evolved gas analysis mass spectrometry (EGA/MS), pyrolysis gas chromatography mass spectrometry (Py-GC/MS) and scanning electron microscopy (SEM).

HEETS and tobacco have a weight loss event prior to pyrolysis, related to the evaporation of low molecular mass compounds, the most prominent being nicotine, but also the additive glycol. The degradation of hemicellulose, cellulose and lignin can be seen in the thermogravimetric data. Kānuka degradation occurs at higher temperatures than the tobaccos, likely due to greater cellulose crystallinity. The heat of pyrolysis trends from endothermic for very small samples to more exothermic for larger sample masses, due to the greater tortuous path distance that the escaping volatiles must travel leading to more secondary reactions. Tobacco and HEETS become exothermic with increasing sample size more quickly than kānuka. They have ten times the ash, which will catalyse reactions. The EGA/MS and Py-GC/MS identified the expected degradation compounds like acetic acid, furfural, mequinol, syringol, levoglucosan and isoeugenol. As a function of temperature, few degradation compounds were present at 180^{o}C, but more appeared with temperature. PAHs were identified. Small molecule PAHs appear at 180°C and increase with temperature. The largest PAHs generally did not appear at 390°C. Specific nitrogen compounds are seen in the tobacco vapours, arising from nicotine ($C_{10}H_{14}N_2$) and tobacco specific nitrosamines.

This research has shown that compounds, like highly carcinogenic benzo(a)pyrene, are less prominent at temperatures below 350^{o}C. Tobacco and kānuka are both plant biomass and have similar components, although the high ash content of tobacco and the large cellulose crystalline structure of kānuka lead to compounds being released from kānuka at higher temperatures. If heat-not-burn technology was applied to wood smoke a higher set point temperature would be required. Overall, this research has shown the dynamics of low temperature heating although more research has been done to quantify health risks. Knowing how composition is affected by temperature is important for improving operational safety and minimizing chemical hazard risk of low temperature devices.

Acknowledgements

I would like to thank Prof Jim Jones, Dr Qun Chen and Dr Penny Truman for their support and guidance throughout my masters. The different backgrounds, insights, and opinions on every aspect of the thesis was incredibly valuable and transformed the work in ways I would never consider. I would also commend them for their consistency and adaptability with communication during the lockdown and global pandemic while there was so much uncertainty.

It was Prof Jim Jones and Dr Qun Chen's encouragement and belief in me in my honours year of engineering that led me to start my masters. This has proven to be a truly life changing opportunity that I will forever be grateful for.

Prof Jim Jones has gone above and beyond his role as a professor and a supervisor. From all the small administrative issues he's sorted for me to the endless amounts of feedback throughout the year and on my draft thesis. It has been very comforting knowing I have support for both my research and my wellbeing.

I am especially thankful for Dr Qun Chen for the all hours of hands on teaching about how to conduct all the experiments in the thesis and how to analyse data. His unwavering kindness when I would make mistakes and he would explain and help me correct them without making me feel bad. It was unbelievable helpful having his expertise just a text message away any time the lab equipment would give me error messages, or the experimental data didn't make sense to me. We thought that detecting polycyclic aromatic hydrocarbons from the biomass in this research was impossible, but it was Dr Qun Chen who never gave up despite all the obstacles and found a method of doing so. I appreciate all the technical skills and knowledge he has given me that I can take to future jobs.

Even without being in the same city, Dr Penny Truman's has constantly been involved with the research. She provided so much technical information on tobacco, as well as opening the conversation to be more than just science and considering economic and societal influences. Her perspective was invaluable and is something I can carry beyond my thesis.

I would like to thank the Manawatu Microscopy Imaging Centre (MMIC) for the use of their scanning electron microscopy. Specifically, Raoul Solomon, who patiently taught me how to use the equipment and advised on the best practices for the types of samples that were analysed.

Table of Contents

Table of Figures

Table of Tables

Nomenclature

HEETS = Philip Morris branded tobacco sticks; HnB = Heat-not-burn device; EGA-MS = Evolved gas analysis mass spectrometry; 3-MCPD = 3-Monochloropropane diol; NDMA = N-Nitrosodimethylamine; NNA = 4-(N-methyl-N-nitrosamino)-4-(3-pyridyl)butanal; NNK = 4-(N-methyl-N-nitrosamino)-1-(3-pyridyl)-1-butanone; NNN = 3-(1-Nitrosopyrrolidin-2-yl)pyridine; PAH = Polycyclic aromatic hydrocarbons; Py-GC/MS = Pyrolysis gas chromatography mass spectrometry; SEM = Scanning electron microscopy

$C_{p,\,Kanuka}$ = Specific heat capacity of kānuka (J/kg K); $C_{p,\,Tobacco}$ = Specific heat capacity of tobacco (J/kg K); H_{py} = Overall heat of pyrolysis (J/g dry biomass); $H_{py,1}$ = Heat of primary reactions (J/g dry biomass); $H_{py,2,HET}$ = Heat of heterogeneous secondary reactions (J/g dry biomass); k'_{HET} = Non dimensional proportionality constant for heterogeneous reactions; $m_{biomass,0}$ = Initial sample mass (mg); m_w = Moisture content of tobacco (kg water/kg dry biomass); P_{atm} = Atmospheric pressure (Pa); P_{sys} = System pressure (Pa); $Q_{biomass}$ = Heat energy of biomass (J); Q_{char} = Heat energy of char (J); Q_{loss} = Heat loss (J); $Q_{sensible}$ = Sensible heat energy (J); T = Temperature (K)

1. Introduction

The pyrolysis of tobacco, with respect to cigarettes, and the pyrolysis of wood has been extensively studied at high temperatures. Heat-not-burn devices produce vapour by heating tobacco at a much lower temperature than cigarettes. Cigarettes can reach up to 950°C (Mallock et al., 2018). Heat-not-burn devices are becoming increasingly popular as they are marketed as a way to "deliver nicotine but limit emissions of tar and carbon monoxide" (Simonavicius et al., 2018), so are perceived as less harmful than cigarettes. There are many versions of these heat-not-burn devices available, but for the purpose of this discussion, two will be described. Dry herb vaporisers (Figure 1) and the Philip Morris iQOS system (Figure 2) are both heat-not-burn devices, although they have different designs and operating procedures.

Figure 1 shows the design of the SMOKA Kush Vaporiser, similar heating methods are common with dry herb vaporisers (Shosha, 2020). Dry herb vaporisers heat loose leaf herbal material which is packed into a chamber with a mesh bottom. Below this is a coil which is heated to around 230^{o}C. This heats the herbal material by radiation, conduction, and internal convection (Smoka Vape, 2019). When the material reaches a set-point temperature, the user draws on the mouthpiece and air flows through holes in the bottom of the device, passing the heated coil and up through the herbal material.

Figure 1: Partial cross-sectional view of the SMOKA Kush Vaporiser. Arrows represent air flow and temperature (Smoka Vape, 2019).

The other heat-not-burn device is the iQOS system by Philip Morris that heats specially designed tobacco sticks called HEETS to around 350°C (Figure 2). Philip Morris International (2020) claim that the iQOS system releases "95% less harmful chemicals compared to cigarettes". The iQOS system uses a heating blade to pierce the centre of the tobacco stick. Once turned on, the heating blade is heated to 350°C for 6 minutes (Philip Morris International, 2020). The user inhales the tobacco vapour through a filter at the end of the tobacco stick, reminiscent of a cigarette. The HEETS consist of four sections, the first being a

tobacco section that the heating blade pierces when the HEETS stick is mounted into the iQOS device (Patent No. WO 2020/035586 A1). The second is a short hollow cellulose acetate tube which acts as a spacer, the third a polylactic acid (PLA) filter, and the fourth a cellulose acetate filter (Patent No. CN 104203015 A). The last of these, cellulose acetate, is the commonly used filter with cigarettes (Li et al., 2020). The polylactic acid filter is described as a cooling zone (Patent No. CN 104203015 A).

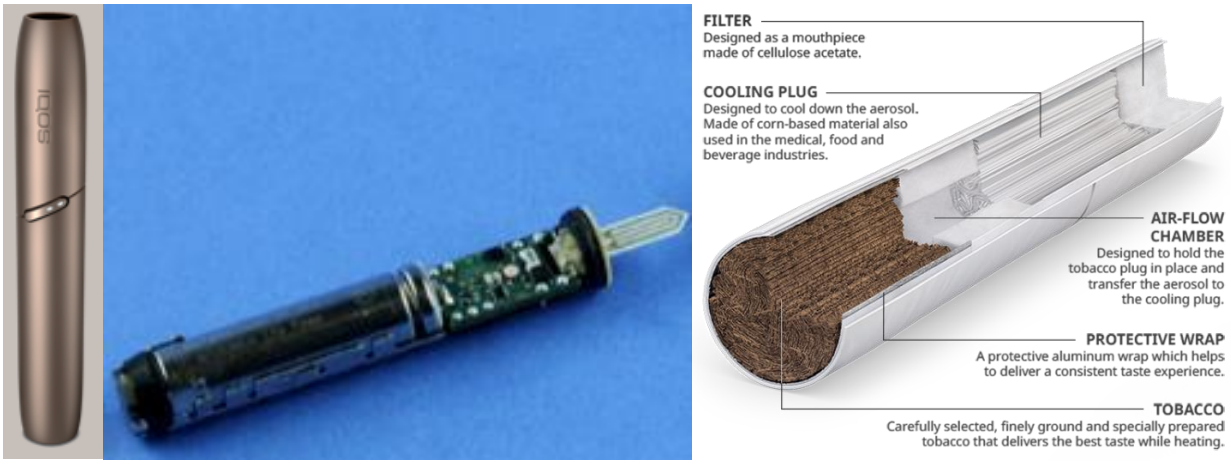

Figure 2: (Left) IQOS 3 DUO device (Philip Morris International, 2020). (Middle) IQOS 3 DUO internals. Outer cosmetic shell has been removed to show the heating blade, circuit board and battery (TechInsights, 2017). (Right) Cross section of Philp Morris tobacco stick branded as “HEETS” (Philip Morris International, 2020)

From an engineering perspective, the key difference between dry herb vaporisers and the iQOS system is the direction of heat transfer. The iQOS system has a central heating blade that will heat the tobacco from the inside of the cylinder. Dry herb vaporisers generally transfer heat from the outside, through the crucible walls into the material. The shape of the sample is also different, with a higher aspect ratio for the HEETS, i.e., they are long and thin whereas the herbal vaporisers are more squat. In both, air is drawn through the material by the user when they inhale.

This research project does not conduct a performance assessment of these devices. The above discussion highlights how they work, which is that they conduct the heating phase essentially without oxygen and therefore can maintain low temperature set-points, because the exothermic smouldering reactions have been excluded. Once the temperature set-point is reached, the user is notified that they can inhale, upon which the volatiles are removed as a fresh plug of air flows into the reaction zone. This air will cause some smouldering, but this is minimal compared to open-air smouldering that occurs with cigarettes.

In terms of low temperature tobacco heating, many papers observe a weight loss below 150°C, which is commonly regarded as water loss (Ahamad & Alshehri, 2012; Calabuig et al., 2019; Gomez-Siurana et al., 2013; Li et al., 2008; Liu et al., 2013; Oja et al., 2006; Polat et al., 2016; and Wang et al. 2019). Forster et al. (2015) conducted more in-depth research into this, by studying the compounds produced while heating tobacco from 100-200°C, at intervals of 20°C. At 100°C the majority of compounds were below the level of detection. By 180°C a significant number of compounds were able to be identified. The pyrolysis of tobacco from around 300 to 900°C, typical in cigarettes, has been studied by many authors with a heavy focus on the higher temperatures where many harmful compounds are formed (examples are Gao et al., 2013; Liao et al., 2017; Sonobe & Worasuwannarak, 2008; Torikai et al., 2004; Wang et al., 2014; and Yang

et al., 2007). These papers do not reveal any significant production of breakdown products at a temperature of 350°C, which is the operating temperature of the iQOS, although it must be noted that these papers were written before the popularisation of the device. Philip Morris Products S.A. (2017) have published the emissions level of 59 compounds from the iQOS system. Li et al. (2019), Mallock et al. (2018), and Auer et al. (2017) conducted similar experiments to validate the results. All these experiments have been done using a smoking machine, where the HEET was heated to around 350°C and air was drawn through the tobacco stick, past the multiple filters and into the analytical equipment. The tobacco in HEETS contains flavouring agents, depending on the product variant, as well as humectants like glycol, propylene glycol and guar gum (Ministry of Health, 2019). The effect of these additives on the emissions from tobacco has not been investigated.

While low temperature heating is gaining traction with respect to tobacco, it has not been considered in the food industry, where there are a number of ways to produce wood smoke for food smoking. Some of these do operate at low temperatures while others, which involve more combustion than pyrolysis, operate at high temperatures. Smoking food products, like meat and fish, is a commonly used to increase shelf life (Wenzl & Zelinkova, 2019), and give a unique flavour (Arvanitoyannis & Kotsanopoulos, 2012). However, in work comparing the polycyclic aromatic hydrocarbon levels in sausages smoked using different smoking methods found that lower PAH levels were obtained from friction smoking device (Pohlmann et al., 2013). These devices have been shown to avoid smouldering and to operate at temperatures in a similar range to the heat-not-burn devices (Seraj et al., 2021). Common smokers have wood chips that are ignited and kept at smouldering conditions in the presence of oxygen. Smouldering wood is usually around 500°C to 700°C (Rebaque et al., 2020). In industrial food smoking systems, the smoke generator is separate from smokehouse (Jones et al., 2017), and the length of smoking is dependent on food type, whether it is hot or cold smoking (i.e., the temperature of the food while being exposed to smoke) and desired outcome (Moody, 2003).

Pyrolysis describes the degradation reactions that occur on thermal lysis of carbonaceous materials. It is generally acknowledged to consist of primary pyrolysis, which is the fragmentation of the hemicellulose, cellulose and lignin in plant material, and secondary pyrolysis, which are the subsequent reactions (Jones et al., 2020). These secondary reactions are many and varied, including dehydration, cracking, polymerisation, oxidation, gasification, reforming, and water-gas shift reactions depending on the temperature and conditions and the presence of catalysts (Neves et al., 2011).

A challenge with smoke generation is the production of polycyclic aromatic hydrocarbons (PAHs). Benzo[a]pyrene is a carcinogen and has been found in some smoked fish at concerning concentrations (Tongo et al., 2016). European Commission Regulation No 835/2011 documents the limits of PAHs on food products (European Union, 2011). Up to 16 PAHs may be measured, although generally four is sufficient to monitor their presence. Compliance with these regulations will give New Zealand smoked food products a competitive edge in the international market.

A unique characteristic of New Zealand smoked food products is the wood used during smoking. Kānuka (*Kunzea ericoides*) is the most common New Zealand wood used in food smoking and so will be investigated in this research. Because it is uniquely NZ wood, there is limited research surrounding kānuka wood and the aerosol compounds produced from it. The purpose of this research is to fill this gap in knowledge and literature.

This thesis focuses on the low temperature heating, from 180°C to 390°C, of tobacco and kānuka wood chips in anoxic conditions. Comparison of the pyrolysis kinetics and compounds produced underlines the similarities more than the differences because, with the advent of heat-not-burn devices for tobacco, the pyrolysis conditions within HnBs and food smoke generators are now similar. They also share the desired

outcomes, to reduce the amount of harmful compounds in tobacco HnBs compared to cigarettes, and similarly for food smoke, to avoid the generation of such harmful compounds. In both cases, there will be a desire to preserve the production of compounds that contribute to desirable aromas. For food, these ultimately contribute to the culinary sensory experience. The selected temperature range encompasses 230°C, which is the operating temperature of dry herb vaporisers, and 350°C, which is the operating temperature of the Philip Morris iQOS. Furthermore, this thesis focuses on heating in the absence of air (i.e., anoxic conditions), which is called pyrolysis and represents the first stage of thermal breakdown inside heated particles. When oxygen gas or air is present, combustion can occur on the outer surfaces or as the pyrolysis gases mix with the air. A small amount of air will cause smouldering or localised combustion, which is exothermic and often sufficient to provide the necessary heat to sustain pyrolysis. Pyrolysis releases a great range of compounds, among these carbonyls can be released, as carbohydrates are present. Carbonyls "have been linked to respiratory disease, cardiovascular disease and carcinogenesis" (Farsalinos et al., 2018).

The aim of this research is to first characterise the three selected biomasses, with proximate and ultimate analysis, and by studying the thermal energetics, then determine how heating temperature affects the release of aromatic compounds and the evolution of degradation products in anoxic environments. This will be done with mass spectrometry on the vapour produced from the biomass. The thermal energetics and mass spectrometry will reveal different decomposition reactions that may be undesirable. Standards of particular compounds have been chosen to aid in identification, some because they are potentially harmful, others are of interest are due to aroma and flavour characteristics. A suite of PAHs has also been included. The goal of this research is to compare a food smoke wood and tobacco under similar conditions of smoke generation. These conditions are at the low end, under 350^{o}C, which are delivered in recently developed heat-not-burn devices. Traditional smoldering combustion for food smoke and cigarette smoke generation occur at much higher temperatures, in excess of 700^{o}C. The work focuses on these lower temperatures, whereas published research focuses on the compounds produced at higher temperatures. Ultimately, this will contribute to improving the control and operational safety of the devices that generate smoke and to minimise the chemical hazard risk that they pose.

It must be noted that this introduction is not followed by a stand-alone literature review. This is because many, many compounds are produced. For this reason, it was decided that it would be easier to introduce the relevant literature alongside the analysis in the results and discussion chapter.

2. Materials and Methods

2.1 Materials

Easy RYO Fine Cut tobacco, manufactured by Joh. Wilh. Von Eicken GmbH, was purchased from Discount T (Kolotex Limited). HEETS Amber Label was purchased from Shosha. Philip Morris produces four non menthol HEETS flavours, marketed as bronze, sienna, amber and yellow, as well as three menthol HEETS flavours, marketed as purple, green and blue. Homogenized tobacco is used in HEETS (Patent No. WO2019206919A1). The tobacco returns from Ministry of Health (2019) can be found in Appendices A, highlighting the added ingredients. Big Smoke Fishermans Blend manuka wood chips were purchased from Bunnings Warehouse. Although they are referred to as manuka wood chips, the wood is actually kānuka. Until 1983 they were assumed to have the same genus, but it is now recognised they are from different genuses (de Lange, 2014). From now on the biomasses will be referred to as tobacco, HEETS and kānuka respectively. The size of the tobacco and HEETS were reduced with scissors and was sieved to be

between 250 and 600 microns. Kānuka wood chips were milled in a hammer mill and sieved by hand to be between 250 and 600 microns in size.

Figure 3: (Left to Right) RYO tobacco, HEETS and kānuka sample at 250-600 microns.

2.1.1 Structural characteristics

The structural analysis of HEETS, tobacco and kānuka has not been completed for this research so assumptions will have to be made from available literature. There is a lot of variation with the tobacco literature as there are different plant species, maturity and sections used. Mendu et al. (2011) studied *Nicotiana benthamiana* stems and found that it had 31.1% cellulose, and 13.6% lignin. Although, Canam et al. (2006) studied another tobacco species, *Nicotiana tabacum* stems, and found that hemicellulose ranged from 14.0% to 17.1%, cellulose ranged from 26.0% to 30.9%, and lignin ranged from 18.6% to 21.0%. Both species are referred to as tobacco but have different structural composition. The HEETS and tobacco sample could use multiple species of tobacco, but it is unclear what species each sample uses. Wang et al. (2019) and Polat et al. (2016) studied tobacco stems. Yuan et al. (2019) and Kulic and Radojicic (2011) compared tobacco stems and leaves. It is not clear what species or sections of the plant have been used for the HEETS and tobacco sample. The structural analysis of the HEETS and tobacco sample can be estimated, but with so many unknowns the estimations won't be precise. It can be assumed the hemicellulose content ranges from 14% to 25% (Canam et al., 2006; Wang et al., 2019; Polat et al., 2016; and Yuan et al., 2019). The upper limit of the range was based on Yuan et al. (2019) finding tobacco stalks had 25.4% matrix polysaccharides. Matrix polysaccharides include hemicellulose, as well as free sugar, starch, and pectin. The cellulose content can be assumed to range from 7% to 31% (Mendu et al., 2011; Canam et al., 2006; Polat et al., 2006; Yuan et al., 2019; and Kulic & Radojicic, 2011). The cellulose has such a wide range because the tobacco and HEETS sample probably utilise both tobacco leaves and stems. Kulic and Radojicic (2011) stated that the cellulose content can be up to 30% in tobacco stems, between 10% to 15% for midrib, and between 7% to 14% for leaves. The 60% cellulose content in tobacco stems found by Wang et al. (2019) does not seem reasonable and there is more literature supporting a lower range. It can be assumed the lignin content ranges from 14% to 21% (Mendu et al., 2011; Canam et al., 2006; Wang et al., 2019; Polat et al., 2016; and Yuan et al., 2019). In Polat et al. (2016) analysis on tobacco

stems they also noted 14.4% extractives. Extractives are compounds, like nicotine, that are naturally present, not bound to the holocellulose, easily volatilised, and will account for a small portion of the tobacco composition.

The structural analysis of kānuka could not be found in literature so it will be assumed from the structural analysis of other woods. Chen et al. (2021) found 36% lignin and 58.4% carbohydrates in kānuka but did not distinguish between hemicellulose and cellulose. The age the kānuka wood was harvested at is unknown, although it can be assumed that the tree was mature. Funda et al. (2019) studied juvenile and mature pine and found aging didn't affect hemicellulose or lignin but cellulose increased from 32.6% to 41.5% and extractives decreased from 7.4% to 1.9%. Luostarinen and Hakkarainen, (2019) studied *Betula pubescens* wood. Garcia-Iruela et al., (2019) studied poplar wood. Snehesh et al. (2017) studied casuarina wood. Azeez et al. (2010) studied beech, spruce, and iroko. From these different sources it can be assumed that hemicellulose ranges from 22% to 24%, cellulose ranges from 33% to 43%, lignin ranges from 22% to 36%, and extractives range from 0% to 8%. The table below summarises the findings of these paragraphs.

Table 1: Structural characteristics of tobacco and kānuka based on literature.

Assumed structural characteristics	HEETS and Tobacco sample	Kānuka sample
Hemicellulose	14% - 25%	22% - 24%
Cellulose	7% - 31%	33% - 43%
Lignin	7% - 14%	22% - 36%
Extractives	~14%*	0% - 8%

*Only one reference source

Table 1 will be a more accurate representation of the tobacco sample than the HEETS, as the tobacco sample is 95.5% tobacco and the HEETS sample is about 76% tobacco (Ministry of Health, 2019). The hemicellulose ranges overlap so it is difficult to make conclusions on the different biomasses. Although the kānuka has a higher range for both cellulose and lignin.

2.2 Standards

Standards were purchased from Sigma Aldrich. The standards purchased and reason for purchase is highlighted in Table 2 below.

Table 2: The standards that were purchased for potential health and environmental concerns as well as for flavour and odour properties. The m/z ratio is mass over charge number used in mass spectrometry. As is typically with GC/MS, m/z represents molecular number.

m/z	Compound	Formula	Reason
53	Acrylonitrile	C_3H_3N	*Potential health effect; cancer, respiratory irritation
78	Benzene	C_6H_6	Potential health effect; cancer, reproductive/developmental
92	Glycerol	$C_3H_8O_3$	**Philip Morris tobacco ingredient
94	Phenol	C_6H_6O	Other

108	M + p + o cresol	C_7H_8O	Potential health effect; cardiovascular
110	Hydroquinone	$C_6H_6O_2$	Other
112	3-Methylcyclopentane-1,2-dione	$C_6H_8O_2$	Other
124	Mequinol	$C_7H_8O_2$	Flavour/odour; caramel, phenol
128	Naphthalene (NAP)	$C_{10}H_8$	***PAH
136	p-Anisaldehyde	$C_8H_8O_2$	Flavour/odour; sweet, floral, aniseed. Philip Morris tobacco ingredient
136	Phenylacetic acid	$C_8H_8O_2$	Other
138	4-Hydroxybenzoic acid	$C_7H_6O_3$	Other
152	Acenaphthylene (ACY)	$C_{12}H_8$	PAH
152	Isovanillin	$C_8H_8O_3$	Flavour/odour; phenolic
152	Vanillin	$C_8H_8O_3$	Flavour/odour; vanilla, caramel. Philip Morris tobacco ingredient
154	Acenaphthene (ACE)	$C_{12}H_{10}$	PAH
154	Syringol	$C_8H_{10}O_3$	Flavour/odour; smoky, phenolic, tarry
162	Levoglucosan	$C_6H_{10}O_5$	Other
164	Eugenol	$C_{10}H_{12}O_2$	Flavour/odour; spicy, floral
164	Isoeugenol	$C_{10}H_{12}O_2$	Flavour/odour; spicy, clove
166	Apocynin	$C_9H_{10}O_3$	Other
166	Fluorene (FLU)	$C_{13}H_{10}$	PAH
178	Phenanthrene (PHEN)	$C_{14}H_{10}$	PAH
178	Anthracene (ANTH)	$C_{14}H_{10}$	PAH
202	Fluoranthene (FLTH)	$C_{16}H_{10}$	PAH
202	Pyrene (PYR)	$C_{16}H_{10}$	PAH
228	Benzo(a)anthracene (B[a]A)	$C_{18}H_{12}$	PAH
228	Chrysene (CHRY)	$C_{18}H_{12}$	PAH
252	Benzo(b)fluoranthene (B[b]F)	$C_{20}H_{12}$	PAH
252	Benzo(k)fluoranthene (B[k]F)	$C_{20}H_{12}$	PAH
252	Benzo(a)pyrene (B[a]P)*	$C_{20}H_{12}$	PAH. Potential health effect; cancer
264	Cinnamyl cinnamate	$C_{18}H_{16}O_2$	Flavour/odour; mild, floral, balsamic
276	Benzo[g,h,i]perylene (B[ghi]P)	$C_{22}H_{12}$	PAH
276	Indeno[1,2,3-cd]pyrene (IND)	$C_{22}H_{12}$	PAH
278	Dibenz[a,h]anthracene (D[ah]A)	$C_{22}H_{14}$	PAH

* Potential health effects as stated by Fowles and Bates (2000).

** Added ingredient listed by Philip Morris International (2018). Flavourings added to HEETS Amber Label is unknown.

*** Polycyclic aromatic hydrocarbons (PAHs) identified as high priority pollutants by the Environmental Protection Agency (Hussar et al., 2012).

2.3 Proximate analysis

Thermogravimetric analysis (TGA) was used to determine the moisture, volatiles, ash, and fixed carbon content of the RYO tobacco, HEETS tobacco and kānuka wood chips. Biomass samples were heated at 10 K/min in triplicate, and the change in mass as a function of temperature was analysed. Each sample had an initial weight of approximately 6 mg. They were placed in the STA 449 F1 Jupiter TG/DSC analyser from NETZSCH (Germany), at room temperature with nitrogen as the purge gas with a flow rate of 50 ml/min and as the protective gas with a flow rate of 20 ml/min. The sample was heated from room temperature to 105°C at 10 K/min. The sample was kept at 105°C for 1 hour, and the mass loss during this time was considered the moisture content of the biomasses. The sample was then heated from 105°C to 900°C at 10 K/min. The sample was kept at 900°C for 10 minutes, and the mass loss during the heating and after the 10 minutes was considered the volatile matter of the biomasses. At 900°C the nitrogen was changed to air and kept at 900°C for 30 minutes. After this the sample was weighed to determine the ash content, and the fixed carbon was calculated from the difference. The result from this experiment is shown in Table 5.

2.4 Heat of pyrolysis investigation

STA TG/DSC stands for simultaneous thermal analysis using thermogravimetry and differential scanning calorimetry. It is also performed by the STA 449 F1 Jupiter from NETZSCH (Germany). The STA TG/DSC was used to determine the mass loss over temperature, as well as the heat of pyrolysis for the biomass. The experiments started with room temperature biomass samples of 3, 6, 12, and 18 mg nitrogen as the purge gas with a flow rate of 50 ml/min and as the protective gas with a flow rate of 20 ml/min. The experimental method was as follows:

1. The sample was heated from room temperature to 105^{o}C at 20K/min.
2. Held at 105°C for 45 minutes to remove free water.
3. Heated from 105°C to 580°C at a rate of 5 K/min.
4. Cooled from 580^{o}C to 105^{o}C at a rate of 5 K/min.
5. Held at 105^{o}C for 30 minutes.
6. Heated again from 105^{o}C to 580^{o}C at 5 K/min.
7. Cooled again from 580^{o}C to 105^{o}C at 5K/min.
8. Held at 105^{o}C for 30 minutes.
9. Heated from 105^{o}C to 580^{o}C at 5K/min.

The results from this experiment are shown from Figure 4 to Figure 12 but not including Figure 7.

2.5 Ultimate analysis

Ultimate analysis determines the composition of nitrogen, carbon, hydrogen, and sulphur. The composition of oxygen in tobacco is calculated from the difference. Biomass samples were analysed by the vario MACRO cube elemental analyser from Elementar (Germany) in triplicate. Each sample was approximately 20 mg of biomass mixed with a catalyst, tungsten trioxide, and wrapped in tinfoil. The samples were combusted to 1000^{o}C in oxidising conditions. Then the flue gas was treated and passed through a thermal conductivity detector to determine the composition. The ultimate analysis was conducted on a dry and ash free basis. The results are shown in Table 6.

2.6 Evolved gas analysis

Evolved gas analysis mass spectrometry (EGA/MS) determined the evolution of compounds present in the vapour during the thermal decomposition process of biomass samples. The analysis was performed using the Shimadzu (Japan) GCMS-QP2010 Ultra coupled with the Frontier Laboratories (Japan) EGA/PY – 3030D Multi-Shot Pyrolyser. Data was analysed using GCMS Postrun Analysis from Shimadzu GCMSsolution Software. Samples of 0.5mg biomass were heated from 85°C to 580°C at 10K/min in the pyrolyser. The EGA/MS was operated with a split ratio of 1:300 and an ionisation energy of 20 eV to minimise fragmentation. The interface temperature was 250^{o}C, and the injection temperature was 300^{o}C. The column flow was 1.00 mL/min at 40^{o}C. The EGA column was a deactivated metal capillary EGA tube UADTM-2.5N (no stationary phase, ID 0.15 mm, length 2.5 m). Specific m/z ratios, corresponding to molecular weights of m/z 17, 27, 28, 30, 44, 53, 54, 60, 74, 76, 78, 92, 108, 110, 162, 166, 177, and 207 were programmed to be detected. The other molecular weights highlighted in tables 2 and 3 were extracted from the total ion chromatogram (TIC). The m/z ratios that were not programmed to be detected and were extracted from the TIC have slightly more noise in the results (Figure 16 and Appendices H). The EGA/MS experiments were repeated 3 times for HEETS and kānuka and 6 times for tobacco for reasons discussed in Figure 7. The results from the EGA/MS are shown in Figure 6, Figure 7, and Figure 16.

Table 3: Compounds of interest being investigated due to flavour and aroma properties. Linoleic acid is not a flavouring but is being investigated as an example of a lipid. There are limits in knowledge of flavours and concentrations added to specific tobacco products.

m/z	Compound	Formula	Flavour/Aroma	Philip Morris Tobacco ingredient*
96	Furfural	$C_5H_4O_2$	Almond-like	
104	Styrene	C_8H_8	Sweet	
106	Benzaldehyde	C_7H_6O	Almond-like	Yes
132	Cinnamaldehyde	C_9H_8O	Cinnamon	Yes
280	Linoleic acid	$C_{18}H_{32}O_2$	-	

*Philip Morris International (2018)

2.7 Pyrolysis gas chromatography mass spectrometry analysis

Pyrolysis gas chromatography mass spectrometry (Py-GC/MS) was also completed to analyse the compounds present in the volatile pyrolysate released from thermally decomposed biomass at different

temperatures. The data was analysed with the GCMS Postrun Analysis from Shimadzu GCMSsolution Software with NIST11 library. The difference between EGA/MS and Py-GC/MS being the EGA/MS detects molecular weights present over a range of temperatures using a constant heating rate, while the Py-GC/MS records mass spectrometry at one temperature to identify individual compounds. Samples of 2 mg biomass were dropped in the pyrolysis furnace (EGA/PY – 3030D Multi-Shot Pyrolyser from Frontier Laboratories, Japan) which was maintained at a set point temperature. There were 10 setpoint temperatures analysed that varied from 180°C to 390°C in 30°C intervals, including two temperatures used in HnB devices. An additional run was done at 230°C, as that is a common temperature utilised by personal use vaporising devices, and 350°C, as that temperature is used with the Philip Morris iQOS system. Vapour released from the sample passed into the GC/MS analyser (GCMS-QP2010 Ultra from Shimadzu, Japan). The GC analysis was performed in a linear velocity control mode with a velocity of 36.1 cm/s and a split ratio of 1:75. The gas chromatography column used was a Shimadzu SH-Rxi-5ms capillary column (stationary phase: 5% diphenyl 95% dimethylpolysiloxane, ID 0.25mm; film thickness 0.25 µm and length 60 m). The column was first kept at 40^{o}C for 4 minutes, then heated in the oven at a rate of 5 ^{o}C/min up to 300^{o}C and kept at 300^{o}C for 15 minutes. The MS interface temperature was set at 250^{o}C and the ion source temperature was 230^{o}C. The electron energy was set at 70 eV with MS scan range (m/z) from 45 to 550. All the kānuka runs, the tobacco runs from 180^{o}C to 300^{o}C, and the HEETS run from 180^{o}C to 270^{o}C had a split ratio of 1:75. The tobacco runs from 330^{o}C to 390^{o}C, and the HEETS run from 300^{o}C to 390^{o}C had a split ratio of 1:150 to avoid oversaturating the Py-GC/MS. The Py-GC/MS were repeated twice, and the results are shown in Figure 17, Table 9, and Table 10.

To help identify compounds, standards were also run through the Py-GC/MS. Pure compounds were purchased from Sigma Aldrich (Table 2). The retention indexes and shape of the peaks were compared to the biomass vapour to determine the compounds present.

For identification of the polycyclic aromatic hydrocarbons (PAHs) a similar method was used, but instead of a split ratio the Py-GC/MS was operated with a splitless method. The tobacco and HEETS were analysed at 180^{o}C, 230^{o}C, 350^{o}C and 500^{o}C. The kānuka was analysed at 230^{o}C, 280^{o}C, 350^{o}C and 500^{o}C due to minimal compounds being identified at the lower temperature range (Table 10). Standards were used to find the retention indexes and relative intensity of fragmentation ions. To identify PAHs in the pyrograms the m/z of the PAH and four fragmentation ions were extracted and compared, shown in Table 4. The results are shown in Table 11.

Table 4: The m/z base peak and fragment ions used to identify polycyclic aromatic hydrocarbons (PAHs) in pyrograms of biomass vapour at various temperatures.

Compound	Number of Carbon Rings	Toxic Equivalency Factor*	m/z Analysed
Naphthalene (NAP)	2	0.001	**128**, 129, 127, 126, 102
Acenaphthylene (ACY)	2	0.001	**152**, 153, 151, 150, 76
Acenaphthene (ACE)	2	0.001	**154**, 153, 152, 151, 76
Fluorene (FLU)	2	0.001	**166**, 165, 163, 164, 167
Anthracene (ANTH)	3	0.01	**178**, 179, 176, 152, 89
Phenanthrene (PHEN)	3	0.001	**178**, 179, 176, 152, 89
Fluoranthene (FLTH)	3	0.001	**202**, 203, 201, 200,101
Pyrene (PYR)	4	0.001	**202**, 203, 201, 200, 101
Benzo[a]anthracene (B[a]A)	4	0.1	**228**, 229, 226, 113, 114
Chrysene (CHRY)	4	0.01	**228**, 229, 226, 113, 114

Benzo[b]fluoranthene (B[b]F)	4	0.1	**252**, 253, 250, 126, 125
Benzo[k]fluoranthene (B[k]F)	4	0.1	**252**, 253, 250, 126, 125
Benzo[a]pyrene (B[a]P)	5	1	**252**, 253, 250, 126, 125
Indeno[1,2,3-cd]pyrene (IND)	5	0.1	**276**, 277, 274, 138, 137
Dibenz[a,h]anthracene (D[ah]A)	5	5	**278**, 279, 276, 139, 138
Benzo[g,h,i]perylene (B[ghi]P)	6	0.01	**276**, 277, 274, 138, 137

Bold numbers are the m/z of the base peak.

*From Nisbet and LaGoy (1992), larger numbers indicate a higher toxicity relative to benzo[a]pyrene.

2.8 Scanning electron microscopy

Scanning electron microscopy (SEM) images were taken at the Manawatu Microscopy and Imaging Centre. The samples were gold coated and analysed with the FEI Quanta 200 Environmental Scanning Electron Microscope with EDAX module. The tobacco, HEETS and kānuka samples, as previously described, were analysed and pine sawdust was also included in the SEM experiment. Monterey Pine sawdust was purchased from Pacific Pine Industries Ltd, New Zealand, and sieved to a particle size less than 1mm was used. The results are shown in Figure 13 and Figure 14.

3. Results

3.1 Proximate analysis

The proximate analysis of biomass was conducted to determine the composition of the samples, shown in Table 5.

Table 5: Proximate analysis of biomass (average ± std dev, wt.%). Raw data in Appendices B. The errors are the standard deviation of three replicates. Volatiles refers to all the compounds released between 105^{o}C to 900^{o}C.

	RYO Tobacco	HEETS	Kānuka
Moisture	16.85 ± 0.59	13.75 ± 2.93	7.58 ± 0.51
Volatiles	60.81 ± 0.25	67.34 ± 1.29	74.71 ± 0.08
Ash	6.30 ± 0.31	7.52 ± 1.39	0.71 ± 0.35
Fixed Carbon*	16.04 ± 0.39	11.39 ± 0.45	17.01 ± 0.25

*Fixed carbon was calculated from the difference.

Tobacco. The moisture content of the tobacco sample used here is higher than that recorded by Senneca et al. (2007) and Wang et al. (2019), where tobacco stems, homogenised tobacco and Kentucky tobacco were found to have moisture contents around 4 to 5 wt.% (Senneca et al., 2007, and Wang et al., 2019). However, flue cured tobacco had a moisture content around 15 to 16 wt.% similar to that recorded here (Wang et al., 2016). The volatile matter of the tobacco sample is similar to tobacco stems (Wang et al.,

2019) and homogenised tobacco (Senneca et al., 2007). The ash content is lower than expected, as reports range from 10 wt.% to 20 wt.% (Senneca et al., 2007; Polat et al., 2016; and Wang et al., 2019). However, tobacco leaf and stem can vary in ash content. According to Wang et al. (2016) tobacco leaves harvested from the top and middle of the plant have an ash content of 7.2 wt.%, whereas tobacco leaves harvested from the bottom of the plant have an ash content of 10.3 wt.%. Here, the proximate analysis was performed on the 'as received' tobacco purchased from the supplier. Tobacco can also receive chemical treatment during processing which is unknown. Another variable is the additives. Here, the tobacco sample contains roughly 4% propylene glycol, and around 0.5% flavourings and additives (Ministry of Health, 2019).

HEETS. The HEETS results are similar to the tobacco sample, as they both are largely tobacco. The moisture content of HEETS is lower than the tobacco sample. The Ministry of Health tobacco returns (2019) report RYO tobacco as having a maximum water content in tobacco of 19.5%, and in HEETS of 12.9%. The difference in tobacco and HEETS water content could be due to different processing methods, and on different varieties of tobacco, both of which are unknown. Added ingredients could also affect moisture content. The tobacco additives are mentioned above. HEETS contain around 16.9% glycerol, 3.8% cellulose, 2.2% guar gum, and 1.0% propylene glycol, and 0.05% flavourings (Ministry of Health, 2019). Furthermore, tobacco and HEETS have obvious visual differences, where loose tobacco is comparable in appearance to string, while HEETS are thin folded sheets of tobacco. The volatile content of HEETS is more than the tobacco but is similar to homogenised tobacco and Kentucky tobacco (Senneca et al., 2007). Processing affects the volatile content. Wang et al. (2019) found that raw tobacco stems had a volatile content of 61.65 wt.%, but when treated with NaOH can increase to 67.15% and when treated with water or HCl can increase to around 70 wt.%. The ash content corresponds with the flue cured tobacco investigated by Wang et al. (2016).

Kānuka. There is limited research on kānuka smoke. Azeez et al. (2010) found for spruce, ikoro and beech the moisture content ranged from 8.4 to 9.7 wt.%, which are slightly higher than the experimental result here, but all are typical of 'as received' dry wood. When oven dried moisture contents are much lower. Chen et al. (2021) found that kānuka had a moisture content of 2.35 wt.%, although this was after drying at 105°C for 24 hours. The volatiles content is lower compared to many different wood species that range from 80 wt.% to 90 wt.% (Chen et al., 2021; Lasode et al., 2014; Snehesh et al., 2017; and Azeez et al., 2010). Ikoro has a low volatile content of 70.4 wt.% (Azeez et al., 2010). Chen et al. (2021) found kānuka had 80.01 wt.% volatiles, while kānuka bark had 73.88 wt.%. They also found that kānuka had an ash content of 0.39 wt.%, while kānuka bark had an ash content of 3.27%. The ash content corresponds with literature. The ash content in New Zealand sapling woods varies from 0.19 to 1.09 wt.% (Chen et al., 2021). Other international smoking woods have ash contents ranging from 0.21 to 1.68 wt.% (Lasode et al., 2014; Luostarinen & Hakkarainen, 2019; Snehesh et al., 2017; and Azeez et al., 2010).

The difference in moisture content between the tobacco and kānuka could be due to either the influence of the propylene glycol on the water activity (Ministry of Health, 2019) or most likely to the structural and functional differences between leaves and wood. The proximate analysis was based on weight loss at specific times and temperatures. The moisture content may not strictly be water but could also include the loss of low molar mass species. Kānuka appears to have a significantly higher volatile content while tobacco has a significantly higher ash content.

3.2 Ultimate analysis

The ultimate analysis of biomass was also conducted to determine the composition of the samples, shown in Table 6.

Table 6: Ultimate analysis of biomass (daf* average ± std dev, wt.%). Raw data in Appendices C. The errors are the standard deviation of four replicates.

	RYO Tobacco	HEETS	Kānuka
N	2.04 ± 0.04	1.91 ± 0.06	0.19 ± 0.02
C	37.83 ± 0.26	39.29 ± 1.28	46.73 ± 0.37
H	5.56 ± 0.15	7.24 ± 0.25	6.73 ± 0.40
S	0.20 ± 0.03	0.12 ± 0.02	0.02 ± 0.04
O**	54.36 ± 0.41	51.44 ± 1.58	46.34 ± 0.45

*Dry and ash free basis

**Oxygen was calculated from the difference.

Tobacco and HEETS. The tobacco and HEETS samples have similar ultimate analyses. The nitrogen content of the tobacco and HEETS samples correspond with the nitrogen content recorded by Akalin and Karagoz (2011), Polat et al. (2016) and Senneca et al. (2007), ranging from 1.9 to 2.6 wt.%. The carbon content of the tobacco sample is within the range reported by Senneca et al. (2007), from 35.8 to 42.5 wt.%, and similarly by Akalin and Karagoz (2011), and Polat et al. (2016). The hydrogen content of the tobacco sample is also within the range reported of 5.4 to 6.5% by Akalin & Karagoz (2011), Bassilakis et al. (2001), Polat et al. (2016), and Senneca et al. (2007). HEETS have the highest hydrogen content for the three biomasses in Table 6 due to the added cellulose being slightly more hydrogenated than the background biomass (Ministry of Health, 2019). The sulphur content is slightly lower than the range reported in literature of 0.4 to 0.8 wt.% (Akalin & Karagoz, 2011; Bassilakis et al., 2001; & Polat et al., 2016). Majewska et al. (2018) found that tobacco leaves have a sulphur content of around 0.5 wt.% and tobacco stems have a sulphur content of 0.4 wt.%.

Kānuka. The nitrogen content of kānuka corresponds with that reported elsewhere. Chen et al. (2021) studied 6 different New Zealand wood species and found that kānuka, silver beech and rewarewa had a nitrogen content of 0.20 wt.%, with close results for the other species. Fir wood had a nitrogen content of 0.23 wt.% (Lin et al., 2019), and pine had a nitrogen content of 0.2 wt. % (Speight, 2011). The carbon content is lower than found by Chen et al. (2021) of 48.94 wt.%. Carbon content in wood ranges from around 42.8 to 53.7 wt.% (Chen et al., 2020; Lasode et al., 2014; Lin et al., 2019; Snehesh et al., 2017; Speight, 2011; and Azeez et al., 2010); poplar has a carbon content of 46.61 wt.% (Lin et al., 2019), and beech has a carbon content of 46.9 wt.% (Azeez et al., 2010). Carbon content will also vary between samples of any one wood depending on whether it is sapwood, heartwood, or bark, and so it can be concluded that the kānuka carbon content is typical of other woods. The hydrogen content is slightly lower than the 7.69 wt.% reported by Chen et al. (2021) for kānuka. However, it is higher than the average hydrogen content for several other wood species, which is around 6.3 wt.% (Lasode et al., 2014; Lin et al., 2019; Speight, 2011; and Azzez et al., 2010). The sulphur content is low, as expected. Many papers do not report the sulphur content in wood, although Speight (2011) found that oak and pine had 0.1 wt.% sulphur content, but also stated that average hardwoods and softwoods have no sulphur. From Appendices C, three out of the four trials had no sulphur content with one trial reporting a sulphur content of 0.07 wt.%, which increased the average result.

Tobacco and HEETS have a higher nitrogen and sulphur content than kānuka. One of the major components in tobacco is nicotine, which has a formula of $C_{10}H_{14}N_2$. Tobacco specific nitrosamines could have also contributed to the higher nitrogen content in the tobacco and HEETS sample. Kānuka has a higher carbon content than tobacco and HEETS.

3.3 Gravimetric curves – general trends

Understanding the stages of pyrolysis will provide knowledge of the expected broad groups of reactions occurring with the biomass.

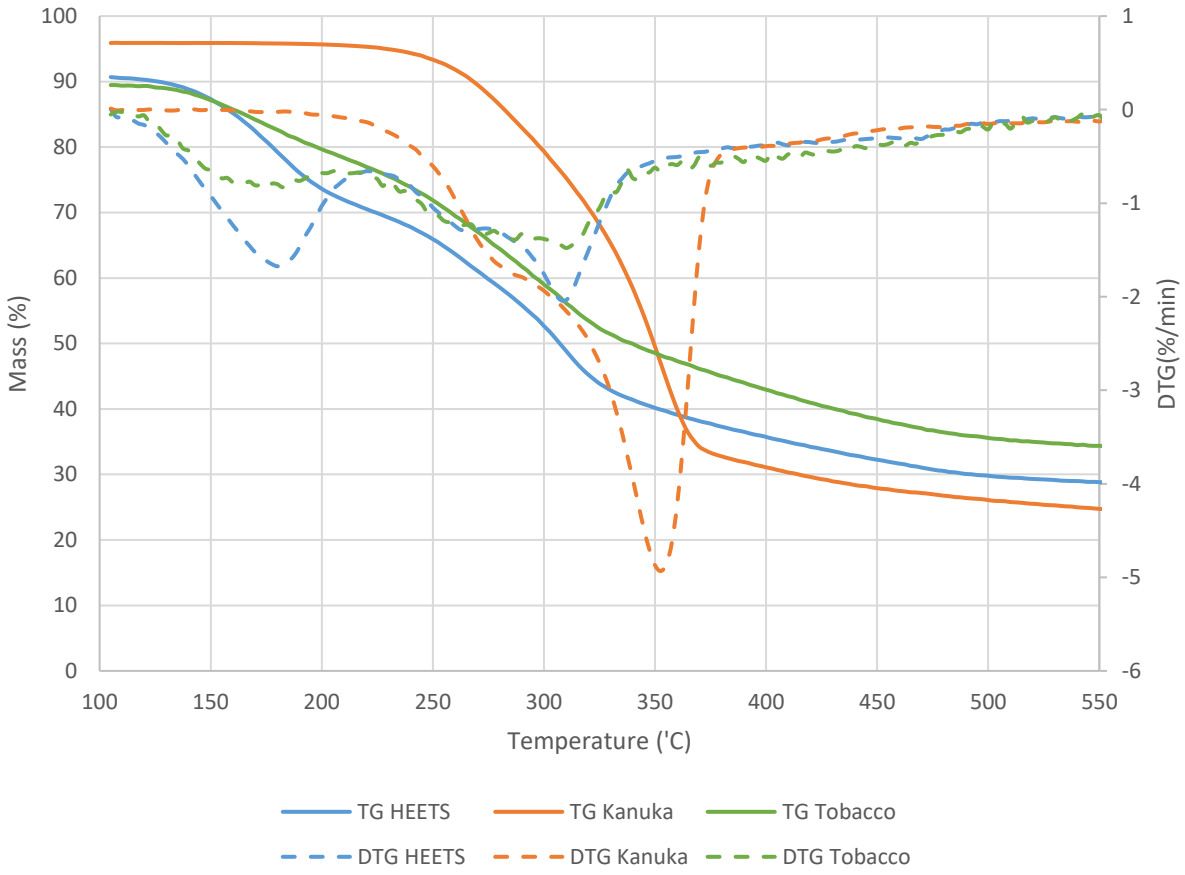

Figure 4: Graph of thermogravimetry (TG) and derivative thermogravimetry (DTG) versus temperature for 12 mg HEETS, kānuka and tobacco samples heated at 5 K/min after being held at 105°C for 45 minutes to remove moisture. The TG curves are relative to the initial air-dry sample mass.

Figure 4 shows the weight loss and differential weight loss curves. These record weight loss as temperature is ramped from 105°C to 550°C. The biomass was heated to 105°C for 45 minutes prior to the temperature ramp to remove free water. Tobacco and HEETS have similar curves with significant weight loss between 150°C to 200°C and again between 250°C to 330°C. Kānuka does not have any weight loss at the lower temperatures, has a similar weight loss to tobacco and HEETS in the middle, and also has a significant weight loss between 320°C and 370°C. For visual simplicity one result for each biomass was displayed in Figure 4. This experiment was completed twice in replicate and with different initial mass.

Figure 4 shows the DTG peaking around 180^{o}C for tobacco and HEETS, indicating the first weight loss event. This is referred to as a distillation phase as it's caused by the release of water and other low molecular mass species (Senneca et al., 2007). The HEETS have a more significant DTG peak at 180^{o}C compared to tobacco, even though tobacco has a higher moisture content shown in Table 5. HEETS contains 17 wt.% added glycerol, while the tobacco sample did not (Ministry of Health, 2019). Gomez-Siurana et al. (2013) and Marcilla et al. (2015) observed a mass loss in a tobacco glycerol mixture from 140^{o}C to 215^{o}C, and concluded it was due to the release of glycerol and other volatiles. The mass loss event from 105^{o}C to 220^{o}C for tobacco and HEETS, shown in Figure 4, is due to a combination of moisture loss, volatile release, and glycerol evaporation.

The thermal decomposition of kānuka is expected to be similar to other woods, although variations will occur due to different holocellulose and lignin compositions. Adeleke et al. (2019) studied the thermal decomposition of melina wood. Islamova and Khamatgalimov (2016) studied the thermal decomposition of coniferous wood. Ondro et al. (2018) studied the thermal decomposition of spruce wood. Sharma and Diwan (2017) studied the thermal decomposition of eucalyptus wood. They all observed a mass loss below 100°C and attributed it to the loss of free water. This was followed by a plateau in the weight loss from around 100°C to 200°C, which was referred to as a "reactive drying phase" (Adeleke et al., 2019). These observations correspond with the results shown in Figure 4.

In Figure 4, the DTG results show all the biomass experience 2 weight loss events close to each other. Tobacco has one peak at 260^{o}C and another at 310^{o}C. HEETS has similar peaks, although the peak at 310^{o}C is more emphasized. Kānuka has significantly larger peaks, but at 290^{o}C and 350^{o}C. The decomposition of cellulose, hemicellulose and lignin can occur at the same time, and due to the dynamics of heating the release of extractives can overlap with the production of degradation products (Shotorban et al., 2018). For tobacco stems, Polat et al. (2016) observed weight loss between 150°C to 275°C and attributed it to the decomposition of cellulose and hemicellulose. They also observed another weight loss from 275°C to 350°C and claimed it was the release of heavier extractives and more complex compounds. Gao et al. (2013) found tobacco had a weight loss peaking at 260°C and determined it was due to the decomposition of hemicellulose, rather than cellulose which they attributed another weight loss at 310°C. Yang et al. (2007), Gomez-Siurana et al. (2013), and Sonobe and Worasuwannarak (2008) had similar findings. In summary, the decomposition of tobacco and HEETS is likely dominated by hemicellulose and for kānuka it is likely dominated by cellulose.

Chen et al. (2021) studied the thermal decomposition of New Zealand wood including kānuka, NZ silver beech, pohutukawa, oak, tawa, and rewarewa, with fairly similar results. Figure 4 results for kānuka correspond very closely to Chen et al. (2021), where hemicellulose dominates the mass loss around 250^{o}C to 300^{o}C, and cellulose dominated the mass loss around 350^{o}C. The kānuka DTG curve also corresponds with Ondro et al. (2018), who studied the thermal decomposition of eucalyptus. There will be minor differences due to the different wood species and environment the tree was grown in.

The size of the cellulose crystal affects the breakdown temperature and weight loss, which varies between leaves and wood (Cheng et al., 2011). In Figure 4, the cellulose dominated peak varies in peak size and temperature for all the biomass due to variations in cellulose crystalline structure. Kānuka shows a very different peak size and temperature to tobacco and HEETS. Wood naturally has larger cellulose crystals than leaves, which increases "Young's modulus, tensile strength, density, and hardness" (Rongpipi et al., 2019). Tobacco and HEETS peak at similar temperatures, but the HEETS peak is larger than tobacco. HEETS is comprised of homogenised tobacco (Patent No. WO2019206919A1), while the tobacco is comprised of fine cut tobacco. The additional processing of the HEETS reduces the cellulose crystalline structure,

making it easier to break down during heating (Cheng et al., 2011). Another reason for the different results is HEETS have 3.8 wt.% added cellulose, while the tobacco sample does not (Ministry of Health, 2019).

Beyond 380^{o}C Figure 4 shows all the DTG curves correspond with each other, while the DTG curves for tobacco and HEETS are very similar from 320^{o}C. This similarity is due to lignin which dominates the mass loss in tobacco and HEETS after 360^{o}C, which is commensurate with the range of 366^{o}C to 541^{o}C attributed by Polat et al. (2016) to lignin decomposition in tobacco stems. The slow mass change after 380^{o}C for kānuka is attributed to lignin degradation (Chen et al., 2020; Adeleke et al., 2019; Ondro et al., 2018; and Sharma & Diwan, 2017). However, lignin decomposes over a wide range of temperatures, from 160°C and continues up to 900°C, although its significance is not generally observed until the hemicellulose and cellulose have decomposed (Gomez-Siurana et al., 2013).

3.4 Thermogravimetry with variable sample mass

Figure 5 highlights some interesting features about mass loss for biomass of varying mass. The TG results have been normalised by dividing by the mass after the sample has been held at 105^{o}C for 45 minutes. Some of the DTG curves show unreasonable results at 105^{o}C, which are artefacts of the analysis software and not an accurate representation of the change in mass. Full scale graphs, with all data points, can be found in Appendices D. There were some issues with the 3 mg and 6 mg results, most likely due to the small sample mass, known as the scale of scrutiny variability, first described by Danckwerts (1958). For example, the 3 mg_3 result shows less mass loss compared to every other sample. Therefore, 6 replicates were completed for 3 mg and 5 replicates were completed for 6 mg, while the other masses only had 3 replicates.

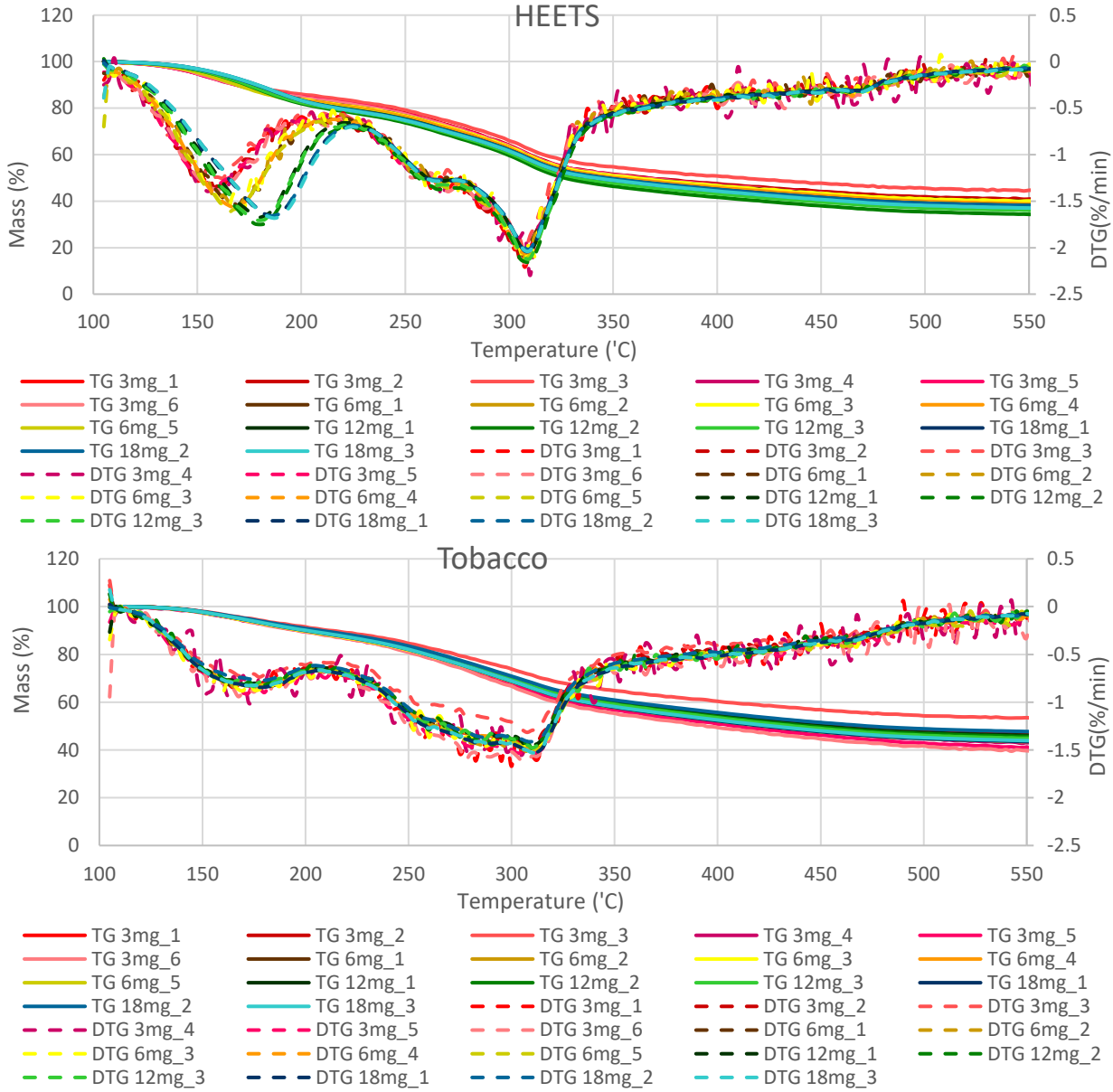
HEETS
Mass (%)
DTG(%/min)
Temperature ('C)
TG 3mg_1
TG 3mg_2
TG 3mg_3
TG 3mg_4
TG 3mg_5
TG 3mg_6
TG 6mg_1
TG 6mg_2
TG 6mg_3
TG 6mg_4
TG 6mg_5
TG 12mg_1
TG 12mg_2
TG 12mg_3
TG 18mg_1
TG 18mg_2
TG 18mg_3
DTG 3mg_1
DTG 3mg_2
DTG 3mg_3
DTG 3mg_4
DTG 3mg_5
DTG 3mg_6
DTG 6mg_1
DTG 6mg_2
DTG 6mg_3
DTG 6mg_4
DTG 6mg_5
DTG 12mg_1
DTG 12mg_2
DTG 12mg_3
DTG 18mg_1
DTG 18mg_2
DTG 18mg_3
Tobacco
Mass (%)
DTG(%/min)
Temperature ('C)
TG 3mg_1
TG 3mg_2
TG 3mg_3
TG 3mg_4
TG 3mg_5
TG 3mg_6
TG 6mg_1
TG 6mg_2
TG 6mg_3
TG 6mg_4
TG 6mg_5
TG 12mg_1
TG 12mg_2
TG 12mg_3
TG 18mg_1
TG 18mg_2
TG 18mg_3
DTG 3mg_1
DTG 3mg_2
DTG 3mg_3
DTG 3mg_4
DTG 3mg_5
DTG 3mg_6
DTG 6mg_1
DTG 6mg_2
DTG 6mg_3
DTG 6mg_4
DTG 6mg_5
DTG 12mg_1
DTG 12mg_2
DTG 12mg_3
DTG 18mg_1
DTG 18mg_2
DTG 18mg_3

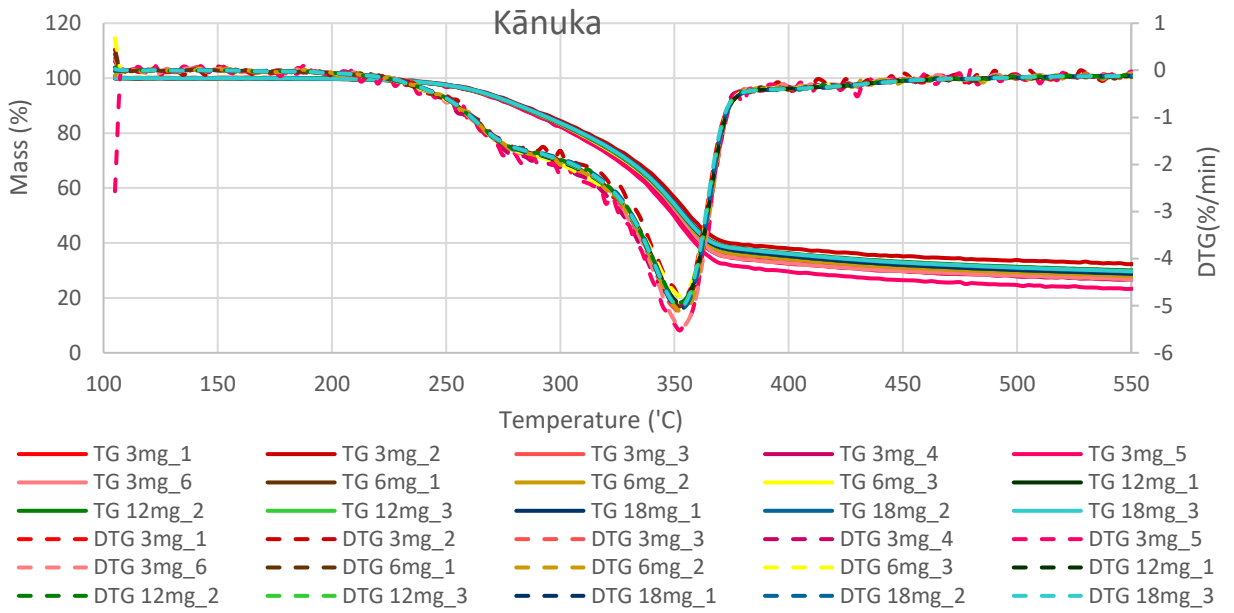

Figure 5: Graphs of normalised thermogravimetry (TG) and derivative thermogravimetry (DTG) versus temperature for HEETS, kānuka and tobacco samples heated at 5K/min after being held at 105°C for 45 minutes to remove moisture. The numbers following the mass represent the replicates, for example 3mg_1 stands for one experiment using a 3mg biomass sample and 3mg_2 is a replicate of that experiment.

The first peak from 150°C to 200°C is significantly affected by initial mass. Previously this peak was attributed to the loss of bound moisture, volatiles, and glycerol. Gomez-Siurana et al. (2011) found there is a linear relationship between the amount of glycerol added to tobacco and the mass loss from 109°C to 220°C. They observed samples with higher ratios of glycerol to tobacco had more mass loss between 109°C to 220°C and the mass peak occurred at higher temperatures. Gomez-Siurana et al. (2011) obtained similar results to the HEETS recorded in Figure 5, with the significant experimental difference that they kept the initial mass constant, with the proportions of tobacco and glycerol changing. In contrast, in this research the proportions of tobacco and glycerol stayed constant, with the initial mass changing. The effect of the increasing amount of glycerol appears the same, that is, the thermal lag between heating ramp and glycerol volatilisation creates a temperature shift. Glycerol is known to volatilise between 150°C to 220°C (Gomez-Siurana et al., 2011).

Masses that had a larger weight loss between 105°C and 230°C, also had a larger final weight loss. The DTG curves for each mass appear uniform after 230°C. At 550°C the amount of weight loss shown in the TG curve corresponds with the DTG curves. Figure 5 shows 12 mg_2 and 12 mg_3 have the largest weight loss event between 105°C and 230°C, and also have the lowest yield at 550°C. This trend of increasing mass loss with increasing sample size becomes less significant as size increases; for example, the 12 mg_1 and 18 mg results are close, indicating that the first weight loss event has a maximum that 18 mg appears to approach.

Kānuka exhibits an intriguing behaviour during drying at 105°C, details of which are in Appendices D, where weight loss increased with initial sample mass. The samples were heated in the same sized crucible, with the only difference that as mass increases the height of the sample increases. The driving pressure

for release of water vapour will be slightly more and the tortuous path distance of effusing molecules will be slightly longer. If desorption – adsorption cycling occurs, then larger samples will have more of this. However, why this trend occurs is not known. After heating to 550^{o}C, Figure 5 shows there is no clear trends in mass loss for the different initial mass. The majority of samples have a 70% mass loss by 550^{o}C, varying between the 3 mg_2 sample with a mass loss of 67.7%, and the 3 mg_5 sample with a mass loss of 76.7%. The kānuka DTG curves are similar with only a slight difference from 3 mg_5 and 3 mg_6. For the peak at 350^{o}C, 3 mg_5 and 3 mg_6 experience a 5.5 %/min mass change, whereas the other samples only experience a 5.0 %/min mass change.

Figure 5 also shows consistent mass loss for tobacco, with no obvious correspondence between initial mass of the sample and weight loss during heating to 550^{o}C. The 3 mg_3 sample has less weight loss than the other samples, which is reflected in the TG and DTG results, and the 3 mg_5 and 3 mg_6 have more weight loss than the other samples. Both results reflecting the before mentioned scale of scrutiny issue with small samples of heterogeneous material (Danckwerts, 1958). The effect of detection noise from the 3mg DTG curves appears more significant in tobacco compared to kānuka because the kānuka DTG graphical scale is about 3 times larger.

3.5 Comparison of thermogravimetry with evolved gas analysis

The total ion count (TIC) from evolved gas analysis is often compared to the differential mass loss. Figure 6 shows one result for each different experiment. As shown in Figure 5, the samples had good repeatability, so the most representative were displayed in Figure 6. The purpose of the comparison is to observe the ability of the EGA/MS to reproduce the pyrolysis behaviour shown by the DTG curves. The DTG curves were obtained by measuring the mass of the sample as it was heated from 105^{o}C to 550^{o}C. The EGA/MS spectrum was obtained from the intensity of a range of evolved gas ions from 45 m/z to 550 m/z, which is the typical detection range of the instrument.

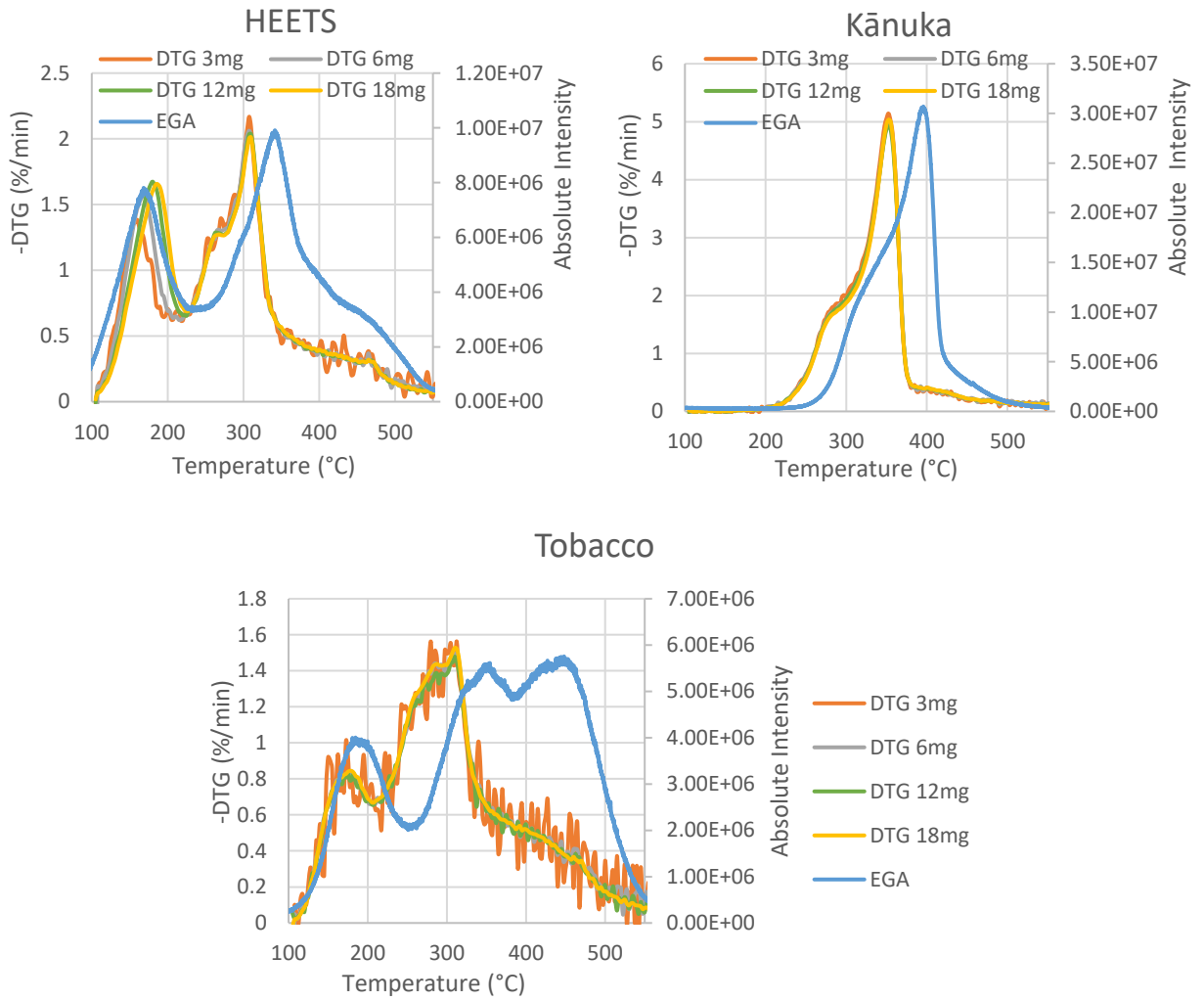

Figure 6: Comparison of derivate thermogravimetry (DTG) curves with an evolved gas analysis mass spectrometry (EGA/MS) spectrum for the biomass. EGA/MS trials used 0.5 mg samples heated at 10 K/min. The thermogravimetry samples were heated at 5 K/min. The scale of the EGA/MS absolute intensity is adjusted to give the curves a comparable height. Full size graphs can be found in Appendices E.

Figure 6 shows that the DTG and EGA/MS results for kānuka are similar, although the EGA/MS results are shifted to a higher temperature. This is because the DTG experiment used a heating rate of 5K/min, while the EGA/MS experiment used a heating rate of 10K/min. The increase in heating rate caused thermal lag so the peaks appear at a higher temperature (Sharma & Diwan, 2017). The DTG and EGA/MS results are also similar for HEETS which again shows evidence of thermal lag in the EGA/MS curve at a higher temperature. There are, however, some slight differences for the HEETS; on the upside of the second peak the shoulder in the DTG curve around 265°C is not as apparent in the EGA/MS curve and on the down side of the second peak, the DTG does not have such an obvious shoulder in the 300°C to 340°C range, where the EGA/MS indicates that many ions are still present. These differences are due to the measurement methods. DTG measures change in sample mass during heating. In contrast, the EGA/MS spectrum is

based on the amount of volatile ions produced during heating and so does not discern whether these ions are from primary or secondary reactions. Clearly, the EGA/MS spectrum is relatively higher than the mass loss rate at high temperatures. Two explanations are possible. One explanation arises by first considering the converse that, in order for the mass loss rate and EGA/MS curves to match each other, the mean molecular weight of degradation species would have to be the same across the whole heating range. This is highly unlikely. Temperature drives the energetics and so smaller degradation products are expected at higher temperatures and, if so, the EGA/MS ion chromatogram will be relatively higher than the mass loss rate curve at higher temperatures, as observed. The other explanation is that primary degradation products undergo secondary reactions to produce more, albeit smaller product molecules. As there will be many more of them, the same result will be observed. Therefore, it is not immediately apparent whether one or both are responsible for the difference at high temperature between the DTG and the EGA/MS results after 370^{o}C.

Tobacco exhibits the most difference between the DTG and EGA/MS curves. The same thermal lag phenomenon is also present as was observed earlier, but here there is an additional third peak at 450^{o}C in the EGA/MS which is not apparent in the DTG results. In the same way as argued above, this indicated extensive generation of species above 390^{o}C. Because tobacco has a clear peak, it also suggests that the mechanism for producing more vapour phase molecules is stronger in tobacco compared to HEETS and kānuka. The reason is unknown, although it is worth speculating that if secondary reactions are responsible, whether these might be homogeneous or heterogeneous. Homogeneous reactions are known to be limited at the temperature range employed in this work and are usually discounted (Jones et al., 2020) and so are unlikely despite the relatively long flight time for the generated volatiles into the EGA column and to the MS (see section 2.5). Heterogeneous reactions are also going to be limited as the sample mass in the EGA/MS trials is only 0.5mg. However, tobacco has the largest particle size, as the leaf tobacco was cut rather than ground, and so as the volatiles are generated, they still need to travel through the leaf before they escape. This greater internal tortuous path distance therefore means tobacco volatiles have more opportunity for secondary reactions; if so, this would explain why the tobacco EGA/MS curve has a third peak. Therefore, it can be concluded that secondary reactions are definitely important above 390°C for tobacco. Further conclusions are able to be drawn later in this thesis.

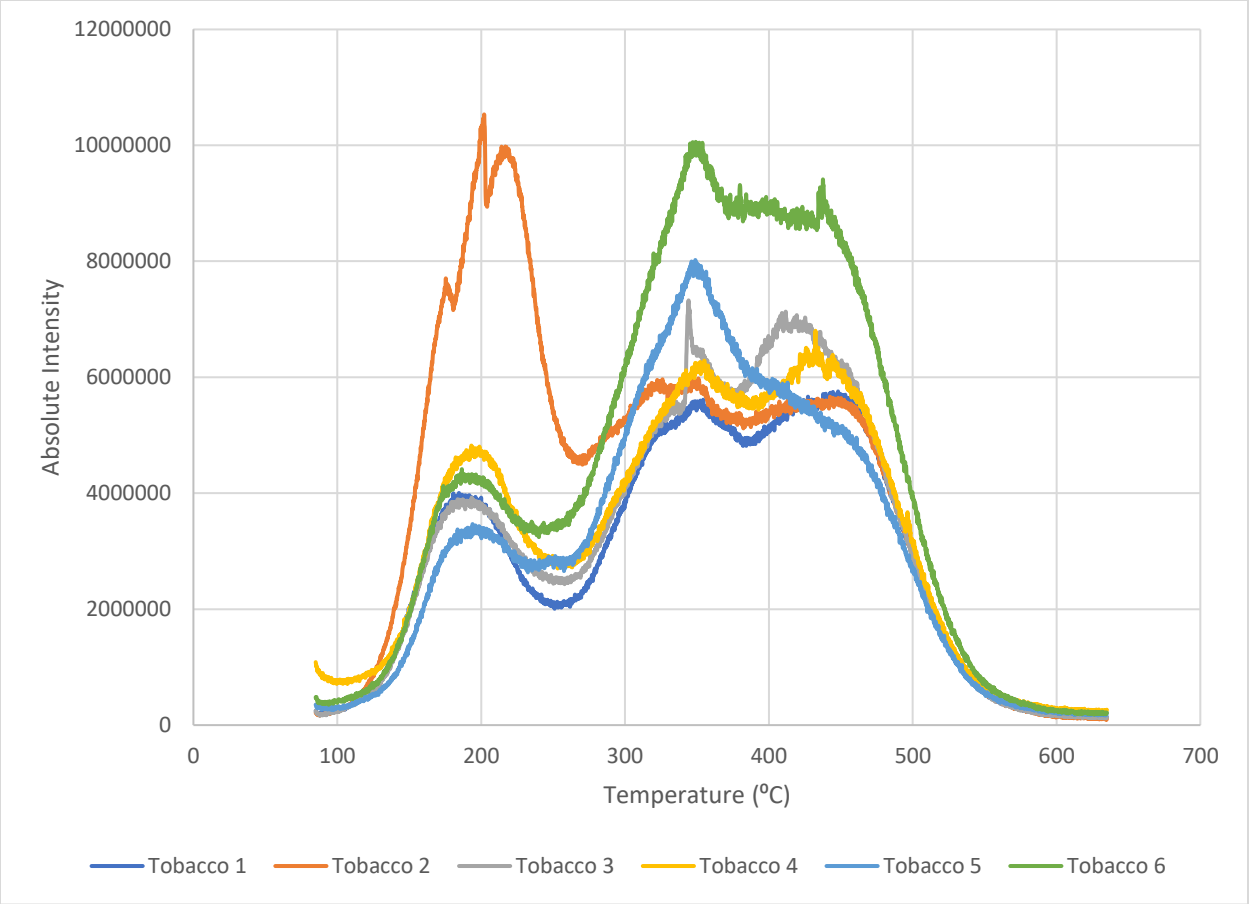

Figure 7: Evolved gas analysis mass spectrometry (EGA/MS) spectrum for a ~0.5mg sample of tobacco heated from 85°C to 630°C at 10 K/min. Appendices F shows the EGA/MS spectrums for HEETS and kānuka. Tobacco 1-6 represent 6 samples of the same tobacco.

Reproducibility was also an issue. HEETS and kānuka achieved consistent results, as shown in Figure 6 and Appendices F. However, there were issues with tobacco as highlighted in Figure 7. Due to using 20eV, small sample sizes were required to obtain accurate results. With a sample mass of 0.5mg and a sample particle size ranging from 250 to 600 microns, and these being a biological material which varies naturally, it is easy for variation in results to occur, noted earlier as the scale of scrutiny problem where the effects of sample heterogeneity and particle distribution are magnified with small sample sizes (Danckwerts, 1958). Tobacco had more variation compared to HEETS and kānuka, but tobacco also had the least uniform starting material. The kānuka wood chips were milled and sieved and so represent a blended material from which samples were taken for analysis. Oversized particles were removed during sifting. The tobacco used in HEETS was a sheet of processed tobacco and also represents a blended material. These sheets were then cut and sieved to get the appropriate sample size. In contrast, the tobacco was a collection of thin strands of leaf material of varying length and thickness. These were cut and sieved to the appropriate size from which samples were selected. For this reason, tobacco is expected to have more variation. The blend of tobacco cultivars used is unknown, which is another factor causing variation in the tobacco sample. Rather than average all the results in Figure 7, tobacco 1 was selected to represent tobacco for the comparison given in Figure 5. This is because the first peak of tobacco 1 matches with 4 other replicates, and the second and third peak match with 3 other replicates.

3.6 Simultaneous Thermogravimetry and Differential Scanning Calorimetry

At the same time as mass loss measurements the heat flows (called the DSC curve) required to maintain the heating temperature ramp from 105°C to 550°C were also recorded. Positive values mean the system requires heat to maintain the temperature ramp, and negative values mean heat loss is required to keep the temperature ramp at the desired value. The decomposition reactions affect the heat flow. Primary reactions from volatiles are endothermic, whereas secondary reactions from char are exothermic (Zobel & Anca-Couce, 2015). Exothermic reactions are more difficult to control because it is generally more difficult to remove heat than to supply heat. While this is not a problem in laboratory analytical equipment where samples are tiny, they are undesirable for larger devices where heat removal is more difficult. By comparing the DTG and DSC curves, a better understanding of heat required during different stages of mass loss can be established.

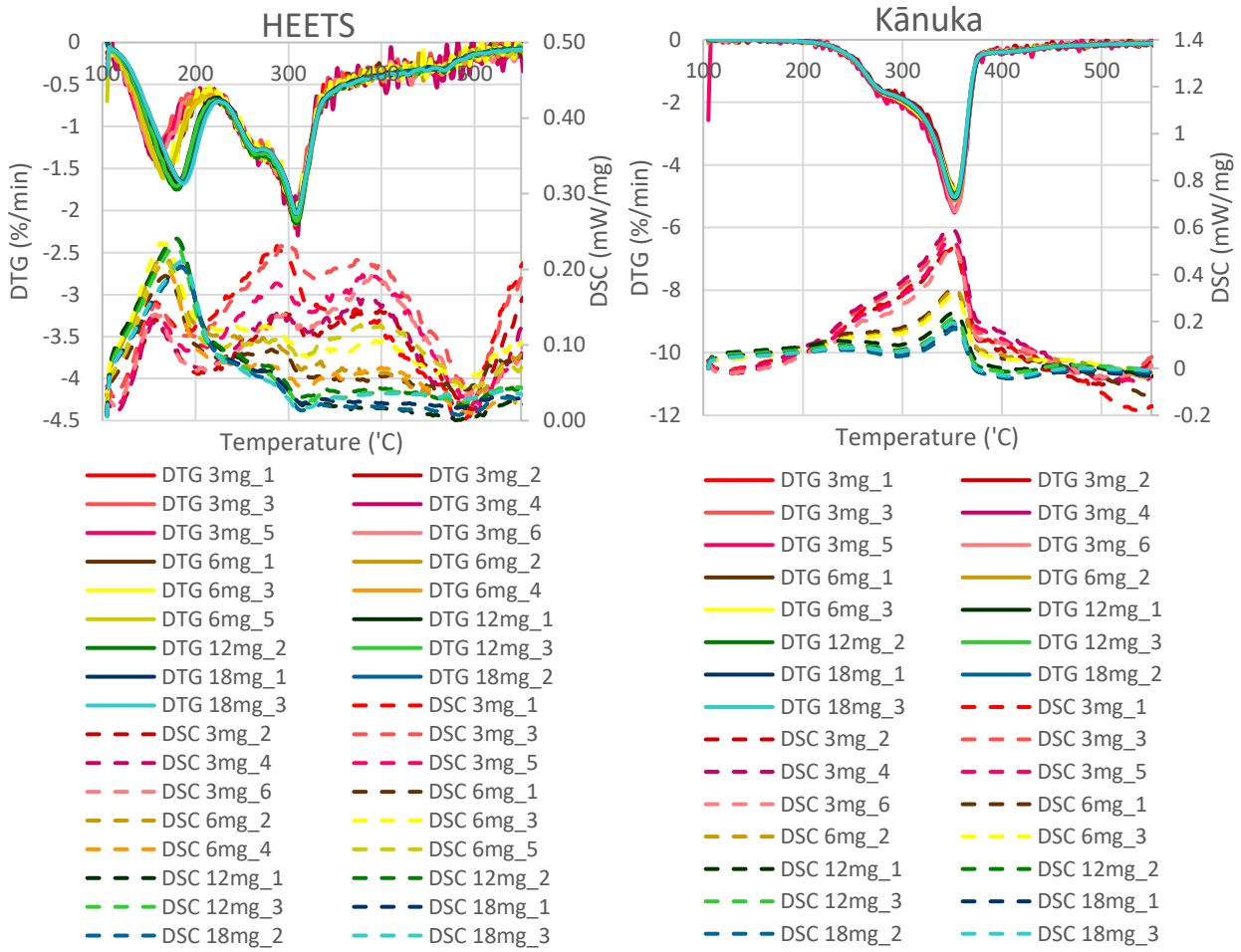

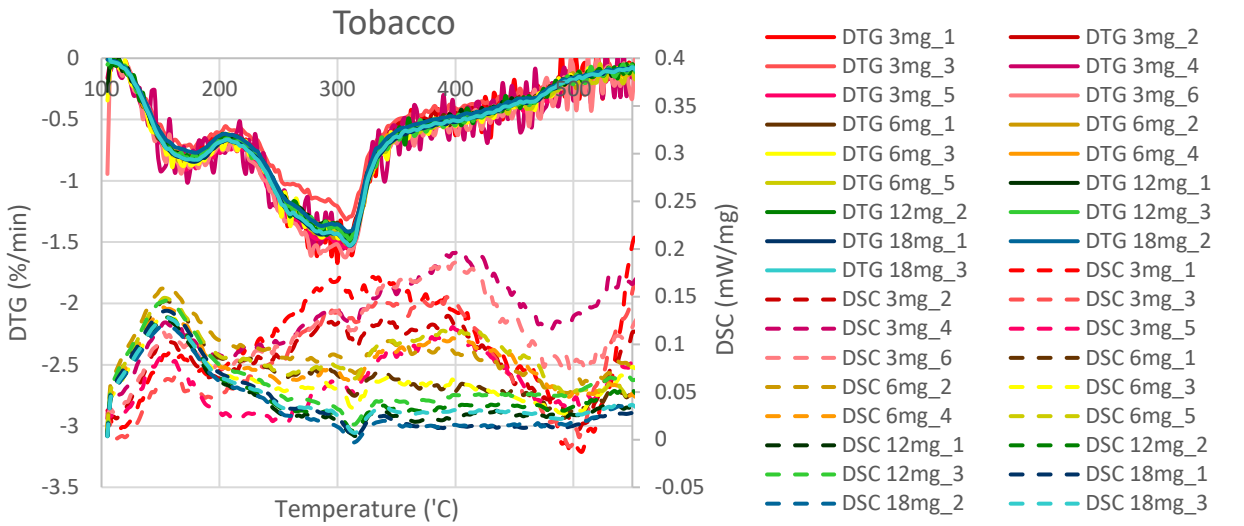

Figure 8: Comparison of derivative thermogravimetry (DTG) curves with differential scanning calorimetry (DSC) curves for the biomass. The number after the mass indicates a replicate trial, for example 3mg_1 is an experiment using 3mg of biomass and 3mg_2 is the experiment repeated with the same conditions. The DTG axis was cropped from 0%/min to -4.5%/min, as there were some large artefacts shown in Appendices D. Full size graphs can be found in Appendices G.

Figure 8 shows the DTG and DSC curves together. For tobacco up to 225^{o}C, which is below the pyrolysis range, the rate of weight loss increases and corresponds to an increase in the heat flow and would be expected for a volatile compound such as nicotine; however, there is not a clear trend with initial sample mass except for the 3 mg samples which require the least heat flow over this early part of the temperature ramp. Above 225^{o}C the initial sample mass significantly affects the heat energy required to change the temperature of the sample. The 3 mg samples require the most heat energy, followed by 6 mg, 12 mg and 18 mg. Basile et al. (2016) noticed a similar trend, while heating corn stalks, poplar, and switchgrass, that smaller sample mass causes the biomass to have a more endothermic behaviour. The reason for this relates to the opportunity for secondary reactions. All the samples were placed in the same sized crucible, so greater sample mass means the height of the sample will be higher. Upon degradation, the volatiles from larger samples have a longer tortuous path distance to travel through the char, which increases the chance of secondary reactions occurring (Basile et al., 2016; Jones et al., 2020). These heterogeneous reactions from volatiles interacting with char tend to be exothermic (Zobel & Anca-Couce, 2015), which is seen in the results where the 18 mg samples require less heat energy than the 3 mg samples. The 3 mg and 6 mg samples have more natural variation as explained earlier, which may be exacerbated by their relative size compared to the crucible, where some of the 3 mg and 6 mg samples may not have completely spread across the horizontal surface area of the crucible. Nevertheless, the trend is still apparent.

For HEETS, Figure 8 shows the same trend as tobacco below 225°C, but with a better correlation between sample size and heat flow. Above 225^{o}C, interestingly for both tobacco and HEETS the heat flow appears to have two peaks, noticeable in the smallest samples, which may be the same two peaks seen in the ion chromatogram from the EGA/MS (Figure 6). The heat flow peaks are at 300^{o}C and 390^{o}C, somewhat less than the shifted peaks of the EGA/MS. In small samples, they probably represent two different reaction mechanisms for the breakdown of holocellulose and lignin. As noted earlier, the highest temperature peak

of the EGA/MS results (Figure 6) was attributed to generation of small molecules, which in tobacco could also be attributed to secondary reactions. As secondary reactions are exothermic (Zobel & Anca-Couce, 2015; Jones et al., 2020), Figure 8 shows that as sample size increases, the heat flow decreases, as would be expected if exothermic secondary reactions were occurring. This trend is ubiquitous across all biomasses, and so supports the conclusion that secondary reactions are present not just in tobacco, but also in HEETS and kānuka. These secondary reactions become more prevalent when sample size increases, which is synonymous with increasing tortuous path distance. That this conclusion was able to be reached earlier for the very smallest sample size of tobacco, clearly shows the influence of individual particles size on this effect.

Kānuka is typical of most woods in that the DTG results are very similar to the DSC results. The only anomaly is that the 3 mg sample requires less heat flow at low temperatures around 110^{o}C compared to the other mass samples. This effect is likely due to the small sample mass where it was difficult to achieve a uniform layer of biomass in the crucible, which affects the radiative heat transfer, due to the biomass and crucible having different surface emissivity and absorptivity (Jones et al., 2020). For kānuka the DSC curves are typical of other woods where they follow main peaks in the DTG, contributing to the degradation of hemicellulose, cellulose, and lignin. The kānuka results appear similar to beech DSC and DTG curves obtained by Gomez et al. (2009). The 18 mg samples require less heat energy than the 3 mg samples due to the secondary reactions as discussed above. He et al. (2006) studied the pyrolysis of pine, peanut shell, cotton stalk, and wheat straw. Their 6 mg biomass samples tend to have a maximum peak of 0.4mW/mg, which correspond with the kānuka results in Figure 8 but not with HEETS or tobacco.

Biomass is dominated by hemicellulose, cellulose, and lignin, which breakdown in a large number of reactions. While treating pyrolysis as a three component decomposition is useful (Miller & Bellan, 1997), it is, in fact, far more complex, as illustrated by the work of Anca-Couce and co-authors who determine heat flow from the differential between the net calorific value of the reactants and products (Anca-Couce, 2016; Anca-Couce & Scharler, 2017; Anca-Couce et al., 2014; and Zobel & Anca-Couce, 2015). Doing so requires a detailed knowledge of the reaction scheme. To date their work provides the correct trends as secondary reactions become more extensive but is not yet a predictive tool. When considering the simpler three component system of hemicellulose, cellulose and lignin, Chen et al. (2014) stated that cellulose degradation is endothermic, but hemicellulose degradation is exothermic. Zobel and Anca-Couce (2015) stated that the decomposition of hemicellulose can be endothermic with small samples, containing less than 2 mg of hemicellulose. The HEETS DSC curves show two dips at 260^{o}C and 310^{o}C, which is when the hemicellulose and cellulose degradation peaks occur as shown in the DTG curves. The tobacco DSC curves have a similar pattern with dips at 255^{o}C and 315^{o}C, when the DTG curves show hemicellulose and cellulose degradation peaks. Again, this shows that at the small size limit, primary reactions are endothermic.

After the cellulose degradation, the main mechanism affecting weight loss is the breakdown of lignin, which is regarded as exothermic (Chen et al., 2014). While the decomposition of hemicellulose, cellulose and lignin can overlap (Shotorban et al., 2018), the kānuka graph clearly delineates the end of cellulose degradation from the underlying lignin decomposition. Here, the 12 mg and 18 mg samples require far less energy after 380^{o}C and indeed are slightly exothermic. While there are a number of factors involved in the interpretation of heat flow, as explained in the next section, this transition to requiring far less energy, indicates that secondary reactions are occurring. Noticeably, the heat flow above 380°C for kānuka is significantly less than that for the sample sizes of 3 mg and 6 mg of HEETS and tobacco. The reason for this is not known but may relate to additives and the ash content. Additives will affect the extent at secondary reactions, which may explain the marked differences between the heat flows above

350°C for kānuka and the two tobacco-based samples. It is the ash content, which is significant in catalysing secondary reactions, which is ten times higher in tobacco and HEETS than for kānuka (Table 5).

Another approach to the study of heat flow in pyrolysis is to use the reaction scheme of Shafizadeh and Chin (1977) where biomass primary reactions produce gas, tar and char, followed by secondary reactions where the tar fraction condenses more char and produces lighter gases. This simple division into endothermic primary reactions and exothermic secondary reactions is used by Jones et al. (2020) to determine an overall heat of reaction based on the extent of secondary reactions. They found that in the small particle size limit, secondary reactions did not occur in pine and in the larger particle size limit, the full extent of secondary reactions was able to occur. The same trend is seen here, that is, as sample size increases the heat flow becomes less endothermic and more exothermic.

Figure 8 shows a dip in the DSC curves for all the biomasses at 500°C, indicating that reactions are exothermic at this temperature. For the HEETS DSC curve, there is a large variation in energy requirements between 215°C to 550°C, although at 500°C all samples have a similar energy requirement. In wood, hydrogen begins to be generated at this temperature (Wang et al., 2009), which is indicative of tar cracking and is an exothermic process (Zobel and Anca-Couce, 2015). Sensible heat "refers to the energy absorbed by the biomass to raise its temperature only" (Daugaard & Brown, 2003). It increases with temperature at high temperatures and is made more difficult by the relative radiative issue between absorptivity and emissivity between the sample crucible and reference crucible, especially when the sample crucible is open, without a lid, as conducted in this work (Jones et al., 2020).

The major experimental result as discussed above and shown in Figure 8 is that smaller initial mass samples require more energy for reactions to occur. This can be further explored by determining the overall heat of pyrolysis by integrating the heat flow over the 105-550°C heating range.

3.7 Heat of pyrolysis

The overall heat of pyrolysis is a way to explore the balance of primary and secondary reactions. Here the heat of pyrolysis is plotted, in Figure 9, as a function of the sample mass for tobacco, HEETS and kānuka. The dry, ash-free basis removes the effect of ash content. In Figure 10, the heat of pyrolysis is on a dry, ash-free, biomass basis. This additionally removes the effect of the additives, which are significant in HEETS. The heat of pyrolysis is not easily extractable from the DSC curves of heat flow. Here the method from Jones et al. (2020) is used, where the differences between the emissivity, absorptivity and surface heat transfer coefficient between the biomass and char need to be removed (Jones et al., 2020). By removing these differences, the heat flow becomes the result of the heat of reaction as well as the sensible heat is as follows.

$$\Delta H_{py} = \frac{1}{m_{wood,0}} \left(\int_{t0}^{t\infty} (Q_{biomass} - Q_{char})_t dt - \int_{t0}^{t\infty} \Delta Q_{sensible,t} dt - \int_{t0}^{t\infty} \Delta Q_{loss,t} dt \right) \quad (1)$$

Abrego et al. (2019) use a similar equation in their research of wood chip pyrolysis. The DSC curves shown in Figure 8 were used to calculate ($Q_{biomass} - Q_{char}$). Due to time constraints, experiments to determine the exact sensible heat ($\Delta Q_{sensible,t}$) and environmental heat loss ($\Delta Q_{loss,t}$) specific to tobacco, HEETS and kānuka were not carried out. Instead, values were chosen from available literature. Assuming the same biomass to char differences here, the environmental heat loss was assumed to be the same as Jones et al. (2020)

work and also because the same equipment was used in this experiment. The sensible heating kānuka was determined from the specific heat capacity of kānuka (Caco et al., 2018), which as a function of temperature is described by:

$$C_{P,Kanuka}(dry) = -7 \times 10^{-7}(T^2) + 4.2 \times 10^{-3}(T) + 1.0505 \quad (2)$$

The sensible heating of tobacco and HEETS was determined from the specific heat capacity of tobacco (Kuroiwa et al., 2008). Buyel et al. (2016) determined the specific heat capacity of tobacco by non-invasive contact-free laser probing, and their results support Kuroiwa et al. (2008). Kuroiwa et al. (2008) defined the specific heat capacity of tobacco relative to temperature as:

$$C_{P,Tobacco} = (6.31\, m_w + 7.35)T - 34.5\, m_w - 434 \quad (3)$$

Where m_w refers to the moisture content of tobacco.

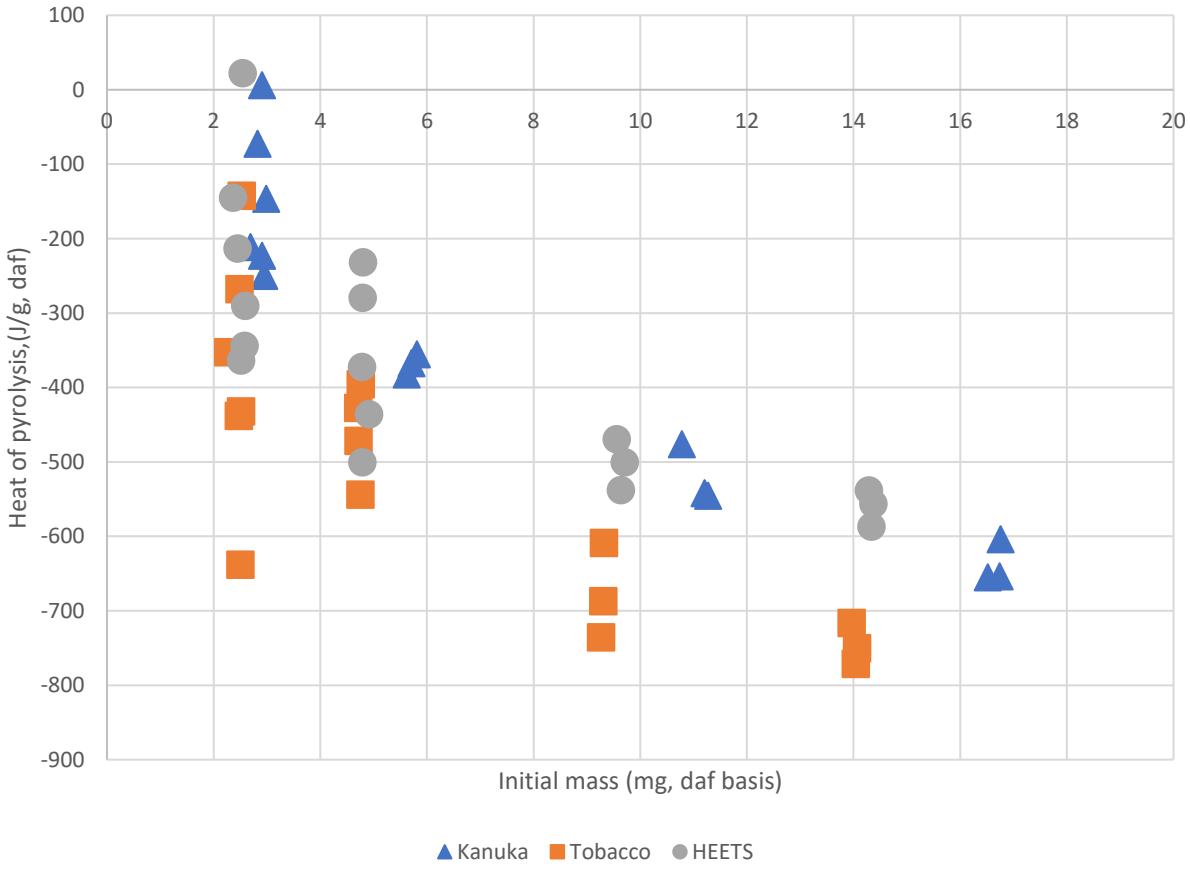

Figure 9: Heat of pyrolysis for biomass of 3 mg, 6 mg, 12 mg, and 18 mg, integrated from 105°C to 550°C, for a heating rate of 5 K/min. Data is plotted on a dry, ash free (daf) basis.

Figure 9 highlights how reactions become less endothermic and more exothermic as sample mass increases. This is due to the effect of secondary reactions, as discussed previously. It also shows how larger samples produce more consistent results, which is related to less variability in the sample. The tobacco results are the most exothermic, followed by HEETS and kānuka, however they all overlap at the lower masses of 3 mg and 6 mg. Chen et al. (2014) stated that cellulose degradation is endothermic, and lignin degradation is exothermic.

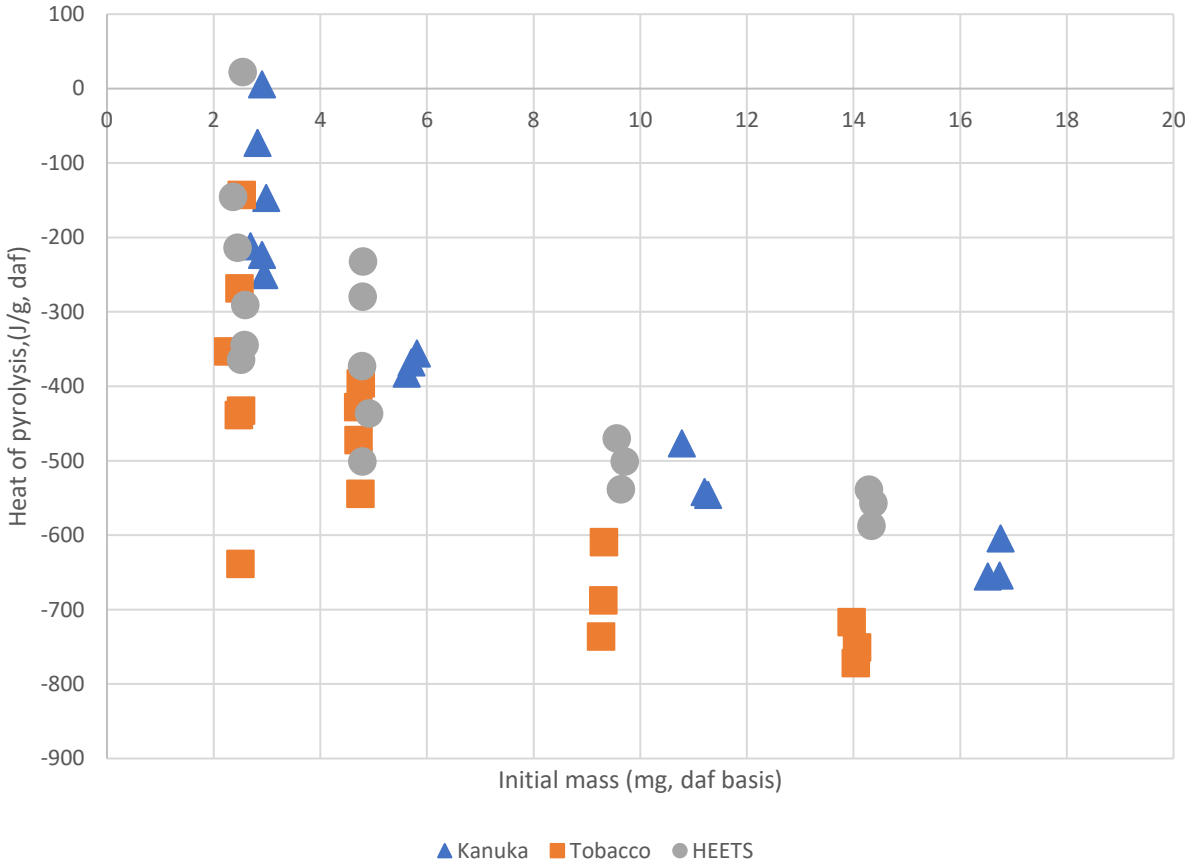

Figure 9 shows the tobacco sample is more exothermic than kānuka, potentially because kānuka has a higher cellulose content (Table 1). Although the results for HEETS and kānuka overlap so it is difficult to conclude that structural analysis is the only factor affecting the heat of pyrolysis. Gomez et al. (2009) studied the pyrolysis of thistle and found that more pre-treatment and processing made the thistle less exothermic. This corresponds with

Figure 9, as HEETS have more pre-treatment and processing than the tobacco sample and are less exothermic comparatively.

The HEETS and tobacco samples are largely tobacco but with some additives (Ministry of Health, 2019). The kānuka sample has minimal processing and it has been assumed not to contain additives. By comparing data on a biomass basis differences between wood and leaves can be investigated.

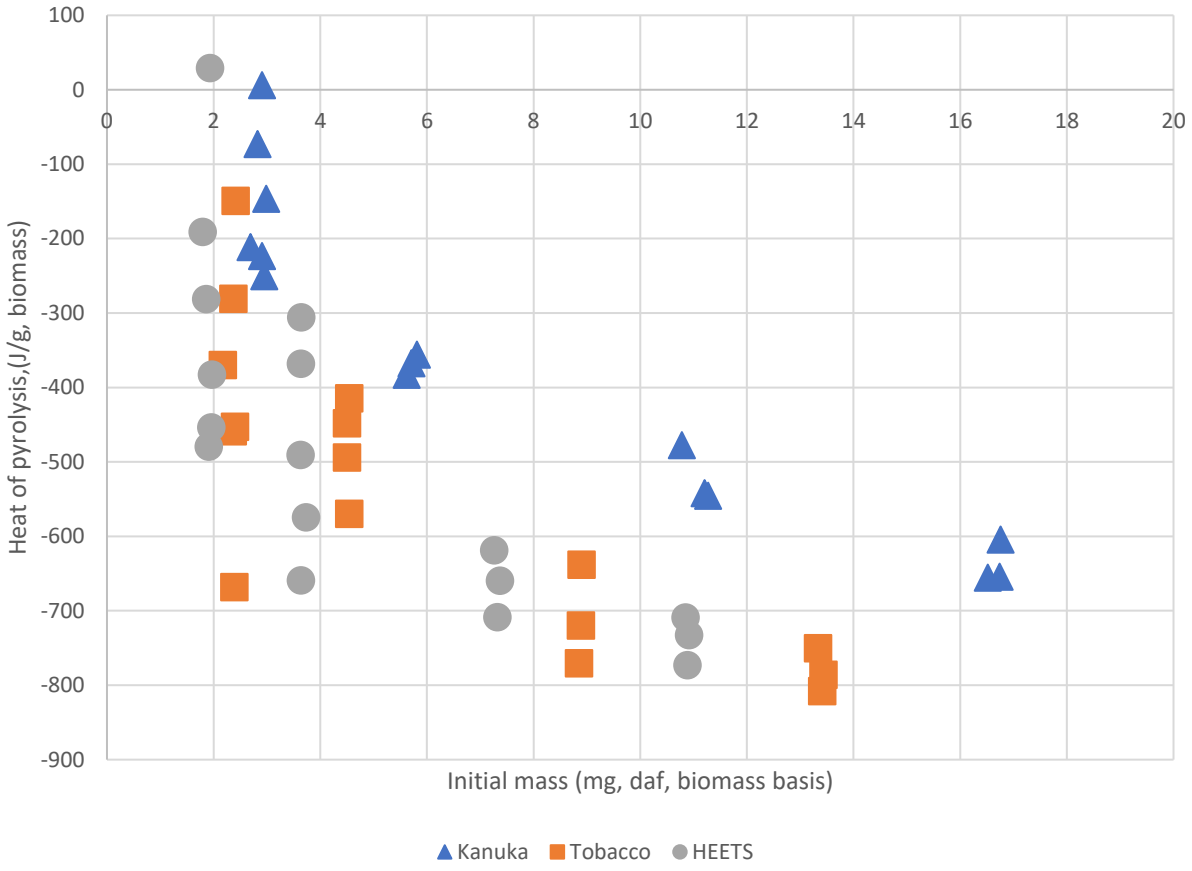

Figure 10: Heat of pyrolysis for biomass of 3 mg, 6 mg, 12 mg, and 18 mg, integrated from 105°C to 550°C, for a heating rate of 5 K/min. Data are plotted on a dry, ash free (daf), biomass basis. Doing this removes the mass effect of the non-biomass additives.

The amount of biomass in the HEETS and tobacco sample was determined from the tobacco returns from Ministry of Health (2019). The tobacco sample had 95.50% tobacco and the HEETS sample had 75.95% tobacco. By removing the non-biomass additives, the heat of pyrolysis for tobacco and HEETS appear to be the same (Figure 9 and Figure 10). Compared to Figure 9, the data points for Figure 10, especially around 3 mg and 6 mg, are further spread out. Completing more trials may highlight an obvious trend.

The heat of pyrolysis may be further analysed by assuming it is the sum of the heat of primary decomposition and heat of secondary reaction multiplied by an extent term. The approach has been used by Jones et al. (2020). Assuming only heterogeneous secondary reactions the relationship takes the following form where the extent is expressed by the bracketed term.

The curves are fitted to an equation by Jones et al. (2020), assuming no homogenous reactions:

$$H_{py} = \Delta H_{py,1} + \Delta H_{py,2,HET}\left[1 - exp\left(-\frac{m_{biomass,0}}{k'_{HET}}\left(\frac{P_{sys}}{P_{atm}}\right)\right)\right] \quad (4)$$

Where:

H_{py} = Overall heat of pyrolysis (J/g dry biomass)

$H_{py,1}$ = Heat of primary reactions (J/g dry biomass)

$H_{py,2,HET}$ = Heat of heterogeneous secondary reactions (J/g dry biomass)

$m_{biomass,0}$ = Initial sample mass (mg)

k'_{HET} = Non dimensional proportionality constant for heterogeneous reactions

P_{sys} = System pressure (Pa)

P_{atm} = Atmospheric pressure (Pa)

Equation 4 was used to fit curves to the data points, shown in Figure 10 for the dry, ash-free, biomass basis, assuming a pressure ratio equal to 1 which is a valid assumption where the particles with the sample are small. The pine curve parameters are from Jones et al. (2020). The parameters for the other biomasses were found using the least square regression method. A limiting factor of the least square regression method is parameters are found for the best fit of the data and does not consider if these are reasonable values in context. To try avoid unreasonable values, a condition was set for non-zero values. Two curve fits were done. The first does not constrain the primary heat of pyrolysis. The second does constrain it to 400 J/g, the value obtained by Jones et al. (2020). The best fits are given in Table 7.

Table 7: The best fit values for the parameters in the heat of pyrolysis model developed by Jones et al. (2020). The pine values are on a dry basis and from Jones et al. (2020). The kānuka, tobacco and HEETS values are from the dry, ash-free, biomass experimental data and the least square regression method.

	$\Delta H_{py,1}$	$\Delta H_{py,2,HET}$	k'_{HET}	R^2
Pine model	400	1237	13.8	-
	Without constraint (Figure 11)			
Kānuka	158.5	844	6.22	0.908
Tobacco	1	791	3.91	0.649
HEETS	54.7	826	3.51	0.656
	With constraint (Figure 12)			
Kānuka	400	1016	3.85	0.896
Tobacco	400	1126	2.15	0.574
HEETS	400	1111	2.08	0.642

Jones et al. (2020) reported the pine model a dry biomass basis, while the other biomasses use a dry, ash-free biomass basis. The ash content of pine is around 0.39% so it would not make a significant difference (Jones et al., 2020).

These parameters give an insight on the types of reactions occurring. $\Delta H_{py,1}$ is the primary pyrolysis of an infinitely small mass without secondary reactions. Primary reactions are more dominant in smaller sample masses. Without constraint, the $\Delta H_{py,1}$ is drastically different for each biomass. It implies that pine requires the most energy for primary reactions, followed by kānuka, then HEETS, then tobacco. $\Delta H_{py,2,HET}$ is the difference between the heat energy of an infinitely large sample and an infinitely small sample. By setting a $\Delta H_{py,1}$ of 400 J/g, the biomasses have a close $\Delta H_{py,2,HET}$ to pine of 1237 J/g. At an infinitely large sample, pine, a softwood, is the most exothermic followed by tobacco and HEETS, tobacco leaf samples, and then kānuka, a hardwood. k'_{HET} is a dimensionless constant but it implies when biomass will reach the overall heat of pyrolysis value for an infinitely large sample. HEETS and tobacco have similar k'_{HET} values, and the

lower k'_{HET} values means they approach their maximum exothermicity at lower masses than kānuka and pine. Pine has the largest k'_{HET} values meaning it will reach its exothermicity of -873 J/g (dry) at larger masses comparably. The accuracy of kānuka without constraint was the best with an R^2 of 0.908, whereas the tobacco and HEETS had a significantly lower R^2 value. This was expected as tobacco and HEETS have significant variation, especially around 3 mg and 6 mg.

The $\Delta H_{py,1}$ of 400 J/g from Jones et al. (2020) would be more representative of kānuka than tobacco and HEETS. $\Delta H_{py,1}$ refers to the heat of primary reactions. Kānuka would have similar primary reactions to pine as they both are wood with large cellulose crystalline structure. Tobacco and HEETS will have a smaller cellulose crystalline structure so are expected to require less energy for primary reactions. Even by comparing $\Delta H_{py,1}$ values without constraint it is clear that kānuka should have a higher $\Delta H_{py,1}$ than tobacco and HEETS.

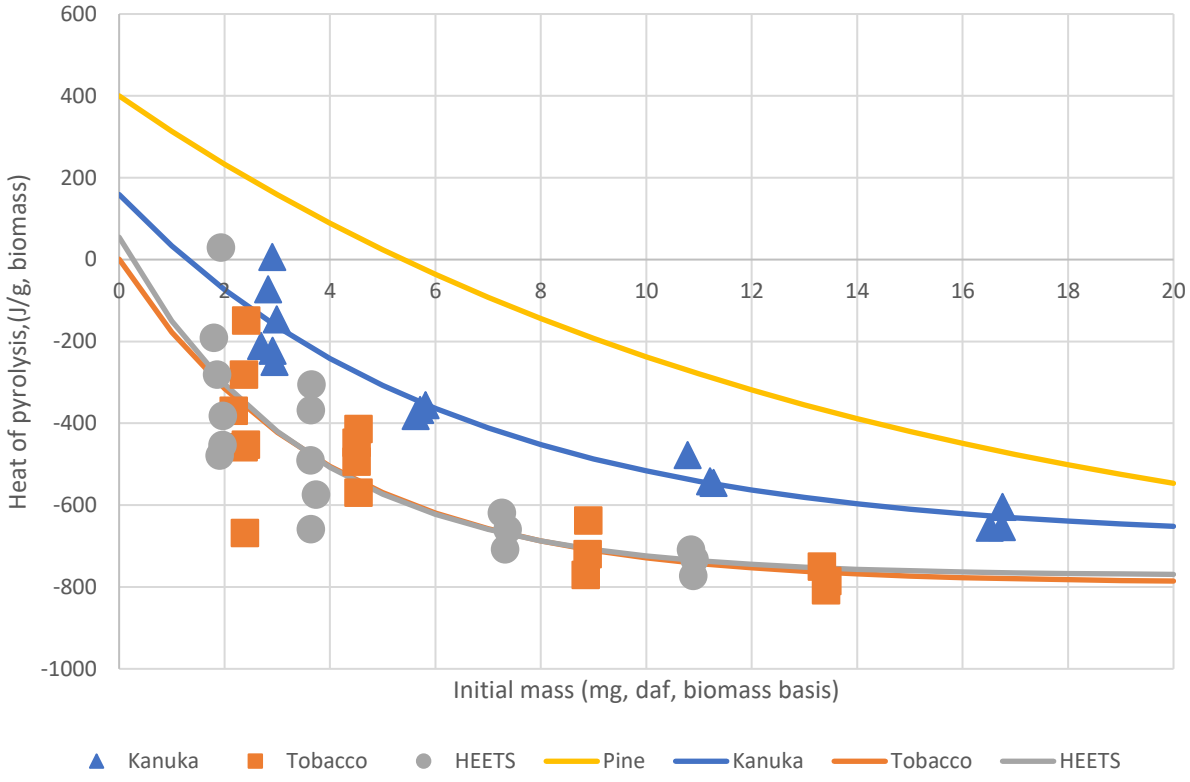

Figure 11: Heat of pyrolysis for kānuka, tobacco and HEETS of 3 mg, 6 mg, 12 mg, and 18 mg, integrated from 105°C to 550°C, for a heating rate of 5 K/min. Data is plotted on a dry, ash free (daf), biomass basis. Curves are fitted based on an equation from Jones et al. (2020). Pine data is from Jones et al. (2020).

Figure 11 shows the "without constraint" curves from Table 7. The pine results from Jones et al. (2020) appear much more endothermic compared to the other biomass, although Figure 11 is limited to 18mg samples. At larger sample masses pine will be the most exothermic, followed by tobacco, HEETS, and then kānuka. The similarities of each parameter, highlighted in Table 7, has led to overlapping results between tobacco and HEETS. This was expected as on a dry, ash-free, biomass basis both samples are tobacco.

In Figure 11 the parameters for the HEETs, kānuka and tobacco curves were chosen based on the best fit, not based on pyrolysis data. Whereas the pine curve from Jones et al. (2020) had more investigation into each parameter.

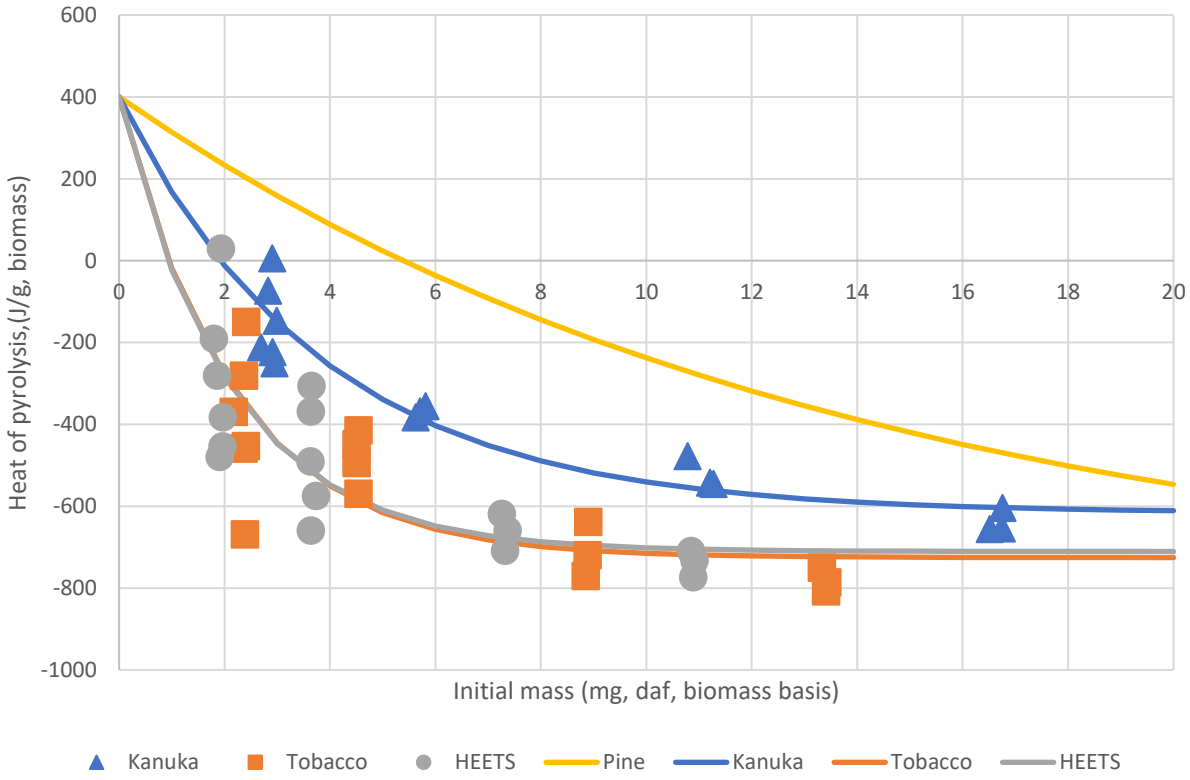

Figure 12: Heat of pyrolysis for kānuka, tobacco and HEETS of 3 mg, 6 mg, 12 mg, and 18 mg, integrated from 105°C to 550°C, for a heating rate of 5 K/min. Data is plotted on a dry, ash free (daf), biomass basis. Curves are fitted based on an equation from Jones et al. (2020), with $\Delta H_{py,1}$ set to 400 J/g. Pine data is from Jones et al. (2020).

Figure 12 shows the "with constraint" curves from Table 7. For the kānuka, tobacco and HEETS there is significant variation around 3 mg, so it is difficult to determine the $\Delta H_{py,1}$ for each of the biomass. Jones et al. (2020) conducted in-depth research into the heat of pyrolysis for pine and found a $\Delta H_{py,1}$ of 400 J/g. The poor R^2 values in Table 7 could imply a bad fit, although visually the curve passes through at least one data point for each mass.

To investigate potential reasons for the endothermic and exothermic behaviour of the biomass in Figure 12 scanning electron microscopy (SEM) images were taken.

3.8 Scanning electron microscopy (SEM)

SEM images were taken to identify differences in the particles of the biomass. The different shapes of the particles highlight how vapour is produced during heating.

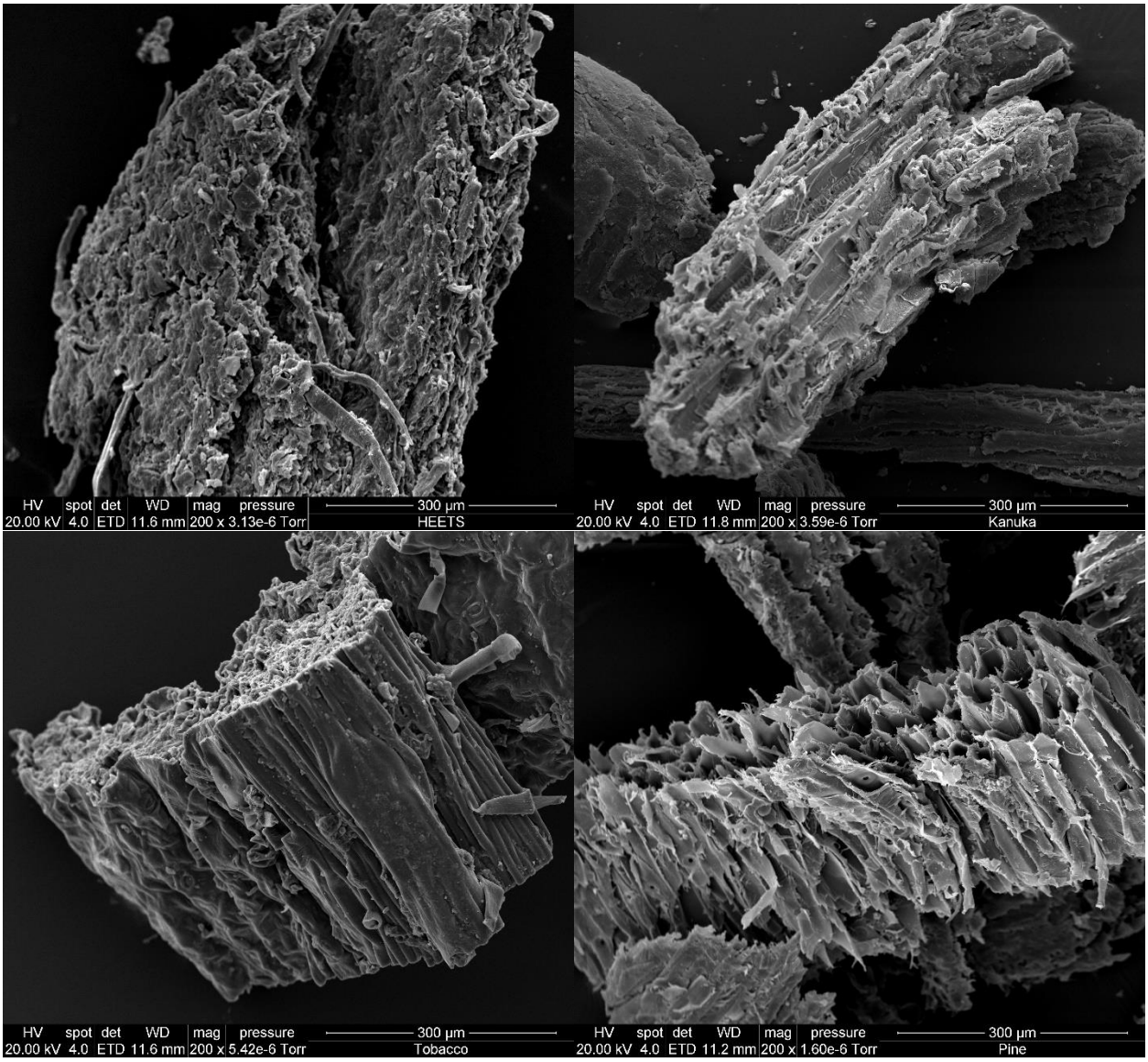

Figure 13: SEM images at 200x magnification of HEETS, kānuka, and tobacco particles sized between 250-600 microns. The pine particles were sized as less than 1 mm.

Figure 13 shows a single particle of each biomass. The HEETS particle is typical of reconstituted tobacco showing tobacco shreds bonded together with additives like guar gum (Li et al., 2018, and Ministry of Health, 2019). The tobacco particle is typical of a leaf with channels in one direction and exposed pores where the leaf was cut. Tobacco does not have obvious stoma on the leaf surface due to dehydration shrinkage and curing reducing their size (Yin et al., 2015). On the cut edge of the tobacco, it is expected

to see vessels and vascular bundles, although due to the angle of the image it is difficult to distinguish these (Kleszyk et al., 2015). The kānuka particle shows layering typical of the growth rings and exposed pores between the grain direction. Pine has larger channels than the other biomass as it is less dense than kānuka, with a density of 450 kg/m^3 (Ripberger, 2016) compared to 785kg/m^3 (Chen et al., 2021). Wood is comprised of longitudinal cells and radial cells. In softwood the longitudinal cells are referred to as tracheids, while in hardwood they are referred to as vessels (Ruffinatto & Crivellaro, 2019). The purpose of both of them is to transport sap from the roots to the top of the tree. The radial cells are mostly parenchyma cells, which are used for storage purposes. Parenchyma radial cells are more prominent in hardwood than softwood, which is why they are seen with kānuka and not pine (Ruffinatto & Crivellaro, 2019). Pore size is not fixed, and variations can occur within the same species of plant due to differences in environmental conditions, plant age, segment analysed and other factors (Yusof et al., 2013, and Yin et al., 2015). Another feature of the kānuka particle is the way it was comminuted, which was using a hammer mill, which has affected the shape, particularly at the end where the particle appears slightly rounded. The pine used for the SEM images is the same as used for Jones et al. (2020), to compare factors that could affect the heat of pyrolysis. Jang and Kang (2019) conducted SEM images of yellow poplar, a hardwood, and Korean red pine, a softwood which can be compared to kānuka, another hardwood and pine, another soft wood. They noticed yellow poplar had a combination of large and small pores facing one direction, with small pores in between facing the alternate direction, similar to the pattern shown by kānuka. They also noticed that Korean red pine had a series of similar sized pores in uniform rows, similar to the pattern shown by pine. These are typical patterns displayed by hardwood and softwood respectively (Filpo et al., 2013; Sun et al., 2012; Zhang & Shen, 2019; and Tanaka et al., 2014).

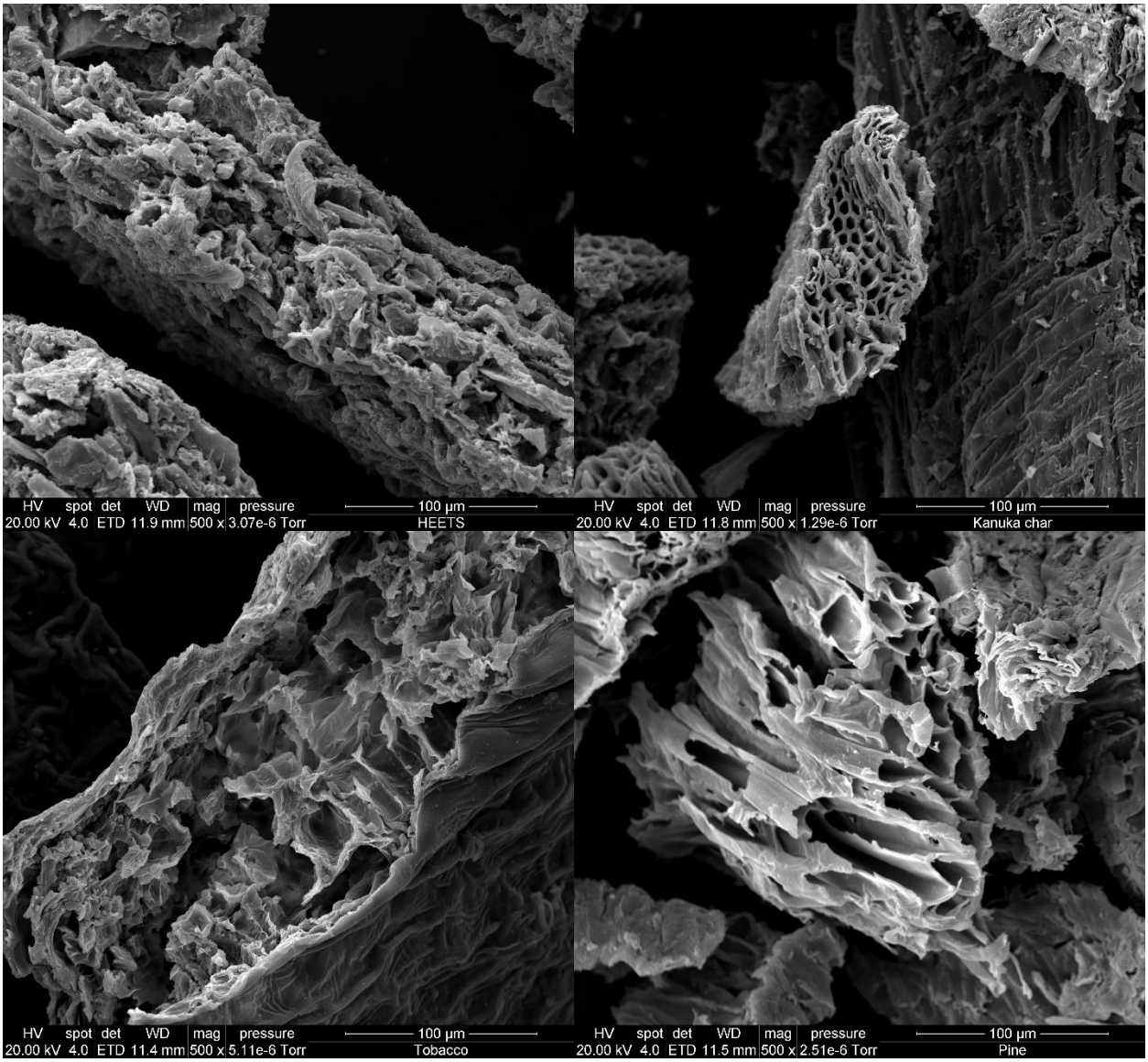

Figure 14: SEM images at 500 times magnification of HEETS, kānuka and tobacco sized between 250-600 micron particle size after being held at 105^{o}C for 45 minutes, then heated from 105^{o}C to 550^{o}C at 5 K/min. The pine was sized at less than 1 mm. It had the same heating profile.

Figure 14 shows the biomasses after pyrolysis to 550^{o}C. The higher magnification, 500x, provides a better cross-sectional view. The HEETS structure appears little changed after pyrolysis, because it is highly processed felted mats of tobacco and additives. Tobacco, in contrast, has a ruptured internal cellular structure due to a build-up of internal pressure from unreleased volatiles (J Chen et al., 2018), but the epidermal tissue layer on the outside has been preserved. Both effects have also been observed by Zi et al. (2019). Kānuka char also preserves its wood structure as is typical of wood charcoal, as does the pine char. This kānuka particle appears to have a clean-cut edge, instead of the rounded edges in Figure 13. In theory, wood pore size reduces after heating because charring involves shrinkage, which affects how easily volatiles can escape the particle (Donaldson et al., 2015). From the SEM images in Figure 13 and Figure 14 this shrinkage is difficult to conclude. For kānuka there was no obvious internal structure as the edge view is not clear.

Relating Figure 13 and Figure 14 to the heat of pyrolysis in Figure 12, pine was shown to be the most endothermic at low masses, which is expected due to the highly porous nature of the pine where volatiles can escape easily and so have less opportunity to undergo secondary reactions. Small pores result in trapped volatiles and a build-up of internal pressure which causes in more secondary reactions to occur (Juan & Ke-qiang, 2009), which most likely explains why pine was the more endothermic at small initial masses than kānuka. Similarly, in Figure 14 tobacco has an open structure, but becomes exothermic far more quickly as sample mass increases (Figure 12). This effect is likely due to the ash content. Pine has an ash content of 0.39 wt.%, kānuka contains 0.71 wt.% ash, tobacco contains 6.30 wt.% ash and HEETS contain 7.52 wt.% ash (Jones et al., 2020, and Table 5). Tobacco and HEETS have very similar heat of pyrolysis relationships with sample mass which are probably due to the catalysing effect of the high ash content (Antal et al., 2000). Inorganic species present in ash have multiple effects on the heat of pyrolysis for biomass (Khelfa et al., 2013), one of which is that inorganic species catalyse secondary reactions (Valin et al., 2015).

3.9 Gravimetric curves – mass loss

Thermogravimetry was also used to study the effect of sample size on mass loss. The term yield refers to the solid residue left after heating to 550°C.

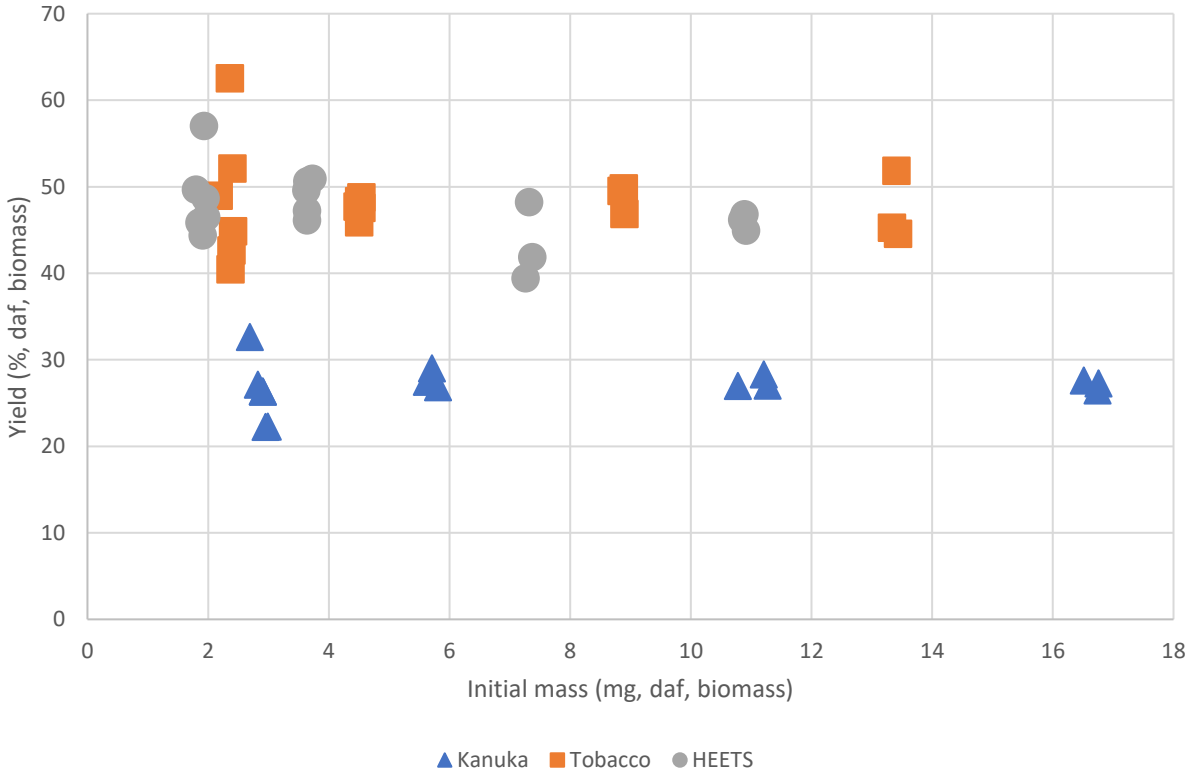

Figure 15: Graphs of yield at 550°C against initial mass for HEETS, kānuka and tobacco samples heated at 5K/min after being held at 105°C for 45 minutes to remove moisture. The biomasses are displayed on a dry ash free (daf), biomass basis.

Figure 15 is displayed on a dry, ash-free, biomass basis to remove the effect of moisture, ash and additives from the biomasses (Table 5 and Ministry of Health, 2019). The HEETS and tobacco appear to have a much higher yield than kānuka, because their ash content is significantly higher than kānuka. The inorganic species present in ash can catalyse secondary reactions leading to more char and a higher yield (Valin et al., 2015, and Khelfa et al., 2013). Another feature of Figure 15 is the yield for all biomasses remains unaffected by initial mass. For HEETS and tobacco this will be due to ash catalysing secondary reactions. For kānuka this will be due to the minimally porous particles (Figure 14).

3.10 Evolved gas analysis- mass spectrometry (EGA-MS)

As shown in the results presented above, there are multiple influences on the behaviour of biomass during heating. To study this further it is worth investigating the individual components that are produced. The EGA/MS is able to report the mass to ion m/z ratio of species or fragments of species produced during pyrolysis. The method does not distinguish between compounds with the same molar mass, however Figure 16 presents selected m/z intensity curves and

Table 8 lists the compounds that are most likely to correspond to the m/z ratios and whether they were identified in each of tobacco, HEETS or kānuka.

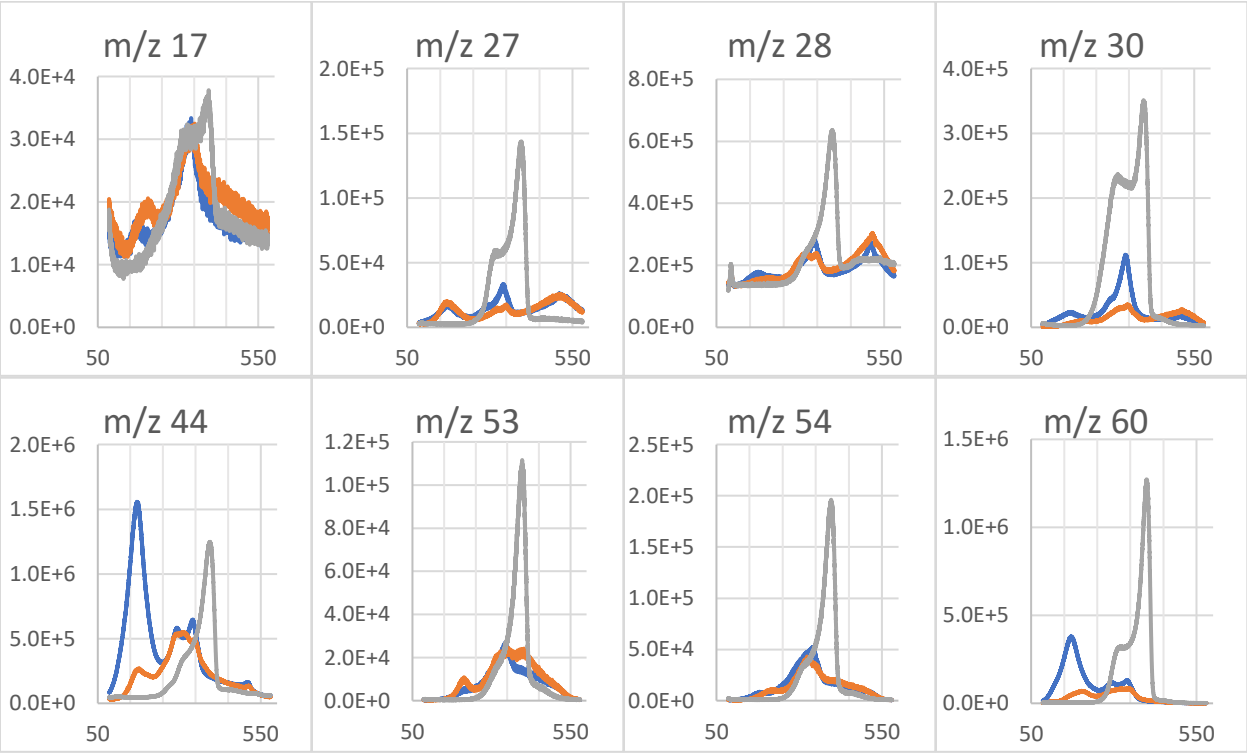

Figure 16: Graphs of absolute intensity versus temperature for evolved gas analysis of 0.5 mg biomass samples for a range of molecular weights. Experiments involve a temp ramp of 10 K/min from 85°C to 580°C and an ionisation energy of 20eV. The blue curves are HEETS, the orange curves are tobacco, and the grey curves are kānuka. The X axis is the temperature from 50°C up to 600°C. The Y axis is the

absolute intensity, and each molecular weight has a different scale. Full size graphs can be found in Appendices H.

Figure 16. continued

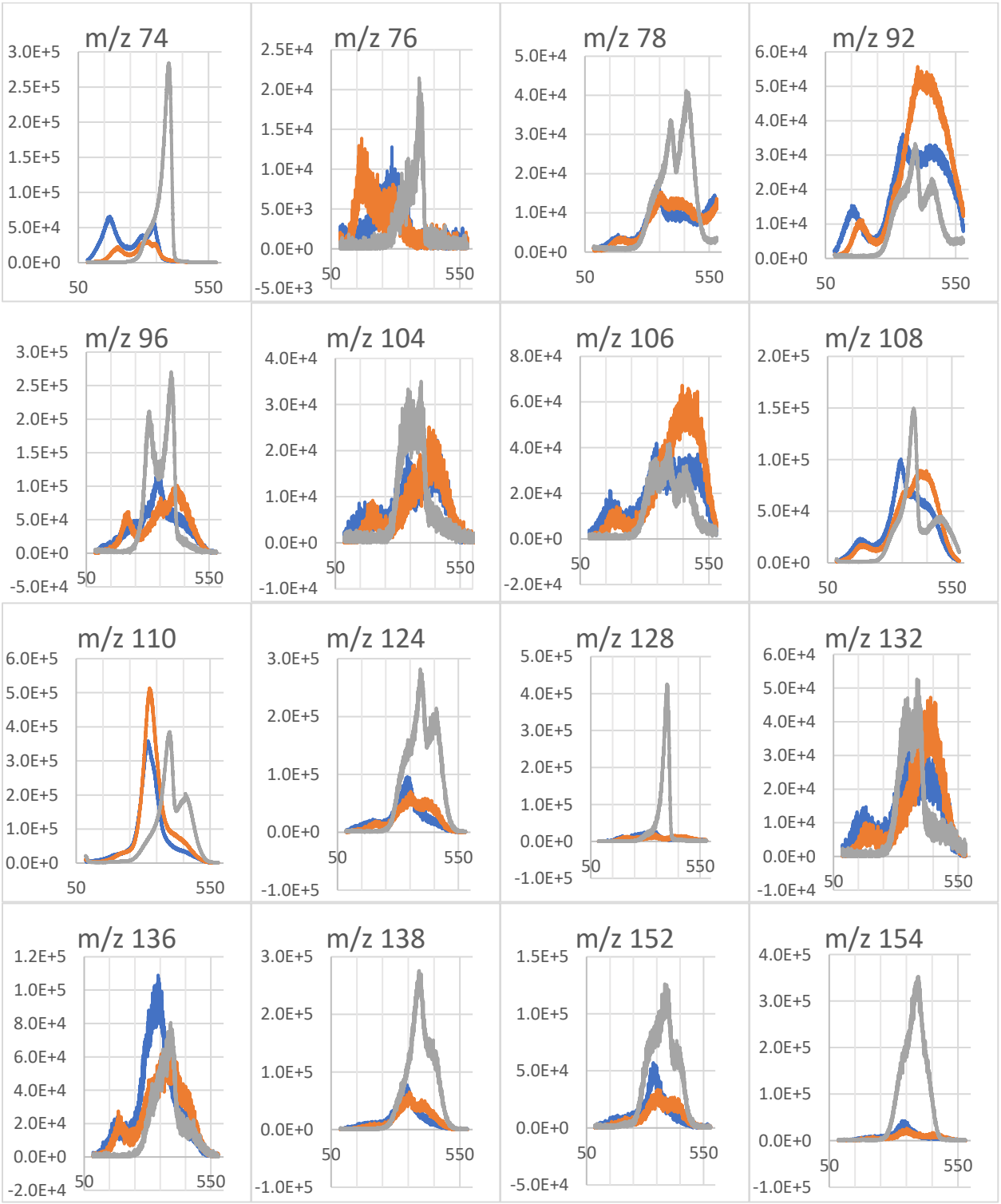

Figure 16. Continued

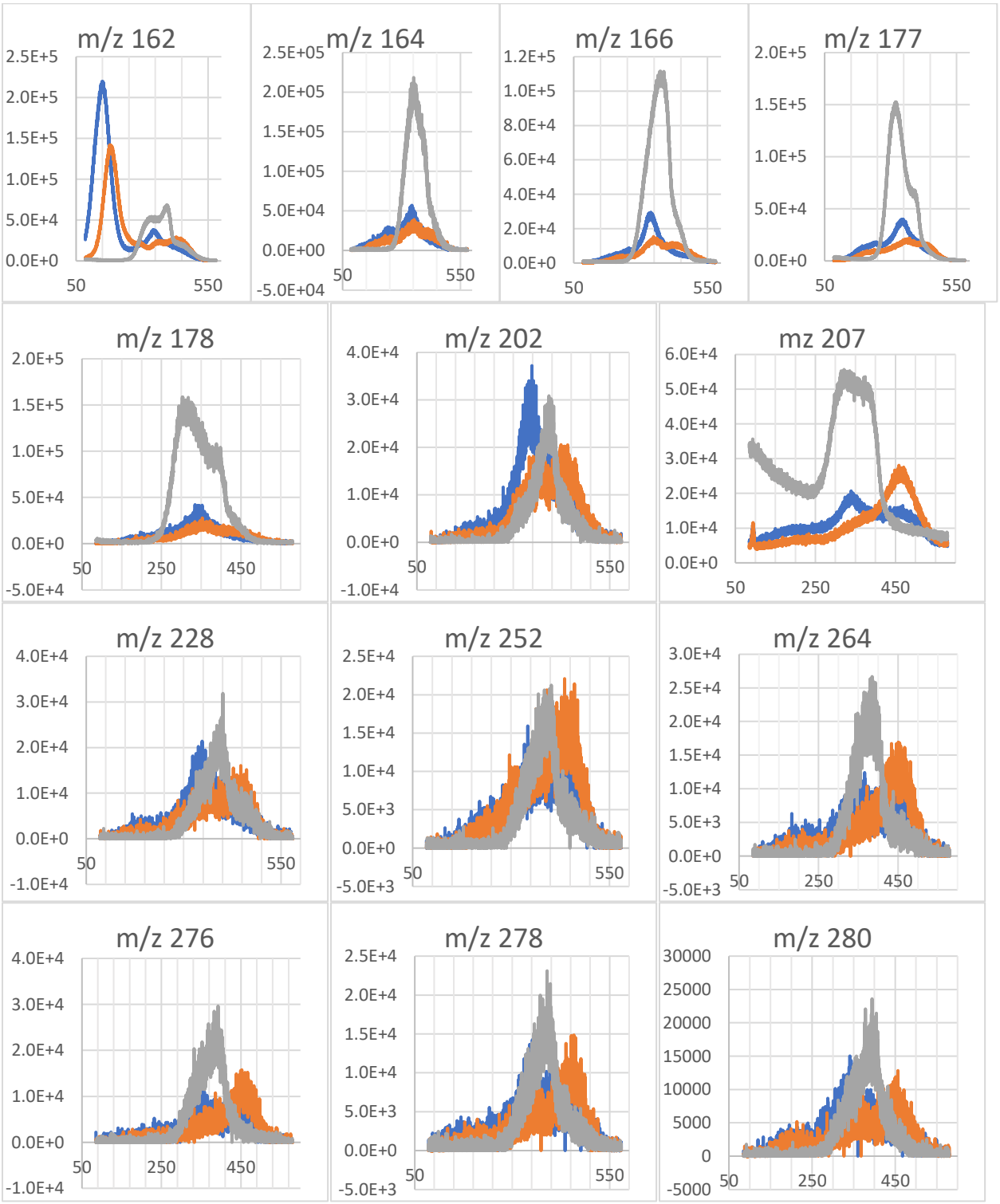

Table 8: Summary of compounds identified from evolved gas analysis. H = HEETS, T = Tobacco, K = Kānuka

m/z	Compounds	Formula	Present in
17	Ammonia	NH_3	H, T, K
17	Hydroxide ions	OH^-	H, T, K
27	Hydrogen cyanide	HCN	H, T
27	$C_2H_3^+$ ions	$C_2H_3^+$	H, T, K
28	Carbon monoxide	CO	H, T, K
28	Ethylene	C_2H_4	H, T
30	Formaldehyde	CH_2O	H, T, K
30	Ethane	C_2H_6	H, T, K
30	Nitric oxide	NO	H, T
44	Carbon dioxide	CO_2	H, T, K
44	Acetaldehyde	C_2H_4O	H, T, K
44	Propane	C_3H_8	H, T, K
44	Ethylene oxide	C_2H_4O	
53	Acrylonitrile	C_3H_3N	H, T
53	$C_4H_5^-$ ions	$C_4H_5^-$	H, T, K
54	1,3-Butadiene	C_4H_6	H, T, K
54	1,2-Butadiene	C_4H_6	H, T, K
54	1-Butyne	C_4H_6	H, T, K
54	2-Butyne	C_4H_6	H, T, K
60	Acetic acid	$C_2H_4O_2$	H, T, K
60	1-Propanol	C_3H_8O	H, T
60	Glycolaldehyde	$C_2H_4O_2$	H, T, K
60	Carbonyl sulfide	COS	
74	N-Nitrosodimethylamine (NDMA)	$C_2H_6N_2O$	H, T
74	Hydroxyacetone	$C_3H_6O_2$	H, T, K
74	n-Butanol	$C_4H_{10}O$	H, T, K
74	Isobutanol	$C_4H_{10}O$	H, T, K
74	Propionic acid	$C_3H_6O_2$	H, T, K
74	Methyl acetate	$C_3H_6O_2$	H, T, K
74	Glycidol	$C_3H_6O_2$	H
74	2-hydroxypropanal	$C_3H_6O_2$	H, T
74	3-hydroxypropanal	$C_3H_6O_2$	H, T, K
76	Propylene glycol	$C_3H_8O_2$	H, T
76	Carbon disulfide	CS_2	H, T
76	2-Methoxyethanol	$C_3H_8O_2$	H, T
76	1,3-Propanediol	$C_3H_8O_2$	H
78	Benzene	C_6H_6	H, T, K
78	Fulvene	C_6H_6	H, T
78	3-Pyridinyl radical	C_5H_4N	H, T
92	Glycerol	$C_3H_8O_3$	H
92	Toluene	C_7H_8	H, T, K
96	Furfural	$C_5H_4O_2$	H, T, K

96	Pyranone	$C_5H_4O_2$	H, T, K
96	2-Cyclopentene-1,4-dione	$C_5H_4O_2$	H
96	2,5-Dimethylfuran	C_6H_8O	H, T, K
96	2-Methyl-2-cyclopentenone	C_6H_8O	H, T, K
96	3-Methyl-2-cyclopentenone	C_6H_8O	H, T, K
104	Styrene	C_8H_8	H, T, K
104	Methional	C_4H_8OS	H, T
104	Cyclooctatetraene	C_8H_8	H, T
106	Benzaldehyde	C_7H_6O	H, T, K
106	Ethylbenzene	C_8H_{10}	H, T, K
106	m-Xylene	C_8H_{10}	H, T, K
106	o-Xylene	C_8H_{10}	H, T, K
106	p-Xylene	C_8H_{10}	H, T, K
106	Glyceric acid	$C_3H_6O_4$	H
108	m-Cresol	C_7H_8O	H, T, K
108	o-Cresol	C_7H_8O	H, T, K
108	p-Cresol	C_7H_8O	H, T, K
108	Benzoquinone	$C_6H_4O_2$	H, T, K
108	Anisole	C_7H_8O	H, T, K
108	Benzyl alcohol	C_7H_8O	H, T, K
108	2,3-Dimethylpyrazine	$C_6H_8N_2$	T
108	2,5-Dimethylpyrazine	$C_6H_8N_2$	H, T
108	2,6-Dimethylpyrazine	$C_6H_8N_2$	T
110	Catechol	$C_6H_6O_2$	H, T, K
110	5-methylfurfural	$C_6H_6O_2$	H, T, K
110	Hydroquinone	$C_6H_6O_2$	H, T, K
110	Resorcinol	$C_6H_6O_2$	H, T, K
110	2,4-Heptadienal	$C_7H_{10}O$	H, T
110	2,3-Dimethyl-2-cyclopenten-1-one	$C_7H_{10}O$	H, T, K
110	2-Ethyl-5-methylfuran	$C_7H_{10}O$	H, T, K
110	2,3,5-Trimethylfuran	$C_7H_{10}O$	H, T, K
110	2-Propylfuran	$C_7H_{10}O$	K
110	3,4,5-Trimethylpyrazole	$C_6H_{10}N$	H, T
110	2-Methyl-1,6-heptadiene	C_8H_{14}	H, T
110	3-Isopropylcyclopentene	C_8H_{14}	H, T
110	2-Acetylfuran	$C_6H_6O_2$	H, T, K
110	3-Monochloropropane diol (3-MCPD)	$C_3H_7ClO_2$	H, T, K
124	Guaiacol	$C_7H_8O_2$	H, T, K
124	Mequinol	$C_7H_8O_2$	H, T, K
124	3-Methoxyphenol	$C_7H_8O_2$	H, T, K
124	6-Methyl-3,5-heptadien-2-one	$C_8H_{12}O$	H, T
128	Naphthalene (NAP)	$C_{10}H_8$	H, T, K
128	Furaneol	$C_6H_8O_3$	K
128	Dihydromaltol	$C_6H_8O_3$	K
132	Cinnamaldehyde	C_9H_8O	H, T
132	Diammonium phosphate	$H_9O_4N_2P$	H, T

132	1-Methyl-4-(1-methylethenyl)benzene	$C_{10}H_{12}$	H, T
132	Ethylstyrene	$C_{10}H_{12}$	K
132	n-Methylbenzofuran	C_9H_8O	K
132	1-Methyl-1-propenylbenzene	$C_{10}H_{12}$	K
136	Anisaldehyde	$C_8H_8O_2$	H, T, K
136	Phenylacetic acid	$C_8H_8O_2$	H, T, K
136	2,3-Diethylpyrazine	$C_8H_{12}N_2$	T
136	2,3,5,6-Tetramethylpyrazine	$C_8H_{12}N_2$	H, T
136	Benzyl formate	$C_8H_8O_2$	H, T
136	3-Phenyl-1-propanol	$C_9H_{12}O$	H, T
136	Limonene	$C_{10}H_{16}$	H, T
136	2,5-Dimethyl-3-methylene-1,5-heptadiene	$C_{10}H_{16}$	H, T
136	2-Ethyl-3,5-dimethylpyrazine	$C_8H_{12}N_2$	H, T
136	Terpinene	$C_{10}H_{16}$	H, T
138	Creosol	$C_8H_{10}O_2$	H, T, K
138	2,3-Dihydroxybenzaldehyde	$C_7H_6O_3$	H, T, K
138	3,4-Dihydroxybenzaldehyde	$C_7H_6O_3$	H, T, K
138	m-Hydroxybenzoic acid	$C_7H_6O_3$	H, T, K
138	o-Hydroxybenzoic acid	$C_7H_6O_3$	H, T, K
138	p-Hydroxybenzoic acid	$C_7H_6O_3$	H, T, K
152	Vanillin	$C_8H_8O_3$	H, T, K
152	4-Ethylguaiacol	$C_9H_{12}O_2$	H, T, K
152	Methyl salicylate	$C_8H_8O_3$	
152	Citral	$C_{10}H_{16}O$	H, T
152	Acenaphthylene	$C_{12}H_8$	H, T, K
152	2,5-Dimethoxytoluene	$C_9H_{12}O_2$	K
154	Syringol	$C_8H_{10}O_3$	H, T, K
154	Eucalyptol	$C_{10}H_{18}O$	H, T
154	Geraniol	$C_{10}H_{18}O$	H, T
154	Isopulegol	$C_{10}H_{18}O$	H, T
154	Linalool	$C_{10}H_{18}O$	H, T
154	Acenaphthene	$C_{12}H_{10}$	H, T, K
162	Nicotine	$C_{10}H_{14}N_2$	H, T
162	Anabasine	$C_{10}H_{14}N_2$	H, T
162	Levoglucosan	$C_6H_{10}O_5$	H, T, K
162	Methyl cinnamate	$C_{10}H_{10}O_2$	H
162	6-Methoxy-3-methylbenzofuran	$C_{10}H_{10}O_2$	K
164	Eugenol	$C_{10}H_{12}O_2$	H, T, K
164	Isoeugenol	$C_{10}H_{12}O_2$	K
164	Raspberry ketone	$C_{10}H_{12}O_2$	
164	Phenethyl acetate	$C_{10}H_{12}O_2$	H, T
166	Fluorene	$C_{13}H_{10}$	H, T, K
166	4-Propylguaiacol	$C_{10}H_{14}O_2$	H, T, K
166	Homovanillin	$C_9H_{10}O_3$	K
166	Acetoguaiacone	$C_9H_{10}O_3$	H, T, K
177	3-(1-Nitrosopyrrolidin-2-yl)pyridine (NNN)	$C_9H_{11}N_3O$	H, T

178	Phenanthrene	$C_{14}H_{10}$	H, T, K
178	Anthracene	$C_{14}H_{10}$	H, T, K
202	Fluoranthene	$C_{16}H_{10}$	H, T, K
202	Pyrene	$C_{16}H_{10}$	H, T, K
207	4-(N-methyl-N-nitrosamino)-1-(3-pyridyl)-1-butanone (NNK)	$C_{10}H_{13}N_3O_2$	H, T
207	4-(N-methyl-N-nitrosamino)-4-(3-pyridyl)butanal (NNA)	$C_{10}H_{13}N_3O_2$	H, T
228	Benzo(a)anthracene	$C_{18}H_{12}$	H, T, K
228	Chrysene	$C_{18}H_{12}$	H, T, K
228	Triphenylene	$C_{18}H_{12}$	H, T, K
228	Myristic acid	$C_{14}H_{28}O_2$	H, T, K
252	Benzo(a)pyrene (B[a]P)	$C_{20}H_{12}$	H, T, K
252	Benzo(e)pyrene (B[e]P)	$C_{20}H_{12}$	H, T, K
252	Benzo(b)fluoranthene (B[b]F)	$C_{20}H_{12}$	H, T, K
252	Benzo(j) fluoranthene (B[j]F)	$C_{20}H_{12}$	H, T, K
252	Benzo(k)fluoranthene (B[k]F)	$C_{20}H_{12}$	H, T, K
264	Cinnamyl cinnamate	$C_{18}H_{16}O_2$	H, T, K
276	Benzo[g,h,i]perylene	$C_{22}H_{12}$	H, T, K
276	Indeno[1,2,3-cd]pyrene	$C_{22}H_{12}$	H, T, K
276	Anthanthrene	$C_{22}H_{12}$	H, T, K
276	Stearidonic acid	$C_{18}H_{28}O_2$	H, T
278	Dibenz[a,h]anthracene (D[ah]A)	$C_{22}H_{14}$	H, T, K
278	Linolenic acid	$C_{18}H_{30}O_2$	H, T, K
278	Neophytadiene	$C_{20}H_{38}$	H, T
280	Linoleic acid	$C_{18}H_{32}O_2$	H, T, K

3.10.1 m/z 17: Hydroxide ions and ammonia

The m/z 17 graph starts with a peak that decreases in intensity for all the biomasses. This could be due to the release of hydroxide ions from dehydration reactions (Wang et al., 2010). The loss of free water would cause the first release of hydroxide ions, although they can be released during thermal decomposition at higher temperatures. Figure 7 shows the EGA for all the biomasses have a peak around 350^{o}C, and kānuka has a larger peak around 400^{o}C. During these large vapour producing events, OH^- ions are likely to be released. This could explain the peak for all biomass at 350^{o}C and the kānuka peak at 400^{o}C. Ammonia also has an m/z of 17. Ammonia provides plants with nitrogen, which is found in HEETS and tobacco (Howitt & Udvardi, 2000), but is much less for kānuka (Table 6). Ahamad and Alshehri (2012) conducted an EGA of bidi tobacco powder at 30K/min using 70eV. They noticed a release of ammonia from 200°C to 300°C and again, with a slightly smaller peak, from 400°C to 500°C. By using a heating rate of 30K/min the peaks from the EGA will appear at a higher temperature than at 10K/min used here. The first peak they found could correspond with the peak 140^{o}C to 250^{o}C, and the second peak from 250^{o}C peaking at 340^{o}C could correspond with the second peak they found. Ahamad and Alshehri (2012) use a 70eV and report results in relation to the ion current, Figure 16 uses 20eV and the results are relative to the absolute intensity. Due to these differences, it is difficult to compare peak heights. Bassilakis et al. (2001) noticed during a TG-FTIR of tobacco, that ammonia generally peaked around 350°C, and had a small shoulder from 160^{o}C to 280^{o}C. They analysed oriental, bright and burley tobacco. Burley tobacco showed a much higher release of ammonia, with a peak from 160^{o}C to 240^{o}C being larger than the peak at 350^{o}C. Of the 3 tobacco varieties, burley was found to have the highest nitrogen content at 5.22%, followed by bright at 3.08%, then oriental at 2.78%. Tobaccos with a higher nitrogen content will release more ammonia (Meng

et al., 2015). Figure 16 does not show a significant difference between HEETS and tobacco, but this could explain the differences with some literature. Baker et al. (2006) observed ammonia in tobacco vapour, in an oxic environment, from 200°C to 700°C with two distinct peaks around 350°C and 525°C. They also observed that inverted sugar does not affect ammonia formation, while the presence of glucose significantly reduced the first peak and slightly reduced the second peak. The tobacco sample uses a small amount of inverted sugar and the HEETS sample uses cellulose, which is made from glucose units (Ministry of Health, 2019). Therefore, this may help explain why HEETS has a more suppressed peak compared to tobacco from 140^{o}C to 250^{o}C. Kānuka does not appear to have a peak at this low temperature. Leaves use ammonia as a nitrogen source for photosynthesis. For trees, during the winter nitrogen is stored in the trunk (Flechard et al., 2013). Kānuka wood chips, which come from the trunk, are suspected to have low ammonia levels as indicated by the low nitrogen in Table 6. Another consideration is that ammonia can be added to tobacco products to increase the amount of unprotonated nicotine released during heating, which makes the tobacco product more addictive (Inaba et al., 2018). It has been described as having a chocolate flavour in smoke, although can be unpleasant if 0.5% or higher is present (Stevenson & Proctor, 2008). The FDA (2019) has identified ammonia as a potentially harmful compound, stating that it is a respiratory toxicant. Philip Morris Products S.A. (2017) released research stating that ammonia concentration in the vapour from HEETS was around 12.2µg/HEET. This is assuming it is used with an iQOS device according to the recommended procedure. The results were verified by Li et al. (2019) who ran the same experiment.

3.10.2 m/z 27: Hydrogen cyanide and $C_2H_3^+$ ions

Hydrogen cyanide can have toxic effects on the human respiratory system (Ahamad & Alshehri, 2012). The FDA (2019) stated that hydrogen cyanide is a respiratory toxicant and a cardiovascular toxicant. Hydrogen cyanide has an m/z of 27. Figure 16 shows peaks around 170^{o}C, 290^{o}C, 340^{o}C, and 510^{o}C for HEETS and tobacco, and peaks around 320^{o}C and 400^{o}C for kānuka. Bassilakis et al. (2001) in TG-FTIR analysis of tobacco showed 3 peaks at 220°C, 480°C and 680°C. These are higher than Figure 16, although they used a heating rate of 30K/min instead of 10K/min so thermal lag would cause a temperature shift of the peaks. Tobacco with higher nitrogen content also had a higher hydrogen cyanide production. Hydrogen cyanide production can be increased with the addition of sugar and glycerol (Baker et al., 2004, and Carmines & Gaworskir, 2005). The HEETS sample contained added sugar and glycerol, while the tobacco sample only has added sugar (Ministry of Health, 2019). Senneca et al. (2007), noticed hydrogen cyanide in tobacco smoke from 180°C to 350°C, and 400°C to 550°C with a heating rate of 5K/min. The slower heating rate used by Senneca et al. (2007) mean that vapour production will occur at lower temperatures than Figure 16. Forster et al. (2015) found that the concentration of hydrogen cyanide was too low to detect in tobacco heated up to 200°C and suggested that higher temperatures were required for formation. Ahamad and Alshehri (2012) conducted an EGA analysis of bidi tobacco powder and attributed the peaks between 250°C to 500°C to hydrogen cyanide and $C_2H_3^+$ ions. In research done by Philip Morris Products S.A. (2017) they were unable to detect hydrogen cyanide in HEETS heated to 350^{o}C but could detect it in a burning 3R4F cigarette and concluded that HEETS provide a >99.5% reduction in hydrogen cyanide. Li et al. (2019) came to the same conclusion. The main production of hydrogen cyanide occurs between 800°C to 1000°C, which is the temperature of a cigarette burning in an oxic environment (Torikai et al., 2004). The HEETS and tobacco, in Figure 16, is reminiscent of the overall EGA curve in Figure 6, which indicates that the vapour production at m/z 27 is dominated by $C_2H_3^+$ ions.

3.10.3 m/z 28: Carbon monoxide and ethylene

Carbon monoxide and ethylene have an m/z of 28. The biomass curves in Figure 16 appear similar to the respective DTG curve in Figure 4, but with a more significant peak after 425^{o}C. Bassilakis et al. (2001) found tobacco, heated at 30K/min, produced carbon monoxide from 200^{o}C, with a large peak at 320^{o}C, a

smaller peak at 500°C, and a large production after 600°C. Senneca et al. (2007) found carbon monoxide from 250°C to 900°C. Meng et al. (2015) concluded that carbon monoxide production was influenced more by cellulose degradation, while carbon dioxide was more influenced by hemicellulose degradation. Philip Morris Products S.A. (2017) claim that HEETS released 347 µg/HEET of carbon monoxide when heated to 350°C. Zhang et al. (2019) completed an FTIR on pine wood sawdust and found a very similar curve to kānuka in Figure 16, although peaks were at slightly lower temperatures due to using particles less than 180 microns compared to 200 to 600 microns. They attributed the shoulder on the main peak to the decomposition of hemicellulose, the largest peak to the decomposition of cellulose and the peak above 415°C to secondary reactions. Carbon monoxide is released during primary and secondary reaction of ether groups (Hrablay & Jelemensky, 2016). Below 250°C the vapour produced from wood consists mostly of water, methane, carbon monoxide and carbon dioxide (Gu et al., 2013). Liu et al. (2008) found for birch, a hardwood like kānuka, carbon monoxide was produced from primary reactions from 135°C to 280°C, and after this was also produced from secondary reactions. They noticed carbon monoxide production below 135°C, but the wood vapour contained significantly more water. Bassilakis et al. (2001) also noticed the production of ethylene from 200°C to 600°C, with peaks at 320°C and 400°C. The ethylene peaks were about ten times smaller than the carbon monoxide peaks. This corresponds with Meng et al. (2015). Therefore, in conclusion, while ethylene will influence Figure 16, it will largely be dominated by carbon monoxide.

3.10.4 m/z 30: Formaldehyde, ethane, nitric oxide

Formaldehyde, ethane, and nitric oxide have an m/z of 30. Figure 16 shows that HEETS and tobacco are similar, while kānuka does not have the low and high temperature peaks. HEETS has a small hump around 170°C, followed by a peak at 340°C with a shoulder around 300°C and a final peak at 510°C. Tobacco shows a similar pattern to HEETS but the absolute intensity of peaks below 400°C is much lower. Kānuka has two peaks at 315°C and 400°C. Bassilakis et al. (2001) analysed the concentration of formaldehyde in tobacco smoke with an FTIR and found production started at 200°C, and peaked at 350°C with a shoulder at 500°C. The peaks of Bassilakis et al. (2001) may be shifted from these here because they use a heating rate of 30K/min while the work here use 10K/min. Baker et al. (2006) noticed formaldehyde was produced in tobacco vapour from 200°C to 500°C with a peak around 325°C. The main production of formaldehyde in tobacco was from 200°C to 500°C (Torikai et al., 2004). Formaldehyde released from tobacco when heating is able to be detected from 180°C (Forster et al., 2015). Formaldehyde is formed from small saccharides that decompose over 250°C (Piade et al., 2013). The decomposition of cellulose can increase formaldehyde concentration in tobacco smoke (Baker et al., 2005, and Banyasz et al., 2001). The HEETS sample has 3.8% added cellulose (Ministry of Health, 2019). Figure 16 shows a larger peak for HEETS compared to tobacco around 340°C which corresponds with this information. At 450°C formaldehyde decomposes to form carbon monoxide and hydrogen (Moldoveanu, 2019). IARC (2006) classified formaldehyde as a carcinogen. Formaldehyde can cause cancer and is a respiratory toxicant (Fowles et al., 2000). Philip Morris Products S.A. (2017) claim that HEETS at 350°C released 14.1 µg/HEET of formaldehyde, although Li et al. (2019) completed the same experiment and found that HEETS released 21.9 µg/HEET. Bacsik et al. (2007) detected ethane present in 4 different tobacco cigarettes. Meng et al. (2015) noticed ethane in the smoke produced from heating tobacco stems from 400°C to 550°C, peaking at 500°C. Formaldehyde and ethane are degradation products also found in wood vapour (Liu et al., 2008, and Hrablay & Jelemensky, 2016). Im et al. (2003) heated tobacco in an anoxic environment at 12K/min and detected nitric oxide present in tobacco smoke from 275°C to 375°C. Senneca et al. (2007) and Piade et al. (2013) had similar findings although Senneca et al. (2007) found nitric oxide from 200°C. Nitric oxide is a degradation product from nitrates in tobacco (Rodgman & Perfetti, 2013). Philip Morris Products S.A. (2017) noticed 12.6µg/HEET of nitric oxide was released while heating HEETS to 350°C. In conclusion, for HEETS and tobacco in Figure 16 it is likely the lower temperature peaks are

dominated by formaldehyde and nitric oxide, while the peak above 400°C is dominated by ethane. For kānuka the overlapping peaks will be due to first formaldehyde then ethane.

3.10.5 m/z 44: Carbon dioxide, acetaldehyde, propane, and ethylene oxide

Carbon dioxide, acetaldehyde, propane, and ethylene oxide have an m/z of 44. In Figure 16, the HEETS curve shows peaks at 170°C, 290°C, 340°C and 510°C. The tobacco curve shows similar peak temperatures and intensities, except for the peak at 170°C which is at a significantly lower intensity. Kānuka shows a main peak around 400°C with a shoulder at 315°C.

Carbon dioxide is a major product of pyrolysis and is released over a wide range of temperatures. Bassilakis et al. (2001) conducted a TG-FTIR of tobacco and their graph for carbon dioxide had a large peak from 250°C to 350°C. Senneca et al. (2007) noticed production of carbon dioxide from tobacco between 180°C to 500°C with a significant dominance from 350°C to 500°C. White et al. (2001) and Meng et al. (2015) had similar findings for tobacco dust and tobacco stems respectively. Zhang et al. (2019) found carbon dioxide production, from heating wood sawdust, peaked at 350°C and 480°C. Gu et al. (2013) found carbon dioxide was released from poplar wood consistently from below 250°C to above 500°C. Carbon dioxide is released due to degradation (Rodgman & Perfetti, 2013).

For acetaldehyde, Bassilakis et al. (2001) noticed that in tobacco vapour it starts being released from 200°C, peaks at 350°C, and decreases till 500°C. Torikai et al. (2004) detected acetaldehyde in tobacco from 25°C to 500°C, which corresponds with Forster et al. (2015) and Ahamad and Alshehri (2012). Hrablay and Jelemensky (2016) heated beech and noticed the production of acetaldehyde from 230°C to 500°C. Gu et al. (2013) had similar findings when heating poplar. Chida et al. (2004) calculated a 1504.92 mmHg vapour pressure for acetaldehyde at 40°C and described it as having a "pungent, ethereal nauseating odor". The main formation of acetaldehyde is due to the decomposition of carbohydrates, hemicellulose, and lignin (Piade et al., 2013), which at around 600°C, decomposes to methane and carbon monoxide (Moldoveanu, 2019). The FDA (2019) has identified acetaldehyde as a potentially harmful compound, stating that it is a carcinogen, respiratory toxicant and is addictive. Philip Morris Products S.A. (2017) detected 192µg/HEET of acetaldehyde production from HEETS heated to 350°C. Auer et al. (2017), Schaller et al. (2016), and Mallock et al. (2018) agree with this result. Li et al. (2019) found a slightly higher production at 210 µg/HEET. Bentley et al. (2020) found acetaldehyde production even higher at 313 µg/HEET.

Propane is a degradation product (Rodgman & Perfetti, 2013). Wood contains phenyl propane monomers, so it is likely kānuka will release propane during heating (Liu et al., 2008). Meng et al. (2015) detected propane while heating tobacco stems from 400°C to 550°C.

For ethylene oxide, Rodgman and Perfetti (2013) has reported its presence in tobacco smoke. After 550°C ethylene oxide begins decomposition, mainly converting to methane and carbon monoxide, with small amounts of "ethane, ethylene, acetylene, acetaldehyde, propane and hydrogen" (Moldoveanu, 2019). Ethylene glycol used to be added to tobacco as a humectant but is no longer used as it produces ethylene oxide (Hoffman and Hoffman, 2001). Ethylene oxide has been recognised as a carcinogen that can increase the risk of lymphoid and breast cancer (EPA, 2008). Philip Morris Products S.A. (2017) were unable to detect ethylene oxide in HEETS, and claimed they gave a >99.3% reduction compared to 3R4F cigarettes. Schaller et al. (2016) heated tobacco blends under the same condition as HEETS and found there was an average reduction of 99.2% ethylene oxide, and there were some tobacco blends with an ethylene oxide concentration too low to be detected.

In the m/z 44 result in Figure 16, it is not clear which peaks correspond to each of carbon dioxide, acetaldehyde, and propane. The addition of glycerol to tobacco can increase acetaldehyde and carbon

dioxide production at low temperatures as it is a glycerol decomposition product (Gomez-Siurana et al., 2013). This corresponds with Figure 16, as HEETS have 17% added glycerol and the tobacco sample has none (Ministry of Health, 2019) In conclusion, it is likely that acetaldehyde appears at the lower temperatures, propane at the higher temperatures and carbon dioxide would dominate across the whole temperature range corresponding to the breakdown of hemicellulose, cellulose and lignin.

3.10.6 m/z 53: Acrylonitrile

Acrylonitrile has an m/z of 53. Acrylonitrile is a degradation compound related to nitric oxide (Piade et al., 2013). Acrylonitrile can cause cancer and is a respiratory toxicant (Fowles et al., 2000). Figure 16 shows HEETS has a main peak at 350^{o}C with shoulders on both sides of the peak. Kānuka has a main peak at 400^{o}C with shoulders on both sides of the peak. Tobacco has peaks at 210^{o}C, 340^{o}C and 400^{o}C. Liu et al. (2011) found acrylonitrile in flue cured tobacco smoke when heating around 800°C. The concentration of acrylonitrile in raw tobacco was 7.73 µg/cigarette which was reduced to 5.17 µg/cigarette after it was homogenized. HEETS is a homogenized tobacco product. In line with this observation, Figure 16 shows that HEETS have some peaks at a lower intensity than the tobacco sample. Forster et al. (2015) was unable to detect acrylonitrile in tobacco vapour below 200°C, as also found here, and concluded that higher temperatures where needed for formation. Torikai et al. (2004) suggest that the main production of acrylonitrile occurs from 500°C to 800°C. Philip Morris Products S.A. (2017) found HEETS at 350^{o}C had an acrylonitrile production of 0.145µg/HEET, which corresponds with the average result found by Schaller et al. (2016). There is limited research to justify each of the peaks shown in Figure 16. The peak around 400^{o}C for tobacco and the shoulder in the same temperature range is likely influenced by acrylonitrile. Due to the low nitrogen content of kānuka it is unlikely that it produces much acrylonitrile (Table 6). Therefore, the kānuka curve is more likely to be the but-2-yn-1-yl radical and but-1-yn-3-yl radical, which both have an m/z of 53 and an empirical formula of C_4H_5. This presence of radicals and ions will also be present for the tobacco samples and so they are probably the main contributing factor to the curves shown in Figure 16.

3.10.7 m/z 54: 1,3-Butadiene, 1,2-butadiene, 1-butyne, and 2-butyne

1,3-Butadiene, 1,2-butadiene, 1-butyne and 2-butyne have an m/z of 54. 1,3-Butadiene is a human carcinogen (Oladipupo et al., 2019). 1,3-Butadiene can cause cancer and harmful reproductive effects (Fowles et al., 2000). Figure 16 shows HEETS and tobacco have a main peak at 320^{o}C. Kānuka has a shoulder at this temperature and a main peak at 400^{o}C. 1,3-Butadiene has been found by other researchers. In anoxic conditions, Torikai et al. (2004) detected 1,3-butadiene in tobacco vapour after heating to 300°C at a rate of 20K/min. Ahamad and Alshehri (2012) reported butadiene was found during the heating of bidi tobacco powder between 250°C and 500°C. Olsson et al. (2004) heated pine and spruce found the concentration of 1,3-butadiene rapidly decreased after roughly 400^{o}C, which corresponds with that observed for kānuka in Figure 16.

1,3-Butadiene is an expected degradation product of cellulose and sugars (Soeteman-Hernandez et al., 2013), which will then further decompose from 425°C to 725°C to cyclohexane, cyclohexadiene, benzene, butenes, propylene, ethylene, methane, vinylacetylene, and hydrogen (Moldoveanu, 2019). Isomerisation occurs between 1,3-butadiene, 1,2-butadiene, 1-butyne and 2-butyne (Lockhart et al., 2017) which, at lower temperatures, is much faster than decomposition (Chambreau et al., 2005). Pan et al. (2013) studied the photon energies of Virginia cigarettes and found that for an m/z of 54, it was made up of 55% 1,3-butadiene, 21% 1,2-butadiene, 22% 1-butyne and 2% 2-butyne. Philip Morris Products S.A. (2017) found 1,3-butadiene production from HEETS heated to 350^{o}C was 0.207µg/HEET. Li et al. (2019), Mallock et al. (2018), and Schaller et al. (2016) had similar findings, but Bentley et al. (2020) found 1,3-butadiene to be higher at 0.716 µg/HEET.

3.10.8 m/z 60: Acetic acid, 1-propanol, glycolaldehyde, and carbonyl sulfide

Acetic acid, 1-propanol, glycolaldehyde, and carbonyl sulfide have an m/z of 60. This m/z is one of the most dominant in EGA/MS analysis; indeed Nardella et al. (2020) conducted an EGA for pine and oak heated to 600^{o}C and found that m/z 60 had the most abundant production for oak and the second most abundant product for pine. The peaks observed in Figure 16 correspond entirely with literature observation. In Figure 16 the profiles are quite noticeably different for the three biomasses. HEETS has peaks at 170^{o}C, 290^{o}C and 340^{o}C. Tobacco has a peak at 210^{o}C that is significantly smaller than the HEETS 170^{o}C peak and also peaks at 290^{o} and 340^{o}C that are slightly lower in absolute intensity than HEETS. Kānuka has peaks at 320^{o}C and 400^{o}C. Therefore, tobacco and HEETS have a mechanism for generation of m/z 60 at lower temperature that is not present in kānuka, and kānuka has a mechanism for generation of m/z 60 at high temperature that is not present in tobacco or HEETS. Acetic acid has been described as having a "pungent, stinging sour odor" (Chida et al., 2004). Chen et al. (2021) identified acetic acid in the vapour produced from heating kānuka to 335°C. Zhang et al. (2020) detected acetic acid in kānuka vapour heated to 480^{o}C. Branca et al. (2003) found in beech, acetic acid production increased from 4.8 wt.% at 275^{o}C to 5.5% at 625^{o}C. Acetic acid is one of the main pyrolysis products from wood between 100°C and 300°C (Dietenberger & Hasburgh, 2016). The decomposition of hemicellulose contributes to the amount of acetic acid released (Meng et al., 2015, and Dietenberger & Hasburgh, 2016). In oxic conditions at 900°C, 95.9% of acetic acid is transferred to vapour, 4.0% is converted to acetic acid anhydride, and 0.1% is converted to ethanol (Baker & Bishop, 2004). Bassilakis et al. (2001) conducted a TG-FTIR of three different tobaccos at 30K/min. There results correspond to those reported here, finding that oriental and bright tobacco had peaks at 200^{o}C and 320^{o}C, whereas burley tobacco only had a peak at 320^{o}C. Gu et al. (2019) noticed acetic acid released while heating a tobacco stem from 160°C to 240°C. The peak decreases till around 400°C, which corresponds with Liu et al. (2013) who detected acetic acid in tobacco smoke at 400°C but not from 500°C to 800°C. Liu et al. (2013) was heating tobacco stems at 10K/min. These results correspond with Figure 16, and acetic acid is likely to contribute heavily to the first 2 peaks from HEETS and tobacco, and slightly to the third peak. The tobacco sample has 0.24 wt.% of added acetic acid to tobacco. Chida et al. (2004) calculated a vapour pressure of 34.93 mmHg for acetic acid at 40°C. The vaporisation of the added acetic acid will also contribute to the low temperature tobacco peaks. Bentley et al. (2020) found acetic acid was the second most prominent component of tobacco smoke and found HEETS had a 994 µg/HEET production.

Gu et al. (2019) also identified 1-propanol when heating tobacco stems from 160°C to 240°C. Kibet et al. (2019) detected the presence of 1-propanol when heating tobacco at 300°C. Chida et al. (2004) also calculated a 52.16 mmHg vapour pressure for 1-propanol at 40°C and stated it had a "mild, nonresidual, alcoholic odor".

Glycolaldehyde was detected by Liu et al. (2009), who conducted an FTIR of poplar. Branca et al. (2003) found the production of glycolaldehyde increased from 0.7 wt.% at 275^{o}C to 2.3 wt.% at 625^{o}C for beech. Sanders et al. (2003) detected glycolaldehyde produced from the thermal decomposition of cellulose at 300°C to 600°C. Glycolaldehyde will be produced from the pyrolysis of kānuka and tobacco (Vitasari, 2012). Glycolaldehyde is also formed from the decomposition of glycerol (Pennings et al., 2019). HEETS has added glycerol and a large first peak in Figure 16, which is likely due to the release of glycolaldehyde (Ministry of Health, 2019).

Carbonyl sulfide has been detected in tobacco smoke from a 2R4F cigarette (Dong & DeBusk, 2009). It can hydrolyse to hydrogen sulfide which causes irritation to skin, eyes, and respiratory system (Svoronos & Bruno, 2002). Bassilakis et al (2001) studied the pyrolysis of different biomasses and found that carbonyl sulfide was released from wheat straw up to 1000°C with multiple peaks in concentration with the three largest peaks at 280°C, 380°C and 880°C. However, with tobacco they found that the

concentration of carbonyl sulfide was too low to detect. The concentration of sulfur in the tobacco, HEETS, and kānuka sample is 0.20 wt.%, 0.12 wt.%, and 0.02 wt.% respectively, so it is unlikely that significant amounts of carbonyl sulfide will be produced (Table 6).

3.10.9 m/z 74: NDMA, hydroxyacetone, n-butanol, isobutanol, propionic acid, etc.

NDMA, hydroxyacetone, n-butanol, isobutanol, propionic acid, methyl acetate, glycidol, 2-hydroxypropanal and 3-hydroxypropanal have an m/z of 74. Figure 16 shows that the profiles for tobacco and HEETS are similar, but that kānuka lacks the low temperature peak and has an additional and large high temperature peak. HEETS has peaks at 170^{o}C, 290^{o}C and 340^{o}C, tobacco has peaks at 200^{o}C, 310^{o}C and 340^{o}C, and kānuka has a peak at 400^{o}C with a shoulder around 320^{o}C. NDMA is a tobacco-specific nitrosamine (Rodgman & Perfetti, 2013) and has been attributed to causing cancer (Ahmad & Alshehri, 2012, and Fowles & Bates 2000). Senneca et al. (2007) noticed the release of NDMA from tobacco from 180°C to 400°C. The addition of glycerol can reduce NDMA production (Carmines & Gaworski, 2005). HEETS have 17 wt.% added glycerol and the tobacco sample does not (Ministry of Health, 2019).

Gu et al. (2019) has identified hydroxyacetone in the vapour released from heating tobacco stems from 160°C to 240°C. Kibet et al. (2019) also noticed the presence of hydroxyacetone when heating tobacco to 300°C. Demirbas (2002) detected hydroxyacetone when heating tobacco stalks from 375°C to 775°C and noticed it peaked around 575°C. Hydroxyacetone was one of the major components of wood vinegar from pine and poplar heated to 500^{o}C (Aguirre et al., 2020). In Chinese Fir, heated to 300^{o}C, hydroxyacetone was one of the main ketones detected by the GC-MS (Li et al., 2020). Branca et al. (2003) found hydroxyacetone, methyl acetate and 3-hydroxypropanal in beech at 525^{o}C. They found that the concentration of hydroxyacetone from beech increased from 1.1 wt.% to 1.6 wt.% from 325^{o}C to 375^{o}C and maintained at 1.6 wt.% up to 625^{o}C. Hydroxyacetone forms from the decomposition of xylan (Demirbas, 2002). Propylene glycerol can also decompose to form a small amount of hydroxyacetone (Pennings et al., 2019). Bentley et al. (2020) studied the top 100 chemicals in HEETS vapour and found 1135 µg/HEET of hydroxyacetone, 53.2 µg/HEET of propanoic acid, and 1.31 µg/HEET of glycidol. St. Helen et al. (2018) also studied the vapour from HEETs at 350^{o}C and found 162 µg/HEET of hydroxyacetone, and 5.71 µg/HEET of glycidol. The difference in results is likely due to the different research methods used. The tobacco sample has 4% added propylene glycerol and the HEETS sample has 1% added propylene glycerol (Ministry of Health, 2019).

n-Butanol has been detected in the tobacco plant and vapour (Rodgman & Perfetti, 2013). Chida et al. (2004) heated flue cured tobacco to 240°C and identified 1-butanol in the vapour produced. Nanda et al., (2014) found n-butanol can be produced from pine. 1-Butanol has a vapour pressure of 18.29 mmHg at 40°C and a “mild fusel-like odor” (Chida et al., 2004). Baker and Bishop (2004) analysed the decomposition of pure compounds heated to 900°C in oxic conditions. For n-butanol, 90.7% of n-butanol can transfer to vapour, 6.3% can convert to isobutanol, and 2.8% can convert to butanal. Isobutanol does not degrade at 900°C.

Propionic acid is a short chain fatty acid found in tobacco (Zeller et al., 2019). Barbero-Lopez et al. (2019) found propionic acid was produced from spruce bark and birch bark after heating to 350^{o}C. For propionic acid, 97.6% of propionic acid transfers to vapour at 900°C in oxic conditions, and so is therefore a relatively stable compound. 1.2% of propionic acid is converted to ethanol, 1.1% converted to propionic anhydride and 0.1% converted to acetic acid (Baker & Bishop, 2004).

Methyl acetate is a potentially harmful toxicant (Lempert et al., 2019). Chida et al. (2004) found methyl acetate in the vapour produced from heating flue cured tobacco to 240°C. They also stated that methyl acetate has a vapour pressure of 405.61mmHg at 40°C and has an “ethereal fruity odor of very poor

tenacity". Demirbas (2002) identified methyl acetate when heating tobacco stalks to 550°C. Methyl acetate starts degradation after 725°C in anoxic conditions (Yang et al., 2015).

Glycidol is formed from the dehydration of glycerol (Sleiman et al., 2016), but appears to be a relatively minor component in m/z 74. 2-Hydroxypropanal is a decomposition product of propylene glycol and 3-hydroxypropanal is a decomposition product from glycerol (Schick et al., 2017, Adam et al., 2009, and Jensen et al., 2017). 3-Hydroxypropanal is also a decomposition product of carbohydrates (del Rio et al., 2002). Costa et al. (2019) detected 3-hydroxypropanal in cork oak wood heated to 650°C. In conclusion, in Figure 16, the dominant compound and largest contribution will be from hydroxyacetone, with decomposition products from propylene glycerol and glycerol contributing to the first peak for HEETS and tobacco and decomposition from lignin responsible for the high temperature peak of kānuka.

3.10.10 m/z 76: Propylene glycol, carbon disulfide, 2-methoxyethanol and 1,3-propanediol

Propylene glycol, carbon disulfide, 2-methoxyethanol and 1,3-propanediol have an m/z of 76. Propylene glycol is a humectant added to the tobacco sample at 4wt%, and the HEETS sample at 1wt% (Ministry of Health, 2019). Bentley et al. (2020) found 643 µg/HEET of propylene glycol was produced from HEETS heated to 350°C, which means that at low temperatures, the majority of propylene glycol is vaporised. Vaporisation was also found to occur at higher temperatures; Laino et al. (2012) found 99.9% of propylene glycol was vaporised at 525°C in anoxic conditions and Baker and Bishop (2004) found 86.3% of propylene glycol was vaporised at 900°C in oxic conditions. Both experiments used pure standards of propylene glycol, not combined with tobacco. Other research does show breakdown of propylene glycol in anoxic environments was found to being at around 400°C (Moldoveanu, 2019, Saliba et al., 2018). Of these, Saliba et al. (2018) studied the decomposition from 80°C to 670°C. In anoxic environments, propionaldehyde was first detected at 413°C, acetone was detected at 460°C, and formaldehyde and acetaldehyde were detected at 670°C. By 670°C propionaldehyde contributed to 57.8% of the vapour, acetone contributed 28.8%, acetaldehyde contributed 6.4% and formaldehyde contributed 3.2%. Propionaldehyde formation was also observed by Moldoveanu (2019), and Diaz et al., (2010) who also found acetone, acetaldehyde, and formaldehyde when heating propylene glycol up to 325°C in an oxic environment. Laino et al. (2012) also found acetone and acetaldehyde from heating propylene glycol to 525°C, as well as hydroxyacetone, ally alcohol, propylene oxide, and propanal. These decomposition products will affect other graphs shown in Figure 16.

Carbon disulfide has been reported in tobacco and tobacco vapour (Rodgman & Perfetti, 2013). Carbon disulfide has been detected in tobacco smoke in 2R4F cigarettes (Dong & DeBusk, 2009). Its concentration was roughly 20 times lower compared to carbonyl sulfide. The amount of carbon disulfide in tobacco and HEETS will be very minimal as tobacco contains 0.20 wt.% sulfur and HEETS contains 0.12 wt.% sulfur. It is unlikely that kānuka would contain carbon disulfide as it has a 0.02 wt.% sulfur composition (Table 6).

2-Methoxyethanol was detected in the smoke from burning Italian cigarettes (Pieraccini et al., 2008). It is unclear if this is from tobacco or a tobacco additive common to the Italian cigarettes analysed. 2-Methoxyethanol was found at a low concentration and is likely to have a slight contribution to the HEETS and tobacco curves, shown in Figure 16, in the lower temperature range.

1,3-Propanediol has been detected in tobacco smoke but not the plant (Rodgman & Perfetti, 2013). It is a decomposition product of glycerol (Diaz et al., 2010), added at 17 wt.% to HEETS (Ministry of Health, 2019). Diaz et al. (2010) found that 1,3-propanediol further decomposed to acrolein when heated to 156°C in oxygen. Since the majority of glycerol is vaporised before degrading, 1,3-propanediol will have only a small effect on the HEETS curve in Figure 16.

Takada et al. (2004) heated sugi wood to 300^{o}C in anoxic conditions and found many compounds had fragmentation ions of m/z 76. They did not discuss the structure of each compound or the fragments. They believe the m/z 76 fragments came from a biphenyl type dimer, a diphenylethane type dimer, and a stilbene type dimer, none of which have been investigated here.

In Figure 16, the first peak for tobacco at 175^{o}C, is likely dominated by the release of propylene glycol. Propylene glycol release for HEETS would occur at the same temperature, although a significant peak is not shown as HEETS has a much smaller addition of propylene glycol (Ministry of Health, 2019). Kānuka does not contain added propylene glycol and shows a low absolute intensity around this temperature. It is unclear exactly what contributed to the other higher temperature peaks, although it is likely dominated by ions from the breakdown of holocellulose and lignin.

3.10.11 m/z 78: Benzene, fulvene and 3-pyridinyl radicals

Benzene and fulvene have an m/z of 78. The FDA (2019) has stated that benzene is a carcinogen, cardiovascular toxicant and reproductive or developmental toxicant. Philip Morris Products S.A. (2017) reported that benzene production was 0.452µg/HEET for HEETS at 350^{o}C. The results correspond with Li et al. (2019), Mallock et al. (2018) and Schaller et al. (2016). Wang et al. (2017) detected benzene and fulvene in smoke from a lit tobacco cigarette and stated that benzene contributes to over 93% of m/z 78 production. Figure 16 shows HEETS and tobacco have a small bump around 190^{o}C, absent in kānuka, followed by a peak at 340^{o}C, another bump around 430^{o}C, and another peak at 570^{o}C. Kānuka has a slight shoulder around 330^{o}C for a peak at 400^{o}C, followed by a larger peak at 460^{o}C and a very small peak at 570^{o}C. The lack of the lowest and almost lack of the highest peak for kānuka indicate that some differences in decomposition occur, or in the pathways of formation. Senneca et al. (2007) identified benzene in tobacco smoke from 200°C to 550°C. Li et al. (2019) found benzene at 350°C when heating a 3R4F cigarette. Branca et al. (2003) found benzene produced from beech heated to 525^{o}C. Ma et al. (2008) heated a Chinese fir extract to 250^{o}C and detected the presence of benzene, the temperature being lower than kānuka experienced in Figure 16 due to the use of an extracted solution instead of raw material. Piade et al. (2013) found that benzene formation starts around 300°C, and the main formation occurs from 450°C to 600°C. Once formed benzene is easily volatilised with a 295.52 mmHg vapour pressure for benzene at 40°C (Chida et al., 2004). However, Figure 16 m/z 78 has multiple peaks and the reasons for these are not known but must relate to a number of formation mechanisms for benzene. The decomposition of catechol, hydroquinone, cinnamic acid, amino acids, cellulose, and other carbohydrates all result in the formation of benzene (Lomnicki et al., 2008, Truong et al., 2008, Liu et al., 2011, O'Connor & Hurley, 2008, Czegeny et al., 2009, and Takada et al., 2004). In tobacco, the decomposition of cotinine, 3-hydroxycotinine, and nicotine-1-N-oxide result in 3-pyridinyl radicals (Zbancioc et al., 2012).

3.10.12 m/z 92: Glycerol and toluene

Glycerol and toluene have an m/z of 92. Figure 16 shows a peak from 100^{o}C to 250^{o}C for tobacco and HEETS, but not for kānuka, followed by large absolute intensities for all biomass from 250^{o}C to 600^{o}C. Glycerol is an added ingredient to HEETS (Ministry of Health, 2019). Glycerol evaporates from tobacco from 123°C to 203°C (Marcilla et al., 2015). Baker and Bishop (2004) found, when heating to 900°C, that 99.8% of glycerol was vaporised. Carmines and Gaworski (2005) had similar findings, also claiming that the remaining glycerol is decomposed to acrolein and glycolaldehyde. According to Moldoveanu (2019) at around 350°C glycerol decomposes to form acrolein, at 450°C acetaldehyde and ally alcohol are also produced, and at 650°C formaldehyde is also produced. Purkis et al. (2013) claims, in cigarettes, that the addition of glycerol does not significantly increase acrolein in vapour compared to cigarettes without added glycerol. In cigarettes, Roemer et al. (2010) found the addition of glycerol reduced phenol and cresol production by 50%, crotonaldehyde and hydrogen production by 25%, and reduced pyridine and quinoline production by 20%. They also found that production of water increases by 150%, and ammonia

production increased by 25%. Philip Morris International (2018) state that 52.3mg glycerol is added to each HEET stick and claim that 5.02mg/HEET of glycerol was detected in the vapour from HEETS heated around 350^{o}C (Philip Morris Products S.A., 2017), which corresponds with St. Helen et al. (2018), but higher than Li et al. (2019) who observed 3.84mg/HEET glycerol in HEETS vapour. The evaporation of glycerol therefore explains the first peak in HEETS in Figure 16, but not the similar peak for tobacco which does not contain added glycerol.

Toluene is formed from the decomposition of carbohydrates (Liu et al., 2011). It is a respiratory toxicant and a reproductive or developmental toxicant (FDA, 2019). Philip Morris Products S.A. (2017) report that toluene production is 1.42µg/HEET in HEETS heated to 350^{o}C. These findings correspond with Li et al. (2019) and Mallock et al. (2018). Bentley et al. (2020) found a slightly higher toluene concentration of 3.80 µg/HEET. Toluene was detected by Gu et al. (2019) in the vapour produced from heating a tobacco stem from 160°C to 240°C. Pieraccini et al. (2008) had corresponding research for Italian cigarettes. Gu et al. (2013) found toluene in poplar wood heated to 600^{o}C in anoxic conditions. Lyu et al. (2019) found toluene in willow lignin vapour from 450^{o}C to 800^{o}C. VanderSchelden et al. (2017) and Sallsten et al. (2006) also found toluene in wood smoke. The main generation of toluene in tobacco vapour occurred from 500°C to 800°C (Torikai et al., 2004). Around 825°C toluene decomposes to benzyl, phenyl and methyl radicals and hydrogen (Moldoveanu, 2019).

As well as glycerol and toluene, fragmentation ions would contribute to Figure 16. Sleiman et al. (2009) found the tobacco-specific nitrosamine, NNA, degrades to an ion with an m/z of 92. Takada et al. (2004) found propioguaiacone in sugi wood and stated that it fragments to an ion of m/z 92.

In summary, the peaks above 250^{o}C for all the biomasses are dominated by toluene and fragmentation ions. Glycerol evaporation influences the first peak for HEETS, although degradation of glycerol appears to be also significant as the graphs at m/z 44 and m/z 60 in Figure 16 suggest, because they contain the known degradation products of acetaldehyde and glycolaldehyde. The low temperature peak for the tobacco remains unknown because then sample does not contain glycerol.

3.10.13 m/z 96: Furfural, pyranone, 2-cyclopenten-1,4-dione, 2,5-dimethylfuran, etc.

Furfural, pyranone, 2-cyclopentene-1,4-dione, 2,5-dimethylfuran, 2-methyl-2-cyclopentenone and 3-methyl-2-cyclopentenone have an m/z of 96. Figure 16 shows different shape curves for each biomass. The absolute intensity for HEETS spans 100^{o}C to 550^{o}C, with a prominent peak at 340^{o}C. Tobacco spans the same range but has peaks at 210^{o}C, 350^{o}C, and 410^{o}C with significant overlap from the latter two peaks. Kānuka has a narrower span from 250^{o}C to 500^{o}C with two distinct peaks at 300^{o}C and 400^{o}C.

Of the above compounds list at m/z 96 furfural is the most significant. Liu et al. (2013) heated tobacco stems from 400^{o}C to 800^{o}C and noticed a decreasing production of furfural from 400^{o}C to 600^{o}C. While they used a 20 K/min heating rate, instead of 10 K/min, and only reported results every 100^{o}C, when considering thermal lag, their results agree with those in Figure 16. Zhang et al. (2020) heated kānuka from 180^{o}C to 480^{o}C and also noticed the production of furfural decreases with increasing temperature. They expected low temperature production, but also noted there could be issues with adsorption onto their adsorption media which they then washed off with a solvent before injection into a GC/MS. Chen et al. (2021) found the production of furfural from kānuka peaked around 300^{o}C, which agrees with Figure 16.

A significant amount of research has focused on furfural. Streibel et al. (2009) found furfural was one of the most prominent compounds in spruce and beech vapour heated to 300^{o}C. Branca et al. (2003) recorded the concentrations of furfural, 2-methyl-2-cyclopentanone, and 3-methyl-2-cyclopentanone while heating beech from 325^{o}C to 625^{o}C. 2-Methyl-2-cyclopentanone and 3-methyl-2-cyclopentanone

concentrations increased with increasing temperature. The furfural concentration was over twice as much as the 2-methyl-2-cyclopentanone concentration and furfural increased from 325°C to 525°C then decreased till 625°C. Furfural is one of the main products from hemicellulose decomposition (Liu et al., 2009). Furfural is produced from the degradation of polysaccharides and sugars (Vasiliou et al., 2013). Furfural can also be produced from the breakdown of cellulose fibres, cocoa extract, guar gum, inverted sugar syrup, and acetic acid (Baker & Bishop, 2005). The HEETS sample has 3.8 wt.% added cellulose and 2.2 wt.% added guar gum. The tobacco sample has 0.24 wt.% added acetic acid, 0.0014% cocoa extract and 0.0006% inverted sugar syrup (Ministry of Health, 2019). Cellulose starts producing furfural from 200°C (Baker et al., 2005). The higher cellulose content of HEETS explains the higher peak in absolute intensity around 340°C compared to tobacco (Figure 16). The main decomposition products from furfural are furan, 1,3-butadienal, and carbon monoxide (Vasiliou et al., 2013).

Direct measurements on HEETS have also been made. Bentley et al. (2020) studied compounds in HEETS vapour at 350°C and found 47.4 µg/HEET of furfural, 51.4 µg/HEET of pyranone, 8.4 µg/HEET of 2-cyclopentene-1,4-dione, and 6.38 µg/HEET of 2,5-dimethylfuran. St. Helen et al. (2018) also studied the vapour from HEETS at 350°C and found 31.1 µg/HEET of furfural, 6.54 µg/HEET of pyranone, and 3.8 µg/HEET of 2-cyclopentene-1,4-dione. Differences could be due to the different experimental methods used.

Of the other compounds listed at m/z 96, pyranone is formed through the thermal degradation of xylose (Huang et al., 2016) and has been detected in oak wood and tobacco (Simon et al., 2010, and Rodgman & Perfetti, 2013). It is unclear if 2-cyclopentene-1,4-dione originates from tobacco or from an added ingredient in HEETS, although it has not been identified in general tobacco literature. 2,5-Dimethylfuran has been identified in tobacco and wood smoke (Adam et al., 2006; Pennings et al., 2019; and Braun & Antonietti, 2017). The thermal decomposition of sugars produces 2,5-dimethylfuran (Pennings et al., 2019). 2-Methyl-2-cyclopentenone and 3-methyl-2-cyclopentenone have been identified in tobacco smoke (Stabbert et al., 2017, and Riveles et al., 2005). Takada et al. (2004) noticed the m/z 96 production during the breakdown of many compounds in sugi wood but did not state the formation of the breakdown compound of the formation of the m/z 96 fragment. In conclusion, it is unclear exactly what compounds are contributing to the peaks in Figure 16, but it will likely be dominated by furfural.

3.10.14 m/z 104: Styrene, methional and cyclooctatetraene

Styrene, methional and cyclooctatetraene have an m/z of 104. In Figure 16, HEETS and tobacco have a small peak around 200°C, followed by at peak around 350°C that is a shoulder for a bigger peak around 440°C. Kānuka does not have either the lowest or highest temperature peaks, but have two middle peaks of equal intensity around 340°C and 390°C. In tobacco vapour, styrene has been detected from 200°C with the main generation from 500°C to 800°C (Torikai et al., 2004, and Akalin & Karagoz, 2011). Branca et al. (2003), found styrene produced from beech wood around 525°C. Kibet et al. (2012) heated lignin and notice the production of styrene from 300°C, peaking around 525°C, and decreasing till 700°C. Styrene is a decomposition product of many ethylbenzene compounds (Blazso et al., 2018), and is carcinogenic and genotoxic (Huff & Infante, 2011). Philip Morris Products S.A. (2017) found that styrene production in HEETS was 0.577 µg/HEET, which approximately agrees with Mallock et al. (2018) who heated two variants of HEETS and found that styrene production was 0.47 µg/HEET and 0.49 µg/HEET respectively. However, as they are sold in flavours, it is unclear what flavour HEETS were analysed. Schaller et al. (2016) heated different tobacco blends under the same condition as HEETS and found there was an average styrene production of 1.067 µg/HEET with results ranging from 0.468 µg/HEET to 1.128 µg/HEET. Methionine has been detected in tobacco leaves and can convert to methional (Adam et al., 2005), which is also a flavour compound that can be added to tobacco (Baker et al., 2004). Methional has been described as having a “boiled potato-like" flavour (Cserhati & Forgacs, 2003). It appears relatively

stable because at 900°C in oxic conditions, 88.1% of methional is transferred to vapour (Baker & Bishop, 2004). Cyclooctatetraene has been detected in tobacco smoke but not the tobacco plant (Rodgman & Perfetti, 2013). Pieraccini et al. (2008) smoked Italian cigarettes and noticed cyclooctatetraene was produced. In conclusions, the peaks above 300^{o}C are most likely to be dominated by styrene. The origins of the low temperature peaks in tobacco and HEETS are unknown.

3.10.15 m/z 106: Benzaldehyde, ethylbenzene, m-xylene, o-xylene, p-xylene, and glyceric acid

Benzaldehyde, ethylbenzene, m-xylene, o-xylene, p-xylene, and glyceric acid have an m/z of 106. Figure 16 shows HEETS and tobacco have a small peak around 170^{o}C, but kānuka does not. Above 250^{o}C detection of m/z 106 occurs in all samples. Tobacco appears to have one large peak around 470^{o}C. HEETS has a series of small peaks from 250^{o}C to 590^{o}C. Kānuka has 3 peaks, a similar size to HEETS, at 340^{o}C, 390^{o}C and 460^{o}C. Pan et al. (2013) studied the photon energies of burning Virginia cigarettes and for an m/z of 106, the vapour is 26% benzaldehyde, 51% ethylbenzene, and 23% xylene. Takada et al. (2004) found sugi wood decomposition had many mechanisms resulting in fragments of m/z 106. Benzaldehyde has been found in biomass, as part of lignin, and will be present in the HEETS, tobacco and kānuka vapour (Rodgman & Perfetti, 2013, and Vasiliou et al., 2013). Benzaldehyde has been detected in wood lignin heated to 450^{o}C (Salem & Bohm, 2013). Chida et al. (2004) detected benzaldehyde in flue cured tobacco heated to 240°C and described it as having a "powerful sweet odor". Stotesbury et al. (2000) and Baker and Bishop (2004) found that at 200°C, benzaldehyde can transfer into the tobacco vapour, but under oxic conditions 23% converted to benzoic acid. At 500°C benzaldehyde breaks down to form benzene and carbon monoxide (Moldoveanu, 2019). Benzaldehyde has a vapour pressure of 133 Pa at 26°C (Pang & Lewis, 2011). Benzaldehyde is a common pyrolysis product from many aroma compounds found in tobacco and tobacco products (Blazso et al., 2018). Benzaldehyde is an added flavouring to HEETS (Philip Morris International, 2018). It is unclear if the HEET used for this research contains added benzaldehyde. The vapour from HEETS has been reported to contain 1.2 µg/HEET benzaldehyde (Auer et al., 2017).

Ethylbenzene has been found in the vapour produced from heating flue cured tobacco to 240°C, and stated it has a "sweet, grassy odor" (Chida et al., 2004). Wang et al. (2016) heated n-benzene up to 800°C and noticed the production of ethylbenzene starting around 650°C. However, Domke et al. (2001) claims that after 600°C ethylbenzene breaks down to styrene, benzene, toluene, methane, and carbon monoxide. Ethylbenzene, m-xylene, o-xylene, and p-xylene has been found in the smoke produced from wood and tobacco (Rey-Salguerio et al., 2016, and Polzin et al., 2007). Gaworski et al. (2008) noticed ethylbenzene and m-xylene when heating potassium sorbate, a tobacco additive, to 1000°C. The tobacco sample contains 0.25% added potassium sorbate (Ministry of Health, 2019). So, while it will cause a slight increase, it will not solely explain the peak around 470^{o}C in Figure 16. Pieraccini et al. (2008) found m-xylene, o-xylene and p-xylene in the vapour produced from smoking Italian cigarettes. Wang et al. (2019) studied the pyrolysis to tobacco stems and found that xylene production peaked around 490°C but can peak at lower temperatures if pre-treatment of the tobacco stems is used. Kibet et al. (2012) observed the lignin p-xylene production from 300°C, peaking just before 500°C and decreasing till 700°C. Zhao et al. (2014) conducted a flash pyrolysis of lignin and detected xylene at 800^{o}C but was unable to detect it below 650^{o}C. Xylene is a potentially harmful compound to the nervous system, mostly causing dizziness and similar symptoms but can be fatal in high concentrations (Kandyala et al., 2010).

Glyceric acid is a decomposition product of glycerol (Schick et al., 2017), which is added to HEETS at 17 wt.% (Ministry of Health, 2019). In Figure 16, the initial peak of the HEETS is only slightly larger than the tobacco. Glycerol become glyceric acid after forming a double bond with an oxygen molecule, so its presence is more likely in an oxic environment (Schick et al., 2017). The EGA/MS experiments were done under anoxic conditions, so the presence of glyceric acid is expected to be minimal. In conclusion, the

peaks above 250°C are dominated by benzaldehyde, ethylbenzene and xylene as noted by Pan et al. (2013). The origin of the peaks below 250°C for tobacco and HEETS appear to relate to the presence of benzaldehyde in the plant material as it is emitted during curing.

3.10.16 m/z 108: m-Cresol, o-cresol, p-cresol, benzoquinone, anisole, benzyl alcohol, etc.

m-Cresol, o-cresol, p-cresol, benzoquinone, anisole, benzyl alcohol, 2,3-dimethylpyrazine, 2,5-dimethylpyrazine, and 2,6-dimethylpyrazine have a m/z of 108. m-Cresol, o-cresol and p-cresol are isomers of each other. Streibel et al. (2009) found cresol was one of the main compounds generated in spruce and beech vapour at 300°C. o-Cresol has a higher production in anoxic conditions, while m-cresol and p-cresol were unaffected by the atmosphere (Torikai et al., 2004). The formation of m-cresol, o-cresol and p-cresol is due to the decomposition of lignin (Liu et al., 2013). Ahmad and Alshehri (2012) detected the cresol compounds when heating bidi tobacco powder. Liu et al. (2013) identified p-cresol in tobacco smoke from 500° to 700°C, but not at 400°C or 800°C. Kibet et al. (2012) detected p-cresol from 250°C to 600°C with a peak at 350°C when heating lignin. Gu et al. (2019) identified o-cresol when heating tobacco stems from 160°C to 240°C. Pieraccini et al. (2008) found m-cresol, o-cresol and p-cresol when smoking Italian cigarettes. McGrath et al. (2009) heated tobacco up to 600°C and measured the relative composition in the vapour. They concluded that 11% of o-cresol was released below 350°C and 89% was released from 350°C to 600°C, 13% of m-cresol was released below 350°C and 87% was released from 350°C to 600°C, and 21% of p-cresol was released below 350°C and 79% was released from 350°C to 600°C. Luo et al. (2017) noticed p-cresol during the thermal decomposition of pine wood from 400°C to 550°C. Zhang et al. (2020) reported the presence of m-cresol in kānuka vapour generated at 480°C.

The FDA (2019) stated that m-cresol, o-cresol, and p-cresol are carcinogens and respiratory toxicants. Philip Morris Products S.A. (2017) analysed vapour from HEETS found production of 0.0424 µg/HEET m-cresol, 0.0779 µg/HEET o-cresol and 0.0706 µg/HEET p-cresol. Schaller et al. (2016) heated tobacco blends in the same condition as HEETS and found there was an average 0.031 µg/HEET m-cresol, 0.052 µg/HEET o-cresol, and 0.068 µg/HEET in p-cresol.

Benzoquinone formation, reported by Truong et al. (2008), occurred from 250°C to 700°C while heating hydroquinone. Hydroquinone has been detected in the tobacco plant and its smoke, while benzoquinone has only been detected in tobacco smoke (Rodgman & Perfetti, 2013). Hydroquinone and compounds containing a benzoquinone functional group have been detected during the decomposition of wood (Fine et al., 2001, and Ngo et al., 2015).

Anisole is a plant component also found in tobacco and wood vapour (Rodgman & Perfetti, 2013, and Nowakowska et al., 2014). At 200°C anisole can transfer to tobacco vapour (Baker & Bishop, 2004). Anisole can be produced from the pyrolysis of anisaldehyde at 800°C (Stotesbury et al., 2000). According to Moldoveanu (2019), from 380°C to 400°C anisole can break down to phenol and ethylene. Baker and Bishop (2004) heated anisole to 900°C in the presence of oxygen, and found 98.7% of anisole was vaporised, 1.1% was converted to methylanisole, and 0.2% was converted to benzaldehyde.

Benzyl alcohol has been found in the tobacco plant (Rodgman & Perfetti, 2013). Sepetdjian et al. (2013) found benzyl alcohol in cigarettes and water pipe tobacco. They found the production of benzyl alcohol was favoured in the water pipe tobacco, potentially because it heats to around 450°C, whereas cigarettes heat to around 950°C. Chida et al. (2004) found benzyl alcohol in the vapour produced from heating flue cured tobacco to 240°C. Safdari et al. (2018) found benzyl alcohol was present in many biomasses, including wood, after heating but it was present in small concentrations. Blazso et al. (2018) heated benzyl alcohol to 300°C and found that 1.87% will decompose to benzaldehyde, with the rest vaporising. At 900°C in oxic conditions, 95.4% of benzyl alcohol will vaporise and 4.8% will convert to benzaldehyde (Baker &

Bishop, 2004). Benzyl alcohol has an almond aroma (Zhai et al., 2018), and is added as a flavouring to HEETS (Philip Morris International, 2018).

Rodgman and Perfetti (2013) have reported the dimethylpyrazines as a tobacco ingredient. Dimethylpyrazines are added for flavour and could improve nicotine delivery (Alpert et al., 2016). It is unclear is benzyl alcohol or dimethylpyrazines have been added to the HEETS or tobacco samples used in this research, as the tobacco returns does not specify flavourings (Ministry of Health, 2019). Akalin and Karagoz (2011) detected 2,5-dimethylpyrazine during the decomposition of tobacco stems at 500°C. Pyrazines can form below 100°C while the tobacco is curing via the Maillard reaction (Alpert et al., 2016). Baker and Bishop (2004) studied pyrolysis products by heating pure substances to 900°C in oxic conditions. They found for 2,3-dimethylpyrazine that 99.7% will vaporise, 0.2% will convert to trimethylpyrazine, and 0.1% will convert to ethyldimethylpyrazine. For 2,5-dimethylpyrazine, 99.7% will vaporise and 0.3% will convert to methylpyrrole. They found for 2,6-dimethylpyrazine that 99.5% will vaporise, 0.3% will be converted to aminodimethylpyridine and 0.2% will convert to dimethylethylpyrazine. The flavour of 2,5-dimethylpyrazine has been described as chocolate (Kaur et al., 2018), and is added to HEETS as a flavouring (Philip Morris International, 2018). The flavour of 2,3-dimethylpyrazine and 2,6-dimethylpyrazine has been described as burley (Alpert et al., 2016). In conclusion, while it is not possible to define precisely which compounds correspond to the peaks in Figure 16 for m/z 108, it is likely that the two peaks for kānuka are the cresol compounds formed from a holocellulose and lignin pathways. These are also reflected in the tobacco and HEETS curves, but with the addition of low temperature peaks likely to relate to the presence of benzyl alcohol and dimethylpyrazines which may be additives within the HEETS and also a residual product within the tobacco from the curing process.

3.10.17 m/z 110: Catechol, hydroquinone, resorcinol, 5-methylfurfural, 2,4-heptadienal, etc.

Catechol, hydroquinone, resorcinol, 5-methylfurfural, 2,4-heptadienal, 2,3-dimethyl-2-cyclopenten-1-one, 3,4,5-trimethylpyrazole, 2-methyl-1,6-heptadiene, 2-ethyl-5-methylfuran, 3-isopropylcyclopentene, 2,3,5-trimethylfuran, 2-propylfuran, 2-acetylfuran and 3-MCPD have an m/z of 110. In Figure 16, HEETS and tobacco show a strong peak around 325^{o}C followed by a shoulder after 400^{o}C. Kānuka is somewhat different, having two peaks, the larger at 400^{o}C corresponding to the shoulder seen in tobacco and HEETS and the smaller at 460^{o}C. Catechol, hydroquinone and resorcinol are isomers of benzenediol. The decomposition of guaiacol leads to the production of catechol (Flamini et al., 2007). Chlorogenic acid is a precursor for catechol and hydroquinone formation (Bassilakis et al., 2001). From tobacco, Senneca et al. (2007) reported catechol release between 180°C to 400°C. McGrath et al. (2009) found for tobacco, 97% of catechol and 96% of hydroquinone was released below 350°C, while 3% of catechol and 4% of hydroquinone was released between 350°C to 600°C. They also found 59% of resorcinol was detected in tobacco vapour below 350°C and 41% was detected from 350°C to 600°C. Resorcinols relative percentage is significantly different compared to catechol and hydroquinone, and it was suggested that resorcinol is produced from the primary decomposition of tobacco as well as from the breakdown of other components (McGrath et al., 2009). At 600°C catechol decomposes to carbon monoxide, “benzene, phenol, cyclopentadiene, acetylene, 1,3-butadiene, and ethylene” (Moldoveanu, 2019). The FDA (2019) defined catechol as a carcinogen. Kibet et al. (2012) detected catechol from 250°C to 450°C with a peak around 325°C when heating lignin. Luo et al. (2017) found catechol while heating pine wood from 400°C to 550°C and noticed a peak in production at 450^{o}C. Kumagai et al. (2015) analysed the relative abundance of m/z 110 in Japanese cedar heated from 100^{o}C to 600^{o}C, and found a single peak increasing from 200^{o}C, peaking at 400^{o}C, and decreasing rapidly after. They attributed this peak to the production of catechol. Lower temperatures were excluded from their research.

Hydroquinone was found by Pieraccini et al. (2008) with GC/MS analysis of smoke from Italian cigarettes. At 500°C hydroquinone decomposes to benzoquinone (Moldoveanu, 2019). Bentley et al. (2020) found 5.71 µg/HEET of hydroquinone was produced from heating HEETS to 350^{o}C. Fine et al. (2001) burned 21 different wood species and found catechol, hydroquinone and resorcinol were present in all wood smoke. Philip Morris Products S.A. analysed vapour produced by HEETS at 350^{o}C and found a catechol production of 14.00 µg/HEET, a hydroquinone production of 6.55 µg/HEET and resorcinol was below the level of detection. Schaller et al. (2016) and St. Helen et al. (2018) found corresponding research.

The compound 5-methylfurfural was investigated by Bassilakis et al. (2001), who conducted a TG-FTIR of tobacco and observed a low concentration single peak for the concentration around 225°C. 5-methylfurfural is a breakdown product from glucose (Fischer et al., 2013). St. Helen et al. (2018) found HEETS had 5-methylfurfural production of 0.995µg/HEET. Bentley et al. (2020) found it was much higher at 14.2 µg/HEET. Gu et al. (2013) found 5-methylfurfural in poplar wood heated to 600^{o}C. Wang et al. (2020) found 5-methylfurfural when heating pine to 500^{o}C.

The flavourant 2,4-Heptadienal can be added to tobacco products (Paschke et al., 2002). Ding et al. (2013) identified 2,4-heptadienal as a free aroma compound in tobacco. Baker and Bishop (2004) heated pure 2,4-heptadienal in oxic conditions, at 900°C, and found that 98.3% of 2,4-heptadienal was transferred to vapour, and 0.4% was converted to benzaldehyde. 2,4-Heptadienal is added as a flavouring to some HEETS (Philip Morris International, 2018), but it is unclear if it has been added to the Amber Label HEETS used in this experiment. 2,4-Heptadienal may have also been used as a flavouring in the tobacco sample, although the company did not list the exact flavourings added. The HEETS sample has 0.05% added flavourings and the tobacco sample has 0.0006% added flavourings (Ministry of Health, 2019), so even if it were added it would not have a significant impact.

The compounds 2,3-dimethyl-2-cyclopenten-1-one and 3,4,5-trimethylpyrazole were noticed by Pieraccini et al. (2008) in Italian cigarette smoke. Yin et al. (2015) identified 2,3-dimethyl-2-cyclopenten-1-one in flue cured tobacco heated to 250°C and stated it had a fresh aroma. Moldoveanu (2019) found 2,3-dimethyl-2-cyclopent-1-one when heating glucose and glutamic acid to 750°C. Bentley et al. (2020) found HEETS at 350^{o}C produced 1.05 µg/HEET of 2,3-dimethyl-2-cyclopenten-1-one.

3-MCPD is a potentially harmful compound as it is possibly carcinogenic (St. Helen, 2018; Bentley et al., 2020; Baer et al., 2010; and FAO/WHO, 2007). St. Helen et al. (2018) compared HEETS at 350^{o}C and burning 3R4F cigarettes and found that HEETS produced 9.94 µg/HEET 3-MCPD and cigarettes produce 5.93 µg/stick 3-MCPD. Higher concentrations were found by Bentley et al. (2020), who obtained 16.1 µg/HEET 3-MCPD for HEETS and 8.21 µg/stick 3-MCPD for 3R4F cigarettes. The differences are likely to be due to experimental methods, but both agree that HEETS at 350^{o}C produce 1.5 to 2 times the amount of 3-MCDP as burning 3R4F cigarettes. 3-MCPD has also been detected in smoked food and smokehouses (Baer et al., 2010; Jira, 2010; FAO/WHO, 2007; and Reece, 2005). 3-MCPD has only been found in “cold smoking” and the amount of 3-MCPD detected was dependant on wood type and smoking time (Reece, 2005, and FAO/WHO, 2007). Cold smoking refers to the smokehouse, which is kept at near ambient temperatures, not the generation temperature of the smoke itself. Hot smoking means the smokehouse is kept at temperatures that also cook the food. (Reece, 2005, and Baer et al., 2010). It was proposed that cellulose breaks down and releases 3-hydroxyacetone which is a precursor for 3-MCPD formation (Baer et al., 2010).

The remaining compounds have been investigated to lesser extents. Liu et al. (2015) identified 3,4,5-trimethylpyrazole in oriental tobacco leaves. The formation of 3,4,5-trimethylpyrazole is due to the Maillard reaction (Yaylayan & Haffenden, 2003). Moldoveanu (2010) studied the smoke from a burning tobacco cigarette and found 0.02% 2,3-dimethyl-2-cyclopent-1-one, 0.09% 2-methyl-1,6-heptadiene,

0.25% 2-ethyl-5-methylfuran, 0.11% 2,3,5-trimethylfuran, 0.03% 3-isopropylcyclopentene. Gu et al. (2013) noticed the production of 2,3,5-trimethylfuran and 2-propylfuran while heating poplar wood to 600^{o}C. At 600^{o}C the concentration of 2-propylfuran was significantly greater compared to catechol, 5-methylfurfual, and 2,3,5-trimethylfuran. Park et al. (2017) found 2-ethyl-5-methyfuran was released while heating larch wood to 250^{o}C, and claimed it was produced from the decomposition of hemicellulose. 2-Acetylfuran is a natural aroma compound from tobacco (Ding et al., 2013). Branca et al. (2003) found 2-acetylfuran, 5-methylfurfural, and 2,3-dimethyl-2-cyclopent-1-one in beech heated to 525^{o}C.

In summary, there are many influences on the curves shown in Figure 16. For all the biomass it is likely that catechol and hydroquinone dominate the first peak, and resorcinol dominates the second. 5-methylfurfural and 2-ethyl-5-methylfuran would contribute to the slight increasing absolute intensity before the largest peak for all biomasses. 2,3,5-Trimethylfuran, 2,3-dimethyl-2-cyclopenten-1-one, 2-acetylfuran and 3-MCPD would have a slight contribution to all biomasses but at unknown temperatures. 3,4,5-Trimethylpyrazole, 2-methyl-1,6-heptadiene, 3-isopropylcyclopentene will have small contributions to the HEETS and tobacco curves but at unknown temperatures. 2-Propylfuran will influence the kānuka curve at unknown temperatures.

3.10.18 m/z 124: Guaiacol, mequinol, 3-methoxyphenol and 6-methyl-3,5-heptadien-2-one

Guaiacol, mequinol, 3-methoxyphenol and 6-methyl-3,5-heptadien-2-one, have an m/z of 124. Figure 16 shows that all three biomasses have significant peaks above 250^{o}C. The main peak for HEETS and tobacco around 340^{o}C is a shoulder in kānuka. Kānuka then has two prominent peaks at 400^{o}C and 460^{o}C, between which tobacco has a well-defined shoulder and HEETS has a lesser shoulder. The two tobacco samples also have a substantially lower peak around 200^{o}C which is absent from kānuka. The first compound listed above, guaiacol is well known, and has the isomers mequinol and 3-methoxyphenol. All three are formed from the thermal decomposition of lignin (Czegeny et al., 2016). Further decomposition of guaiacol produces catechol and mequinol decomposes to phenol (Wang et al., 2019). Guaiacol and the last compound on the list, 6-methyl-3,5-heptadien-2-one are flavourings which may be added in HEETS (Philip Morris International, 2018). It is unclear if these flavourings have been added to the HEETS used in this research. 6-Methyl-3,5-heptadien-2-one is a common tobacco flavour ingredient (Rodgman & Perfetti, 2013). It is also unclear what flavourings are used in the tobacco sample.

Guaiacol has been detected in tobacco and tobacco smoke (Purkis et al., 2011). McGrath et al. (2009) heated tobacco to 600°C and found that 95% of guaiacol was released below 350°C. Guaiacol has been found in kānuka vapour heated at 480^{o}C (Zhang et al., 2020). Wang et al. (2018) identified guaiacol when heating ginkgo to 400°C. Wang et al. (2019) heated ginkgo from 450^{o}C to 750^{o}C and found the concentration of guaiacol, relative to all compounds in the produced vapour, decreased from 19.46% to 5.85% and mequinol decreased from 3.48% to 0.00%. Sebio-Punal et al. (2012) heated *Castannea sativa* and *Pinus pinaster* and found guaiacol intensity increasing from 200^{o}C, peaking at 350^{o}C, and then decreasing to 400^{o}C. Hua et al. (2016) heated poplar lignin and fir lignin to 600^{o}C and measured the relative composition of the vapour produced. Poplar lignin released 3.20% guaiacol and fir lignin released 13.07% guaiacol. Kibet et al. (2012) heated lignin and noticed the production of guaiacol from 200°C, peaking at 400°C, and decreasing till 600°C. From 300°C to 900°C in anoxic conditions, 99.79% of guaiacol is vaporised and 0.21% degrades to 2-methylphenol (Czegeny et al., 2016). Guaiacol, mequinol, and 3-methoxyphenol have been identified in tobacco cigarettes (Stabbert et al., 2017, and Moldoveanu et al., 2008). 3-Methoxyphenol has not been reported in wood vapour but is likely to be present in a small quantity. Moldoveanu et al. (2018) ignited 10 different cigarettes and found the smoke contained an average of 1.72 µg/cigarette guaiacol, 0.49 µg/cigarette mequinol and 0.30 µg/cigarette 3-methoxyphenol. In summary, Figure 16 will be dominated by the production of guaiacol, with the two

main peaks in each biomass indicating to generalised reaction pathways, the higher being from lignin and the lower being from cellulose or a lower temperature lignin mechanism.

3.10.19 m/z 128: Naphthalene, furaneol and dihydromaltol

Naphthalene (NAP), furaneol and dihydromaltol have an m/z 128. For Figure 16, HEETS and tobacco have a comparatively low absolute intensity to kānuka, which shows a large single peak at 400^{o}C. However, tobacco and HEETS do show a low intensity plateau around 300^{o}C to 350^{o}C, which appears to coincide with a low shoulder in kānuka. Naphthalene is the smallest of the polycyclic aromatic hydrocarbons (Table 4) and is produced from the decomposition of cellulose (Czegeny et al., 2009). Naphthalene has been identified as potentially carcinogenic (Charles et al., 2007, and Bailey et al., 2016). Naphthalenes odour profile has been described as "spicy, smoke, cold ashes" (Varlet et al., 2006). Because it is indicative of the presence of other PAHs, naphthalene has been well studied. Hofer et al. (2019) determined that HEETS contain 0.0116 µg/HEET of naphthalene. Ding et al. (2005) found naphthalene concentration in 100% reconstituted tobacco was 230 ng/cigarette, and other tobaccos and tobacco blends ranged from 630 ng/cigarette to 1055 ng/cigarette. Czegeny et al. (2009) heated Virginia and burley tobacco with a heating rate of 400 K/s and analysed the production of naphthalene. Minimal naphthalene was detected below 600^{o}C, but was detected when heated directly at 900^{o}C. There was also minimal naphthalene found when heating successively from 450^{o}C up to 900^{o}C. They determined that the naphthalene precursors are degraded before 450^{o}C. The fast pyrolysis of tobacco experimental results of Liu et al. (2013) and Adam et al. (2009) correspond with Czegeny et al. (2009). Liu et al. (2013) also investigated slow pyrolysis of tobacco stems at 20K/min. They found naphthalene was released in tobacco vapour from 400^{o}C to 700^{o}C. In ignited poplar, naphthalene was found to be the third most prominent polycyclic aromatic hydrocarbon (PAH) in the smoke produced (Skrbic et al., 2018).

Furaneol and dihydromaltol have been identified in toasted Spanish *Quercus pyrenaica*, French oak, American oak, false acacia, cherry wood, chestnuts wood, and ash wood (de Simon et al., 2010, de Simon et al., 2009, Cullere et al., 2013, and Guillen & Manzanos, 2005). Furaneol has a "toasty carmel (*sic*)" odour (Cullere et al., 2013). Dihydromaltol is "responsible for "toasty caramel (*sic*)" and "honey" odors" (de Simon et al., 2010). Furaneol and dihydromaltol are formed during heating by the Maillard reaction (Moreno-Arribas & Polo, 2008, and de Simon et al., 2010). These odour compounds have not been reported in tobacco literature.

In conclusion, the large peak, in Figure 16, only experienced by kānuka is probably these compounds. Naphthalene is only minimally present due, most likely, to the slow heating rate reported here, and that the precursors have either decomposed or volatilised away before the temperatures needed to form naphthalene have been reached.

3.10.20 m/z 132: Cinnamaldehyde, diammonium phosphate, ethylstyrene, etc.

Cinnamaldehyde, diammonium phosphate, 1-methyl-4-(1-methylethenyl)benzene, ethylstyrene, n-methylbenzofuran, and 1-methyl-1-propenylbenzene have an m/z of 132. Figure 16 shows tobacco and HEETS have a small peak around 170^{o}C, and all the biomass experience flattened peaks between 300^{o}C and 500^{o}C. Which appears to be a combination of two peaks, the first between 350^{o}C to 400^{o}C is dominant in kānuka and the second around 450^{o}C is dominant in tobacco. For HEETS both peaks have similar intensity.

Cinnamaldehyde is a decomposition product and is also a common flavourant (Rodgman & Perfetti, 2013). Khachatryan et al. (2016) studied the thermal decomposition from 400°C to 800°C of cinnamyl alcohol, which is found in lignin. They found that the production cinnamaldehyde was favoured at 400°C and were able to detect cinnamaldehyde at 700°C but not 800°C. Pyrolysis products of cinnamaldehyde include phenol, allylbenzene, and benzaldehyde (Wang & Luo, 2017, and Nystoriak et al., 2018). Cinnamaldehyde

can be added to tobacco products to provide a cinnamon flavour, when added it will start decomposing from 210^{o}C (Nystoriak et al., 2018). The addition of cinnamaldehyde has been "Generally Recognised as Safe" (GRAS) by the FDA and FEMA (Cocchiara et al., 2005). Although the GRAS rating is more for food or cosmetic products and does not evaluated inhalation risks (Clapp et al., 2019). Nystoriak et al. (2019) reported that heating and inhalation of cinnamaldehyde could be potentially cardiotoxic. Cinnamaldehyde is added to HEETS as a flavour ingredient (Philip Morris International, 2018). It is unclear if cinnamaldehyde has been used in the Amber Label HEETS or RYO tobacco for this research.

Diammonium phosphate is added to tobacco to enhance flavour and reduce irritation (Stavanja et al., 2008). Marcilla et al. (2015) studied the effect of diammonium phosphate on the thermal decomposition of tobacco. Marcilla et al. (2015) suggested that at 157°C diammonium phosphate produced ammonia and ammonium dihydrogen phosphate. They observed a large weight loss event, peaking at 216°C, from the degradation diammonium phosphate. Which between 170°C to 216°C, produced ammonia and phosphoric acid. From 240°C to 540°C phosphoric acids were dehydrated, and phosphorus pentoxide was formed. By 658°C no diammonium phosphate was found in the tobacco as it had degraded or vaporised. They also found the addition of diammonium phosphate lowered the decomposition temperatures of hemicellulose, cellulose, and lignin. Baker et al. (2006) observed three weight loss events during the heating of diammonium phosphate, these were two small events from 140°C to 280°C and 340°C to 370°C, as well as a larger event from 600°C to 760°C. It is unclear if diammonium phosphate has been added to HEETS or tobacco used in this research. The HEETS used in this research has 0.05% added flavourings and the tobacco used in this research has 0.0006% added flavourings (Ministry of Health, 2019).

1-Methyl-4-(1-methylethenyl)benzene has been found in tobacco vapour but not the tobacco plant (Rodgman & Perfetti, 2013). It was detected by Pieraccini et al. (2008) from the vapour produced when burning Italian cigarettes.

Ethylstyrene, n-methylbenzofuran, and 1-methyl-1-propenylbenzene have been detected in the smoke from wood fires (Johnson et al., 2013; International Maritime Organization, 2001; Buist et al., 2012; and, Chitsamphandhvej et al., 2017). 2-Methylbenzofuran is commonly utilized as a flavour compound in liquid smoke used for food smoking (Nollet et al., 2008). It is a holocellulose decomposition product, and its formation is more prominent in oxic environments (Stockwell et al., 2015).

The m/z 132 ion chromatogram (Figure 16) is also known to contain many fragments. Xylose is a component of hemicellulose found in tobacco and wood (Akpinar et al., 2011, and Cheng et al., 2019). Nakahara et al. (2014) found while heating beech wood, xylose units fragment off larger compounds. Xylose fragments could contribute to the peaks in Figure 16, and other fragments are also present. While heating *Acacia saligna* biochar, Yang (2012) found m/z 132 was a common fragment ion produced from the breakdown of carboxylic acids by the McLafferty rearrangement. Takada et al. (2004) and Mammela (2001) found that m/z 132 was a common fragment ion for many compounds in sugi and beech respectively, but neither was able to describe the structure or formula for the fragments at m/z 132, nor did they report the concentrations and temperature ranges that these m/z 132 compounds exist.

In summary, given the peaks at m/z 132 (Figure 16) are common to both kānuka and the tobaccos, it is unlikely they are additives that are not found naturally in the kānuka, which rules out diammonium phosphate. The peaks are therefore cinnamaldehyde, the other named compounds, xylose fragments and other unnamed fragments. As expected, when the ion to charge ratio increases it becomes harder to attribute peaks to compounds in Figure 16.

3.10.21 m/z 136: Anisaldehyde, phenylacetic acid, 2,3-diethypyrazine, benzyl formate, etc.

Anisaldehyde, phenylacetic acid, 2,3-diethylpyrazine, 2,3,5,6-tetramethylpyrazine, benzyl formate, 3-phenyl-1-propanol, limonene, 2,5-dimethyl-3-methylene-1,5-heptadiene, 2-ethyl-3,5-dimethylpyrazine and terpinene have an m/z of 136. In Figure 16, tobacco and HEETS have a small peak around 180^{o}C not showed by kānuka. HEETS has a larger peak at 340^{o}C and tobacco and kānuka have a larger peak at 390^{o}C., although each seems to have a shoulder at the other values. Of the above compounds, anisaldehyde is added to HEETS as a flavour ingredient (Philip Morris International, 2018). Anisaldehyde has been detected in the tobacco plant and vapour (Rodgman & Perfetti, 2013). In a study on tobacco ingredient heating, Baker and Bishop (2004) found that 99.3% anisaldehyde will volatilise by 400°C. They also found that 0.3% will convert to anisyl alcohol, 0.2% will convert to mequinol and 0.1% will convert to anisole. Stotesbury et al. (2000) also found when heating anisaldehyde from 200°C to 400°C, it volatilises but a small amount converts to methyl-4-hydroxy benzoate and methyl-4-methoxy benzoate. Flamini et al. (2007), analysed acacia, chestnut, cherry, European ash, American ash, Spanish oak, American oak, and French oak, and was only able to detect anisaldehyde in cherry wood. De Simon et al. (2009) analysed acacia, chestnut, cherry, mulberry and oak, and only detected anisaldehyde in acacia, chestnut, and oak. They concluded the low quantities of anisaldehyde make it difficult to detect (de Simon et al., 2009).

Phenylacetic acid has been detected in the tobacco plant and vapour (Rodgman & Perfetti, 2013). It is synthesised by the tobacco plant to regulate growth and development (Sumayo et al., 2018), and has been identified as one of the main odour compounds in Scots pine (Schreiner et al., 2018). Blazso et al. (2018) analysed the vapour produced from heating phenylacetic acid to 300°C and found the majority consisted of phenylacetic acid, but with 4.67% converting to benzaldehyde and 0.4% becoming benzoic acid, phenol, benzyl alcohol, and 2,3-diphenylmaleic anhydride. Baker and Bishop (2004) found at 900°C in oxic conditions, 51.6% of phenylacetic acid vaporises and the remainder decomposes to a range of products including benzaldehyde, ethylphenyl acetate, diphenylethanone, benzoic acid, dibenzyl, benzyl phenylacetate, toluene, and acetophenone. Phenylacetic acid is added as a flavouring to HEETS (Philip Morris International, 2018). Schreiner et al. (2018) describes phenylacetic acid as having a “honey-like” odour.

2,3-Diethylpyrazine and 2,3,5,6-tetramethylpyrazine are present in tobacco and also can be added as they provide a “nutty, coffee, popcorn, cocoa, chocolate, earthy and baked potato” flavour and smell (Coggins et al., 2011). Baker and Bishop (2004) heated pure samples of these compounds to 900°C in the presence of oxygen. They found 99.6% of 2,3-diethylpyrazine will vaporise and 0.4% will be converted to methylisopropylpyrazine. They also found that 2,3,5,6-tetramethylpyrazine does not degrade at 900°C. Philip Morris International (2018) have listed 2,3,5,6-tetramethylpyrazine as an added flavouring to HEETS, but it is unclear if it is used in the Amber label HEETS used here.

Benzyl formate is a natural component of the tobacco plant (Rodgman & Perfetti, 2004). When benzyl formate is heated to 300°C the majority of the vapour contains benzyl formate, with 1.64% converting to benzyl alcohol and 0.25% convert to benzaldehyde (Blazso et al., 2018). 3-Phenyl-1-propanol has been detected in the tobacco plant and vapour (Rodgman & Perfetti, 2013). In oxic conditions, at 900°C, 90.4 % of 3-phenyl-1-propanol will transfer to vapour. The decomposition products of 3-phenyl-1-propanol include phenylpropanal, benzaldehyde, styrene, phenylpropenal, phenyl vinyl ketone, and acetophenone (Baker & Bishop, 2004).

Limonene has been detected in the tobacco plant and vapour (Rodgman & Perfetti, 2013). Chida et al. (2004) found limonene in the vapour produced from heating flue cured tobacco to 240°C and described it as having a “fresh, light, sweet citrusy odor”. Cardoso and Ataide (2013) heated tobacco dust to 400°C and detected limonene in the vapour produced. Yildiz and Ceylan (2019) found limonene was produced

during the thermal decomposition of tobacco waste at 600°C. Sugi tree leaves were found to have limonene as a natural component and as part of the smoke (Yamada & Yatagai, 2007). Maleknia et al. (2009) found limonene, terpinene, pinene, and myrcene in pyrolysed eucalyptus leaves and in small eucalyptus branches. It is unknown if these compounds are also present in the tree trunk. It is unlikely that kānuka wood contains limonene, terpinene, pinene, and myrcene as they are all odorous compounds. Pieraccini et al. (2008) lit Italian cigarettes and noted the presence of limonene and 2,5-dimethyl-3-methylene-1,5-heptadiene in the smoke produced. Nystoriak et al. (2018) identified limonene as potentially cardiotoxic. The last two compounds, listed at the beginning of this section, 2-ethyl-3,5-dimethylpyrazine and terpinene, are added as flavourings to HEETS (Philip Morris International, 2018). However, the flavour ingredients added the HEETS and tobacco samples in this research is unknown. In summary, the lower peaks around 180^{o}C, which are present only in the tobacco and HEETS are likely to be one of the many additives mentioned here. The higher peaks seem to be an amalgam in differing proportions of three compounds that are all present in kānuka and the two tobaccos, which probably rules out the odorous compounds as they are not likely to be present in kānuka volatiles. It is not possible to draw any further conclusions.

3.10.22 m/z 138: Creosol, 3,4-dihydroxybenzaldehyde, 2,3-dihydroxybenzaldehyde, etc.

Creosol, 3,4-dihydroxybenzaldehyde, 2,3-dihydroxybenzaldehyde, m-hydroxybenzoic acid, o-hydroxybenzoic acid, and p-hydroxybenzoic acid have an m/z of 138. Figure 16 shows that all three biomasses have peaks between 250^{o}C to 500^{o}C but proportioned differently. HEETS has a single peak around 350^{o}C. Tobacco has a similar peak followed by a shoulder around 400^{o}C. Kānuka has a similar shape to tobacco, but at a much higher absolute intensity and slightly higher temperatures with a peak at 390^{o}C and shoulder at 440^{o}C. Creosol has been well-studied. Wang et al. (2019) claims that the breakdown of 4-ethyl-2-methoxyphenol in lignin causes the production of creosol from 500°C to 700°C. Creosol forms from the decomposition of many compounds including 2-methoxy-4-(1-hydroxypropyl)phenol and homovanillic acid (Takada et al., 2004). In fast pyrolysis, Guo et al. (2019) detected the release of creosol from tobacco stalk lignin at 300°C, peaking at 600°C, and with a smaller production at 900°C. Creosol and 3,4-dihydroxybenzaldehyde have been identified in tobacco cigarette smoke (Stabbert et al., 2017). Chen et al. (2021) has identified cresol and 2,3-dihydroxybenzaldehyde in the vapour produced from heating kānuka at 335°C. Zhang et al. (2020) found the production of creosol from kānuka increased peaked at 380^{o}C, which corresponds with Figure 16, where the slight difference is because Figure 16 records temperature every 0.1^{o}C during heating while Zhang et al. (2020) analysed set temperatures between 180^{o}C and 480^{o}C. Luo et al. (2017) detected creosol when heating pine wood from 400°C to 550°C. Wang et al. (2018) observed creosol when heating ginkgo at 400°C. Creosol has been described as having a spicy, clove, vanilla and phenolic odour and flavour (Czoli et al., 2019), and has been listed as an added flavouring in HEETS (Philip Morris International, 2018), although it is unclear is this flavouring has been added to the HEETS or tobacco used in this research.

The isomers of dihydroxybenzaldehyde and hydroxybenzoic acid are likely to be in kānuka, HEETS and tobacco. Hydroxybenzoic acid is a lignin derived compound and is expected to be present in higher quantities in biomass with higher lignin content (Muller-Tautges et al., 2016, and Wan et al., 2019). o-Hydroxybenzoic acid plays an important role in plants defence mechanism against pathogens (Chong et al., 2001). Chen et al. (2018) found p-hydroxybenzoic acid and o-hydroxybenzoic acid in tobacco leaves. Nolte et al. (2001) observed the production of p-hydroxybenzoic acid in oak, eucalyptus, and pine smoke. Christensen et al. (2017) was able to detect hydroxybenzoic acid and creosol in aspen and oak heated to 500^{o}C. In conclusion, as creosol is known as one of the most abundant breakdown products in lignin, it is

expected to dominate the ion chromatogram for m/z 138 in Figure 16. Contributions will also be present from dihydroxybenzaldehyde and hydroxybenzoic acid but the peaks attributable are unknown.

3.10.23 m/z 152: Vanillin, 4-ethylguaiacol, methyl salicylate, citral, acenaphthylene and 2,5-dimethoxytoluene

Vanillin, 4-ethylguaiacol, methyl salicylate, citral, acenaphthylene and 2,5-dimethoxytoluene have an m/z of 152. From the shape of the curves in Figure 16, all biomasses show differing intensity between 250^{o}C to 500^{o}C. Within this, HEETS has one significant peak, tobacco has 2 peaks and kānuka has 3 over lapping peaks. All the biomasses have a peak of different intensity at 340^{o}C. Kānuka has a second peak at 390^{o}C, and kānuka and tobacco have another peak at 440^{o}C.

Vanillin has been detected in tobacco smoke from 200°C (Lemus et al., 2007). Vanillin occurs naturally in tobacco and can also be an added ingredient in tobacco products (Lemus et al., 2007, and Rodgman & Perfetti, 2013). Chen et al. (2021) found vanillin in the vapour produced from heating kānuka wood chips to 335°C. Wang et al. (2018) identified vanillin while heating ginkgo to 400°C. Stotesbury et al. (2000) found that at 200°C vanillin was transferred to vapour without degrading, and at 800°C some of the vanillin was degraded to phenol, 2-methoxyphenol, o-cresol, 2-hydroxy benzaldehyde and toluene. Wang et al. (2016) claims that vanillin starts decomposing around 650°C. Baker and Bishop (2004) found at 900°C in oxic conditions, 99.6% of vanillin vaporises, 0.2% converts to guaiacol, 0.1% converts to veratraldehyde, and 0.1% converts to piperonal. Vanillin is the main pyrolysis product from vanilla absolute, which can be added to tobacco products (Baker & Bishop, 2005). Vanillin is listed as a flavour ingredient used in HEETS, but it is unknown if it has been added to Amber label HEETS (Philip Morris International, 2018). It is unclear what specific flavourings have been added to the tobacco and HEETS used in this experiment.

4-Ethylguaiacol has been detected in the tobacco plant and vapour (Rodgman & Perfetti, 2013). Pieraccini et al. (2008) detected 4-ethylguaiacol in the smoke produced from burning Italian cigarettes. Zhang et al. (2020) reported 4-ethylguaiacol was present in kānuka vapour heated to 480^{o}C. Luo et al. (2017) found 4-ethylguaiacol from 400°C to 550°C when heating pine wood. 4-Ethylguaiacol is produced from the decomposition of lignin (Mullery et al., 2017). Kibet et al. (2012) heated lignin and noticed the production of 4-ethylguaiacol from 250°C, peaking at 400°C, and decreasing till 550°C. Mullery et al. (2017) heated 4-ethylguaiacol in anoxic conditions and found that it decomposes from 350°C to 600°C. They also found that methane and ethane are produced above 400°C, ethylene, propane, propylene, and propadiene are produced above 450°C, carbon monoxide and 1,3-butadiene are produced above 500°C and benzene is produced above 550°C. Blazso et al. (2018) found that at 300°C only 0.33% of 4-ethylguaiacol will decompose to 4-vinylguaiacol, with the rest vaporising. Baker and Bishop (2004) heated 4-ethylguaiacol to 900°C in oxic conditions and found 97.5% of 4-ethylguaiacol vaporises, with the rest decomposing to vinylmethoxyphenol, hydroxymethoxyacetophenone, and methylguaiacol. The aroma 4-ethylguaiacol was described as smoky and woody (Wang et al., 2018). 4-Ethylguaiacol is listed as an added flavouring in HEETS (Philip Morris International, 2018). It is unclear if it's added to the Amber label HEETS used here.

Methyl salicylate has been detected in the tobacco plant and vapour (Rodgman & Perfetti, 2013). Methyl salicylate is formed from salicylic acid and is released from the tobacco plant as a defence response (Huang et al., 2003). Staub et al. (2011) noted that methyl salicylate was not present in Chinese weeping cypress wood smoke or flaky juniper wood smoke. With oxygen present, at 900°C, 98.6% of methyl salicylate will vaporise, 1.1% will convert to ethyl salicylate and 0.3 % will convert to phenol (Baker & Bishop, 2004). Methyl salicylate gives tobacco a wintergreen flavour and provides a "local anaesthetic effect" (Kostygina & Ling, 2016). Methyl salicylate can be added to menthol tobacco products, although

small amounts have been found in regular tobacco products (Chen et al., 2010). Merckel et al. (2006) analysed 55 different cigarette packs and methyl salicylate was only able to be detected in 1 pack. Philip Morris International (2018) state methyl salicylate and citral are added flavourings, but do not disclose which products they are added to. It is unlikely that that methyl salicylate will be added to the HEETS or tobacco used in this research as they were not advertised as menthol flavoured. It is unclear if citral has been added to HEETS or tobacco used in this experiment.

Acenaphthylene has been found in tobacco and wood smoke (Skrbic et al., 2018; Paschke et al., 2016; and Rodgman & Cook, 2009). Acenaphthylene contributes to 9.8% of the total PAHs in ignited tobacco smoke (Lu & Zhu, 2007). Tsekos et al. (2020) was only able to detect acenaphthylene production from poplar after heating to 700^{o}C. Auer et al. (2017) found the acenaphthylene production from HEETS at 350^{o}C was 1.9 ng/HEET and from burning cigarettes was 235 ng/cigarette. Ding et al. (2005) found for burning 100% reconstituted tobacco the acenaphthylene concentration was 54 ng/HEETS and other tobaccos and tobacco blends ranged from 140 ng/cigarette to 210 ng/cigarette. The higher production in cigarettes is most probably due to the higher temperature at which smoke was produced at the burning interface and is not an added ingredient in HEETS. The last compound listed at the top of this m/z 152 section, 2,5-dimethoxytoluene, was observed by Chen et al. (2021) in kānuka wood chip vapour at 335°C. In summary, it is clear that only vanillin and 4-ethylguaiacol will be present in quantities large enough to influence the m/z 152 ion chromatogram. It is not known which peak refers to each compound. In kānuka there are conceivably three overlapping peaks indicating more than one mechanism of production for one or other of the compounds.

3.10.24 m/z 154: Syringol, eucalyptol, geraniol, isopulegol, linalool and acenaphthene

Syringol, eucalyptol, geraniol, isopulegol, linalool and acenaphthene have an m/z of 154. Figure 16 shows an order of magnitude difference in detection intensity, with kānuka the larger. HEETS and tobacco have a small peak at 340^{o}C at which kānuka has a shoulder with its peak at 400^{o}C.

Syringol is a well-known decomposition product of lignin, and provides a smoky flavour (Wu et al., 2016, and Kaur et al., 2018). Syringol has been detected in the tobacco plant and vapour (Rodgman & Perfetti, 2013). Chen et al. (2021) found syringol was produced when heating kānuka wood chips to 335°C. de Macedo et al. (2018) found syringol in the vapour produced from heating eucalyptus to 275^{o}C. Kibet et al. (2012) heated lignin and noticed the production of syringol from 200°C, peaking around 425°C and decreasing till 700°C. Kawamoto (2017) and Branca et al. (2003) obtained similar results. These authors all correspond with kānuka in Figure 16, with the differences in peak attributable to variations in experimental materials and methods. In Figure 16 the kānuka peak ends around 475^{o}C instead of 700^{o}C because plant material contains a limited amount of lignin, while the other research papers used excess lignin. At 600°C in anoxic conditions the only decomposition product from syringol was benzofuran (Akazawa et al., 2015).

Eucalyptol, geraniol, isopulegol and linalool are all fragrant plant extractives and are listed as additives to HEETS by Philip Morris International (2018), and to other tobacco products (Lisko et al., 2014, and Reger et al., 2018). The flavour ingredients added to Amber label HEETS and tobacco used in this research is unknown. Eucalyptol can be extracted from eucalyptus wood (Zhang et al., 2008), and has been detected in tobacco plants and tobacco smoke (Rodgman & Perfetti, 2013). Geraniol was able to be extracted from *Mydocarpus lanceolatus* wood but not *Mydocarpus fraxinifolius* or *Mydocarpus viellardii* (Lebouvier et al., 2014). Zhu et al. (2013) was able to detect geraniol in untreated camphor wood. Linalool was found in brutian pine, Brazilian rosewood, *Mydocarpus lanceolatus* and *Mydocarpus viellardii* (Guler, 2019; Zellner et al., 2006; and Lebouvier et al., 2014). The odour of linalool has been described as “sweet, citric,

herbaceous" (Zellner et al., 2006). They have not been investigated in kānuka. Another factor is that the flavour compounds have been identified in wood extract, and not wood smoke.

The last compound in them/z 154 list above, acenaphthene, was found by Auer et al. (2017) to be present at 350^{o}C in HEETS at 145 ng/HEET acenaphthene compared to 49 ng/cigarette from conventional burning cigarettes. Ding et al. (2005) found acenaphthene while burning reconstituted tobacco at 70 ng/cigarette, and while burning other tobacco and tobacco blends ranged from 90 ng/cigarette to 200 ng/cigarette Acenaphthene has also been found in wood smoke at unknown concentrations (Tiwo et al., 2019, and Alcanzare, 2006). Szramowiat-Sala et al. (2019) found, in combusted Norway spruce, that acenaphthene and benzo(a)pyrene were the 2 most dominant polycyclic aromatic hydrocarbons produced. In summary, syringol will dominate the m/z 154 ion chromatogram (Figure 16) due to its prevalence as a lignin breakdown product, which is produced in far greater quantities from kānuka then from the tobacco and HEETS which are plant leaf and stalk product. It is also likely due to the peak and shoulder that there are two mechanisms for the formation of syringol.

3.10.25 m/z 162: Nicotine, anabasine, levoglucosan, methyl cinnamate and 6-methoxy-3-methylbenzofuran

Nicotine, anabasine, levoglucosan, methyl cinnamate and 6-methoxy-3-methylbenzofuran have an m/z of 162. Figure 16 shows distinct differences between the two tobaccos and kānuka. HEETS and tobacco have peaks at 150^{o}C and 190^{o}C respectively which are absent from kānuka. Above 250^{o}C, all three biomasses exhibit peaks. Kānuka appears to have a shoulder at around 340^{o}C a peak at 390^{o}C and another shoulder at 450^{o}C. Both tobacco and HEETS appear to have a similar spread of peaks. Detection of m/z 162 peters out by 500^{o}C.

Of the above compounds, nicotine is the most controversial. Nicotine is rapidly absorbed into the body and causes the brain to release dopamine, which provides a positive emotional response. The positive emotional response can cause nicotine addiction (Benowitz, 2010). However, there are also side effects. Mishra et al. (2015) claims that nicotine contributes to "an increased risk of cardiovascular, respiratory, and gastrointestinal disorders". The FDA (2019) has stated nicotine is a reproductive or developmental toxicant and is addictive. Philip Morris Products S.A. (2017) claim that HEETS have a nicotine production of 1.29 mg/HEET when heated to 350^{o}C. Although Li et al. (2019) found it was slightly higher at 1.35 mg/HEET. Schaller et al. (2016) heated different tobacco blends in the same conditions as HEETS and found that on average 1.38 mg/HEET of nicotine was produced but found extremes with 0.62 mg/HEET and 1.62 mg/HEET of nicotine. Farsalinos et al. (2018) analysed HEETS and found a similar average to Schaller et al. (2016). Anabasine is an isomer of nicotine and will likely be released around the same temperature (Adam et al., 2009). Forster et al. (2015) found nicotine when heating tobacco as low as 100°C and as temperature increased to 200°C the concentration detected increased. White et al. (2001) heated tobacco powder from 250°C to 550°C and noticed a high nicotine yield at 250° that decreased as temperatures increased. Bassilakis et al. (2001) heated different types of tobacco at 30 K/min and found nicotine peaked around 200^{o}C, with a hump from 300^{o}C to 600^{o}C. Nicotine is a natural component of tobacco plants and when heated above 400°C, fragmentation occurs, and different volatiles are released (Rodgman & Perfetti, 2013). Bassilakis et al. (2001) determined the high temperature release of nicotine was due to condensation and re-vaporisation of nicotine within the TG-FTIR. The peak at 200^{o}C was more intense when there was a greater nitrogen content in the tobacco. Due to the faster heating rate peaks will appear at higher temperatures than Figure 16. The large peaks below 200^{o}C for HEETS and tobacco, shown in Figure 16, will be dominated by nicotine production. Table 6 shows the tobacco sample has a higher nitrogen concentration than HEETS, so should have a larger intensity peak if it follows Bassilakis et al. (2001) trend. However, Figure 16 shows that the first peak in HEETS is larger and occurs at a slightly lower temperature. Why it is larger is unknown, but the fact that it occurs earlier is probably

due to the more homogenised nature of the tobacco, whereas leaf tobacco may offer more resistance to nicotine release. Baker and Bishop (2004) found when heating to 900^{o}C that 97.7% of nicotine vaporised, while 1.4% converted to nicotyrine, 0.6% converted to myosmine, and 0.3% converted to cotinine.

Levoglucosan is a product from cellulose decomposition (Gu et al., 2019; Zhou et al., 2017; and Bassilakis et al., 2001). Gu et al. (2019) noticed levoglucosan in the vapour produced from heating tobacco stems from 160°C to 240°C. Chen et al. (2021) found levoglucosan was produced when heating kānuka wood chips to 335°C. Zhou et al. (2017) found levoglucosan in pine vapour from 200^{o}C to 380^{o}C with a peak at 310^{o}C, using TGA coupled with Time of Flight Mass Spectrometry (TOF MS). Heigenmoser et al. (2011) found levoglucosan in beech and larch wood at 340^{o}C and 450^{o}C. Levoglucosan fragments into compounds of m/z 144, 126, and 98 (Zhou et al., 2017), where the compound of m/z 98 is cyclohexanone (Hrablay & Jelemensky, 2016).

Methyl cinnamate is listed as a HEETS flavour ingredient (Philip Morris International, 2018), but it is unclear if methyl cinnamate has been added to the Amber label HEETS or tobacco sample used in this experiment. Bentley et al. (2020) heated HEETS to 350^{o}C, although they did not disclose which of the flavours was used and found 0.101 µg/HEET methyl cinnamate. Blazso et al. (2018) state that at 300°C only 0.1% of methyl cinnamate decomposes to benzaldehyde, with the rest vaporising. Baker and Bishop (2004) claim that methyl cinnamate will vaporise at 400°C with only 1% decomposing. Decomposition products of methyl cinnamate include ethyl cinnamate, benzaldehyde and styrene. The last compound in the m/z 162 list is 6-methoxy-3-methylbenzofuran that was detected by Gu et al. (2013) who heated poplar wood to 600^{o}C.

In summary, nicotine is released at low temperatures as shown by the two peaks for tobacco and HEETS below 200^{o}C. Above that levoglucosan is ubiquitous to all biomass thermal decompositions being produced from cellulose, and seemingly by more than one reaction pathway.

3.10.26 m/z 164: Eugenol, isoeugenol, raspberry ketone, and phenethyl acetate

Eugenol, isoeugenol, raspberry ketone, and phenethyl acetate have an m/z of 164. Figure 16 shows HEETS and tobacco have a first peak around 250^{o}C, followed by a larger peak around 350^{o}C and shoulder around 400^{o}C experienced by all the biomasses.

Eugenol and isoeugenol are known lignin breakdown products. Eugenol has been detected in the tobacco plant and smoke (Rodgman & Perfetti, 2013). Chen et al. (2021) reported the presence of eugenol and isoeugenol in kānuka wood chips heated to 335°C. Eugenol and isoeugenol have been identified in vapour from pine and ginkgo wood heated to 400°C (Luo et al., 2017; and Wang et al., 2018). Takada et al. (2004) found eugenol and isoeugenol in sugi wood vapour and found coniferyl aldehyde breaks down to isoeugenol. Kibet et al. (2012) heated lignin in anoxic conditions and reported the production of eugenol from 200°C, peaking at 400°C, and decreasing till 600°C. At 300°C eugenol mostly vaporised, degrading 0.21% to 5-methoy-1H-inden-6-ol and 0.14% to vanillin (Blazso et al., 2018). Eugenol is known to have a “spicy, clove-like” scent (Bendre et al., 2016). Eugenol concentration in U.S. cigarettes at around 0.61 µg/cigarette (Stanfill & Ashley., 2000). Cigarettes containing cloves could produce up to 60,000 times more eugenol than traditional cigarettes (Polzin et al., 2007). Philip Morris International (2018) do not list cloves or clove oil as an added ingredient in HEETS, although eugenol-like flavours may be added and eugenol could be present in mixed flavours (Krusemann et al., 2018). Cinnamon bark oil contains eugenol, but not as much as clove oil, and is listed as an added flavour ingredient in HEETS (Philip Morris International, 2018; Moricz et al., 2016; Li et al., 2013; and Kim et al., 2015). Eugenol has numerous health effects including “respiratory infection, aspiration pneumonitis, hemoptysis and hemorrhagic pulmonary edema” (Lisko et al., 2014).

Raspberry ketone has only been detected in tobacco smoke (Rodgman & Perfetti, 2013). Blazso et al. (2018) heated raspberry ketone to 300°C and found that 99.66% vaporised, 0.25% converted to 4-(4-hydroxyphenyl)but-3-en-2-one and 0.09% converted to 4-hydroxybenzaldehyde. Raspberry ketone is often added to raspberry flavoured tobacco products, although is not commonly used in traditional tobacco products (Smith et al., 2002). Philip Morris International (2018) listed raspberry ketone and phenethyl acetate as added flavourings but do not specify which products used this flavour. Phenethyl acetate has a floral odour and may be present in tobacco products (McGinty et al., 2012).

In summary, for Figure 16, the release of eugenol and isoeugenol will explain the higher peak and shoulder for the biomasses. The lower temperature peak for HEETS and tobacco could be the release of added eugenol.

3.10.27 m/z 166: Fluorene, 4-propylguaiacol, homovanillin, and acetoguaiacone

Fluorene, 4-propylguaiacol, homovanillin, and acetoguaiacone have an m/z of 166. Figure 16 shows that all the biomasses have peaks between 250^{o}C to 500^{o}C. HEETS and tobacco have a peak at 340^{o}C and kānuka has a peak at 370^{o}C. Kānuka and tobacco also have a shoulder off the main peak around 430^{o}C, which is absent from HEETS. Fluorene is the second most present polycyclic aromatic hydrocarbon (PAH) in tobacco smoke, behind naphthalene (Lu and Zhu, 2007; Vu et al., 2015; and Ding et al., 2005). Ding et al. (2005) found fluorene in burning 100% reconstituted tobacco cigarettes was 229 ng/cigarette and for other tobaccos and tobacco blends ranged from 350 ng/cigarette to 625 ng/cigarette. In poplar wood chip smoke, Skrbic et al. (2018) found fluorene was the second most prominent PAH behind phenanthrene. They also found for poplar sawdust smoke, phenanthrene, naphthalene and acenaphthylene have higher concentrations than fluorene and attributed this to more air present during heating than for the wood chips. Hedberg et al. (2002) found for birch wood smoke, fluorene had the fourth highest PAH production behind phenanthrene, fluoranthene and pyrene. Nakajima et al. (2007) studied the generation of PAHs for cypress and chestnut wood from 400^{o}C to 1000^{o}C. From 400^{o}C to 600^{o}C fluorene production dominates. For cypress fluorene production continues to dominate up to 1000^{o}C. For chestnut wood phenanthrene overtakes at 800^{o}C and acenaphthylene overtakes fluorene at 1000^{o}C. Fluorene is a respiratory irritant (Smith et al., 2020).

4-Propylguaiacol, homovanillin, and acetoguaiacone are produced from the thermal decomposition of lignin (Lupoi et al., 2015, and Kim et al., 2015). 4-Propylguaiacol and acetoguaiacone have been identified in tobacco smoke (Rodgman & Perfetti, 2013). Zhang et al. (2020) found the production of 4-propylguaiacol from kānuka started from 280^{o}C and peaked at 380^{o}C. This corresponds with Figure 16 where the slight differences are likely due to the experimental methods. The apparat et al. (2015) heated red river gum, river tamarind, rubber wood, and neem wood to 400^{o}C and found 4-propylguaiacol was the second most generated pyrolysis product following acetic acid. Takada et al. (2004) found propylguaiacol, homovanillin, and acetoguaiacone while heating sugi wood. Homovanillin has also been detected in the smoke from Scots pine (Lourenco et al., 2018). Acetoguaiacone has been identified in Monterey pine (Wagner et al., 2011). Wang et al. (2018) found ginko wood lignin produces 9.14% acetoguaiacone at 400^{o}C and its relative concentration decreases as temperature increases past 400^{o}C.

In summary, all the m/z 166 compounds discussed seem to be released from the biomass over a similar temperature range and the peaks shown in Figure 16 are likely to be an amalgam of these compounds and other fragments.

3.10.28 m/z 177: NNN

3-(1-Nitrosopyrrolidin-2-yl)pyridine (NNN) has an m/z of 177. Figure 16 shows the ion chromatogram for m/z 177. Tobacco and HEETS have some low level detection below 250^{o}C. Above 250^{o}C, kānuka has much higher detection intensity with a peak at 310^{o}C and a shoulder at 390^{o}C. HEETS has one peak in the middle

at 340^{o}C and tobacco is broad with a minor peak at 370^{o}C and a shoulder around 440^{o}C. NNN is formed "by nitrosation of nicotine" and will be present in tobacco vapour after 154°C (Piade et al., 2013). Li et al. (2019) noticed NNN when burning 3R4F reference cigarettes. Forster et al. (2015) was able to detect NNN in tobacco vapour from 100°C. Tobacco plants produce NNN during the curing stage. The NNN then vaporises during pyrolysis (Brown et al., 2013). NNN is carcinogenic and can be cancer inducing (FDA, 2019; Fowles et al., 2000; and Konstantinou et al., 2018). Carmines and Gaworski (2005) found the addition of glycerol to tobacco reduced the production of NNN. HEETS has added glycerol while tobacco does not (Ministry of Health, 2019). The only point in Figure 16 where the HEETS absolute intensity is lower than the tobacco absolute intensity is after 410^{o}C. The EGA curves are formed from the release of a combination of compounds at the same molecular weight, so cannot be used to validity Carmines and Gaworski (2005) statement. Philip Morris Products S.A. (2017) states 10.1 ng/HEET of NNN is released from HEETS at 350^{o}C. This corresponds with Li et al. (2019). Bekki et al. (2017) found that 19.2ng/HEET of NNN was released from HEETS. Schaller et al. (2016) heated different tobacco blends in the same method as HEETS and found that NNN had an average production of 14.2 ng/stick with extremes found at 3.0 ng/stick and 57.1 ng/stick. Kānuka does not contain nicotine so will not have NNN. Therefore, the detection spectrum for m/z 177 must be due to other compounds or fragments.

Protonated cotinine has an m/z of 177 (Dunlop et al., 2013). Protonated cotinine mostly fragments to a compound at m/z 80, but also fragments in compounds at m/z 98 and m/z 146 (Pellegrini et al., 2007). Although cotinine is a nicotine metabolite, so while it has been found in tobacco smokers' bodies it will not be present in tobacco smoke or Figure 16 (Khattab et al., 2015). Tokareva et al. (2010) heated trigalacturonic acid, a component of wood lignin, and noticed the presence of m/z 177. They assumed it was a fragment ion from the breakdown of galacturonic acid. Yang (2012) also noticed the presence of m/z 177 and concluded it was from fragmentation ions. In summary, aside from NNN in tobacco and HEETS, the peaks in Figure 16 will be made up from a range of mostly unknown compounds and fragments.

3.10.29 m/z 178: Phenanthrene and anthracene

Phenanthrene and anthracene have an m/z of 178. In Figure 16 shows little detection below 250^{o}C for each biomass. HEETS and tobacco have a peak at 350^{o}C, while kānuka shows two substantial peaks, a larger one at 300^{o}C and a smaller one at 400^{o}C.

Both phenanthrene and anthracene are polycyclic aromatic hydrocarbons (PAH) that are present in smoke. In burning cigarette smoke phenanthrene is the third most common PAH and anthracene is the fourth (Kalaitzoglou & Samara, 2006, and Zha et al., 2002). Paschke et al. (2016) conducted fast pyrolysis with tobacco in anoxic conditions at set temperatures from 400^{o}C to 1000^{o}C and found the concentration of phenanthrene and anthracene did not obviously change. This implies that phenanthrene and anthracene formation occurred before 400^{o}C and was stable because it did not significantly degrade at higher temperatures. Connolly et al. (2005) obtained similar results. Ding et al. (2005) found for 100% reconstituted tobacco around 89 ng/cigarette phenanthrene and 62 ng/cigarette anthracene is released while the other tobacco and blends containing reconstituted tobacco ranged from 212-300 ng/cigarette phenanthrene and 125-150 ng/cigarette anthracene. Vu et al. (2015) and Geiss and Kotzias (2007) found corresponding results. HEETS contains reconstituted tobacco, while RYO tobacco contains chopped tobacco (Philip Morris International., 2018). In Figure 16, tobacco has a slightly higher absolute intensity than HEETS after 400^{o}C which could be related to the higher levels of phenanthrene and anthracene released.

Varlet et al. (2007) heated beech wood chips in three different smoke generators, one at 380^{o}C, one between 400^{o}C and 450^{o}C, and one at 500^{o}C. They found that phenanthrene production increased with increasing temperature, while anthracene production was the highest using the heating method between

400°C and 450°C. For birch log smoke phenanthrene was found to be the most prominent PAH with 99.1 mg/kg wood present, and anthracene was the fourth most prominent with 19.3 mg/kg wood (Hedberg et al., 2002). The high concentrations of phenanthrene compared to anthracene in biomass smoke is due to phenanthrene having more resonance structures and therefore being more thermodynamically stable (Skrbic et al., 2018). Although biomass smoke has high concentrations of phenanthrene and anthracene, both have a toxic equivalence factor of 0.0005 compared to benzo(a)pyrene (Conde et al., 2005). For this reason, phenanthrene is considered to be noncarcinogenic but its metabolites have been associated with increased cancer risk (Yershova et al., 2016). In summary, the presence of phenanthrene and anthracene is undisputed, and appears to be far more prevalent in kānuka volatiles than tobacco or HEETS. Nevertheless, for the relatively high mass to ion ratio, m/z 178, there will be other contributing but unknown compounds and fragments some of which may also be more prevalent in kānuka.

3.10.30 m/z 202: Fluoranthene and pyrene

Fluoranthene and pyrene have an m/z of 202. Figure 16 shows all biomass peak between 250°C and 500°C. HEETS and tobacco have peaks at 350°C and 430°C, with HEETS having a higher absolute intensity for the first and tobacco having a higher absolute intensity for the second. In between this, kānuka has a single peak at 400°C.

Fluoranthene and pyrene are polycyclic aromatic hydrocarbons that are present in smoke. From a smoking machine, tobacco cigarette smoke was found to contain 12.3-70.0 ng/cigarette fluoranthene and 57.0-293.8 ng/cigarette pyrene, which behaved independently (Lodovici et al., 2004). Vu et al. (2015) results agree for the pyrene range but found fluoranthene ranged from 74-189 ng/cigarette in smoked tobacco cigarettes. Ding et al. (2005) analysed smoke from different tobacco and tobacco blends, and found reconstituted tobacco had the lowest fluoranthene concentration at 79 ng/cigarette and burley tobacco had the lowest pyrene concentration at 48.9 ng/cg. The HEETS used in this research contains reconstituted tobacco, but the tobacco used in the RYO tobacco is unknown (Philip Morris International., 2018). Li et al. (2003) found that lighting a cigarette with a match or lighter can increase fluoranthene concentration by 8% and pyrene concentration by 16%. This is because the yellow tipped flame contains incandescent carbon associated with PAH formation. Hedberg et al. (2002) found for birch wood smoke there is 29.4 mg/kg fluoranthene and 25.5 mg/kg pyrene. Samae et al. (2021) found corresponding research for rubber wood smoke. Phenylalanine, an amino acid in tobacco and wood, decomposes to form 11 ng/mg phenylalanine of fluoranthene and 16 ng/mg phenylalanine of pyrene at 700°C and at 900°C decomposes to form 760 ng/mg phenylalanine of fluoranthene and 340 ng/mg phenylalanine of pyrene (Wang et al., 2004). In summary, while fluoranthene and pyrene will contribute to the detection spectrum of m/z 202, other compounds of m/z 202 can also arise as fragmentation ions from the thermal breakdown of larger compounds (Takada et al., 2004).

3.10.31 m/z 207: NNK and NNA

4-(N-methyl-N-nitrosamino)-1-(3-pyridyl)-1-butanone (NNK) and 4-(N-methyl-N-nitrosamino)-4-(3-pyridyl)butanal (NNA) have an m/z of 207. Figure 16 shows a very different intensity spectrum for kānuka. At 105°C kānuka has an absolute intensity of 32000, which decreases until 250°C, rises again until 320°C, declines to 390°C, then decreases quickly and plateaus. HEETS and tobacco both show two major peaks. HEETS has a larger peak at 340°C and a smaller at 460°C. Tobacco has a smaller peak at 340°C and a larger at 460°C. NNK and NNA are tobacco-specific nitrosamines that will be present in tobacco and HEETS, but not kānuka (Brown et al., 2003) Forster et al. (2015) was able to detect NNK in tobacco vapour at 100°C. Nicotine can oxidise to pseudooxynicotine, which can nitrosate to NNK (Piade et al., 2013). The majority of NNK and NNA is formed during the curing stage of tobacco, not the pyrolysis stage, and vaporises upon heating (Brown et al., 2003). NNK and NNA are carcinogenic and can lead to cancer (Konstantinou et al., 2018, and Sleiman et al., 2009). Carmines and Gaworski (2005) found the addition of glycerol was able to

reduce NNK production in tobacco vapour. HEETS contains glycerol while tobacco does not (Ministry of Health, 2019). The increase of tobacco over HEETS after 400^{o}C, in Figure 16 could indicate more NNK being released from tobacco. NNA is difficult to detect in burning cigarette smoke due to the "reactivity and instability at high temperatures during tobacco pyrolysis" (Sleiman et al., 2010). Philip Morris Products S.A. (2017) found that HEETS produced 7.8ng/HEET NNK at 350^{o}C. Li et al. (2019) and Schaller et al. (2016) had similar findings. Bekki et al. (2017) found a slightly higher production of 12.3 ng/HEET NNK. The thermal breakdown of NNA can lead to fragmentation ions at m/z 148, 120, and 92, while the breakdown of NNK can lead to fragmentation ions at m/z 177, 159, 146, and 106 (Sleiman et al., 2009). Most compounds of m/z 207 contain nitrogen, which is unlikely to be found in high concentrations in kānuka as it contains 0.19 wt.% nitrogen (Table 6). Therefore, the curve showed by kānuka in Figure 16 is likely to be fragmentation ions from other compounds. Biomass compounds without nitrogen that were found to break down to m/z 207 include 4,4'-dihydroxy-3,3'-dimethoxy stilbene, lupeol and taraxasterol (Takada et al., 2004, and Doshi et al., 2015). In summary, the higher temperature peaks for tobacco and HEETS may be NNK and NNA as kānuka does not have a peak here. The lower temperature peaks for all three biomasses are likely to be fragmentation ions, expect the 105^{o}C to 200^{o}C intensity spectrum for kānuka which remains unknown.

3.10.32 m/z 228: Benzo(a)anthracene, chrysene, triphenylene and myristic acid

Benzo(a)anthracene, chrysene, and triphenylene and myristic acid have an m/z of 228. In Figure 16, detection activity ranges between 250^{o}C and 500^{o}C, where HEETS and kānuka have a single peak at 350^{o}C and 400^{o}C respectively, and tobacco has two smaller peaks at 350^{o}C and 450^{o}C. Benzo(a)anthracene, chrysene, and triphenylene are polycyclic aromatic hydrocarbons (PAHs). From a smoking machine, tobacco cigarettes were found to contain 3.9-9.2 ng/cigarette benzo(a)anthracene, and 6.6-79.7 ng/cigarette chrysene (Lodovici et al., 2004). Akpan et al. (2006) agrees with the chrysene range from Lodovici et al. (2004), although found benzo(a)anthracene ranged slightly higher at 7.7-25.3 ng/cigarette. Djinovic-Stojanovic et al., (2013) found benzo(a)anthracene accounts for 9.23-15.46% of the total PAHs in beech smoke and chrysene accounts for 23.78-28.27% of the total PAHs. Although the amount of benzo(a)anthracene and chrysene release from wood smoke is very dependent on the type of wood (Racovita et al., 2020). Jimenez et al. (2017) found the benzo(a)anthracene content in Tasmanian blue gum smoke was 207.6 µg/kg wood, Patagonia oak smoke was 341.0 µg/kg wood, and silver wattle smoke was 106.1 µg/kg wood. They also found the chrysene content in Tasmanian blue gum smoke was 266.6 µg/kg wood, Patagonia oak smoke was 445.1 µg/kg wood, and silver wattle smoke was 131.9 µg/kg wood. Benzo(a)anthracene is formed from the thermal decomposition of sugars, lipids, amino acids, and nicotine (Smith et al., 2000). Phenylalanine, an amino acid in tobacco and wood, degrades to 8.8 ng/mg phenylalanine of benzo(a)anthracene and 15 ng/mg phenylalanine of chrysene when heated at 700^{o}C but when heated at 900^{o}C degrades to 290 ng/mg phenylalanine of benzo(a)anthracene and 580 ng/mg phenylalanine of chrysene (Wang et al., 2004). Benzo(a)anthracene and chrysene have been classified as "probably carcinogenic to humans" (Smith et al., 2000, and IARC, 2010).

Triphenylene has been identified in tobacco and wood smoke (Rodgman & Perfetti, 2013; Forchhammer et al., 2012; and Alcanzare, 2006). Triphenylene is non carcinogenic and is often present in low concentrations below the limit of detection in smoke (IARC, 2010, and Gustafson et al., 2008). There may be a slight contribution from these PAHs to Figure 16, although they are more likely at high temperatures outside the range analysed.

Lu et al. (2003) identified myristic acid in Virginia cigarette smoke condensate. The content of myristic acid in tobacco leaves increases with the curing time (Daheng et al., 2001). Myristic acid is naturally occurring in tobacco and can also be added to tobacco as a flavouring (Fowles & Bates, 2000). Myristic acid has a "waxy, fatty, soapy" odour (Martinez-Garcia et al., 2017). Bentley et al. (2020) detected myristic

acid in HEETS heated to 350°C at 4.62 µg/HEET, and in burning cigarettes at 18.7 µg/cigarette. Rencoret et al. (2007) analysed 5 different wood extracts and found myristic acid ranged from 0.6-3.2 mg/kg wood. For a mahaleb cherry tree, the relative concentration of myristic acid able to be extracted from leaves was 2.5% and from wood was 6.4% (Mastelic et al., 2006). Presence of these compounds may explain why kānuka has a higher absolute intensity than HEETS and tobacco in Figure 16. The decomposition of larger compounds can also result in the formation of m/z 228 ions, although the breakdown mechanisms and contribution to Figure 16 is unknown (Takada et al., 2004).

3.10.33 m/z 252: Benzo(a)pyrene, benzo(e)pyrene, benzo(b)fluoranthene, etc.

Benzo(a)pyrene, benzo(e)pyrene, benzo(b)fluoranthene, benzo(j)fluoranthene and benzo(k)fluoranthene all have a m/z of 252. Figure 16 shows that all biomasses have peaks of similar intensity, with HEETS and kānuka peak temperature around 400°C and tobacco peak temperature around 450°C. Benzo(a)pyrene is "one of the strongest carcinogens in tobacco smoke" (Yang et al., 2018), benzo(b)fluoranthene, benzo(j)fluoranthene and benzo(k)fluoranthene are probably carcinogens (Abdel-Shafy & Mansour, and IARC, 2010) and benzo(e)pyrene is noncarcinogenic (Vienneau et al., 1995). Benzo(a)pyrene has a vapour pressure of 7 x 10^{-6} Pa at 25°C (Piade et al., 2013). Figure 16 shows the absolute intensity from HEETS and tobacco starts increasing from 100°C, which corresponds with Klauser et al. (2018) who stated that benzo(a)pyrene is partially gaseous from 100°C to 350°C and so any of this compound present in the tobacco will be released over this range; the amount appears small, however. Tobacco leaves harvested from the top of the plant had a higher benzo(a)pyrene concentration than leaves harvested lower down due to differences in sugar content (Cai et al., 2019). Benzo(a)pyrene is formed from the decomposition of carbohydrates (Liu et al., 2011). Further benzo(a)pyrene is formed during heating. McGrath et al. (2007) heated tobacco and noticed the production of benzo(a)pyrene and benzo(b)fluoranthene starting from 400°C and peaking around 500°C to 550°C. Torikai et al. (2004) found benzo(a)pyrene was largely formed from 500°C to 800°C. Washing tobacco with water reduces the benzo(a)pyrene concentration by half, because precursors that form benzo(a)pyrene are removed (Liao et al., 2017). Benzo(a)pyrene is "one of the strongest carcinogens in tobacco smoke" (Yang et al., 2018). Philip Morris Products S.A. (2017) stated that benzo(a)pyrene production in HEETS at 350°C was 0.736 ng/HEET. Auer et al. (2017) found HEETS at 350°C produced 0.8 ng/HEET benzo(a)pyrene, 0.5 ng/HEET benzo(b)fluoranthene and 0.4 ng/HEET benzo(k)fluoranthene. Schaller et al. (2016) heated different tobacco blends using the same method and found benzo(a)pyrene had an average production of 1.02 ng/HEET, with some blends having concentrations too low to detect, and a maximum production of 4.46 ng/HEET. Hedberg et al. (2002) measured PAH concentration in birch wood smoke and found benzo(a)pyrene at 3.6 mg/kg wood, benzo(e)pyrene at 1.8 mg/kg wood, benzo(b)fluoranthene at 6.1 mg/kg wood and was unable to detect benzo(k)fluoranthene. Szramowiat-Sala et al. (2019) found corresponding results for European spruce. The concentration of benzo(a)pyrene in vapour increases with oxic environments (Klauser et al., 2018), noting that the EGA/MS experiment (Figure 16) was conducted under anoxic conditions. Djinovic-Stojanovic et al. (2013) measured the smoke from beech wood and found benzo(a)pyrene contributes 3.95-8.33% of the total PAHs, benzo(b)fluoranthene contributes 7.99-24.36%, benzo(j)fluoranthene contributes 3.54-7.84%, and benzo(k)fluoranthene contributes 2.42-6.27%. Klauser et al. (2018) obtained similar results. In summary, the spectrum for m/z 252 will certainly contain benzo(a)pyrene and for kānuka, probably also benzo(b)fluoranthene. However, with this high m/z, 252, there will be other fragment conditions.

3.10.34 m/z 264: Cinnamyl cinnamate

Cinnamyl cinnamate has an m/z of 264. For Figure 16, HEETS has two small peaks at 350°C and 420°C, tobacco has a peak at 450°C, and kānuka has a slightly larger peak at 390°C. Cinnamyl cinnamate has been identified in the tobacco plant and vapour (Rodgman & Perfetti, 2013). Xu et al. (2015) analysed 6

different types of wood with a GC/MS and only found 4.82% cinnamyl cinnamate per mass of wood in *Liquidambar formosana*. Cinnamyl cinnamate provides a spicy cinnamon flavour and balsamic odour (Guedes et al., 2004, and Xu et al., 2015). Baker and Bishop (2004), found at 900°C in oxic conditions, 53.6% of cinnamyl cinnamate will vaporise. The rest decomposes to benzaldehyde, diphenylhexadiene, styrene, diphenylpentadiene, cinnamaldehyde, phenol, propnylbenzene. Blazso et al. (2018) obtained similar results; they heated cinnamyl cinnamate to 300°C and found that 69.22% of cinnamyl cinnamate vaporises and obtains the same decomposition products as Baker and Bishop (2004) except for diphenylpentadiene. The most prominent decomposition products from Blazso et al. (2018) were benzaldehyde, 2-oxo-3-phenylpropyl cinnamate and cinnamyl cinnamate isomers. Fragmentation ions will also contribute to the curves in Figure 16. Isocorydine, sphinganine and sphingosine have been found in biomass and breakdown to m/z 264 (Singh et al., 2017, and Sullards et al., 2007).

3.10.35 m/z 276: Benzo(g,h,i)perylene, indeno(1,2,3-cd)pyrene, anthanthrene and stearidonic acid

Benzo(g,h,i)perylene, indeno(1,2,3-cd)pyrene, anthanthrene and stearidonic acid have an m/z 276. Figure 16 suggests that HEETS has two peaks, the lower, around 340^{o}C, shared with kānuka and the higher around 450^{o}C shared with tobacco. These temperatures correspond to shoulders in the kānuka spectrum which has its main peak at 390^{o}C. Out of the PAHs, benzo(g,h,i)perylene and anthanthrene are noncarcinogenic and indeno(1,2,3-cd)pyrene is carcinogenic (IARC, 2010). Kentucky cigarettes in a smoking machine produce 0.4-2.1 ng/cigarette benzo(g,h,i)perylene (Zha et al., 2002). Lodovici et al. (2004) noticed a similar range and found some cigarettes produced up to 3.5 ng/cigarette benzo(g,h,i)perylene. Smith and Hansch (2000) found a slightly higher range with 31.5 ng/cigarette benzo(g,h,i)perylene, 12 ng/cigarette indeno(1,2,3-cd,)pyrene and 11 ng/cigarette anthanthrene. Dusautoir et al. (2021) agrees with this result and also found that the concentration of these PAHS in HEETS at 350^{o}C is less than 7% of the comparative PAH in burning cigarette emissions. Lu and Zhu (2007) found a very different range in 12 brands of tobacco cigarettes with benzo(g,h,i)pyrene averaging 274.6 ng/cigarette and indeno(1,2,3-cd)pyrene averaging 48.92 ng/cigarette. Indeno(1,2,3-cd)pyrene was also found to have the second smallest concentration of the 17 PAHs that Lu and Zhu (2007) analysed. The amount of PAHs in tobacco smoke is unknown, but they will be more prominent at temperatures above 580^{o}C, which is the maximum used in this work (Figure 16).

Benzo(g,h,i)perylene, indeno(1,2,3-cd)pyrene, and anthanthrene have been reported in wood smoke (Alcanzare, 2006). In beech smoke benzo(g,h,i)perylene contributes to 3.87-8.26% of the total PAHs and indeno(1,2,3-cd)pyrene contributes to 3.09-5.55% of the total PAHs (Djnovic-Stojanovic et al., 2013). Barbosa et al. (2006) found, in eucalyptus smoke, that indeno(1,2,3-cd)pyrene was the third lowest PAH concentration after benzo(g,h,i)perylene and dibenz(a,h)anthracene. Fine et al. (2004) analysed the smoke from 5 different woods and found the general trend for m/z 276 PAHs was indeno(1,2,3-cd)pyrene with the highest concentration, followed by benzo(g,h,i)perylene, and anthanthrene had the lowest concentration. Bruns et al. (2015) reports similar findings. These PAHs can be formed from high temperature catechol pyrolysis (Wornat et al., 2001). There is potential that benzo(g,h,i)perylene could "promote the carcinogenesis of benzo(a)pyrene" (Cherng et al., 2001).

The last compound in this m/z 276 list, stearidonic acid, is a common fatty acid in plants, but is only present in very small amounts making it difficult to detect (Cholewski et al., 2018). Bentley et al. (2020) found 4.56 µg/HEET of stearidonic acid in HEETS at 350^{o}C and 21.3 µg/cigarette of stearidonic acid in burning cigarettes. In summary, no conclusions can be drawn to relate the compounds to the m/z 272 spectra. There will also be many contributing ion fragments.

3.10.36 m/z 278: Dibenz(a,h)anthracene, linolenic acid and neophytadiene

Dibenz(a,h)anthracene, linolenic acid, and neophytadiene have an m/z of 278. Similarly, HEETs and tobacco have peaks at 350^{o}C and 450^{o}C, with HEETS having a larger first peak and tobacco having a larger second. Kānuka has a single peak around 390^{o}C. Dibenz(a,h)anthracene has been detected in tobacco smoke, although its concentration was extremely low between 0-7.5 ng/cigarette (Jeffery et al., 2018; Ding et al., 2008; and Paschke et al., 2016). Dibenz(a,h)anthracene is potentially carcinogenic to humans (IARC, 2010). In beech wood smoke, dibenz(a,h)anthracene accounts for 0.79-2.58% of the total PAHs (Djinovic-Stojanovi et al., 2013).

Linolenic acid is a polyunsaturated fatty acid commonly found in tobacco and wood (Kirkova et al., 2016, Salehi, 2012). The concentration of linolenic acid in tobacco leaves decreases with increased curing time (Daheng et al., 2001). Bentley et al. (2020) found HEETS at 350^{o}C released 57.9 µg/HEET linolenic acid and burning cigarettes release 157 µg/cigarette linolenic acid. Fine et al. (2002) found the concentration of linolenic acid in yellow poplar wood was 16.44 mg/g organic carbon, while the linolenic concentration in 5 other woods was much lower between 1.10-2.00 mg/g organic carbon. The linolenic acid concentration in trees was found to increase towards the heartwood (Piispanen & Saranpaa, 2002).

Of the neutral aroma compounds in flue-cured tobacco, studied by Hou-long et al. (2016), neophytadiene was the most prevalent. Cai et al. (2002) also found that neophytadiene was a major free aromatic volatile from flue-cured tobacco. Bentley et al. (2020) found HEETS at 350^{o}C produced 23.8 µg/HEET neophytadiene, while burning cigarettes produced 43.0 µg/cigarette neophytadiene. Neophytadiene has a boiling point of 346^{o}C (Yokoi & Shimoda, 2016). The decomposition of chlorophyll leads to the production of neophytadiene (Rodgman & Perfetti, 2013) and so will be absent from kānuka wood. There are many factors affecting the concentration of neophytadiene in tobacco, such as the species, processing conditions, width/length ratio of the leaves, and height leaves were harvest at (Palic et al., 2002, and Hou-long et al., 2016). Mastelic et al. (2006) analysed chemicals in the mahaleb cherry tree and identified neophytadiene in the leaves, but not in the bark or wood. In summary, Figure 16 will be dominated by the release of linolenic acid, and HEETS and tobacco will have some contribution from neophytadiene.

3.10.37 m/z 280: Linoleic acid

Linoleic acid has an m/z of 280. Figure 16 shows HEETS has a main peak around 350^{o}C and a smaller peak around 190^{o}C. Tobacco also has a small peak around 190^{o}C and a slight peak at 350^{o}C that's dominated by a larger peak at 450^{o}C. Kānuka has a single peak around 400^{o}C. Linoleic acid accounts for roughly 62% to 72% of the fatty acid in tobacco seeds (Popova et al., 2018, and Mukhtar et al., 2007). In tobacco leaves for a 6-week-old plant, linoleic acid accounts for 12.5% of the fatty acid (Popov et al., 2011). Whereas in pine wood it accounts for 39% to 46% of the fatty acid (Piispanen & Saranpaa, 2001). Popov et al., (2011) found tobacco roots had a higher linoleic acid composition than leaves. While it is unlikely that roots will be part of the HEETS and tobacco sample, they probably will use leaves, stems, and seeds. The research from Popov et al., (2011) highlights how variation in linoleic acid content can arise from using different segments of the same plant. Piispanen and Saranpaa (2001) found the linoleic acid concentration in pine decreased towards heartwood, while Arisandi et al. (2020) found the linoleic acid concentration in eucalyptus increased toward heartwood. Although these papers came to differing conclusions, they both agree that linoleic acid concentration is dependent on the area of tree used. Plants from colder climates had higher linoleic acid concentrations than plants in warmer climates (Piispanen & Saranpaa, 2001; and Popov et al., 2011). Linoleic acid has been detected in tobacco and tobacco vapour (Rodgman & Perfetti, 2013). Bentley et al. (2020) found HEETS at 350^{o}C released 43 µg/HEET of linoleic acid. Asomaning et al. (2014) heated linoleic acid to 390°C and noted the presence of hexane, decane, heptanoic acid, octanoic acid, nonanoic acid, 8-heptadecene, n-heptadecane, 8-octadecenoic acid, and octadecanoic acid. In

summary, the spectra in Figure 16 will be significantly influenced by linoleic acid with differences due to plant species, growing conditions, and section of the plant used.

3.11 Pyrolysis gas chromatography mass spectrometry

As shown in previous experiments, the biomass vapour changes with temperature. To identify the evolution of compounds present in biomass vapour, the Py-GC/MS was used. Heat-not-burn devices utilise specific temperature set points to maximise delivery of desirable compounds, like nicotine, while minimising delivery of undesirable compounds, like carcinogens. The differences in vapour produced from a heat-not-burn device that heats to 230°C and an iQOS device that heats to 350°C is unknown. The purpose of the Py-GC/MS analysis was used to identify specific compounds from 180°C to 390°C.

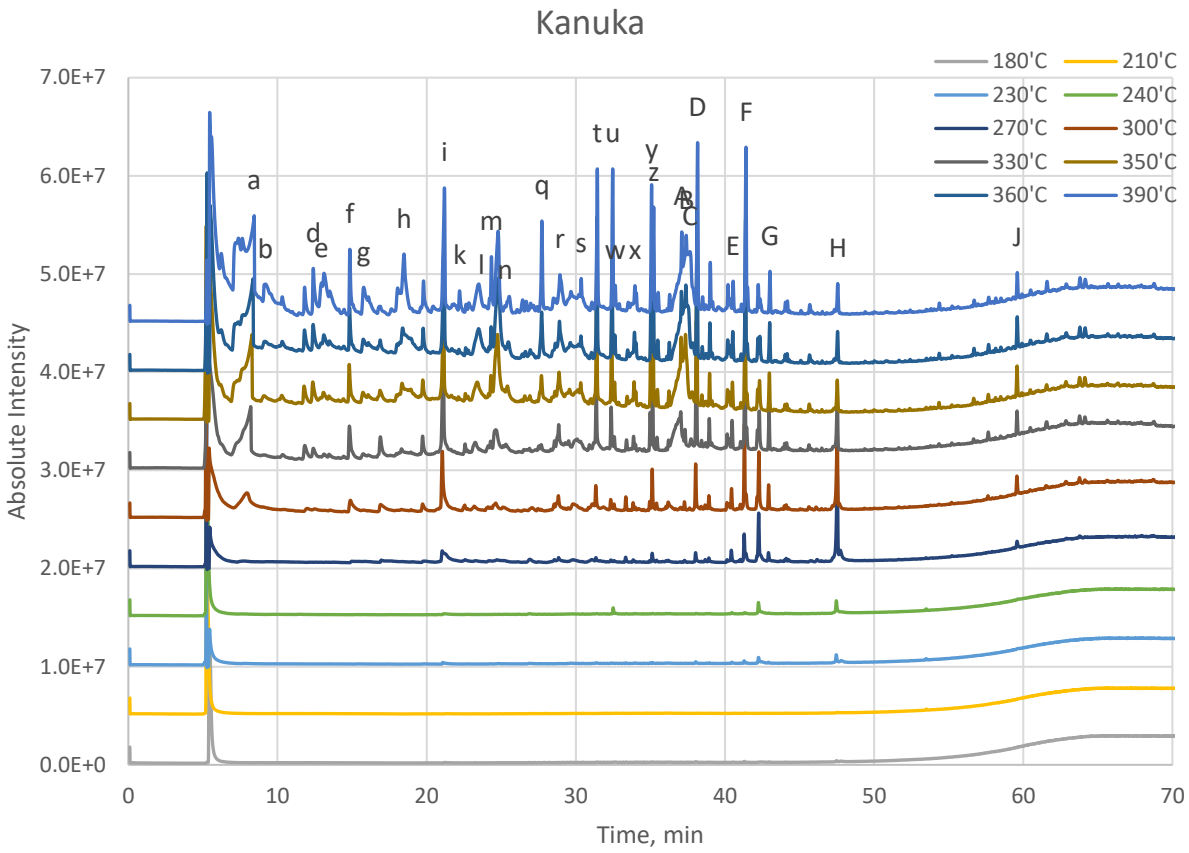

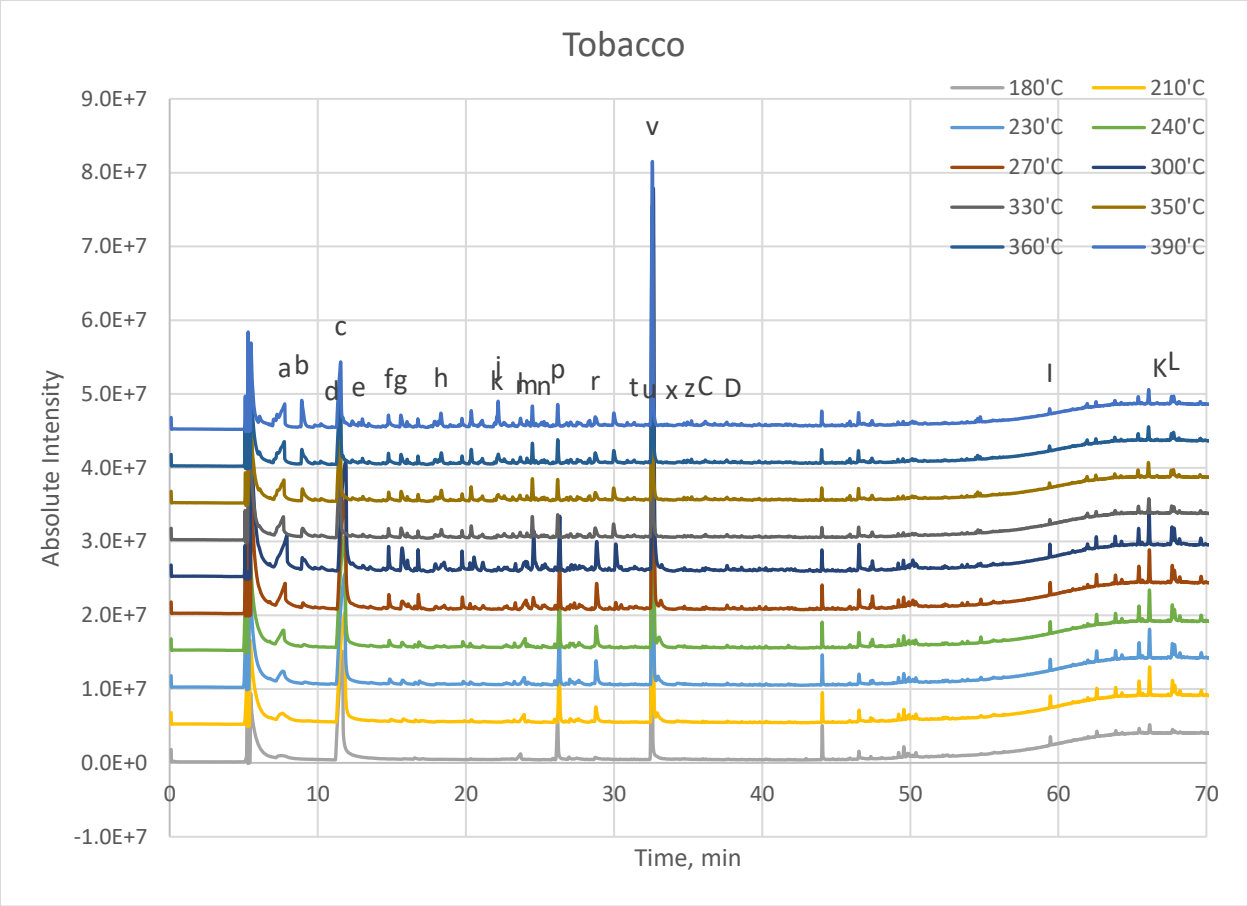
Tobacco
180'C
210'C
230'C
240'C
270'C
300'C
330'C
350'C
360'C
390'C
Absolute Intensity
Time, min
9.0E+7
8.0E+7
7.0E+7
6.0E+7
5.0E+7
4.0E+7
3.0E+7
2.0E+7
1.0E+7
0.0E+0
-1.0E+7
0
10
20
30
40
50
60
70
a
b
c
d
e
f
g
h
i
k
l
m
n
p
r
t
u
v
x
z
C
D
I
K
L

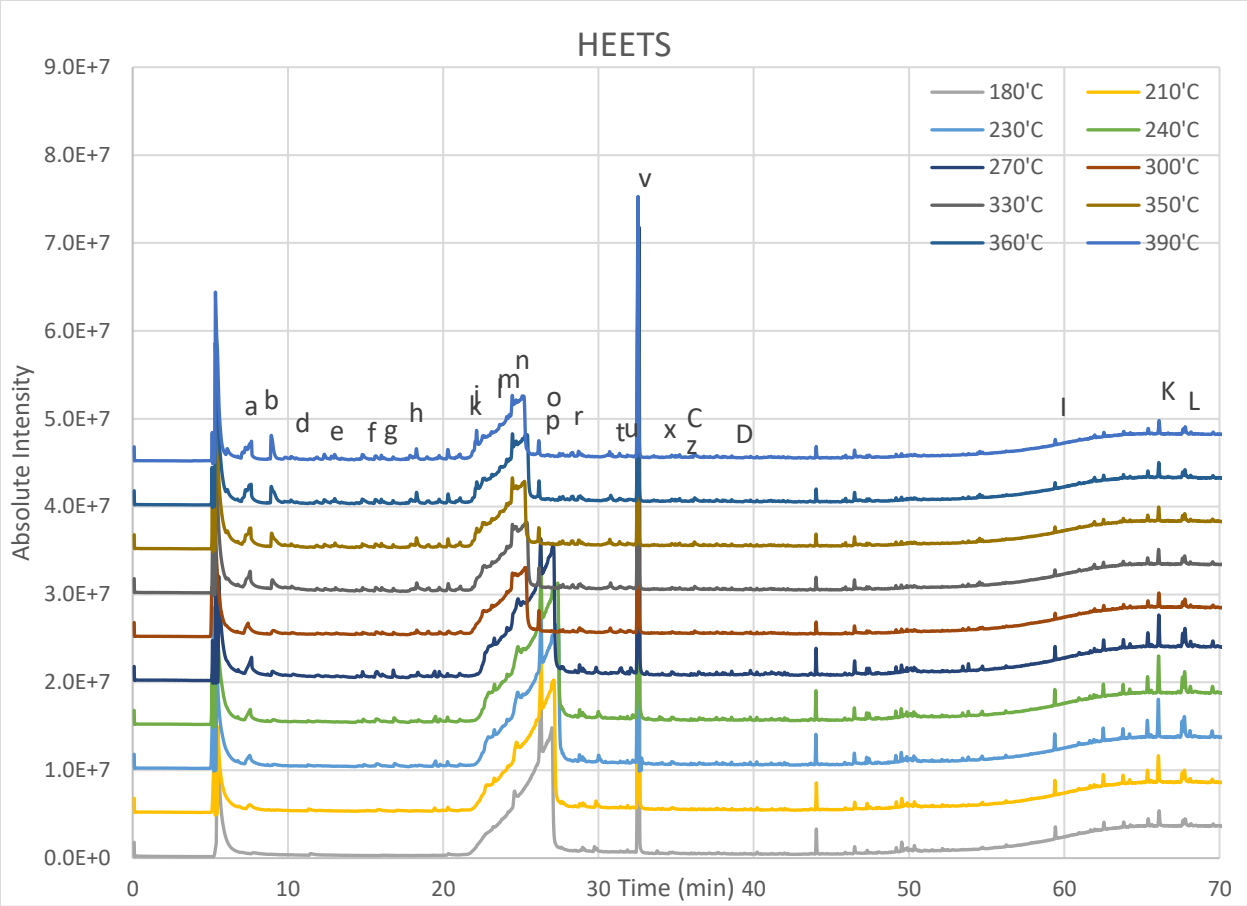

Figure 17: Graph of absolute intensity versus time for 2mg samples of kānuka, tobacco and HEETS, heated to temperatures ranging from 180°C to 390°C. The different temperature runs have been separated by an absolute intensity of 5.0E+6 for visual display purposes. Labelled peaks have been identified in Table 9.

Table 9: List of major compounds identified from Figure 17. Retention index and absolute intensity is from one run at 390°C. Retention index refers to the dimentionless retention time taken for a compound to pass through the column, generally with heavier compounds having larger retention indexes.

Label	Compound	Kānuka		Tobacco		HEETS	
		Retention Index	Absolute Intensity	Retention Index	Absolute Intensity	Retention Index	Absolute Intensity
a	Acetic acid	664	$1.09x10^7$	644	$3.66x10^6$	640	$2.45x10^6$
b	Hydroxyacetone	688	$3.96x10^6$	679	$4.15x10^6$	679	$3.11x10^6$
c	Propylene Glycol			760	$9.35x10^6$		
d	Acetic anhydride	786	$5.57x10^6$	741	$5.58x10^5$	741	$4.21x10^5$
e	Succindialdehyde	803	$4.07x10^6$	797	$1.13x10^6$	799	$7.42x10^5$
f	Furfural	861	$7.51x10^6$	859	$2.15x10^6$	859	$9.33x10^5$
g	Furfuryl alcohol	890	$3.64x10^6$	885	$2.14x10^6$	885	$7.64x10^5$
h	2-Hydroxycyclopent-2-en-1-one	973	$7.03x10^6$	968	$2.40x10^6$	966	$1.58x10^6$
i	Squaric acid	1056	$1.38x10^7$				

j	Limonene			1086	$4.02x10^6$	1086	$3.68x10^6$
k	**3-Methyl-1,2-cyclopentanedione**	1087	$3.28x10^6$	1084	$1.93x10^6$	1083	$2.42x10^6$
l	**m-Cresol**	1132	$2.33x10^6$	1133	$1.71x10^6$	1132	$4.35x10^6$
m	**Mequinol**	1153	$6.76x10^6$	1147	$1.38x10^6$	1150	$5.46x10^6$
n	2-Cyclopenten-1-one, 2-hydroxy-, 3,4-dimethyl-	1181	$1.76x10^6$	1181	$1.26x10^6$	1176	$7.60x10^6$
o	**Glycerol**					1179	$7.57x10^6$
p	4H-Pyran-4-one, 2,3-dihydro-3,5-dihydroxy-6-methyl-			1211	$3.58x10^6$	1210	$2.51x10^6$
q	Creosol	1266	$1.04x10^7$				
r	5-Hydroxymethylfurfural	1308	$4.29x10^6$	1301	$1.90x10^6$	1301	$1.30x10^6$
s	4-Ethylguaiacol	1358	$4.54x10^6$				
t	2-Methoxy-4-vinylphenol	1397	$1.57x10^7$	1394	$1.15x10^6$	1394	$1.06x10^6$ 6
u	**Syringol**	1437	$1.57x10^7$	1434	$9.15x10^5$	1433	$7.73x10^5$
v	Nicotine			1442	$3.65x10^7$	1441	$3.03x10^7$
w	**Eugenol**	1444	$3.84x10^6$				
x	**Vanillin**	1497	$3.81x10^6$	1495	$7.56x10^5$	1491	$6.72x10^5$
y	Vanillic acid	1542	$1.41x10^7$				
z	**Isoeugenol**	1547	$1.18x10^7$	1543	$9.88x10^5$	1543	$7.77x10^5$
A	Ethanone, 1-(2,6-dihydroxy-4-methoxyphenyl)-	1625	$9.29x10^6$				
B	Homovanillyl alcohol	1639	$8.94x10^6$				
C	**Levoglucosan**	1650	$7.26x10^6$	1585	$1.30x10^6$	1586	$1.01x10^6$
D	2,5-Dimethoxy-4-methylbenzaldehyde	1673	$1.84x10^7$	1666	$9.44x10^5$	1666	$7.26x10^5$
E	Syringaldehyde	1779	$4.26x10^6$				
F	Phenol, 2,6-dimethoxy-4-(2-propenyl)-	1819	$1.79x10^7$				
G	3,5-Dimethoxy-4-hydroxyphenylacetic acid	1899	$5.28x10^7$				
H	2-Methoxyphenanthrene	2136	$4.02x10^7$				
I	Triacontane			2893	$3.01x10^6$	2894	$2.24x10^6$
J	Quinalizarin	2906	$5.14x10^6$				
K	Tetratriacontane			3317	$5.61x10^6$	3318	$4.80x10^6$
L	Vitamin E			3405	$4.71x10^6$	3405	$4.09x10^6$

Bold Compounds have been confirmed using standards, other compounds are the most likely possibility from GCMS Postrun Analysis from Shimadzu GCMSsolution Software with NIST11 library.

Figure 17 shows the Py-GC/MS results where samples were dropped into the pyrolyser at temperatures ranging from 180^{o}C to 390^{o}C. A repeat was done with very similar results, shown in Appendices I. Table 9 shows the major compounds identified in the biomasses vapour after heating at 390^{o}C. By comparing the different temperatures, it is clear that higher temperatures have more peaks, referring to more compounds present, but they did not necessarily have the highest absolute intensity for each compound. In Figure 17 peaks were arranged by retention index; the larger retention index means that the compounds took longer to pass through the Py-GC/MS. Peaks having an absolute intensity larger than 2 x 10^6 were considered major peaks. Not every peak was able to be identified, as some peaks include multiple compounds. The first large unidentified peak, around 5 minutes for all of the biomasses, is likely due to a combination of water vapour and other low molecular mass compounds. The retention indexes for most compounds are consistent across all biomasses. Acetic acid, acetic anhydride and levoglucosan have higher retention indexes for kānuka compared to tobacco and HEETS. The absolute intensity for the biomass is affected by the split ratio. The split ratio refers to how much of the vapour produced passes through the column or is lost to atmosphere. Kānuka, at 390^{o}C used a split ratio of 1:75, meaning 1 part in 75 passed through the column for detection. Tobacco and HEETS used a split ratio of 1:150, due to the nicotine peak from tobacco and HEETS dominating the Py-GC/MS results, and so requiring a higher split ratio to avoid over saturation.

Syringol, isoeugenol, and 2,5-dimethoxy-4-methylbenzaldehyde are significantly more prominent in kānuka than tobacco and HEETS. There are also compounds that have been detected in one biomass and are either not present or unable to be detected in the other biomass. Glycerol is one such compound, being an added ingredient in HEETS (Ministry of Health, 2019) and has only been detected in HEETS. Another additive is propylene glycerol, which is 4 wt.% in the tobacco sample and 1 wt.% in the HEETS sample (Ministry of Health, 2019). However, propylene glycerol was only detected in tobacco and not HEETS. The Py-GC/MS arranges compounds by retention index so compounds can overlap each other. For example, in Table 9 eugenol was only identified in kānuka, while isoeugenol was identified in all the biomass. Eugenol has a retention index of 1444 and nicotine has a retention index of 1442. Due to nicotine being so prominent in the tobacco and HEETS smoke, the peak for eugenol could have been obscured. From Figure 17 and Table 9 the general composition of each biomass can be established. The temperature, 390^{o}C, was the maximum temperature investigated in this research so it was displayed as it would include any extractives and degradation products present in the lower temperature. The evolution of the overall smoke composition from 180^{o}C to 390^{o}C was also investigated.

Table 10: Compounds identified in biomass by Py-GC/MS

m/z		180	210	230	240	270	300	330	350	360	390
60	Acetic acid ($C_2H_4O_2$)	H, T	H, T	H, T	H, T	H, T	H, T, K	H, T, K	H, T, K	H, T, K	H, T, K
74	Hydroxyacetone ($C_3H_6O_2$)			H, T	H, T	H, T	H, T	H, T, K	H, T, K	H, T, K	H, T, K
76	Propylene Glycol ($C_3H_8O_2$)	T	T	T	T	T	T	T	T	T	T
78	**Benzene (C_6H_6)**							T	H, T	H, T	H, T
86	Succindialdehyde ($C_4H_6O_2$)							H, T	H, T, K	H, T, K	H, T, K

92	**Glycerol ($C_3H_8O_3$)**	H	H	H	H	H	H	H	H	H	H
94	**Phenol (C_6H_6O)**					H, T	H, T	H, T, K	H, T, K	H, T, K	H, T, K
96	2-Cyclopentene-1,4-dione ($C_5H_4O_2$)		H	H, T	H, T	H, T	H, T	H, T	H, T	H, T	H, T
96	Furfural ($C_5H_4O_2$)	T	H, T	H, T	H, T	H, T, K	H, T, K	H, T, K	H, T, K	H, T, K	H, T, K
98	2-Hydroxycyclopent-2-en-1-one ($C_5H_6O_2$)			H, T	H, T	H, T	H, T, K	H, T, K	H, T, K	H, T, K	H, T, K
98	Furfuryl alcohol ($C_5H_6O_2$)		H, T	H, T	H, T	H, T	H, T	H, T, K	H, T, K	H, T, K	H, T, K
100	Acetylpropionyl ($C_5H_8O_2$)						H	H, T	H, T	H, T	H, T
102	Acetic anhydride ($C_4H_6O_3$)					H, T, K	H, T, K	H, T, K	H, T, K	H, T, K	H, T, K
108	**m-Cresol (C_7H_8O)**						T	H,T	H, T, K	H, T, K	H, T, K
110	5-Methylfurfural ($C_6H_6O_2$)		H, T	H, T	H, T	H, T	H, T	H, T	H, T	H, T	H, T
110	**Hydroquinone ($C_6H_6O_2$)**			T	T	H, T	H, T	H, T	H, T, K	H, T, K	H, T, K
112	1,2-Cyclohexanedione ($C_6H_8O_2$)						H	H, T	H, T	H, T	H, T
112	**3-Methylcyclopentane-1,2-dione ($C_6H_8O_2$)**							H, T	H, T, K	H, T, K	H, T, K
114	Squaric acid ($C_4H_2O_4$)				K	K	K	K	K	K	K
117	Indole (C_8H_7N)						H	H, T	H, T	H, T	H, T
120	2,3-Dihydrobenzofuran (C_8H_8O)							T	T	H, T	H, T
124	**Mequinol ($C_7H_8O_2$)**					T	T, K	H, T, K	H, T, K	H, T, K	H, T, K
126	5-Hydroxymethylfurfural ($C_6H_6O_3$)	H, T	H, T	H, T	H, T	H, T, K	H, T, K	H, T, K	H, T, K	H, T, K	H, T, K
126	2-Cyclopenten-1-one, 2-hydroxy-, 3,4-dimethyl- ($C_7H_{10}O_2$)							H, T	H, T	H, T	H, T, K
136	Limonene ($C_{10}H_{16}$)							H, T	H, T	H, T	H, T
138	Creosol ($C_8H_{10}O_2$)						K	K	K	K	K
144	4H-Pyran-4-one,2,3-dihydro-3,5-dihydroxy-6-methyl- ($C_6H_8O_4$)	H, T	H, T	H, T	H, T	H, T	H, T	H, T	H, T	H, T	H, T
150	2-Methoxy-4-vinylphenol ($C_9H_{10}O_2$)	H	H, T	H, T	H, T	H, T, K	H, T, K	H, T, K	H, T, K	H, T, K	H, T, K
152	4-Ethylguaiacol ($C_9H_{12}O_2$)								K	K	K

152	**Vanillin ($C_8H_8O_3$)**			T	T	H, T, K	H, T, K	H, T, K	H, T, K	H, T, K	H, T, K
154	**Syringol ($C_8H_{10}O_3$)**			H	H	H, K	H, T, K	H, T, K	H, T, K	H, T, K	H, T, K
162	**Levoglucosan ($C_6H_{10}O_5$)**					H	H, T	H, T, K	H, T, K	H, T, K	H, T, K
162	Nicotine ($C_{10}H_{14}N_2$)	H, T	H, T	H, T	H, T	H, T	H, T	H, T	H, T	H, T	H, T
164	**Eugenol ($C_{10}H_{12}O_2$)**					K	K	K	K	K	K
164	**Isoeugenol ($C_{10}H_{12}O_2$)**					H, T, K	H, T, K	H, T, K	H, T, K	H, T, K	H, T, K
166	4-Propylguaiacol ($C_{10}H_{14}O_2$)					K	K	K	K	K	K
166	**Acetoguaiacone ($C_9H_{10}O_3$)**					K	K	K	K	K	K
168	Homovanillyl alcohol ($C_9H_{12}O_3$)						K	K	K	K	K
168	Vanillic acid ($C_8H_8O_4$)					K	K	K	K	K	K
180	2,5-Dimethoxy-4-methylbenzaldehyde ($C_{10}H_{12}O_3$)			T, K	H, T, K	H, T, K	H, T, K	H, T, K	H, T, K	H, T, K	H, T, K
182	Ethanone, 1-(2,6-dihydroxy-4-methoxyphenyl)- ($C_9H_{10}O_4$)						K	K	K	K	K
182	Syringaldehyde ($C_9H_{10}O_4$)		K	K	K	K	K	K	K	K	K
194	Phenol, 2,6-dimethoxy-4-(2-propenyl)- ($C_{11}H_{14}O_3$)	K	K	K	K	K	K	K	K	K	K
208	2-Methoxyphenanthrene ($C_{15}H_{12}O$)	K	K	K	K	K	K	K	K	K	K
212	3,5-Dimethoxy-4-hydroxyphenylacetic acid ($C_{10}H_{12}O_5$)					K	K	K	K	K	K
272	Quinalizarin ($C_{14}H_8O_6$)					K	K	K	K	K	K
278	Linolenic acid ($C_{18}H_{30}O_2$)	T	T	H, T	H, T	H, T	H, T	H, T	H, T	H, T	H, T
284	Octadecanoic acid ($C_{18}H_{36}O_2$)	H, T	H, T	H, T	H, T	H, T, K	H, T, K	H, T, K	H, T, K	H, T, K	H, T, K
422	Triacontane ($C_{30}H_{62}$)	H, T	H, T	H, T	H, T	H, T	H, T	H, T	H, T	H, T	H, T
430	Vitamin E ($C_{29}H_{50}O_2$)	H, T	H, T	H, T	H, T	H, T	H, T	H, T	H, T	H, T	H, T
478	Tetratriacontane ($C_{34}H_{70}$)	H, T	H, T	H, T	H, T	H, T	H, T	H, T	H, T	H, T	H, T

Where H = HEETS, T = Tobacco, and K = Kānuka

Bold Compounds have been confirmed using standards, other compounds are the most likely possibility from GCMS Postrun Analysis.

Standards were used to help identify some of the compounds in the biomass. The standards investigated, shown in Table 2, were associated with negative health effects, desirable flavour compounds, or general interest. The standards were run to identify the retention index and shape of the peak. This information could be compared to the biomass vapour to confirm specific compounds.

For each temperature from 180^{o}C to 390^{o}C there were two trials done for each biomass, which were found to be in agreement with each other. At the lowest temperature, 180^{o}C, there were a number of compounds detected, mostly with tobacco and HEETS but also a few with kānuka. This was expected as Figure 4 shows tobacco and HEETS lose many compounds at the lower temperature range, while kānuka had minimal change. The detection of acetic acid, hydroxyacetone, propylene glycol, glycerol, 2-cyclopentene-1,4-dione, furfural, 5-methylfurfural, hydroquinone and nicotine at these low temperatures corresponds with the EGA results (Figure 16) and with literature (Saliba et al., 2018; Marcilla et al., 2015; Zhang et al., 2020; Forster et al., 2015; and Bassilakis et al., 2001). Creosol, 4-ethylguaiacol, eugenol, 4-propylguaiacol, and acetoguaiacone were detected in kānuka but were also expected to be detected in tobacco and HEETS (Rodgman & Perfetti, 2013). From Figure 16 and Senneca et al. (2007), benzene was expected to appear at lower temperatures for tobacco and HEETS, and appear in kānuka around the 330^{o}C. The reason why it did not is unknown.

The m/z ratios analysed in the EGA/MS were chosen with the intention of identifying potentially harmful compounds and desirable flavour or aroma compounds. For this project, the EGA/MS experiments were completed first and due to issues with the equipment the Py-GC/MS experiments were completed much later. Ideally the compounds listed in Table 11 would be cross referenced with Figure 16 but some were not because of time constraints.

For the compounds not investigated by the EGA/MS, succindialdehyde is a breakdown product from furfural which is why it is present at temperatures over 330^{o}C (Tshabala et al., 2012). Li et al. (2019) noted succindialdehyde was produced from *Osmanthus fragrans* wood heated to 500^{o}C, and Yang et al. (2020) found the same for *Toona sinesis* wood. Succindialdehyde has been extracted from pine wood, orange wood and oriental tobacco (Chen et al., 2016, Kravetz et al., 2020 and Liu et al., 2015).

Phenol generation starts from around 300^{o}C (Kibet et al., 2015; McGrath et al., 2009, and Torikai et al., 2004) and is a common breakdown product of lignin (Kibet et al., 2012). It has been detected in tobacco and wood (McGrath et al., 2009; Czegeny et al., 2009; Torikai et al., 2004; Guzelciftci et al., 2020; Murwanashyaka et al., 2001, and Luo et al., 2017).

2-Hydroxycyclopent-2-en-1-one is a cellulose breakdown product (Peng et al., 2018), so the lower temperature formation from the tobaccos compared to kānuka, in Table 11, would be due to crystalline structure. 2-Hydroxycyclopent-2-en-1-one has been reported in tobacco vapour (Marcilla et al., 2011) and no literature was found for wood vapour, although, Tekin et al. (2013) extracted 3,4-dimethyl-2-hydroxycyclopent-2-en-1-one from Scotch pine wood.

Furfuryl alcohol has been identified in kānuka vapour, at 335^{o}C, by Chen et al., (2021). It has also been found in tobacco and other woods (Yuan et al., 2007; Schmeltz et al., 1978; Blasi et al., 2009, and Chen et al., 2021).

Acetylpropionyl is an added ingredient in tobacco products (Pierce et al., 2013, and Ilies et al., 2020), which explains why it was not detected in kānuka.

3-Methylcyclopentane-1,2-dione is a degradation product from cellulose (Peng et al., 2018), and was extracted from *Toona sinensis* wood (Adfa et al., 2017) and *Cinnamomum parthenoxylon* wood (Adfa et al., 2020). Indole provides a "strong, burley tobacco taste" (Yan et al., 2018) and has only been identified in tobacco not kānuka (Senneca et al., 2007, and Adam et al., 2005).

2,3-Dihydrobenzofuran in tobacco vapour was studied by Lee et al. (2000), who detected it as low as 330^{o}C in the lamina section of leaf but not the midrib section. 5-Hydroxymethylfurfural is formed from the Maillard reaction and has been detected in tobacco and wood vapour (Severin et al., 2010, and Hosoya et al., 2007).

4H-Pyran-4-one,2,3-dihydro-3,5-dihydroxy-6-methyl- has been extracted by Ishiguro et al. (1976) from Flue-cured tobacco. Homovanillyl alcohol is a lignin degradation product (Wang et al., 2015) and has been identified in kānuka vapour after heating to 335^{o}C (Chen et al., 2021). Vanillic acid forms from the decomposition of lignin (Gnomes & Rodrigues, 2019), and has been identified in kānuka heated to 335^{o}C (Chen et al., 2021) but also should have been identified in tobacco (Xe et al., 2010).

2,5-Dimethoxy-4-methylbenzaldehyde is a degradation product from xylene (Sangthong et al., 2016), and Chen et al. (2018) detected its presence after heating rubber wood to 500^{o}C. Ethanone, 1-(2,6-dihydroxy-4-methoxyphenyl)- has been reported in willow wood vapour by Nowakowshi et al. (2007).

Syringaldehyde is a naturally occurring component in cellulose and lignin (Ibrahim et al., 2012). It has been detected in kānuka vapour at 335^{o}C (Chen et al., 2021) and should have also been detected in tobacco (Yang & Wender, 1964). Phenol, 2,6-dimethoxy-4-(2-propenyl)- is a natural component of lignin (Liu et al., 2015, and Wang et al., 2011) and Zhang et al. (2009) extracted it from Chinese fir wood.

3,5-Dimethoxy-4-hydroxyphenylacetic acid has been extracted from *Cinnamomum parthenoxylon* at 450^{o}C by Adfa et al. (2020). Octadecanoic acid is a common fatty acid found in tobacco and wood (Moon et al., 1995; Mecca et al., 2018; Guitierrez et al., 1999; Peng et al., 2017, Ivanov et al., 2012).

Triacontane and tetratriacontane are common long chain alkane hydrocarbons found in tobacco vapour (Saffari et al., 2014; Choi et al., 2011; Han et al., 2013; Ruiz-Rodriguez et al., 2008, and Popova et al., 2019). Vitamin E is a natural component synthesised in tobacco leaves (Han et al., 2013).

Compounds from kānuka are generally found at the higher end of the temperature range investigated here. The larger crystalline structure of cellulose in kānuka requires more energy to breakdown and so explains why degradation products form at a higher temperature compared to tobacco and HEETS. Levoglucosan, which is a primary cellulose degradation product, was found at 270^{o}C for HEETS, 300^{o}C for tobacco and 330^{o}C for kānuka most likely for this reason. Acetic acid, a ubiquitous degradation product of biomass pyrolysis, was first observed at 180^{o}C for tobacco and HEETS but at 300^{o}C for kānuka. The EGA/MS results in Figure 16 show that tobacco and HEETS start releasing an m/z 60 compound from around 150^{o}C, while kānuka releases m/z 60 compounds at 300^{o}C. This early release in tobacco and HEETS will be because acetic acid is an added ingredient to the tobacco sample (Ministry of Health, 2019) and so volatilises. At higher temperatures, and exclusively in kānuka, it forms during decomposition of the biomass. However, its presence at these higher temperatures is much less in tobacco and HEETS, which may be because it is known to interact extensively with glycerol which is an additive in these products (Hu et al., 2019).

The Py-GC/MS is not able to easily differentiate isomers. Table 10 states that m-cresol was identified in the biomass, but m-cresol, o-cresol, and p-cresol have a retention index of 1014 and the same chemical formula. The isomers in Table 10, are likely to be a combination of their arrangements.

3.12 Polycyclic aromatic hydrocarbons from pyrolysis gas chromatography mass spectrometry

Polycyclic aromatic hydrocarbons (PAHs) are important to identify as they are carcinogenic or potentially carcinogenic (Abdel-Shafy & Mansour, 2016). Highlighted by the toxic equivalency factors (Table 4), the health risk from PAHs varies, the most toxic being benzo[a]pyrene and dibenz[a,h]anthracene, which severely increases cancer risk (Alcanzare, 2006; Fowles & Bates, 2000; and Nisbet & LaGoy, 1992). PAH generation tends to occur significantly at higher temperatures, so many papers investigate the generation of PAHs from 400°C to 1000°C (Adam et al., 2009; Czegeny et al., 2009; Kalaitzoglou et al., 2006; Lu & Zhu, 2007; Nakajima et al., 2007; Szramowiat-Sala et al., 2019; and Tsekos et al., 2020). There is little research on the generation of PAHs below 400°C, so this work aims to fill a gap in knowledge. PAHs are usually present in low concentrations so can be difficult to detect with oversaturation from other compounds (Figure 17). The pyrograms shown in Figure 17 (and Appendices I) were compared to the pyrogram for a standardised mixture of 16 polycyclic aromatic hydrocarbons. By comparing the base peak and fragmentation ions some PAHs were found present in biomass vapour, as shown in Table 11. The presence of each PAH is noted by a '+' and the peak intensity by the number of the '+' symbols. In cases where the identifying peaks are all present but overlap occurs with other compounds, which changes the peak height order for the PAH and its fragmentation ions from that expected, it is not possible to positively identify the presence of a particular PAH and so '(+)' is given.

Table 11: PAHs identified with the Py-GC/MS for a 2mg samples of biomass heated at various temperatures between 180°C and 500°C.

m/z	Compounds	HEETS				Tobacco				Kānuka			
		180	230	350	500	180	230	350	500	230	280	350	500
128	Naphthalene (NAP) ($C_{10}H_8$)	+	+	++	++	+	+	++	+++	+	+	+	++
152	Acenaphthylene (ACY) ($C_{12}H_8$)	+	(+)	++	++	+	+	++	++	+	+	+	++
154	Acenaphthene (ACE) ($C_{12}H_{10}$)	+	(+)	++	++	+	+	++	+	(+)	+	(+)	(+)
166	Fluorene (FLU) ($C_{13}H_{10}$)	+	+	+	++	+	+	+	++	(+)	(+)	(+)	(+)
178	Phenanthrene (PHEN) ($C_{14}H_{10}$)	+	(+)	+	++	+	+	++	++	+	+	(+)	+
178	Anthracene (ANTH) ($C_{14}H_{10}$)	(+)	(+)	+	(+)	+	+	(+)	(+)	+	+	+	+
202	Fluoranthene (FLTH) ($C_{16}H_{10}$)	+	+	(+)	+	+	+	+	+	(+)	+	+	+
202	Pyrene (PYR) ($C_{16}H_{10}$)	+	+	+	+	(+)	+	+	++	+	+	+	+
228	Benzo(a)anthracene (B[a]A) ($C_{18}H_{12}$)	+	+	+	+	n.d.	+	+	+	+	(+)	+	+
228	Chrysene (CHRY) ($C_{18}H_{12}$)	+	+	+	+	n.d.	+	+	+	n.d.	(+)	(+)	+
252	Benzo(b)fluoranthene (B[b]F) ($C_{20}H_{12}$)	(+)	(+)	(+)	(+)	n.d.	(+)	(+)	(+)	n.d.	+	(+)	(+)
252	Benzo(k)fluoranthene (B[k]F) ($C_{20}H_{12}$)	(+)	(+)	(+)	(+)	n.d.	(+)	(+)	(+)	n.d.	(+)	+	+
252	Benzo(a)pyrene (B[a]P) ($C_{20}H_{12}$)	(+)	(+)	(+)	+	n.d.	(+)	(+)	+	n.d.	(+)	(+)	+

276	Benzo[g,h,i]perylene (B[ghi]P) ($C_{22}H_{12}$)	n.d.	n.d.	n.d.	n.d.	n.d.	n.d.	n.d.	+	n.d.	n.d.	n.d.	n.d.
276	Indeno[1,2,3-cd]pyrene (IND) ($C_{22}H_{12}$)	n.d.	n.d.	+	+	n.d.	n.d.	(+)	+	n.d.	n.d.	n.d.	n.d.
278	Dibenz[a,h]anthracene (D[ah]A) ($C_{22}H_{14}$)	n.d.	n.d.	n.d.	+	n.d.	n.d.	n.d.	(+)	n.d.	n.d.	n.d.	n.d.

+ = compounds identified with the base peak intensity lower than 9,000

++ = compounds identified with the base peak intensity between 9,000 and 90,000

+++ = compounds identified with the base peak intensity higher than 90,000

(+) = the relative intensity of the MS peaks does not match with the peaks of standard, due to interference

n.d. = compounds not identified

Across the four temperatures from 180^{o}C to 500, the increase of the base peak values indicates how the concentration of a PAH changes relative to itself. This is a qualitative tool and it cannot be used to quantify concentration relative to the biomass vapour production. As expected, the base peak intensity for some PAHs shows an increasing trend with higher temperatures (Auer et al., 2017; Hofer et al., 2017; Liu et al., 2013; Varlet et al. 2007; and Torikai et al., 2004). Some PAHs, at the higher m/z range, do not show much change from 180^{o}C to 500^{o}C. The PAHs were identified by comparing the ratio of the base peak with surrounding peaks (Table 4). Due to compounds having similar retention indices they could overlap and affect the relative intensity of a peak, leading it to be labelled as (+) , as noted, in Table 11. Such a compounds is anthracene, identified in kānuka from 180^{o}C to 500^{o}C which, although denoted (+), is also likely to be present in HEETS and tobacco at the same temperature range. PAHs like naphthalene, anthracene, fluoranthene and benzo[a]anthracene are expected at low temperatures as they are decomposition product from cellulose and polyphenols (Czegeny et al., 2009, and Paschke et al., 2002). The heavier PAHs like benzo[a]anthracene, chrysene, benzo[b] fluoranthene and benzo[a]pyrene are expected at higher temperatures as they are degradation products of lignin (Racovita et al., 2020, and Liu et al., 2011). Many papers have struggled with the identification of benzo[g,h,i]perylene, indeno[1,2,3-cd]pyrene and dibenz[a,h]anthracene in biomass vapour (Skrbic et al., 2018; Paschke et al., 2016; and Auer et al., 2017). In general, for combusted biomass low molecular mass PAHs are more prominent in the vapour phase, while high molecular mass PAHs are more prominent in the particulate phase (Lu & Zhu, 2007; Djinovic-Stojanovic et al., 2013; and Jimenez et al., 2017). Varlet et al. (2007) used a friction smoker to produce vapour from beech wood at roughly 380^{o}C and detected trace amounts of benzo(a)pyrene and benzo[g,h,i]pyrene. Tobacco and HEETS results are similar, with indeno[1,2,3-cd]pyrene and dibenz[a,h]anthracene being detected or probably detected at high temperatures, but not detected in kānuka. Some PAHs like dibenz[a,h]anthracene, benzo(a)pyrene and benzo[a]anthracene would be more likely in the tobaccos as they can be also formed from the decomposition of nicotine and other tobacco components (Smith et al., 2000).

The production of PAHs increases in the presence of oxygen (Czegeny et al., 2009; Adam et al., 2009; and Skrbic et al., 2018), which was not studied here. High temperatures, long smouldering time, and larger samples promote the formation of high molecular mass PAHs are they are mainly formed from secondary reactions (Alcanzare, 2006, and McGrath et al., 2007). Therefore, it should be noted that the conditions used in these experiments, no oxygen and 2 mg sample mass, should have minimised the production of PAHs, but nevertheless they were still detected. The work therefore isolates temperature as the determining factor for PAH formation. That the two PAHs with the highest toxic equivalency factors, benzo(a)pyrene and dibenz[a,h]anthracene, are observed at 500°C is significant. It is therefore recommended that smoke generation from kānuka or tobacco products not be carried out at this

temperature. Such recommendations are important for the operational safety of these devices. Some temperatures below this received (+) for these compounds, indicating overlapping, and so requiring further study.

4. Conclusions

The aim of this report was to investigate the compounds produced during anoxic low temperature heating on tobacco, HEETS and kānuka. The work is an anoxic study because the focus is on the pyrolysis products produced in Heat not Burn (HnB) devices used for tobacco and in food smokers such as friction smokers. These devices aim to avoid the higher temperatures that occur in smouldering combustion systems, like cigarette smoking and smouldering smoke generation. Three materials were studied, loose leaf tobacco, HEETS, and kānuka. Generic heat-not-burn (HnB) devices heat loose leaf tobacco (and other herbaceous material) to 230^{o}C. HEETS are Philip Morris branded tobacco sticks, designed to be used with their IQOS device and heated to 350^{o}C. Kānuka woodchips are used in food smoker generators. They make the most popular wood smoke in New Zealand. The temperature ranges from 180^{o}C to 390^{o}C was of particular interest in this study, because most primary pyrolysis reactions are completed over this temperature range. A number of analysis methods were used to compare these three biomasses.

Proximate analysis determined the moisture, volatile, ash and fixed carbon content for the biomass, based on weight loss while heating. The tobacco moisture content was found to be 16.85 wt.%, HEETS was 13.75 wt.%, and kānuka was 7.58 wt.%. Tobacco and HEETS have a higher moisture content than kānuka because leaves contain more water and they have added humectants, like glycerol and propylene glycol. The ash content was significantly different with tobacco containing 6.30 wt.% ash, HEETS 7.52 wt.% ash, and kānuka an order of magnitude lower at 0.71 wt.% ash.

Ultimate analysis determined the nitrogen, carbon, hydrogen, sulphur, and oxygen content of the biomass. The nitrogen content varied with tobacco at 2.04 wt.% nitrogen, HEETS at 1.91 wt.% nitrogen and kānuka again an order of magnitude lower at 0.19% nitrogen. The major component of tobacco containing nitrogen is nicotine ($C_{10}H_{14}N_2$), with small amounts of tobacco-specific nitrosamines, like NNK ($C_{10}H_{13}N_3O_2$) and NNN ($C_9H_{11}N_3O$). These types of components are responsible for the higher nitrogen content in tobacco and HEETS.

Mass loss during heating was measured by thermogravimetry. Four peaks in the differential mass loss curve for tobacco and HEETS are at 180^{o}C, 260^{o}C, 310^{o}C, and 350^{o}C, and three peaks for kānuka are at 280^{o}C, 350^{o}C, and 380^{o}C. The early peak at 180^{o}C is related to the loss of moisture and volatile extractives such as nicotine. The other three peaks are dominated by hemicellulose, cellulose, and lignin degradation respectively. The kānuka peaks occur at higher temperatures most likely due to it having a larger cellulose crystalline structure than tobacco and HEETS and thus requiring more energy to break down.

The STA-TG/DSC was used to investigate the heat of pyrolysis. Exothermicity increased with sample size. Larger samples had higher fill levels within the crucible, which means vapour had more contact with solid particles as it egressed. Greater contact increases the chance of heterogeneous secondary reactions, which condense more secondary char. Tobacco and HEETS were also found to progress to more exothermic behaviour than kānuka, likely due to their higher ash content catalysing secondary reactions. Another factor may also be the less crystalline nature of the cellulose in tobacco and HEETS compared to kānuka, as mentioned above, and so requiring less energy to break down.

The EGA total ion chromatogram (TIC) was compared to the differential mass loss curve (dTG). It compared well for kānuka in the same way as for other woods but, for tobacco at higher temperatures,

showed an extra peak, which was observed as a long shoulder in HEETS. This extra peak was caused by the generation of many small molecules which greatly increase the ion count and are likely to be from both primary reactions and secondary heterogeneous reactions catalysed by the ash content. Gas phase homogeneous reactions can generally be discounted because the temperatures are well below where they are expected. Indeed, the heat of pyrolysis model, developed by Jones et al. (2020), disregards homogeneous reactions as they do not significantly affect the pyrolysis of wood. The balance between primary and secondary reaction, which are regarded as endothermic and exothermic respectively, can be seen in the DSC heat flow data, where the heat flow reduces significantly after cellulose degradation. Integrated over the temperature range, the overall heat of pyrolysis transitions from endothermic to exothermic as sample mass increases, reflecting the role of the tortuous path distance of volatile as they escape from the sample and the opportunity for secondary reactions to take place. Tobacco and HEETS become more exothermic with sample size than kānuka, due most likely to their high ash content catalysing secondary reactions more readily.

SEM images revealed kānuka had a tighter porous structure than tobacco and HEETS. This property will favour secondary reactions when the local pressure increases inside the pores. However, secondary reactions seemed to occur more readily in the tobacco and HEETS, driven most likely by their order of magnitude higher ash content.

EGA/MS and Py-GC/MS were used to identify compounds in the biomass vapour at different temperatures. Some major compounds found in all the biomass were acetic acid, hydroxyacetone, furfural, cresol, mequinol, vanillin, syringol, levoglucosan and isoeugenol. Many compounds begin to appear at higher temperatures for kānuka because of the higher energy needed to lyse the more crystalline cellulose structure in kānuka. Nicotine and limonene are major compounds only found in tobacco and HEETS. Nicotine is an extractive and so volatilises mostly below 200^{o}C. Some compounds were able to be detected as low as 180^{o}C, but at low intensities. The number of compounds identified and their absolute intensities increased with temperature. The Py-GC/MS identified PAHs and other potentially harmful compounds, like benzene and m-cresol, within the range of interest produced from low temperature heating. Indeno[1,2,3-cd]pyrene, which increases cancer risk, was detected in HEETS vapour at 350^{o}C. Benzene, which increases cancer risk and effects reproductive health, was detected in tobacco vapour from 330^{o}C and HEETS vapour from 350^{o}C. The compound m-cresol, which effects cardiovascular health, was detected in all three biomasses vapour at 350^{o}C and was detected as low as 300^{o}C in tobacco vapour. The method used here was qualitative, and so did not determine exact concentrations. Now that compounds have been identified, further research should be conducted for a better understanding of the chemical hazard risk.

Overall, this research has highlighted some interesting points that should be further explored to increase operational safety and minimize chemical hazard risk in low temperature heating devices.

Overall, this research highlights the similarities and differences in smoke made from tobacco products and wood smoke. A clear similarity is that the conditions of smoke generation are common to recreational heat-not-burn devices and friction smoke generators for food smoking. A clear difference is the kānuka wood is additive free, unlike tobacco or HEETS. While the additives and their functions have not been explored *per se*, one of the consequences is that the ash content is nearly ten times higher in tobacco and HEETS: their samples become more exothermic at small sample sizes and, at temperatures above 390^{o}C, generate more mole molecular volatiles. In all three biomasses, this research shows that temperature is the determining factor for the appearance of compounds. For designers of these devices, careful control of temperature is paramount to strike the right balance between the generation of desirable compounds. For designers of these devices, careful control of temperature is paramount to strike the right balance

between the generation of desirable compounds and prevention of undesirable compounds. It is recommended that temperatures must be no higher than 350^{o}C

References

Abdel-Shafy, H. I., & Mansour, M. S. M. (2016). A review on polycyclic aromatic hydrocarbons: Source, environmental impact, effect on human health and remediation. *Egyptian Journal of Petroleum, 25*(1), 107-123. https://doi.org/10.1016/j.ejpe.2015.03.011

Abrego, J., Atienza-Martinez, M., Plou, F., & Arauzo, J. (2019). Heat requirement for fixed bed pyrolysis of beechwood chips. *Energy, 178*, 145-157. https://doi-org.ezproxy.massey.ac.nz/10.1016/j.energy.2019.04.078

Adam, T., Baker, R. R., & Zimmermann, R. (2007). Investigation, by single photon ionisation (SPI)-time-of-flight mass spectrometry (TOFMS), of the effect of different cigarette-lighting devices on the chemical composition of the first cigarette puff. *Analytical and Bioanalytical Chemistry, 387*, 575-584. https://doi.org/10.1007/s00216-006-0945-9

Adam, T., Mitschke, S., & Baker, R. R. (2009). Investigation of tobacco pyrolysis gases and puff-by-puff resolved cigarette smoke by single photon ionisation (SPI) – time-of-flight mass spectrometry (TOFMS). *Beitrage zur Tabakforschung International/ Contributions to Tobacco Research, 23*(4), 203-226. https://doi.org/10.2478/cttr-2013-0860

Adam, T., Streibel, T., Mitschke, S., Muhlberger, F., Baker, R. R., & Zimmermann, R. (2005). Application of time-of-flight mass spectrometry with laser-based photoionization methods for analytical pyrolysis of PVC and tobacco. *Journal of Analytical and Applied Pyrolysis, 74*(1-2), 454-464. https://doi.org/10.1016/j.jaap.2004.11.021

Adeleke, A. A., Odusote, J. K., Lasode, O. A., Ikubanni, P. P., Madhurai, M., & Paswan, D. (2019). Evaluation of thermal decomposition characteristics and kinetic parameters of melina wood. *Biofuels*. https://doi.org/10.1080/17597269.2019.1646541

Adfa, M., Kusnanda, A. J., Saputra, W. D., Banon, C., Efdi, M., & Koketsu, M. (2017). Termiticidal activity of *Toona sinesis* wood vinegar against *Coptotermes curvignathus* Holmgren. *Rasayan Journal of Chemistry, 10*(4), 1088-1093. http://dx.doi.org/10.7324/RJC.2017.1041866

Adfa, M., Romayasa, A., Kusnanda, A. J., Avidlyandi, A., Yudha, S., Banon, C., & Gustian, I. (2020). Chemical components, antitermite and antifungal activities of *Cinnamomum parthenoxylon* wood vinegar. *Journal of the Korean Wood Science and Technology, 48*(1), 107-116. https://www.koreascience.or.kr/article/JAKO202012764215922.pdf

Aguirre, J. L., Baena, J., Martin, M. T., Nozal, L., Gonzalez, S., Manjon, J. L., & Peinado, M. (2020). Composition, ageing and herbicidal properties of wood vinegar obtained through fast biomass pyrolysis. *Energies, 13*(10), 2418. https://doi.org/10.3390/en13102418

Ahamad, T., & Alshehri, S. M. (2012). TG-FTIR-MS (Evolved Gas Analysis) of bidi tobacco powder during combustion and pyrolysis. *Journal of Hazardous Materials, 199-200,* 200-208. https://doi-org.ezproxy.massey.ac.nz/10.1016/j.jhazmat.2011.10.090

Akalin, M. K., & Karagoz, S. (2011). Tobacco residue pyrolysis: Part 1. Thermal. *BioResources, 6*(2), 1520-1531. https://pdfs.semanticscholar.org/4e5a/d5b83ef628a0393f2bb76c5e3d539357bab6.pdf

Akazawa, M., Kojima, Y., & Kato, Y. (2015). Formation of polycyclic compounds from phenols by fast pyrolysis. *EC Agriculture, 1*(2), 67-85. https://www.ecronicon.com/ecag/agriculture-ECAG-01-00007.php

Akpan, V., Huang, S., Lodovici, M., & Dolara, P. (2006). High levels of carcinogenic polycyclic aromatic hydrocarbons (PAH) in 20 brands of Chinese cigarettes. *Journal of Applied Toxicology, 26*, 480-483. https://doi.org/10.1002/jat.1165

Akpinar, O., Levent, O., Sabanci, S., Uysal, R. S., & Sapci, B. (2011). Optimization and comparison of dilute acid pretreatment of selected agricultural residues for recovery of xylose. *BioResources, 6*(4), 4103-4116. https://bioresources.cnr.ncsu.edu/BioRes_06/BioRes_06_Unsecured/BioRes_06_4_4103_Akpinar_LSUS_Optim_Dil_Acid_Pretreat_Ag_Res_Xylose_1745.pdf

Alcanzare, R. J. C. (2006). *Polycyclic aromatic compounds in wood soot extracts from Henan, China* [Master's thesis, Louisiana State University]. LSU Digital Commons. https://core.ac.uk/download/pdf/217390758.pdf

Alpert, H. R., Agaku, I. T., & Connolly, G. N. (2016). A study of pyrazines in cigarettes and how additive might be used to enhance tobacco addiction. *Tobacco Control, 25*(4), 444-450. https://dx.doi.org/10.1136%2Ftobaccocontrol-2014-051943

Anca-Couce, A. (2016). Reaction mechanisms and multi-scale modelling of lignocellulosic biomass pyrolysis. *Progress in Energy and Combustion Science, 53*, 41-79. https://doi-org.ezproxy.massey.ac.nz/10.1016/j.pecs.2015.10.002

Anca-Couce, A., Mehrabian, R., Scharler, R., & Obernberger, I. (2014). Kinetic scheme of biomass pyrolysis considering secondary charring reactions. *Energy Conversion and Management, 87*, 687-696. https://doi-org.ezproxy.massey.ac.nz/10.1016/j.enconman.2014.07.061

Anca-Couce, A., & Scharler, R. (2017). Modelling heat of reaction in biomass pyrolysis with detailed reaction schemes. *Fuel, 206*, 572-579. https://doi.org/10.1016/j.fuel.2017.06.011

Antal, M. J., Allen, S. G., Dai, X., Shimizu, B., Tam, M. S., & Gronli, M. (2000). Attainment of the theoretical yield of carbon from biomass. *Industrial & Engineering Chemistry Research, 39*(11), 4024-4031. https://pubs-acs-org.ezproxy.massey.ac.nz/doi/full/10.1021/ie000511u

Arisandi, R., Ashitani, T., Takahashi, K., Marsoem, S. N., & Lukmandaru, G. (2020). Lipophilic extractives of the wood and bark from *Eucalyptus pellita* F. Muell grown in Merauke, Indonesia. *Journal of Wood Chemistry and Technology, 40*(2). https://doi-org.ezproxy.massey.ac.nz/10.1021/ie000511u

Arvanitoyannis, I. S., & Kotsanopoulos, K. V. (2011). Smoking of fish and seafood: History, methods and effects on physical, nutritional and microbiological properties. *Food and Bioprocess Technology, 5*, 831-853. https://doi-org.ezproxy.massey.ac.nz/10.1007/s11947-011-0690-8

Asomaning, J., Mussone, P., & Bressler, D. C. (2014). Pyrolysis of polyunsaturated fatty acid. *Fuel Processing Technology, 120*, 89-95. https://doi-org.ezproxy.massey.ac.nz/10.1016/j.fuproc.2013.12.007

Auer, R., Concha-Lozano, N., & Jacot-Sadowski, I. (2017). Heat-not-burn tobacco cigarettes: Smoke by any other name. *JAMA Internal Medicine, 177*(7), 1050-1052. https://doi.org/10.1001/jamainternmed.2017.1419

Azeez, A. M., Meier, D., Odermatt, J., & Wilner, T. (2010). Fast pyrolysis of African and European lignocellulosic biomasses using Py-GC/MS and fluidized bed reactor. *Energy Fuels, 24*(3), 2078-2085. https://doi-org.ezproxy.massey.ac.nz/10.1021/ef9012856

Bacsik, Z., McGregor, J., & Mink, J. (2007). FTIR analysis of gaseous compounds in the mainstream smoke of regular and light cigarettes. *Food and Chemical Toxicology, 45*(2), 266-271. https://doi.org/10.1016/j.fct.2006.08.018

Baer, I., De la Calle, B., & Taylor, P. (2010). 3-MCPD in food other than soy sauce or hydrolysed vegetable protein (HVP). *Analytical & Bioanalytical Chemistry, 396*(1), 443-456. https://doi.org/10.1007/s00216-009-3177-y

Bailey, L. A., Nascarella, M. A., Kerper, L. E., & Rhomberg, L. R. (2016). Hypothesis-based weight-of-evidence evaluation and risk assessment for naphthalene carcinogenesis. *Critical Reviews in Toxicology, 46*(1), 1-42. https://doi.org/10.3109/10408444.2015.1061477

Baker, R. R., & Bishop, L. J. (2005). The pyrolysis of non-volatile tobacco ingredients using a system that simulates cigarette combustion conditions. *Journal of Analytical and Applied Pyrolysis, 74*(1-2), 145-170. https://doi-org.ezproxy.massey.ac.nz/10.1016/j.jaap.2004.10.011

Baker, R. R., & Bishop, L. J. (2004). The pyrolysis of tobacco ingredients. *Journal of Analytical and Applied Pyrolysis, 71*(1), 223-311. https://doi-org.ezproxy.massey.ac.nz/10.1016/S0165-2370(03)00090-1

Baker, R. R., Coburn, S., & Liu, C. (2006). The pyrolytic formation of formaldehyde from sugars and tobacco. *Journal of Analytical and Applied Pyrolysis, 77*(1), 12-21. https://doi-org.ezproxy.massey.ac.nz/10.1016/j.jaap.2005.12.009

Baker, R. R., Coburn, S., Liu, C., & Tetteh, J. (2005). Pyrolysis of saccharide tobacco ingredients: A TGA-FTIR investigation. *Journal of Analytical and Applied Pyrolysis, 74*(1-2), 171-180. https://doi.org/10.1016/j.jaap.2004.09.005

Banyasz, J. L., Li, S., Lyons-Hart, J., & Shafer, K. H. (2001). Gas evolution and the mechanism of cellulose pyrolysis. *Fuel, 80*(12), 1757-1763. https://doi-org.ezproxy.massey.ac.nz/10.1016/S0016-2361(01)00060-6

Barbero-Lopez, A., Chibily, S., Tomppo, L., Salami, A., Ancin-Murguzur, F. J., Venalainen, M., Lappalainen, R., & Haapala, A. (2019). Pyrolysis distillates from tree bark and fibre hemp inhibit the growth of wood-decaying fungi. *Industrial Crops and Products, 129*, 604-610. https://doi-org.ezproxy.massey.ac.nz/10.1016/j.indcrop.2018.12.049

Barbosa, J. M. S., Re-Poppi, M., & Santiago-Silva. (2006). Polycyclic aromatic hydrocarbons from wood pyrolysis in charcoal production furnaces. *Environmental Research, 101*(3), 304-311. https://doi-org.ezproxy.massey.ac.nz/10.1016/j.envres.2006.01.005

Basile, L., Tugnoli, A., Stramigioli, C., & Cozzani, V. (2016). Thermal effects during biomass pyrolysis. *Thermochimica Acta, 636*, 63-70. https://doi-org.ezproxy.massey.ac.nz/10.1016/j.tca.2016.05.002

Bassilakis, R., Carangelo, R. M., & Wojtowicz, M. A. (2001). TG-FTIR analysis of biomass pyrolysis. *Fuel, 80*(12), 1765-1786. https://doi-org.ezproxy.massey.ac.nz/10.1016/S0016-2361(01)00061-8

Bekki, K., Inaba, Y., Uchiyama, S., & Kunugita, N. (2017). Comparison of chemicals in mainstream smoke in heat-not-burn tobacco and combustion cigarettes. *Journal of UOEH, 39*(3), 201-207. https://www.jstage.jst.go.jp/article/juoeh/39/3/39_201/_pdf/-char/en

Bendre, R. S., Rajput, J. D., Bagul, S. D., & Karandikar, P. S. (2016). Outlooks on medicinal properties of eugenol and its synthetic derivatives. *Natural Products Chemistry & Research, 4*(3). https://doi.org/10.4172/2329-6836.1000212

Benowitz, N. L. (2010). Nicotine addiction. *The New England Journal of Medicine, 362*(24), 2295-2303. https://dx.doi.org/10.1056%2FNEJMra0809890

Bentley, M. C., Almstetter, M., Arndt, D., Knorr, A., Martin, E., Pospisil, P., & Maeder, S. (2020). Comprehensive chemical characterization of the aerosol generated by a heated tobacco product by untargeted screening. *Analytical and Bioanalytical Chemistry, 412*(11), 2675-2685. https://doi.org/10.1007/s00216-020-02502-1

Blasi, C. D., Galgano, A., & Branca, C. (2009). Effects of potassium hydroxide impregnation on wood pyrolysis. *Energy Fuels, 23*(2), 1045-1054. https://doi.org/10.1021/ef800827q

Blazso, M., Babinszki, B., Czegeny, Z., Barta-Rajnai, E., Sebestyen, Z., Jakab, E., Nicol, J., Liu, C., & McAdam, K. (2018). Thermo-oxidative degradation of aromatic flavour compounds under simulated tobacco heating product condition. *Journal of Analytical and Applied Pyrolysis, 134*, 405-414. https://doi-org.ezproxy.massey.ac.nz/10.1016/j.jaap.2018.07.007

Branca, C., Giudicianni, P., & Blasi, C. D. (2003). GC/MS characterization of liquids generated from low-temperature pyrolysis of wood. *Industrial & Engineering Chemistry Research, 42*(14), 3190-3202. https://doi-org.ezproxy.massey.ac.nz/10.1021/ie030066d

Braun, M., & Antonietti, M. (2017). A continuous flow process for the production of 2,5-dimethylfuran from fructose using (non-noble metal based) heterogeneous catalysis. *Green Chemistry, 19*, 3813-3819. https://doi.org/10.1039/C7GC01055A

Brown, B. G., Borschke, A. J., & Doolittle, D. J. (2003). An analysis of the role of tobacco-specific nitrosamines in the carcinogenicity of tobacco smoke. *Nonlinearity in Biology, Toxicology, Medicine, 1*(2), 179-198. https://dx.doi.org/10.1080%2F15401420391434324

Bruns, E. A., Krapf, M., Orasche, J., Huang, Y., Zimmermann, R., Drinovec, L., Mocnik, G., El-Haddad, I., Slowik, J. G., Dommen, J., Baltensperger, U., & Prevot, A. S. H. (2015). Characterization of primary and secondary wood combustion products generated under different burner loads. *Atmospheric Chemistry and Physics, 15*, 2825-2841. https://doi.org/10.5194/acp-15-2825-2015

Buist, J. M., Grayson, S. J., & Woolley, W. D. (2012). *Fire and Cellular Polymers*. Springer Science & Business Media.

Bunnings Warehouse. (2020). *Big Smoke Fisherman's Blend Wood Chips.* https://www.bunnings.co.nz/big-smoke-fisherman-s-blend-wood-chips-2kg_p0310581

Buyel, J. F., Gruchow, H. M., Todter, N., & Wehner, M. (2016). Determination of the thermal properties of leaves by non-invasive contact-free laser probing. *Journal of Biotechnology, 217*, 100-108. https://doi-org.ezproxy.massey.ac.nz/10.1016/j.jbiotec.2015.11.008

Caco, N. S. A., Jones, J. R., Chen, Q., Ripberger, G. D., & Eyres, G. T. (2018). Precise determination of specific heat of culinary smoking wood by means of DSC (Differential Scanning Calorimetry). *Chemeca 2018, 182*, 1-8. https://search.informit.com.au/documentSummary;dn=047557047467513;res=IELENG;type=pdf

Cai, B., Li, Z., Wang, R., Geng, Z., Shi, Y., Xie, S., Wang, Z., Yang, Z., & Ren, X. (2019). Emission level of seven mainstream smoke toxicants from cigarette with variable tobacco leaf constituents. *Regulatory Toxicology and Pharmacology, 103*, 181-188. https://doi-org.ezproxy.massey.ac.nz/10.1016/j.yrtph.2019.01.032

Cai, J., Liu, B., Ling, P., & Su, Q. (2002). Analysis of free and bound volatiles by gas chromatography and gas chromatography-mass spectrometry in uncased and cased tobaccos. *Journal of Chromatography A, 947*(2), 267-275. https://doi-org.ezproxy.massey.ac.nz/10.1016/S0021-9673(02)00015-8

Calabuig, E., Juarez-Serrano, N., & Marcilla, A. (2019). TG-FTIR study of evolved gas in the decomposition of different types of tobacco. Effect of the addition of SBA-15. *Thermochimica Acta, 671*, 209-219. https://doi-org.ezproxy.massey.ac.nz/10.1016/j.tca.2018.12.006

Canam, T., Park, J., Yu, K. Y., Campbell, M. M., Ellis, D. D., & Mansfield, S. D. (2006). Varied growth, biomass and cellulose content in tobacco expressing yeast-derived invertases. *Planta, 224*, 1315-1327. https://doi.org/10.1007/s00425-006-0313-1

Cardoso, C. R., & Ataide, C. H. (2013). Analytical pyrolysis of tobacco residue: Effect of temperature and inorganic additives. *Journal of Analytical and Applied Pyrolysis, 99*, 49-57. https://doi-org.ezproxy.massey.ac.nz/10.1016/j.jaap.2012.10.029

Carmines, E. L., & Gaworski, C. L. (2005). Toxicological evaluation of glycerin as a cigarette ingredient. *Food and Chemical Toxicology, 43*(10), 1521-1539. https://doi-org.ezproxy.massey.ac.nz/10.1016/j.fct.2005.04.010

Chambreau, S. D., Lemieux, J., Wang, L., & Zhang, J. (2005). Mechanistic studies of the pyrolysis of 1,3-butadiene, 1,3-butadiene-1,1,4,4,-d_4, 1,2-butadiene, and 2-butyne by supersonic jet/photoionization mass spectrometry. *Journal of Physical Chemistry A, 109*(10), 2190-2196. https://doi-org.ezproxy.massey.ac.nz/10.1021/jp045010r

Charles, S. M., Batterman, S. A., & Jia, C. (2007). Composition and emissions of VOCs in main and side-stream smoke of research cigarettes. *Atmospheric Environment, 41*(26), 5371-5384. https://doi-org.ezproxy.massey.ac.nz/10.1016/j.atmosenv.2007.02.020

Chen, J., Fang, D., & Duan, F. (2018). Pore characteristics and fractal properties of biochar obtained from the pyrolysis of coarse wood in a fluidized-bed reactor. *Applied Energy, 218*, 54-65. https://doi-org.ezproxy.massey.ac.nz/10.1016/j.apenergy.2018.02.179

Chen, Q., Ripberger, G., Jones, J., Caco, N., Archer, R., Telfer, S., Eyres, G., & Silcock, P. (2021). Characterisation of New Zealand woods for food smoking. ***Not yet published.***

Chen, Q, Yang, R., Zhao, B., Li, Y., Wang, S., Wu, H., Zhou, Y., & Chen, C. (2014). Investigation of heat of biomass pyrolysis and secondary reactions by simultaneous thermogravimetry and differential scanning caorimetry. *Fuel, 134*, 467-476. https://doi-org.ezproxy.massey.ac.nz/10.1016/j.fuel.2014.05.092

Chen, W., Wang, C., Kumar, G., Rousset, P., Hsieh, T. (2018). Effect of torrefaction pretreatment on the pyrolysis of rubber wood sawdust analysed by Py-GC/MS. *Bioresource Technology, 259*, 469-473. https://doi.org/10.1016/j.biortech.2018.03.033

Chen, Y., Cao, W., & Atreya, A. (2016). An experimental study to investigate the effect of torrefaction temperature and time on pyrolysis of centimetre-scale pine wood particles. *Fuel Processing Technology, 153*, 74-80. https://doi.org/10.1016/j.fuproc.2016.08.003

Chen, Y., Chen, W., Lan, Y., Wang, K., Wu, Y., Zhong, X., Ying, K., Li, J., & Yang, G. (2018). Determination of 18 phenolic acids in tobacco and rhizosphere soil by ultra high performance liquid chromatography combined with triple quadrupole mass spectrometry. *Journal of Separation Science, 42*(4), 816-825. https://doi-org.ezproxy.massey.ac.nz/10.1002/jssc.201800819

Cheng, G., Varanasi, P., Li, C., Liu, H., Melnichenko, Y. B., Simmons, B. A., Kent, M. S., Singh, S. (2011). Transition of cellulose crystalline structure and surface morphology of biomass as a function of ionic liquid pretreatment and its relation to enzymatic hydrolysis. *Biomacromolecules, 12*(4), 933-941. https://doi.org/10.1021/bm101240z

Cheng, K., Wenming, Z., Chen, H., & Zhang, Y. P. (2019). Upgrade of wood sugar D-xylose to a value-added nutraceutical by in vitro metabolic engineering. *Metabolic Engineering, 52*, 1-8. https://doi.org/10.1016/j.ymben.2018.10.007

Cheng, S., Lin, P., Yang, J., Hsu, S., & Lee, H. (2001). Benzo[g,h,i]perylene synergistically transactivates benzo[a]pyrene-induced CYP1A1 gene expression by aryl hydrocarbon receptor pathway. *Toxicology and Applied Pharmacology, 170*(1), 63-68. https://doi-org.ezproxy.massey.ac.nz/10.1006/taap.2000.9082

Chida, M., Sone, Y., & Tamura, H. (2004). Aroma characteristics of stored tobacco cut leaves analyzed by a high vacuum distillation and canister system. *Journal of Agricultural and Food Chemistry, 52*(26), 7918-7924. https://doi-org.ezproxy.massey.ac.nz/10.1021/jf049223p

Chien, Y., Yang, T., Hung, K., Li, C., Xu, J., & Wu, J. (2018). Effects of heat treatment on the chemical compositions and thermal decomposition kinetics of Japanese cedar and beech wood. *Polymer Degradation and Stability, 158*, 220-227. https://doi-org.ezproxy.massey.ac.nz/10.1016/j.polymdegradstab.2018.11.003

Chitsamphandhvej, W., Asavasanti, S., Sukhummek, B., Angkaew, S., Titawong, K., & Saichunyoon, P. (2017). Volatile organic compounds of charcoal combustion smoke. In Y. Pornputtkul (Ed.), *Proceedings of the Pure and Applied Chemistry International Conference 2017 (PACCON2017)* (pp. 222-228). https://www.researchgate.net/publication/327287220_Volatile_organic_compounds_of_charcoal_combustion_smoke

Choi, Y. E., Lim, S., Kim, H., Han, J. Y., Lee, M., Yang, Y., Kim, J., & Kim, Y. (2011). Tobacco *NtLTP1*, a glandular-specific lipid transfer protein is required for lipid secretion from glandular trichomes. *The Plant Journal, 70*(3), 480-491. https://doi.org/10.1111/j.1365-313X.2011.04886.x

Cholewski, M., Tomczykowa, M., & Tomczyk, M. (2018). A comprehensive review of chemistry, sources and bioavailability of omega-3 fatty acids. *Nutrients, 10*(11), 1662. https://dx.doi.org/10.3390%2Fnu10111662

Chong, J., Pierrel, M., Atanassova, R., Werck-Reichhart, D., Fritig, B., & Saindrenan, P. (2001). Free and conjugated benzoic acid in tobacco plants and cell cultures. Induced accumulation upon elicitation of defence responses and role as salicylic acid precursors. *Plant Physiology, 125*(1), 318-328. https://dx.doi.org/10.1104%2Fpp.125.1.318

Christensen, E., Evans, R. J., & Carpenter, D. (2017). High-resolution mass spectrometric analysis of biomass pyrolysis vapors. *Journal of Analytical and Applied Pyrolysis, 124*, 327-334. https://doi-org.ezproxy.massey.ac.nz/10.1016/j.jaap.2017.01.015

Clapp, P. W., Lavrich, K. S., Heusden, C. A., Lazarowski, E. R., Carson, J. L., & Jaspers, I. (2019). Cinnamaldehyde in flavored e-cigarette liquids temporarily suppresses bronchial epithelial cell ciliary motility by dysregulation of mitochondrial function. *American Journal of Physiology, 316*(3), 470-486. https://doi.org/10.1152/ajplung.00304.2018

Cocchiara, J., Letizia, C. S., Lalko, J., Lapczynski, A., & Api, A. M. (2005). Fragrance material review on cinnamaldehyde. *Food and Chemical Toxicology, 43*(6), 867-923. https://doi-org.ezproxy.massey.ac.nz/10.1016/j.fct.2004.09.014

Coggins, C. R. E., Edmiston, J. S., Jerome, A. M., Langston, T. B., Sena, E. J., Smith, D. C., & Oldham, M. J. (2011). A comprehensive evaluation of the toxicology of cigarette ingredients: essential oils and resins. *Inhalation Toxicology, 23*(S1), 41-69. http://search.ebscohost.com/login.aspx?direct=true&db=edb&AN=61081847&site=eds-live&scope=site

Coggins, C. R. E., Merki, J. A., & Oldham, M. J. (2011). A comprehensive evaluation of the toxicology of cigarette ingredients: heterocyclic nitrogen compounds. *Inhalation Toxicology, 23*(S1), 84-89. https://doi.org/10.3109/08958378.2010.545841

Coggon, M. M., Veres, P. R., Yuan, B., Koss, A., Warneke, C., Gilman, J., Lerner, B., Peischl, J., Aikin, K. C., Stockwell, C. E., Hatch, L. E., Ryerson, T. B., Roberts, J. M., Yokelson, R. J., & de Gouw, J. A. (2016). Emissions of nitrogen-containing organic compounds from the burning of herbaceous are arboraceous

biomass: Fuel composition dependence and the variability of commonly used nitrile tracers. *Geophysical Research Letters, 43*(18), 9903-9912. https://doi.org/10.1002/2016GL070562

Conde, F. J., Ayala, J. H., Afonso, A. M., & Gonzalez, V. (2005). Polycyclic aromatic hydrocarbons in smoke used to smoke cheese produced by the combustion of rock rose (*Cistus monspeliensis*) and tree heather (*Erica arborea*) Wood. *Journal of Agricultural and Food Chemistry, 53*(1), 176-182. https://doi-org.ezproxy.massey.ac.nz/10.1021/jf0492013

Connolly, G. N., Alpert, H. R., Rees, V., Carpenter, C., Wayne, G. F., Vallone, D., & Koh, H. Effect of the New York State cigarette fire safety standard on ignition propensity, smoke constituents, and the consumer market. *Tobacco Control, 14*, 321-327. http://dx.doi.org.ezproxy.massey.ac.nz/10.1136/tc.2005.011759

Costa, R., Lourenco, A., Oliveria, V., & Pereira, H. (2019). Chemical characterization of cork, phloem and wood from different *Quercus suber* provenances and trees. *Heliyon, 6*(3). https://doi.org/10.1016/j.heliyon.2019.e02910

Cserhati, T., & Forgacs, E. (2003). Flavor (Flavour) Compounds | Structures and Characteristics. In B. Caballero (Ed.), *Encyclopedia of Food Science and Nutrition* (2nd ed., pp. 2509-2517). Academic Press. https://doi.org/10.1016/B0-12-227055-X/00483-1

Cullere, L., de Simon, B. F., Cadahia, E., Ferreira, V., Hernandez-Orte, P., & Cacho, J. (2013). Characterization by gas chromatography-olfactometry of the most odor-active compounds in extracts prepared from acacia, chestnust, cherry, ash and oak woods. *LWT – Food Science and Technology, 53*(1), 240-248. https://doi-org.ezproxy.massey.ac.nz/10.1016/j.lwt.2013.02.010

Czegeny, Z., Blazso, M., Varhegyi, G., Jakab, E., Liu, C., & Nappi, L. (2009). Formation of selected toxicants from tobacco under different pyrolysis conditions. *Journal of Analytical and Applied Pyrolysis, 85*(1-2), 47-53. https://doi-org.ezproxy.massey.ac.nz/10.1016/j.jaap.2008.10.001

Czegeny, Z., Bozi, J., Sebstyen, Z., Blazso, M., Jakab, E., Barta-Rajnai, E., Forster, M., Nicol, J., McAdam, K. G., & Liu, C. (2016). Thermal behaviour of selected flavour ingredients and additives under simulated cigarette combustion and tobacco heating conditions. *Journal of Analytical and Applied Pyrolysis, 121*, 190-204. https://doi.org/10.1016/j.jaap.2016.07.020

Czoli, C. D., Goniewicz, M. L., Palumbo, M., Leigh, N., White, C. M., & Hammond, D. (2019). Identification of flavouring chemicals and potential toxicants in e-cigarette products in Ontario, Canada. *Canadian Journal of Public Health, 110*(5), 542-550. https://doi.org/10.17269/s41997-019-00208-1

Daheng, Z., Jinfeng, H., Chunyun, G., & Ru, C. (2001). Changes in higher fatty acids and related biochemical characteristics of flue-cured tobacco during aging. *Beitrage zur Tabakforschung International/ Contributions to Tobacco Research, 19*(6). https://doi.org/10.2478/cttr-2013-0718

Danckwerts, P. V. (1958). The effect of incomplete mixing on homogeneous reactions. *Chemical Engineering Science, 8*(1-2), 93-102. https://doi.org/10.1016/0009-2509(58)80040-8

Daugaard, D. E., & Brown, R. C. (2003). Enthalpy for pyrolysis for several types of biomass. *Energy & Fuels, 17*, 934-939. https://lib.dr.iastate.edu/cgi/viewcontent.cgi?article=1156&context=me_pubs

De Lange, P. (2014). A revision of the New Zealand *Kunzea ericoides* (Myrtaceae) complex. *PhytoKeys, 40*, 1-185. https://doi.org/10.3897/phytokeys.40.7973

De Macedo, L. A., Commandre, J., Rousset, P., Valette, J., & Petrissans, M. (2018). Influence of potassium carbonate addition on the condensable species released during wood torrefaction. *Fuel Processing Technology, 168*, 248-257. https://doi-org.ezproxy.massey.ac.nz/10.1016/j.fuproc.2017.10.012

De Simon, B. F., Esteruelas, E., Munoz, A. M., Cadahia, E., & Sanz, M. (2009). Volatile compounds in acacia, chestnut, cherry, ash, and oak woods, with a view to their use in cooperage. *Journal of Agricultural and Food Chemistry, 57*(8), 3217-3227. https://doi-org.ezproxy.massey.ac.nz/10.1021/jf803463h

De Simon, B. F., Muino, I., & Cadahia, E. (2010). Characterization of volatile constituents in commercial oak wood chips. *Journal of Agricultural and Food Chemistry, 58*(17), 9587-9596. https://doi-org.ezproxy.massey.ac.nz/10.1021/jf101301a

Del Rio, J. C., Speranza, M., Gutierrez, A., Martinez, M. J., & Martinez, A. T. (2002). Lignin attack during eucalypt wood decay by selected basidiomycetes: a Py-GC/MS study. *Journal of Analytical and Applied Pyrolysis, 64*, 421-431. https://digital.csic.es/bitstream/10261/39873/3/2002-DELRIO-JAAP-64-421.pdf

Demirbas, A. (2002). Analysis of liquid products from biomass via flash pyrolysis. *Energy Sources, 24*(4), 337-345. https://doi.org/10.1080/00908310252888718

Diaz, E., Sad, M. E., & Iglesia, E. (2010). Homogeneous oxidation reactions of propanediols at low temperatures. *ChemSusChem, 3*(9), 1063-1070. https://doi-org.ezproxy.massey.ac.nz/10.1002/cssc.201000142

Dietenberger, M., & Hasburgh, L. (2016). *Wood Products: Thermal Degradation and Fire.* https://www.fpl.fs.fed.us/documnts/pdf2016/fpl_2016_dietenberger001.pdf

Ding, Y., Trommel, J. S., Yan, X. J., Ashley, D., & Watson, C. H. (2005). Determination of 14 polycyclic aromatic hydrocarbons in mainstream smoke from domestic cigarettes. *Environmental Science & Technology, 39*(2), 471-478. https://doi-org.ezproxy.massey.ac.nz/10.1021/es048690k

Ding, Y., Zhang, L., Ram, B., Jain, N., Wang, R. Y., Ashley, D. L., & Watson, C. H. (2008). Levels of tobacco-specific nitrosamines and polycyclic aromatic hydrocarbons in mainstream smoke from different tobacco varieties. *Cancer Epidemiology Biomarkers & Prevention, 17*(12). https://doi.org/10.1158/1055-9965.EPI-08-0320

Ding, Y., Zhu, L., Liu, S., Yu, H., & Dai, Y. (2013). Analytical method of free and conjugated neutral aroma compounds in tobacco by solvent extraction coupled with comprehensive two-dimensional gas chromatography-time-of-flight mass spectrometry. *Journal of Chromatography A, 1280*, 122-127. https://doi-org.ezproxy.massey.ac.nz/10.1016/j.chroma.2013.01.028

Discount T. (2017). *Easy RYO Fine Cut Tobacco.* https://www.discountt.co.nz/shop/TOBACCO/EASY/Easy+FINE+CUT+30g/x_sku/02140.html

Djinovic-Stojanovic, J., Popovic, A., Spiric, A., & Jira, W. (2013). Emission of polycyclic aromatic hydrocarbons from beech wood combustion. *Energy Sources, Part A: Recovery, Utilization, and Environmental Effects, 35*(4), 328-336. https://doi.org/10.1080/15567036.2010.503234

Domke, S. B., Pogue, R. F., Van Neer, F. J. R., Smith, C. M., & Wojciechoeski, B. W. (2001). Investigation of the kinetics of ethylbenzene pyrolysis using a temperature-scanning reactor. *Industrial & Engineering Chemistry Research, 40*(25), 5878-5884. https://doi-org.ezproxy.massey.ac.nz/10.1021/ie010483v

Donaldson, L. A., Kroese, H. W., Hill, S. J., & Franich, R. A. (2015). Detection of wood cell wall porosity using small carbohydrate molecules and confocal fluorescence microscopy. *Journal of Microscopy, 259*(3), 228-236. https://doi.org/10.1111/jmi.12257

Dong, J. & DeBusk, S. M. (2009). GC-MS analysis of hydrogen sulfide, carbonyl sulfide, methanethiol, carbon disulfide, methyl thiocyanate and methyl disulfide in mainstream vapour phase cigarette smoke. *Chromatographia, 71*, 259-265. https://doi-org.ezproxy.massey.ac.nz/10.1365/s10337-009-1434-z

Doshi, G. M., Nalawade, V. V., Mukadam, A. S., Chaskar, P. K., Zine, S. P., Somani, R. R., & Une, H. D. (2015). Structural elucidation of chemical constituents from *Benincasa hispida* seeds and *Carissa congesta* roots by gas chromatography: Mass spectroscopy. *Pharmacognosy Research, 7*(3), 282-293. https://dx.doi.org/10.4103%2F0974-8490.157179

Dunlop, A. J., Clunie, I., Stephen, D. W. S., Allison, J. J. (2014). Determination of cotinine by LC-MS-MS with automated solid-phase extraction. *Journal of Chromatographic Science, 52*(4), 351-356. https://doi.org/10.1093/chromsci/bmt038

Dusautoir, R., Zarcone, G., Verriele, M., Garcon, G., Fronval, I., Beauval, N., Allorge, D., Riffault, V., Locoge, N., Lo-Guidice, J., & Antherieu, S. (2021). Comparison of the chemical composition of aerosols from heated tobacco products, electronic cigarettes and tobacco cigarettes and their toxic impacts on the human bronchial epithelial BEAS-2B cells. *Journal of Hazardous Materials, 401*(5), 123417. https://doi.org/10.1016/j.jhazmat.2020.123417

EPA. (2008). *Ethylene Oxide.* https://www.epa.gov/sites/production/files/2016-09/documents/ethylene-oxide.pdf

European Union. (2011). Commission Regulation (EU) No 835/2011. *Official Journal of the European Union, 54,* 4-8. https://eur-lex.europa.eu/legal-content/EN/TXT/?uri=uriserv:OJ.L_.2011.215.01.0004.01.ENG&toc=OJ:L:2011:215:TOC

FAO/WHO. (2007). *Discussion Paper on Chloropropanols Derived from the Manufacture of Acid-HVP and the Heat Processing of Foods.* Codex Committee on Contaminants in Foods. http://www.fao.org/tempref/codex/Meetings/CCCF/cccf1/cf01_13e.pdf

Farsalinos, K. E., Yannovits, N., Sarri, T., Voudris, V., Poulas, K., & Leischow, S. J. (2018). Carbonyl emissions from a novel heated tobacco products (IQOS): comparison with an e-cigarette and a tobacco cigarette. *Addiction, 113*(11), 2099-2106. https://doi-org.ezproxy.massey.ac.nz/10.1111/add.14365

FDA. (2019). *Harmful and Potentially Harmful Constituents in Tobacco Products and Tobacco Smoke: Established List.* https://www.fda.gov/tobacco-products/rules-regulations-and-guidance/harmful-and-potentially-harmful-constituents-tobacco-products-and-tobacco-smoke-established-list

Filpo, G. D., Palermo, A. M., Rachiele, F., & Nicoletta, F. P. (2013). Preventing fungal growth in wood by titanium dioxide nanoparticles. *International Biodeterioration & Biodegradation, 85*, 217-222. https://doi-org.ezproxy.massey.ac.nz/10.1016/j.ibiod.2013.07.007

Fine, P. M., Cass, G. R., & Simoneit, B. R. T. (2004). Chemical characterization of fine particle emissions from the wood stove combustion of prevalent United States tree species. *Environmental Engineering Science, 21*(6), 705-720. http://www.bioenergylists.org/stovesdoc/Roden/ees.2004.21.705.pdf

Fine, P. M., Cass, G. R., & Simoneit, R. T. (2002). Chemical characterization of fine particle emissions from the fireplace combustion of woods grown in the Southern United States. *Environmental Science & Technology, 36*(7), 1442-1451. https://doi-org.ezproxy.massey.ac.nz/10.1021/es0108988

Fine, P. M., Cass, G. R., & Simoneit, B. R. T. (2001). Chemical characterization of fine particle emissions from fireplace combustion of woods grown in Northeastern United States. *Environmental Science & Technology, 35*(13), 2665-2675. https://doi-org.ezproxy.massey.ac.nz/10.1021/es001466k

Flamini, R., Vedova, A. D., Cancian, D., Panighel, A., & Rosso, M. D. (2007). GC/MS-positive ion chemical ionization and MS/MS study of volatile benzene compounds in five different woods used in barrel making. *Journal of Mass Spectrometry, 42*(5), 641-646. https://doi-org.ezproxy.massey.ac.nz/10.1002/jms.1193

Flechard, C. R., Massad, R., S., Loubert, B., Personne, E., Simpson, D., Bash, J. O., Cooter, E. J., Nemitz, E., & Sutton, M. A. Advances in understanding, models and parameterizations of biosphere-atmosphere ammonia exchange. *Biogeosciences, 10*, 5183-5225. https://doi.org/10.5194/bg-10-5183-2013

Forchhammer, L., Moller, P., Riddervold, I. S., Bonlokke, J., Massling, A., Sigsgaard, T., & Loft, S. (2012). Controlled human wood smoke exposure: oxidative stress, inflammation and microvascular function. *Particle and Fibre Toxicology, 9*(7). https://doi.org/10.1186/1743-8977-9-7

Forster, M., Lui, C., Duke, M. G., McAdam, K. G., & Proctor, C. J. (2015). An experimental method to study emissions from heated tobacco between 100-200°C. *Chemistry Central Journal, 9*(20). https://doi.org/10.1186/s13065-015-0096-1

Fowles, J., & Bates, M. (2000). *The Chemical Constituents in Cigarettes and Cigarette Smoke: Priorities for Harm Reduction.* https://www.moh.govt.nz/notebook/nbbooks.nsf/0/FBC6507272B60331CC257B81000F5EF4/$file/chemicalconstituentscigarettespriorities.pdf

Funda, T., Fundova, I., Gorzsas, A., Fries, A., & Wu, H. X. (2019). Predicting the chemical composition of juvenile and mature woods in Scots pine (*Pinus sylvestris L.*) using FTIR spectroscopy. *Wood Science and Technology, 54*, 289-311. https://doi.org/10.1007/s00226-020-01159-4

Gao, W., Chen, K., Xiang, Z., Yang, F., Zeng, J., Li, J., Yang, R., Rao, G., & Tao, H. (2013). Kinetic study on pyrolysis of tobacco residues from the cigarette industry. *Industrial Crops and Products, 44,* 152-157. https://doi-org.ezproxy.massey.ac.nz/10.1016/j.indcrop.2012.10.032

Garcia-Iruela, A., Esteban, L. G., Fernandez, F. G., Palacios, P., Rodriguez-Navarro, A. B., Martin-Sampedro, R., & Eugenio, M. E. (2019). Effect of vacuum/pressure cycles on cell wall composition and structure of poplar wood. *Cellulose, 26*, 8543-8556. https://doi-org.ezproxy.massey.ac.nz/10.1007/s10570-019-02692-7

Gaworski, C. L., Lemus-Olalde, R., & Carmines, E. L. (2008). Toxicological evaluation of potassium sorbate added to cigarette tobacco. *Food and Chemical Toxicology, 46*(1), 339-351. https://doi-org.ezproxy.massey.ac.nz/10.1016/j.fct.2007.08.012

Geiss, O., & Kotzias, D. (2007). *Tobacco, Cigarettes and Cigarette Smoke: An Overview.* https://publications.jrc.ec.europa.eu/repository/bitstream/111111111/8885/1/7472%20-%20EUR22783EN_Geiss_Kotzias.pdf

Gomes, E. D., & Rodrigues, A. E. (2019). Lignin biorefinery: Separation of vanillin, vanillic acid and actovanollone by adsorption. *Separation and Purification Technology, 216*, 92-101. https://doi.org/10.1016/j.seppur.2019.01.071

Gomez, C., Velo, E., Barontini, F., & Cozzani, V. (2009). Influence of secondary reactions on the heat of pyrolysis of biomass. *Industrial & Engineering Chemistry Research, 48*(23), 10222-10233. https://doi-org.ezproxy.massey.ac.nz/10.1021/ie9007985

Gomez-Siurana, A., Marcilla, A., Beltran, M., Berenguer, D., Martinez-Castellanos, I., & Menargues, S. (2013). TGA/FTIR study of tobacco and glycerol-tobacco mixtures. *Thermochimica Acta, 573*, 146-157. https://doi-org.ezproxy.massey.ac.nz/10.1016/j.tca.2013.09.007

Gomez-Siurana, A., Marcilla, A., Beltran, M., Martinez, I., Berenguer, D., Garcia-Martinez, R., & Hernandez-Selva, T. (2011). Thermogravimetric study of the pyrolysis of tobacco and several ingredients used in the fabrication of commercial cigarettes: Effect of the presence of MCM-41. *Thermochimica Acta, 523*(1-2), 161-169. https://doi-org.ezproxy.massey.ac.nz/10.1016/j.tca.2011.05.018

Gu, W., Yu, Z., Fang, S., Dai, M., Chen, L., & Ma, X. (2019). Effects of hydrothermal carbonization on catalytic fast pyrolysis of tobacco stems. *Biomass Conversion and Biorefinery, 9*(35), 1-16. https://doi-org.ezproxy.massey.ac.nz/10.1007/s13399-019-00509-y

Gu, X., Ma, X., Li, L., Liu, C., Cheng, K., & Li, Z. (2013). Pyrolysis of poplar wood sawdust by TG-FTIR and Py-GC/MS. *Journal of Analytical and Applied Pyrolysis, 102*, 16-23. https://doi-org.ezproxy.massey.ac.nz/10.1016/j.jaap.2013.04.009

Guedes, C. M., Pinto, A. B., Moreira, R. F. A., & de Maria, C. A. B. (2004). Study of the aroma compounds of rose apple (*Syzygium jambos* Alston) fruit from Brazil. *European Food Research and Technology, 219*, 460-464. https://doi-org.ezproxy.massey.ac.nz/10.1007/s00217-004-0967-5

Guillen, M. D., & Manzanos, M. J. (2005). Characteristics of smoke flavourings obtained from mixtures of oak *(Quercus* sp.) wood and aromatic plants (*Thymus vulgaris* L. and *Salvia lavandulifolia* Vahl.). *Flavour and Fragrance Journal, 20*, 676-685. https://doi.org/10.1002/ffj.1599

Guler, G. (2019). A comparison of brutian pine (*Pinus brutia Ten.*) root volatile compounds vs. the stem wood. *BioResources, 14*(4), 9307-9316. https://doi.org/10.15376/biores.14.4.9307-9316

Guo, G., Liu, X., Ran, L., Qiang, L., Yu, H., & Li, M. (2019). Characterization of tobacco stalk lignin using nuclear magnetic resonance spectrometry and its pyrolysis behavior at different temperatures. *Journal of Analytical and Applied Pyrolysis, 142*, 104665. https://doi-org.ezproxy.massey.ac.nz/10.1016/j.jaap.2019.104665

Gustafson, P., Ostman, C., & Sallsten, G. (2008). Indoor levels of polycyclic aromatic hydrocarbons in homes with or without wood burning for heating. *Environmental Science & Technology, 42*(14), 5074-5080. https://doi-org.ezproxy.massey.ac.nz/10.1021/es800304y

Gutierreez, A., del Rio, J. C., Gonzalez-Vila, F. J., & Martin, F. (1999). Chemical composition of lipophilic extractives from *Eucalyptus globulus* Labill. wood. *Holzforschung, 53*(5). https://citeseerx.ist.psu.edu/viewdoc/download?doi=10.1.1.723.4385&rep=rep1&type=pdf

Guzelciftci, B., Park, K., & Kim, J. (2020). Production of phenol-rich bio-oil via a two-stage pyrolysis of wood. *Energy, 200*, 117536. https://doi.org/10.1016/j.energy.2020.117536

Han, J., Wang, H., & Choi, Y. (2013). Production of dammarenediol-II triterpene in a cell suspension culture of transgenic tobacco. *Plant Cell Reports, 33*, 225-233. https://doi.org/10.1007/s00299-013-1523-1

He, F., Yi, W., & Bai, X. (2006). Investigation on caloric requirement of biomass pyrolysis using TG-DSC analyzer. *Energy Conversion and Management, 47*(15-16), 2461-2469. https://doi-org.ezproxy.massey.ac.nz/10.1016/j.enconman.2005.11.011

Hedberg, E., Kristensson, A., Ohlsson, M., Johansson, C., Johansson, P., Swietlicki, E., Vesely, V., Wideqvist, U., & Westerholm, R. (2002). Chemical and physical characterization of emissions from birch wood combustion in a wood stove. *Atmospheric Environment, 36*(30), 4823-4837. https://doi-org.ezproxy.massey.ac.nz/10.1016/S1352-2310(02)00417-X

Heigenmoser, A., Fuchs, R., Windeisen, E., & Wegener, G. (2011). Characterization of different wood samples using a new combined method of evolved gas analysis and pyrolysis-gas chromatography/mass spectrometry. *Wood Science and Technology, 46*, 637-642. https://doi-org.ezproxy.massey.ac.nz/10.1007/s00226-011-0435-x

Hofer, I., Gautier, L., Sauteur, E. C., Dobler, M., Python, A., O'Reilly, C., Gisi, D., Tinguely, E., Wehren, & Fidalgo, E. G. (2019). A screening method by gas chromatography-mass spectrometry for the quantification of 24 aerosol constituents from heat-not-burn tobacco products. *Beitrage zur Tabakforschung International/ Contributions to Tobacco Research, 28*(7), 317-328. https://doi.org/10.2478/cttr-2019-0013

Hoffman, D., & Hoffman, I. (2001). The Changing Cigarette: Chemical and Bioassays. In D. R. Shopland (Eds.), *Risks associated with smoking cigarettes with low machine-measured yields of tar and nicotine* (pp. 152-192). U.S. Department of Health and Human Services. https://cancercontrol.cancer.gov/brp/tcrb/monographs/13/m13_complete.pdf

Hosoya, T., Kawamoto, H., & Saka, S. (2007). Pyrolysis behaviors of wood and its constituent polymers at gasification temperature. *Journal of Analytical and Applied Pyrolysis, 78*(2), 328-336. https://doi.org/10.1016/j.jaap.2006.08.008

Hou-long, J., Chen, X., Dai-bin, W., Li-na, G., Ming, Z., & Xiao-wei, Z. (2016). Effect of tobacco leaf width-length ratio on tobacco quality: a case study in the Chongqing tobacco production area. *Australia Journal of Crop Science, 10*(10), 1455-1459. https://doi.org/10.21475/ajcs.2016.10.10.p7670

Howitt, S. M., & Udvardi, M. K. (2000). Structure, function and regulation of ammonium transporters in plants. *Biochimica et Biophysica Acta (BBA) – Biomembranes, 1465*(1-2), 152-170. https://doi.org/10.1016/S0005-2736(00)00136-X

Hrablay, I., & Jelemensky, L. (2016). Kinetic study of thermochemical degradation of lignocellulosic materials based on TG-FTIR, Py-GC/MS and 13C NMR experiments. *Chemical and Biochemical Engineering Quarterly, 30*(3), 359-372. https://doi.org/10.15255/cabeq.2015.2309

Hu, B., Lu, Q., Wu, Y., Liu, J., Li, K., Dong, C., & Yang, Y. (2019). Interaction between acetic acid and glycerol: A model for secondary reactions during holocellulose pyrolysis. *The Journal of Physical Chemistry A, 123*(3), 674-681. https://doi.org/10.1021/acs.jpca.8b11264

Huang, J., He, C., Wu, L., & Tong, H. (2016). Thermal degradation reaction mechanism of xylose: A DFT study. *Chemical Physics Letters, 658*, 114-124. https://doi-org.ezproxy.massey.ac.nz/10.1016/j.cplett.2016.06.025

Hua, W., Liu, C., Wu, S., & Li, X. (2016). Analysis of structural units and their influence on thermal degradation of alkali lignins. *BioResources, 11*(1), 1959-1970. https://doi.org/10.15376/biores.11.1.1959-1970

Huff, J., & Infante, P. F. (2011). Styrene exposure and risk of cancer. *Mutagenesis, 26*(5), 583-584. https://dx.doi.org/10.1093%2Fmutage%2Fger033

Hussar, E., Richards, S., Lin, Z., Dixon, R. P., & Johnson, K. A. (2012). Human health risk assessment of 16 priority polycyclic aromatic hydrocarbons in soils of Chattanooga, Tennessee, USA. *Water, Air, and Soil Pollution, 223*(9), 5535-5548. https://dx.doi.org/10.1007%2Fs11270-012-1265-7

IARC. (2006). Formaldehyde, 2-Butoxyethanol and 1-tert-Butoxypropan-2-ol. *IARC Monographs on the Evaluation of Carcinogenic Risks to Humans, 88*. https://www.ncbi.nlm.nih.gov/books/NBK326468/

IARC. (2010). Some Non-heterocyclic Polycyclic Aromatic Hydrocarbons and Some Related Exposures. *IARC Monographs on the Evaluation of Carcinogenic Risks to Humans, 92.* https://www.ncbi.nlm.nih.gov/books/NBK321713/

Ibrahim, M. N. M., Sriprasanthi, R. B., Shamsudeen, S., Adam, F., & Bhawani, S. A. (2012). A concise review of the natural existence synthesis, properties, and applications of syringaldehyde. *BioResources, 7*(3), 4377-4399.

https://ojs.cnr.ncsu.edu/index.php/BioRes/article/view/BioRes_07_3_Ibrahim_SSAB_Review_Synthesis_Properties_Applications_Syringaldehyde

Ilies, B. D., Moosakutty, S. P., Kharbatia, N. M., & Sarathy, S. M. (2020). Identification of volatile constituents released from IQOS heat-not-burn tobacco HeatSticks using a direct sampling method. *Tobacco control,* 055521. https://doi.org/10.1136/tobaccocontrol-2019-055521

Im, H., Rasouli, F., & Hajaligol, M. (2003). Formation of nitric oxide during tobacco oxidation. *Journal of Agricultural and Food Chemistry, 51*(25), 7366-7372. https://doi-org.ezproxy.massey.ac.nz/10.1021/jf030393w

Inaba, Y., Uchiyama, S., & Kunugita, N. (2018). Spectrophotometric determination of ammonia levels in tobacco fillers of and sidestream smoke from different cigarette brands in Japan. *Environmental Health and Preventive Medicine, 23*(15). https://doi.org/10.1186/s12199-018-0704-5

Intani, K., Latif, S., Kabir, R., & Muller, J. (2016). Effect of self-purging pyrolysis on yield of biochar from maize cobs, husks and leaves. *Bioresource Technology, 218*, 541-551. https://doi-org.ezproxy.massey.ac.nz/10.1016/j.biortech.2016.06.114

International Maritime Organization (2001). *Advanced Training in Fire Fighting.* IMO Publishing.

Ishiguro, S., Yano, S., Sugawara, S., & Kaburaki, Y. (2005). Comparisons of acids in smoke of lamina and midrib of flue-cured tobacco leaves. *Agricultural and Biological Chemistry, 40*(10), 2005-2011. https://doi.org/10.1080/00021369.1976.10862328

Islamova, S. I., & Khamatgalimov, A. R. (2016). Thermogravimetric and kinetic analyses of the thermal decomposition of fuel wood. *Solid Fuel Chemistry, 51*(2), 83-87. https://doi.org/10.3103/S0361521917020045

Ivanov, A. G., Allakhverdiev, S. I., Huner, N. P. A., & Murata, N. (2012). Genetic decrease in fatty acid unsaturation of phosphatidylglycerol increased photoinhibition of photosystems I at low temperature in tobacco leaves. *Biochimica et Biophysica Acta (BBA) – Bioenergetics, 1817*(8), 1374-1379. https://doi-org.ezproxy.massey.ac.nz/10.1016/j.bbabio.2012.03.010

Jang, E., & Kang, C. (2019). Changes in gas permeability and pore structure of wood under heat treating temperature conditions. *Journal of Wood Science, 65*, 37. https://doi.org/10.1186/s10086-019-1815-3

Jeffery, J., Carradus, M., Songin, K., Pettit, M., Pettit, K., & Wright, C. (2018). Optimized method for determination of 16 FDA polycyclic aromatic hydrocarbons (PAHs) in mainstream cigarette smoke by gas chromatography-mass spectrometry. *Chemistry Central Journal, 12*(27). https://doi.org/10.1186/s13065-018-0397-2

Jensen, R. P., Strongin, R. M., & Peyton, D. H. (2017). Solvent chemistry in the electronic cigarette reaction vessel. *Scientific Report, 7*(42549). https://doi.org/10.1038/srep42549

Jimenez, J., Farias, O., Quiroz, R., & Yanez, J. (2017). Emission factors of particulate matter, polycyclic aromatic hydrocarbons, and levoglucosan from wood combustion in south-central Chile. *Journal of the Air & Waste Management Association, 67*(7), 806-813. https://doi.org/10.1080/10962247.2017.1295114

Jira, W. (2010). 3-Monochloropropane-1,2-diol (3-MCPD) in smoked meat products: investigation of contents and estimation of the uptake by the consumption of smoke meat products. *Fleischwirtschaft, 90*, 115-118. https://www.semanticscholar.org/paper/3-Monochloropropane-1%2C2-diol-(3-MCPD)-in-smoked-of-Jira/5fca5903c499d1e745c547d26b3ac60d55dad204

Johnson, T. J., Yokelson, R. J., Akagi, S. K., Burling, I. R., Weise, D. R., Urbanski, S. P., Stockwell, C. E., Reardon, J., Lincoln, E. N., Profeta, L. T. M., Mendoza, A., Schneider, M. D. W., Sams, R. L., Williams, S. D., Wold, C. E., Griffith, D. W. T., Cameron, M., Gilman, J. B., Warneke, C., … de Gouw, J. (2013). *Final Report for SERDP Project RC-1649: Advanced Chemical Measurements of Smoke from DoD-prescribed Burns.* https://www.pnnl.gov/main/publications/external/technical_reports/PNNL-23025.pdf

Jones, J., Chen, Q., & Ripberger, G. D. (2020). Secondary reactions and the heat of pyrolysis of wood. *Energy Technology, 8*(6). https://doi-org.ezproxy.massey.ac.nz/10.1002/ente.202000130

Jones, J., Ripberger, G., Eyres, G., Silcock, P., & Archer, R. (2017, June/July). Adding Value by Culinary Smoking. *Food New Zealand, 17*(3), 12-14. http://www.foodnz.co.nz/uploads/PDFs/FNZvol17No3FIETCulinarySmoking.pdf

Juan, Y., & Ke-qiang, Q. (2009). Preparation of activated carbon by chemical activation under vacuum. *Environmental Science & Technology, 43*(9), 3385-3390. https://doi-org.ezproxy.massey.ac.nz/10.1021/es8036115

Kalaitzoglou, M., & Samara, C. (2006). Gas/particle partitioning and yield levels of polycyclic aromatic hydrocarbons and n-alkanes in the mainstream cigarette smoke of commercial cigarette brands. *Food*

and Chemical Toxicology, 44(8), 1432-1442. https://doi-org.ezproxy.massey.ac.nz/10.1016/j.fct.2006.03.010

Kandyala, R., Raghavendra, S. P. C., Rajasekharan, S. T. (2010). Xylene: An overview of its health hazards and preventive measures. *Journal of Oral and Maxillofacial Pathology, 14*(1), 1-5. https://dx.doi.org/10.4103%2F0973-029X.64299

Kaur, G., Muthumalage, T., & Rahman, I. (2018). Mechanisms of toxicity and biomarkers of flavoring and flavor enhancing chemicals in emerging tobacco and non-tobacco products. *Toxicology Letters, 15*(288), 143-155. https://dx.doi.org/10.1016%2Fj.toxlet.2018.02.025

Kawamoto, H. (2017). Lignin pyrolysis reactions. *Journal of Wood Science, 63*, 117-132. https://doi.org/10.1007/s10086-016-1606-z

Khachatryan, L., Xu, M., Wu, A., Pechagin, M., & Astryan, R. (2016). Radicals and molecular products from the gas-phase pyrolysis of lignin model compounds. Cinnamyl alcohol. *Journal of Analytical and Applied Pyrolysis, 121*, 75-83. https://doi-org.ezproxy.massey.ac.nz/10.1016/j.jaap.2016.07.004

Khattab, A. R., Ibrahim, A. S., Ibrahim, S. M., El-Seoud, K. A. A., Soliman, W. E., & El-Fiky, F. K. (2015). LC-MS/MS based-comparative study of (S)-nicotine metabolism by microorganisms, mushrooms and plant cultures: Parallels to its mammalian metabolic fate. *Bulletin of Faculty of Pharmacy, Cairo University, 53*(2), 93-99. https://doi.org/10.1016/j.bfopcu.2015.04.002

Khelfa, A., Bensakhria, A., & Weber, J. V. (2013). Investigations into the pyrolytic behaviour of birch wood and its main components: Primary degradation mechanisms, additivity and metallic salt effects. *Journal of Analytical and Applied Pyrolysis, 101*, 111-121. https://doi-org.ezproxy.massey.ac.nz/10.1016/j.jaap.2013.02.004

Kibet, J. K., Jebet, A., & Kinyanjui, T. (2019). Molecular oxygenates from the thermal degradation of tobacco and material characterization of tobacco char. *Scientific African, 5*(153). https://doi.org/10.1016/j.sciaf.2019.e00153

Kibet, J., Khachatryan, L., & Dellinger, B. (2012). Molecular products and radicals from pyrolysis of lignin. *Environmental Science & Technology, 46*(23) 12994-13001. https://doi-org.ezproxy.massey.ac.nz/10.1021/es302942c

Kim, J., Lee, J. H., Park, J., Kim, J. K., An, D., Song, I. K., Choi, J. W. (2015). Catalytic pyrolysis of lignin over HZSM-5 catalysts: Effect of various parameters on the production of aromatic hydrocarbon. *Journal of Analytical and Applied Pyrolysis, 114*, 273-280. https://doi-org.ezproxy.massey.ac.nz/10.1016/j.jaap.2015.06.007

Kim, Y., Lee, J., Kim, S., Baek, K., & Lee, J. (2015). Cinnamon bark oil and its components inhibit biofilm formation and toxin production. *International Journal of Food Microbiology, 195,* 30-39. https://doi-org.ezproxy.massey.ac.nz/10.1016/j.ijfoodmicro.2014.11.028

Kirkova, S., Srbinoska, M., Ivanova, S., & Georgieva, A. (2016). Determination of fatty acid composition of seed of oriental tobacco. *TyTyH, Tobacco, 66*(1-6), 53-58. https://doi.org/10.13140/RG.2.2.18885.14560

Klauser, F., Carlon, E., Kistler, M., Schmidl, C., Schwabl, M, Sturmlechner, R., Haslinger, W., & Kasper-Giebl, A. (2018). Emission characterization of modern wood stoves under real-life oriented operating conditions. *Atmospheric Environment, 192,* 257-266. https://doi-org.ezproxy.massey.ac.nz/10.1016/j.atmosenv.2018.08.024

Klauser, F., Schwabl, M., Kistler, M., Sedlmayer, I., Kienzl, N., Weissinger, A., Schmidl, C., Haslinger, W., & Kasper-Giebl, A. (2018). Development of a compact technique to measure benzo(a)pyrene emissions from residential wood combustion, and subsequent testing in six modern wood boilers. *Biomass and Bioenergy, 111*, 288-300. https://doi-org.ezproxy.massey.ac.nz/10.1016/j.biombioe.2017.05.004

Kleszyk, P., Ratajczak, P., Skowron, P., Jagiello, J., Abbas, Q., Frackowiak, E., & Beguin, F. (2015). Carbons with narrow pore size distribution prepared by simultaneous carbonization and self-activation of tobacco stems and their application to supercapacitors. *Carbon, 81*, 148-157. https://doi-org.ezproxy.massey.ac.nz/10.1016/j.carbon.2014.09.043

Konstantinou, E., Fotopoulou, F., Drosos, A., Dimakopoulou, N., Zagoriti, Z., Niarchos, A., Makrynioti, D., Kouretas, D., Farsalinos, K., Lagoumintzis, G., & Poulas, K. (2018). Tobacco-specific nitrosamines: A literature review. *Food and Chemical Toxicology, 118*, 198-203. https://doi-org.ezproxy.massey.ac.nz/10.1016/j.fct.2018.05.008

Kravetz, C., Leca, C., Brito, J. O., Saloni, D., & Tilotta, D. C. (2020). Characterization of selected pyrolysis products of diseased orange wood. *BioResources, 15*(3), 7118-7126. https://ojs.cnr.ncsu.edu/index.php/BioRes/article/view/BioRes_15_3_7118_Kravetz_Selected_Pyrolysis_Products

Krusemann, E. J., Visser, W. F., Cremers, J. W., Pennings, J. L., & Talhout, R. (2018). Identification of flavour additives in tobacco products to develop a flavour library. *Tobacco Control, 27*(1), 105-111. https://tobaccocontrol.bmj.com/content/27/1/105

Kulic, G. J., & Radojicic, V. B. (2011). Analysis of cellulose content in stalks and leaves of large leaf tobacco. *Journal of Agricultrual Sciences, 56*(3), 207-215. https://doi.org/10.2298/JAS1103207K

Kumagai, S., Matsuno, R., Grause, G., Kameda, T., Yoshioka, T. (2015). Enhancement of bio-oil production via pyrolysis of wood biomass by pretreatment with H_2SO_4. *Bioresource Technology, 178*, 76-82. https://doi-org.ezproxy.massey.ac.nz/10.1016/j.biortech.2014.09.146

Kuroiwa, T., Araki, N., & Nakanishi, Y. (2008). Measurement of thermal conductivity of cured tobacco material. *Food Science and Technology Research, 14*(2), 124-131. https://www.jstage.jst.go.jp/article/fstr/14/2/14_2_124/_pdf

Laino, T., Tuma, C., Moor, P., Martin, E., Stolz, S., & Curioni, A. (2012). Mechanisms of propylene glycol and triacetin pyrolysis. *Journal of Physical Chemistry A, 116*(18), 4602-4609. https://doi-org.ezproxy.massey.ac.nz/10.1021/jp300997d

Lasode, O. A., Balogun, A. O., & McDonald, A. G. (2014). Torrefaction of some Nigerian lignocellulosic resources and decomposition kinetics. *Journal of Analytical and Applied Pyrolysis, 109*, 47-55. https://doi.org/10.1016/j.jaap.2014.07.014

Lebouvier, N., Lawes, D., Hnawia, E., Page, M., Brophy, J., & Nour, M. (2014). The leaf, wood and bark oils of three species of *Mydocarpus* (Myodocarpaeceae) endemic to New Caledonia. *Natural Product Communications, 9*(9), 1223-1227. https://journals-sagepub-com.ezproxy.massey.ac.nz/doi/pdf/10.1177/1934578X1400900901

Lee, J., Jang, H., Kwag, J., & Lee, D. (2000). Comparison of pyrolytic components in lamina and midrib of flue-cured tobacco leaves. *Journal of the Korean Society of Tobacco Science, 22*(2), 176-183. https://www.koreascience.or.kr/article/JAKO200011922997987.pdf

Lempert, L. K., St.Helen, G., Gotts, J., Kozlovich, S., Springer, M., Halpern-Felsher, B., & Glantz, S. A. (2019). *In addition to the 19 constituents FDA proposes to add to the list of Harmful and Potentially Harmful Constituents, FDA should also add compounds that may be carcinogenic or cause pulmonary or cardiovascular harms when inhaled, especially oils and chemicals and chemical classes found in e-cigarette flavorants, and FDA should use as additional criteria California's Proposition 65 list of carcinogens and reproductive toxicants and the California Air Resources Board's list of Toxicant Air*

Contaminants. https://tobacco.ucsf.edu/sites/g/files/tkssra4661/f/wysiwyg/UCSF%20comment%20on%20additional%20HPHCs%20-%20Oct.%202%2C%202019%2BAppendix.pdf

Lemus, R., Carmines, E. L., Miert, E. V., Coggins, C. R. E., Anskeit, E., Gerstenberg, B., Meisgen, T. J., Schramke, H., Stabbert, R., Volkel, H., & Terpstra, P. M. (2007). Toxicology comparisons of cigarettes containing different amounts of vanillin. *Inhalation Toxicology, 19*, 683-699. https://doi.org/10.1080/08958370701353205

Li, C., Yue, X., Yang, J, Zhao, Y., Lv, C., Dong, S., Luo, X., Sun, Z., Zhang, Y., Li, B., Yang, Y., Zhang, Q., Bi, H., Zheng, D., & Peng, W. (2019). Pyrolysis produces from *Osmanthus Fragrans* wood. *Ekoloji, 28*(108), 105-109. http://www.ekolojidergisi.com/download/pyrolysis-products-from-osmanthus-fragrans-wood-6442.pdf

Li, J., Hu, J., Li, S., Li, J., & Liu, J. (2018). The effect of guar gum and chitosan on fiber and fiber fine micromorphology in paper-process reconstituted tobacco pulp. *Carbohydrate Polymers, 196*, 102-109. https://doi-org.ezproxy.massey.ac.nz/10.1016/j.carbpol.2018.04.125

Li, L., Jia, C., Zhu, X., & Zhang, S. (2020). Utilization of cigarette butt waste as functional carbon precursor for supercapacitors and adsorbents. *Journal of Cleaner Production, 256*, 120326. https://doi-org.ezproxy.massey.ac.nz/10.1016/j.jclepro.2020.120326

Li, S., Olegario, R. M., Banyasz, J. L., & Shafer, K. H. (2003). Gas chromatography – mass spectrometry analysis of polycyclic aromatic hydrocarbons single puff of cigarette smoke. *Journal of Analytical and Applied Pyrolysis, 66*(1-2), 155-163. https://doi-org.ezproxy.massey.ac.nz/10.1016/S0165-2370(02)00111-0

Li, W., Peng, J., Zhang, L., Xia, H., Li, N., Yang, K., & Zhu, X. (2008). Investigations on carbonization processes of plain tobacco stems and H3PO4- impregnated tobacco stems used for the preparation of activated carbons with H3PO4 activation. *Industrial Crops and Products, 28*(1), 73-80. https://doi-org.ezproxy.massey.ac.nz/10.1016/j.indcrop.2008.01.006

Li, X., Cai, J., Kong, H., Wu, M., Hua, R., Zhao, M., Liu, J., & Xu, G. (2003). Analysis of cigarette smoke condensates by comprehensive two-dimensional gas chromatography/time-of-flight mass spectrometry | Acidic fraction. *Analytical Chemistry, 75*(17), 4441-4451. https://doi-org.ezproxy.massey.ac.nz/10.1021/ac0264224

Li, X., Luo, Y., Jiang, X., Zhang, H., Zhu, F., Hu, S., Hou, H., Hu, Q., & Pang, Y. (2019). Chemical analysis and simulated pyrolysis of tobacco heating system 2.2 compared to conventional cigarettes. *Nicotine & Tobacco Research, 21*(1), 111-118. http://xqdoc.imedao.com/165dd67c46d1e4ef3fe4864d.pdf

Li, Y., Chen, J., Yang, Y., Li, C., & Peng, W. (2020). Chemical compositions and functions of Chinese fir volatiles. *Thermal Science, 24*(3A), 1853-1859. https://doi.org/10.2298/TSCI190601073L

Li, Y., Kong, D., & Wu, H. (2013). Analysis and evaluation of essential oil components of cinnamon barks using GC-MS and FTIR spectroscopy. *Industrial Crops and Products, 41*, 269-278. https://doi-org.ezproxy.massey.ac.nz/10.1016/j.indcrop.2012.04.056

Liao, J., Lu, Z., Hu, S., Li, Q., Che, L., & Chen, X. D. (2017). Effects of prewash on the pyrolysis kinetics of cut tobacco. *Drying Technology, 35*(11), 1368-1378. https://doi.org/10.1080/07373937.2017.1320803

Lin, B., Silveira, E. A., Colin, B., Chen, W., Lin, Y., Leconte, F., Petrissans, A., Rousset, P., & Petrissans, M. (2019). Modelling and prediction of devolatilization and elemental composition of wood during mild pyrolysis in a pilot-scale reactor. *Industrial Crops and Products, 131*, 357-370. https://doi-org.ezproxy.massey.ac.nz/10.1016/j.indcrop.2019.01.065

Lisko, J. G., Stanfill, S. B., & Clifford, H. W. (2014). Quantification of ten flavor compounds in unburned tobacco products. *Analytical Methods, 6*(13), 4698-4704. https://doi-org.ezproxy.massey.ac.nz/10.1039/C4AY00271G

Liu, B., Li, Y., Wu, S., Li, Y., Deng, S., & Xia, Z. (2013). Pyrolysis characteristics of tobacco stem studied by Py-GC/MS, TG-FTIR, and TG-MS. *BioResources, 8*(1), 220-230. http://eds.a.ebscohost.com.ezproxy.massey.ac.nz/eds/pdfviewer/pdfviewer?vid=9&sid=88510098-1bd8-4cc6-ba17-93954e62095f%40sdc-v-sessmgr06

Liu, C., DeGrandpre, Y., Porter, A., Griffiths, A., McAdam, K., Voisine, R., Cote, F., & Proctor, C. (2011). The use of a novel tobacco treatment process to reduce toxicant yields in cigarette smoke. *Food and Chemical Toxicology, 49*(9), 1904-1917. https://doi.org/10.1016/j.fct.2011.02.015

Liu, C., Liang, J., Wu, S., & Deng, Y. (2015). Effect of Chemical Structure on Pyrolysis Behavior of Alcell Mild Acidolysis Lignin. *BioResources, 10*(1), 1073-1084. https://ojs.cnr.ncsu.edu/index.php/BioRes/article/view/BioRes_10_1_1073_Liu_Pyrolysis_Behavior_Alcell_Lignin

Liu, Q., Wang, S., Wang, K., Luo, Z, & Cen, K. (2009). Pyrolysis of wood species based on the compositional analysis. *Korean Journal of Chemical Engineering, 26*(2), 548-553. https://link-springer-com.ezproxy.massey.ac.nz/content/pdf/10.1007/s11814-009-0093-y.pdf

Liu, Q., Wang, S., Zheng, Y., Luo, Z., & Cen, K. (2008). Mechanism study of wood lignin pyrolysis by using TG-FTIR analysis. *Journal of Analytical and Applied Pyrolysis, 82*(1), 170-177. https://doi-org.ezproxy.massey.ac.nz/10.1016/j.jaap.2008.03.007

Liu, S., He, P., Tian, Z., Li, X., & Xu, C. (2015). Ultrasound-assisted extraction and characterization of pectic polysaccharide from oriental tobacco leaves. *Journal of the Chemical Society of Pakistan, 37*(4), 621-628. https://jcsp.org.pk/PublishedVersion/fdd52c5e-1684-41fc-b023-e4c0850575c0Manuscript%20no%201,%20Final%20Gally%20Proof%20of%2010166%20(CHUNPING%20XU).pdf

Lockhart, J. P. A., Goldsmith, C. F., Randazzo, J. B., Ruscic, B., & Tranter, R. S. (2017). An experimental and theoretical study of the thermal decomposition of C_4H_6 isomers. *Journal of Physical Chemistry A, 121*(20), 3827-3850. https://doi.org/10.1021/acs.jpca.7b01186

Lodovici, M., Akpan, V., Evangelisti, C., & Dolara, P. (2004). Sidestream tobacco smoke as the main predictor of exposure to polycyclic aromatic hydrocarbons. *Journal of Applied Toxicology, 24*, 277-281. https://doi.org/10.1002/jat.992

Lomnicki, S., Truong, H., Dellinger, B. (2008). Mechanisms of product formation from the pyrolytic thermal degradation of catechol. *Chemosphere, 73*(4), 629-633. https://doi.org/10.1002/jat.992

Lourenco, A., Giminho, J., & Pereira, H. (2018). Chemical characterization of lignocellulosic materials by analytical pyrolysis. In P. Kusch (Ed.), *Analytical Pyrolysis*. https://doi.org/10.5772/intechopen.80556

Lu, H., & Zhu, L. (2007). Pollution patterns of polycyclic aromatic hydrocarbons in tobacco smoke. *Journal of Hazardous Materials, 139*(2), 193-198. https://doi-org.ezproxy.massey.ac.nz/10.1016/j.jhazmat.2006.06.011

Luo, H., Bao, L., Kong, L., & Sun, Y. (2017). Low temperature microwave-assisted pyrolysis of wood sawdust for phenolic rich compounds: Kinetics and dielectric properties analysis. *Bioresource Technology, 238*, 109-115. https://doi-org.ezproxy.massey.ac.nz/10.1016/j.biortech.2017.04.030

Luostarinen, K., & Hakkarainen, K. (2019). Chemical composition of wood and its connection with wood anatomy in *Betula pubescens*. *Scandinavian Journal of Forest Research, 34*(7), 577-584. https://doi.org/10.1080/02827581.2019.1662939

Lupoi, J. S., Singh, S., Parthasarathi, R., Simmons, B. A., & Henry, R. J. (2015). Recent innovations in analytical methods for the qualitative and quantitative assessment of lignin. *Renewable and Sustainable Energy Reviews, 49*, 871-906. https://doi.org/10.1016/j.rser.2015.04.091

Lyu, G., Wu, Q., Li, T., Jiang, W., Ji, X., Yang, G. (2019). Thermochemical properties of lignin extracted from willow by deep eutectic solvents (DES). *Cellulose, 26*, 8501-8511. https://doi-org.ezproxy.massey.ac.nz/10.1007/s10570-019-02489-8

Ma, Q., Zhang, D., Peng, W., Liu, Q., & Wu, Y. (2008). Determination of chemical components of benzene/ethanol extractives of Chinese-fir wood GC/MS. *2008 2nd International Conference on Bioinformatics and Biomedical Engineering.* https://doi.org/10.1109/ICBBE.2008.1128

Mahernia, S., Amanlou, A., Kiaee, G., & Amanlou, M. (2015). Determination of hydrogen cyanide concentration in mainstream smoke of tobacco products by polarography. *Journal of Environmental Health Science & Engineering, 13*(57). https://dx.doi.org/10.1186%2Fs40201-015-0211-1

Majewska, U., Piotrowska, M., Sychowska, I., Banas, D., Kubala-Kukus, A., Wudarczyk-Mocko, J., Stabrawa, I., & Gozdz, S. (2018). Multielemental analysis of tobacco plant and tobacco products by TXRF. *Journal of Analytical Toxicology, 42*(6), 409-416. https://doi-org.ezproxy.massey.ac.nz/10.1093/jat/bky016

Maleknia, S. D., Bell, T. L., & Adams, M. A. (2009). Eucalypt smoke and wildfires: Temperature dependent emissions of biogenic volatile organic compounds. *International Journal of Mass Spectrometry, 279*(2-3), 126-133. https://doi-org.ezproxy.massey.ac.nz/10.1016/j.ijms.2008.10.027

Mallock, N., Boss, L., Burk, R., Danzinger, M., Welsch, T., Hahn, H., Trieu, H., Hahn, J., Pieper, E., Henkler-Stephani, F., Hutzler, C., & Luch, A. (2018). Levels of selected analytes in the emissions of "heat not burn" tobacco products that are relevant to assess human health risks. *Archives of Toxicology, 92*, 2145-2149. https://doi-org.ezproxy.massey.ac.nz/10.1007/s00204-018-2215-y

Mammela, P. (2001). Phenolics in selected European hardwood species by liquid chromatography-electrospray ionisation mass spectrometry. *Analyst, 9*. https://pubs-rsc-org.ezproxy.massey.ac.nz/en/content/articlelanding/2001/AN/b104584a#!divRelatedContent&articles

Marcilla, A., Beltran, M., Gomez-Siurana, A., Martinez, I., & Berenguer, D. (2011). Catalytic effect of MCM-41 on the pyrolysis and combustion processes of tobacco. Effect of the aluminium content. *Thermochimica Acta, 518*(1-2), 47-52. https://doi.org/10.1016/j.tca.2011.02.005

Marcilla, A., Beltran, M. I., Gomez-Siurana, A., Martinez-Castellanos, I., Berenguer, D., Pastor, V., & Garcia, A. N. (2015). TGA/FTIR study of the pyrolysis of diammonium hydrogen phosphate-tobacco mixtures. *Journal of Analytical and Applied Pyrolysis, 112*, 48-55. https://doi-org.ezproxy.massey.ac.nz/10.1016/j.jaap.2015.02.023

Martinez-Garcia, R., Garcia-Martinez, T., Puig-Pujol, A., Mauricio, J. C., & Moreno, J. (2017). Changes in sparkling wine aroma during the second fermentation under CO_2 pressure in sealed bottle. *Food Chemistry, 237*, 1030-1040. https://doi-org.ezproxy.massey.ac.nz/10.1016/j.foodchem.2017.06.066

Mastelic, J., Jerkovic, I., & Mesic, M. (2006). Volatile constituents from flowers, leaves, bark and wood of *Punus mahaleb* L. *Flavour and Fragrance Journal, 21*, 306-313. https://doi.org/10.1002/ffj.1596

McGinty, D., Vitale, D., Letizia, C. S., & Api, A. M. (2012). Fragrance material review on phenethyl acetate. *Food and Chemical Toxicology, 50*(2), 491-497. https://doi-org.ezproxy.massey.ac.nz/10.1016/j.fct.2012.02.089

McGrath, T. E., Brown, A. P., Meruva, N. K., & Chan, W. G. (2009). Phenolic compound formation from the low temperature pyrolysis of tobacco. *Journal of Analytical and Applied Pyrolysis, 84*(2), 170-178. https://doi-org.ezproxy.massey.ac.nz/10.1016/j.jaap.2009.01.008

McGrath, T. E., Wooten, J. B., Chan, W. G., & Hajaligol, M. R. (2007). Formation of polycyclic aromatic hydrocarbons from tobacco: The link between low temperature residual solid (char) and PAH formation. *Food and Chemical Toxicology, 45*(6), 1039-1050. https://doi-org.ezproxy.massey.ac.nz/10.1016/j.fct.2006.12.010

Mecca, M., D'Auria, M., & Todaro, L. (2018). Effect of heat treatment on wood chemical composition extraction yield and quality of the extractive of some wood species by the use of molybdenum catalysts. *Wood Science and Technology, 53*, 119-133. https://doi.org/10.1007/s00226-018-1057-3

Mendu, V., Harman-Ware, A. E., Crocker, M., Jae, J., Stork, J., Morton, S., Placido, A., Huber, G., & DeBolt, S. (2011). Identification and thermochemical analysis of high-lignin feedstocks for biofuel and biochemical production. *Biotechnology for Biofuels, 4*(43). https://doi.org/10.1186/1754-6834-4-43

Meng, A., Zhang, Y., Zhuo, J., Li, Q., & Qin, L. (2015). Investigation on pyrolysis and carbonization of Eupatorium adenophorum Spreng and tobacco stem. *Journal of the Energy Institute, 88*(4), 480-489. https://doi.org/10.1016/j.joei.2014.10.003

Miller, R. S., & Bellan, J. (1997). A Generalized Biomass Pyrolysis Model Based on Superimposed Cellulose, Hemicelluloseand Liqnin Kinetics. *Combustion Science and Technology, 126* (1-6). https://doi.org/10.1080/00102209708935670

Ministry of Health. (2019). *New Zealand Tobacco Group Tobacco Returns 2019.* https://www.health.govt.nz/system/files/documents/pages/nztg-tobacco-return-2019.pdf

Ministry of Health. (2019). *Philip Morris Tobacco Returns 2019.* https://www.health.govt.nz/system/files/documents/pages/philipmorris-tobacco-return-2018.pdf

Mishra, A., Chaturvedi, P., Datta, S., Sinukumar, S., Joshi, P., & Garg, A. (2015). Harmful effects of nicotine. *Indian Journal of Medical and Paediatric Oncology, 36*(1), 24-31. https://dx.doi.org/10.4103%2F0971-5851.151771

Moody, M. W. (2003). Fish | Processing. In *Encyclopedia of Food Sciences and Nutrition* (2nd ed., pp. 2453-2457). https://doi.org/10.1016/B0-12-227055-X/00474-0

Moon, B. Y., Higashi, S., Gombos, Z., Murata, N. (1995). Unsaturation of the membrane lipids of chloroplasts stabilizes the photosynthetic machinery against low-temperature photoinhibition in transgenic tobacco plant. *Proceedings of the National Academy of Sciences, 92*(14), 6219-6223. https://www.pnas.org/content/pnas/92/14/6219.full.pdf

Moldoveanu, S. C. (2019). *Pyrolysis of Organic Molecules: Applications to Health and Environmental Issues* (2nd ed.). Elsevier Science. https://doi.org/10.1016/C2016-0-05137-9

Moldoveanu, S. C. (2010). Analysis of acrylonitrile and a-methacrylonitrile in vapour phase of mainstream cigarette smoke using a charcoal trap for collection. *Beitrage zur Tabakforschung International/Contributions to Tobacco Research, 24*(3), 145-156. https://doi.org/10.2478/cttr-2013-0892

Moldoveanu, S. C., Coleman, W., Wilkins, J., & Reynolds, R. J. (2008). Determination of hydroxybenzenes in exhaled cigarette smoke. *Beitrage zur Tabakforschung International/ Contributions to Tobacco Research, 23*(2), 98-106. https://doi.org/10.2478/cttr-2013-0852

Moreno-Arribas, M.V., & Polo, M. C. (2008). *Wine chemistry and biochemistry.* Springer.

Moricz, A. M., Horvath, G., Boszormenyl, A., & Ott, P. G. (2016). Detection and identification of antibacterial and antioxidant components of essential oils by TLC-Biodetection and GC-MS. *Natural Product Communications, 11*(11), 1705-1708. https://journals-sagepub-com.ezproxy.massey.ac.nz/doi/pdf/10.1177/1934578X1601101120

Mukhtar, A., Ullah, H., & Mukhtar, H. (2007). Fatty acid composition of tobacco seed oil and synthesis of alkyd resin. *Chinese Journal of Chemistry, 25*, 705-708. https://onlinelibrary-wiley-com.ezproxy.massey.ac.nz/doi/pdfdirect/10.1002/cjoc.200790132

Muller-Tautges, C., Eichler, A., Schwikowski, M., Pezzatti, G. B., Conedera, M., & Hoffmann, T. (2016). Historic records of organic compounds from a high Alpine glacier: influences of biomass burning, anthropogenic emissions, and dust transport. *Atmospheric Chemistry and Physics, 16*(2), 1029-1043. https://doi.org/10.5194/acp-16-1029-2016

Murwanashyaka, J. N., Pakdel, H., & Roy, C. (2001). Separation of syringol from birch wood-derived vacuum pyrolysis oil. *Separation and Purification Technology, 24*(1-2), 155-165. https://doi.org/10.1016/S1383-5866(00)00225-2

Nakahara, Y., Yamauchi, K., & Saka, S. (2014). MALDI-TOF/MS analyses of decomposition behavior of beech xylan as treated by semi-flow hot-compressed water. *Journal of Wood Science, 60*, 225-231. https://doi.org/10.1007/s10086-014-1396-0

Nakajima, D., Nagame, S., Kuramochi, H., Sugita, K., Kageyama, S., Shiozaki, T., Takemura, T., Shiraishi, F., & Goto, S. (2007). Polycyclic aromatic hydrocarbon generation behavior in the process of carbonization of wood. *Bulletin of Environmental Contamination and Toxicology, 79*, 221-225. https://doi-org.ezproxy.massey.ac.nz/10.1007/s00128-007-9177-8

Nanda, S., Dalai, A. K., & Kozinski, J. A. (2014). Butanol and ethanol production from lignocellulosic feedstock: biomass pretreatment and bioconversion. *Energy Science & Engineering, 2*(3), 138-148. https://doi.org/10.1002/ese3.41

Nardella, F., Mattonai, M., & Ribechini, E. (2020). Evolved gas analysis-mass spectrometry and isoconversional methods for the estimation of component-specific kinetic data in wood pyrolysis. *Journal of Analytical and Applied Pyrolysis, 145*. https://doi-org.ezproxy.massey.ac.nz/10.1016/j.jaap.2019.104725

Neves, D., Thunman, H., Matos, A., Tarelho, L., & Gomez-Barea, A. (2011). Characterization and prediction of biomass pyrolysis products. *Progress in Energy and Combustion Science, 37*(5), 611-630. https://doi.org/10.1016/j.pecs.2011.01.001

Ngo, T. A., Kim, J., & Kim, S. S. (2015). Fast pyrolysis of spent coffee waste and oak wood chips in a micro-tubular reactor. *Energy Sources, Part A: Recovery, Utilization, and Environmental Effects, 37*(11), 1186-1194. https://doi.org/10.1080/15567036.2011.608779

Nisbet, I. C. T., & LaGoy, P. K. (1992). Toxic equivalency factors (TEFs) for polycyclic aromatic hydrocarbons (PAHs). *Regulatory Toxicology and Pharmacology, 16*(3), 290-300. https://doi.org/10.1016/0273-2300(92)90009-X

Nollet, L. M. L., Boylston, T., Chen, F., Coggins, P. C., Gloria, M. B., Hyldig, G., Kerth, C. R., McKee, L. H., & Hui, Y. H. (2008). *Handbook of Meat, Poultry and Seafood Quality*. John Wiley & Sons.

Nolte, C. G., Schauer, J. J., Cass, G. R., & Simoneit, B. R. T. (2001). Highly polar organic compounds present in wood smoke and in the ambient atmosphere. *Environmental Science & Technology, 35*(10), 1912-1919. https://doi-org.ezproxy.massey.ac.nz/10.1021/es001420r

Nowakowska, M., Herbinet, O., Dufour, A., & Glaude, P. (2014). Detailed kinetic study of anisole pyrolysis and oxidation to understand tar formation during biomass combustion and gasification. *Combustion and Flame, 161*(6), 1474-1488. https://doi-org.ezproxy.massey.ac.nz/10.1016/j.combustflame.2013.11.024

Nowakowski, D. J., Jones, J. M., Brydson, R. M. D., & Ross, A. B. (2007). Potassium catalysis in the pyrolysis behaviour of short rotation willow coppice. *Fuel, 86*(15), 2389-2402. https://doi.org/10.1016/j.fuel.2007.01.026

Nystoriak, M. A., Kilfoil, P. J., Lorkiewicz, P. K., Conklin, D. J., & Bhatnagar, A. (2018). Arrhythmic risk evaluation of native and combusted tobacco flavor additives in human induced pluripotent stem cell-derived cardiomyocytes. *Circulation, 136*(1). https://www.ahajournals.org/doi/abs/10.1161/circ.136.suppl_1.20782

Nystoriak, M. A., Kilfoil, P. J., Lorkiewicz, P. K., Ramesh, B., Kuehl P. J., McDonald, J., Bhatnagar, A., & Conklin, D. J. (2019). Comparative effects of parent and heated cinnamaldehyde on the function of human iPSC-derived cardiac myocytes. *Toxicology in Vitro, 61*. https://doi-org.ezproxy.massey.ac.nz/10.1016/j.tiv.2019.104648

O'Connor, R. J., & Hurley, P. J. (2008). Existing technologies to reduce specific toxicant emissions in cigarette smoke. *Tobacco Control, 17*(1), 39-48. http://dx.doi.org.ezproxy.massey.ac.nz/10.1136/tc.2007.023689

Oja, V., Hajaligol, M. R., & Waymack, B. E. (2006). The vaporization of semi-volatile compounds during tobacco pyrolysis. *Journal of Analytical and Applied Pyrolysis, 76*(1-2), 117-123. https://doi-org.ezproxy.massey.ac.nz/10.1016/j.jaap.2005.08.005

Oladipupo, O. A., Dutta, D., & Chong, N. S. (2019). Analysis of chemical constituents in mainstream bidi smoke. *BMC Chemistry, 13*(93). https://doi.org/10.1186/s13065-019-0614-7

Olsson, M., Ramnas, O., & Petersson, G. (2004). Specific volatile hydrocarbons in smoke from oxidative pyrolysis of softwood pellets. *Journal of Analytical and Applied Pyrolysis, 71*(2), 847-854. https://doi-org.ezproxy.massey.ac.nz/10.1016/j.jaap.2003.11.003

Ondro, T., Vitazek, I., Hulan, T., Lawson, M. K., & Csaki, S. (2018). Non-isothermal kinetic analysis of the thermal decomposition of spruce wood in air atmosphere. *Research in Agricultural Engineering, 64*(1), 41-46. https://doi.org/10.17221/115/2016-RAE

Palic, R., Stojanovic, G., Alagic, S., Nikolic, M., & Lepojevic, Z. (2002). Chemical composition and antimicrobial activity of the essential oil and CO_2 extracts of the oriental tobacco, Prilep. *Flavour and Fragrance Journal, 17*, 323-326. https://doi.org/10.1002/ffj.1084

Pan, Y., Hu, Y., Wang J., Ye, L., Liu, C., & Zhu, Z. (2013). Online characterization of isomeric/isobaric components in the gas phase of mainstream cigarette smoke by tunable synchrotron radiation vacuum ultraviolet photoionization time-of-flight mass spectrometry and photoionization efficiency curve simulation. *Analytical Chemistry, 85*(24), 11993-12001. https://doi-org.ezproxy.massey.ac.nz/10.1021/ac402955k

Pang, X., & Lewis, A. C. (2011). Carbonyl compounds in gas and particle phases of mainstream cigarette smoke. *Science of The Total Environment, 409*(23), 5000-5009. https://doi-org.ezproxy.massey.ac.nz/10.1016/j.scitotenv.2011.07.065

Park, Y., Jang, S., Park, J., Yang, S., Chung, H., Han, Y., Chang, Y., Choi, I., Yeo, H. (2017). Changes of major chemical components in larch wood through combined treatment of drying and heating treatment using superheated steam. *Journal of Wood Science, 63*, 635-643. https://doi.org/10.1007/s10086-017-1657-9

Paschke, T., Scherer, G., & Heller, W. (2002). Effects of ingredients on cigarette smoke composition and biological activity: A literature overview. *Beitrage zur Tabakforschung International/ Contributions to Tobacco Research, 20*(3), 107-247. https://doi.org/10.2478/cttr-2013-0736

Paschke, M., Hutzler, C., Henkler, F., & Luch, A. (2016). Oxidative and inert pyrolysis on-line coupled to gas chromatography with mass spectrometric detection: On the pyrolysis products of tobacco additives. *International Journal of Hygiene and Environmental Health, 219*(8), 780-791. https://doi-org.ezproxy.massey.ac.nz/10.1016/j.ijheh.2016.09.002

Pellegrini, M., Marchei, E., Rossi, S., Vagnarelli, F., Durgbanshi, A., Garcia-Algar, O., Vall, O., & Pichini, S. (2007). Liquid chromatography/electrospray ionization tandem mass spectrometry assay for determination of nicotine and metabolites, caffeine and arecoline in breast milk. *Rapid Communications in Mass Spectrometry, 21*, 2693-2703. https://doi.org/10.1002/rcm.3137

Peng, J., Liu, X., & Bao, Z. (2018). Experimental study on the liquefaction of cellulose in supercritical ethanol. *IOP Conference Series: Materials Science and Engineering, 322*, 022024. https://doi.org/10.1088/1757-899X/322/2/022024

Peng, W., Li, D., Zhang, M., Ge, S., Mo, B., Li, S., Ohkoshi, M. (2017). Characteristics of antibacterial molecular activities in poplar wood extractives. *Saudi Journal of Biological Sciences, 24*(2), 399-404. https://doi.org/10.1016/j.sjbs.2015.10.026

Pennings, J. L. A., Cremers, J. W. J. M., Becker, M. J. A., Klerx, W. N. M., & Talhout, R. (2019). Aldehyde and volatile organic compound yields in commercial cigarette mainstream smoke are mutually related and depend on the sugar and humectant content in tobacco. *Nicotine & Tobacco Research, 22*(10), 1748-1756. https://doi.org/10.1093/ntr/ntz203

Philip Morris International. (2020). *Discover the taste of IQOS HEETS.* https://za.iqos.com/product/iqos-device/taste

Philip Morris International. (2020). *IQOS Official Website.* https://nz.iqos.com/

Philip Morris International. (2018). *Making Heated Tobacco Products.* https://www.pmi.com/investor-relations/overview/making-heated-tobacco-products

Philip Morris Products SA. (2020). *Patent No. WO 2020/035586 A1*. https://worldwide.espacenet.com/patent/search?q=pn%3DWO2020035586A1

Philip Morris Products S.A. (2017). *Philip Morris Products S.A. Modified Risk Tobacco Product (MRTP) Applications.* https://www.fda.gov/tobacco-products/advertising-and-promotion/philip-morris-products-sa-modified-risk-tobacco-product-mrtp-applications#6

Philip Morris Products SA. (2014). *Patent No. CN 104203015 A*. https://worldwide.espacenet.com/patent/search?q=pn%3DCN104203015A

Philip Morris Products SA. (2019). *Patent No. WO2019206916A1.* https://worldwide.espacenet.com/patent/search/family/062046794/publication/WO2019206916A1?q=pn%3DWO2019206916A1

Piade, J. J., Wajrock, S., Jaccard, G., Janeke, G. (2013). Formation of mainstream cigarette smoke constituents prioritized by the World Health Organization – Yield patterns observed in market surveys, clustering and inverse correlations. *Food and Chemical Toxicology, 55*, 329-347. https://doi.org/10.1016/j.fct.2013.01.016

Pieraccini, G., Furlanetto, S., Orlandini, S., Bartolucci, G., Giannini, I., Pinzauti, S., & Moneti, G. (2008). Identification and determination of mainstream and sidestream smoke components in different brands and types of cigarettes by means of solid-phase microextraction-gas chromatography-mass spectrometry. *Journal of Chromatography A, 1180*(1-2), 138-150. https://doi-org.ezproxy.massey.ac.nz/10.1016/j.chroma.2007.12.029

Pierce, J. S., Abelmann, A., Spicer, L. J., Adams, R. E., & Finely, B. L. (2014). Diaceyl and 2,3-pentanedione exposure associated with cigarette smoking: implications for risk assessment of food and flavouring workers. *Critical Reviews in Toxicology, 44*(5), 420-435. https://doi.org/10.3109/10408444.2014.882292

Piispanen, R., & Saranpaa, P. (2002). Neutral lipids and phospholipids in Scots pine (*Pinus sylvestris)* sapwood and heartwood. *Tree Physiology, 22*, 661-666. https://doi-org.ezproxy.massey.ac.nz/10.1093/treephys/22.9.661

Pohlmann, M., Hitzel, A., Schwagele, F., Speer, K., & Jira, W. (2013). Influence of different smoke generation methods on the contents of polycyclic aromatic hydrocarbons (PAH) and phenolic substances in Frankfurtuer-type sausages. *Food Control, 34*(2), 347-355. https://doi.org/10.1016/j.foodcont.2013.05.005

Polat, S., Apaydin-Varol, E., & Putun, A. E. (2016). Thermal decomposition behavior of tobacco stem Part I: TGA-FTIR-MS analysis. *Energy Sources, Part A: Recovery, Utilization, and Environmental Effects, 38*(20), 3065-3072. https://doi.org/10.1080/15567036.2015.1129373

Polzin, G. M., Kosa-Maines, R. E., Ashley, D. L., & Watson, C. H. (2007). Analysis of volatile organic compounds in mainstream cigarette smoke. *Environmental Science & Technology, 41*(4), 1297-1302. https://doi-org.ezproxy.massey.ac.nz/10.1021/es060609l

Polzin, G. M., Stanfill, S. B., Brown, C. R., Ashley, D. L., Watson, C. H. (2007). Determination of eugenol, anethole, and coumarin in the mainstream cigarette smoke of Indonesian clove cigarettes. *Food and Chemical Toxicology, 45*(10), 1948-1953. https://doi-org.ezproxy.massey.ac.nz/10.1016/j.fct.2007.04.012

Popov, V. N., Antipina, O. V., Pchelkin, V. P., & Tsydendambaev, V. D. (2012). Changes in the content and composition of lipid fatty acids in tobacco leaves and roots at low-temperature hardening. *Russian Journal of Plant Physiology, 59*(2), 177-182. https://doi.org/10.1134/S1021443712020124

Popova, V., Petkova, Z., Ivanova, T., Stoyanova, M., Lazarov, L., Stoyanova, A., Hristeva, T., Docheva, M., Nikolova, V., Nikolov, N., & Zheljazkov, V. D. (2018). Biologically active components in seeds of three *Nicotiana* species. *Industrial Crops and Products, 117*, 375-381. https://doi-org.ezproxy.massey.ac.nz/10.1016/j.indcrop.2018.03.020

Popova, V., Tumbarski, Y., Ivanova, T., Hadjikinova, R., & Stoyanova, A. (2019). Tobacco resinoind (*Nicotiana tabacum* L.) as an active ingredient of comestic gels. *Journal of Applied Pharmaceutical Science, 9*(9), 111-118. http://dx.doi.org/10.7324/JAPS.2019.90916

Purkis, S. W., Mueller, C., & Intorp, M. (2011). The fate of ingredients in and impact on cigarette smoke. *Food and Chemical Toxicology, 49*(12), 3238-3248. https://doi-org.ezproxy.massey.ac.nz/10.1016/j.fct.2011.09.028

Racovita, R. C., Secuianu, C., Ciuca, M. D., & Israel-Roming, F. (2020). Effects of smoking temperature, smoking time, and type of wood sawdust on polycyclic aromatic hydrocarbon accumulation levels in directly smoked pork sausages. *Journal of Agricultural and Food Chemistry, 68*(35), 9530-9536. https://doi-org.ezproxy.massey.ac.nz/10.1021/acs.jafc.0c04116

Rebaque, V., Ertesvag, I. S., Mikalsen, R. F., & Steen-Hansen, A. (2020). Experimental study of smouldering in wood pellets with and without air draft. *Fuel*, *264*. https://doi-org.ezproxy.massey.ac.nz/10.1016/j.fuel.2019.116806

Reece, P. (2005). *The Origin and Formation of 3-MCPD in Foods and Food Ingredients.* https://citeseerx.ist.psu.edu/viewdoc/download?doi=10.1.1.611.8907&rep=rep1&type=pdf

Reger, L., Mob, J., Hahn, H., & Hahn, J. (2018). Analysis of menthol, menthol-like, and other tobacco flavoring compounds in cigarettes and in electrically heated tobacco products. *Beitrage zur Tabakforschung International/ Contributions of Tobacco Research, 28*. https://doi.org/10.2478/cttr-2018-0010

Rencoret, J., Gutierrez, A., & del Rio, J. C. (2007). Lipid and lignin composition of woods from different eucalypt species. *Holzforschung, 61*, 165-174. https://doi.org/10.1515/HF.2007.030

Rey-Salguerio, L., Omil, B., Merino, A., Martine-Carballo, E., & Simal-Gandara, J. (2016). Organic pollutants profiling of wood ashes from biomass power plants linked to the ash characteristics. *Science of The Total Environment, 544*, 535-543. https://doi-org.ezproxy.massey.ac.nz/10.1016/j.scitotenv.2015.11.134

Ripberger, G. D. (2016). *A Study of the Importance of Secondary Reactions in Char Formation and Pyrolysis* [Doctoral dissertation, Massey University]. https://mro.massey.ac.nz/handle/10179/11429

Riveles, K., Roza, R., & Talbot, P. (2005). Phenols, quinolines, indoles, benzene, and 2-cyclopenten-1-ones are oviductal toxicants in cigarette smoke. *Toxicological Sciences, 86*(1), 141-151. https://doi.org/10.1093/toxsci/kfi112

Rodgman, A., & Cook, L. C. (2009). The composition of cigarette smoke. An historical perspective of several polycyclic aromatic hydrocarbons. *Beitrage zur Tabakforschung International/Contributions to Tobacco Research, 23*(6), 384-410. https://doi.org/10.2478/cttr-2013-0873

Rodgman, A., & Perfetti, T. A. (2013). *The Chemical Components of Tobacco and Tobacco Smoke.* https://doi-org.ezproxy.massey.ac.nz/10.1201/b13973

Roemer, E., Wittke, S., Sticken, E. T., Piade, J., Bonk, T., & Schorp, M. K. (2010). The addition of cocoa, glycerol, and saccharose to tobacco of cigarettes: Implications for smoke chemistry, in vitro cytotoxicity, mutagenicity and further endpoints. *Beitrage zur Tabakforschung International/ Contributions to Tobacco Research, 24*(3), 117-138. https://doi.org/10.2478/cttr-2013-0890

Rongpipi, S., Ye, D., Gomez, E. D., & Gomez, E. W. (2019). Progress and opportunities in the characterization of cellulose – An important regulator of cell wall growth and mechanics. *Frontiers in Plant Science, 9*, 1894. https://doi.org/10.3389/fpls.2018.01894

Ruffinatto, F., & Crivellaro, A. (2019). *Atlas of Macroscopic Wood Identification.* Springer, Cham. https://link-springer-com.ezproxy.massey.ac.nz/book/10.1007%2F978-3-030-23566-6#toc

Ruiz-Rodrigues, A., Bronze, M. & Ponte, M. N. (2008). Supercritical fluid extraction of tobacco leaves: A preliminary study on the extraction of solanesol. *The Journal of Supercritical Fluids, 45*(2), 171-176. https://doi.org/10.1016/j.supflu.2007.10.011

Safdari, M., Rahmati, M., Amini, E., Howarth, J. E., Berryhill, J. P., Dietenberger, M., Weise, D. R., & Fletcher, T. H. (2018). Characterization of pyrolysis products from fast pyrolysis of live and dead vegetation naïve to the Southern United States. *Fuel, 229*, 151-166. https://doi.org/10.1016/j.fuel.2018.04.166

Saffari, A., Daher, N., Ruprecht, A., Marco, C. D., Pozzi, P., Boffi, R., Hamad, S. H., Shafer, M. M., Schauer, J. J., Westerdahl, D., Sioutas, C. (2014). Particulate metals and organic compounds from electronic and tobacco-containing cigarettes: comparison of emission rates and secondhand exposure. *Environmental Science: Processes & Impacts, 16*, 2259-2267. https://doi.org/10.1039/C4EM00415A

Salehi, A. (2012). *Chemical Interactions Between Fatty Acids and Wood Components During Oxidation Processes* [Doctoral dissertation, Royal Institute of Technology]. KTH Chemical Science and Engineering. https://www.diva-portal.org/smash/get/diva2:556760/FULLTEXT01.pdf

Salem, M. Z. M., & Bohm, M. (2013). Understanding of formaldehyde emission from solid wood: An overview. *BioResources, 8*(3), 1-16. http://search.ebscohost.com/login.aspx?direct=true&db=aph&AN=89393541&site=eds-live&scope=site

Saliba, N. A., Hellani, A. E., Honein, E., Salman, R., Talih, S., Zeaiter, J., & Shihadeh, A. (2018). Surface chemistry of electronic cigarette electrical heating coils: Effects of metal types on propylene glycol thermal decomposition. *Journal of Analytical and Applied Pyrolysis, 134*, 520-525. https://dx.doi.org/10.1016%2Fj.jaap.2018.07.019

Sallsten, G., Gustafson, P., Johansson, L., Johannesson, S., Molnar, P., Strandberg, B., Tullin, C., & Barregard, L. (2006). Experimental wood smoke exposure in humans. *Inhalation Toxicology, 18*(11), 855-864. https://doi.org/10.1080/08958370600822391

Samae, H., Tekasakul, S., Tekasakul, P., & Furuuchi, M. (2021). Emission factors of ultrafine particulate matter (PM <0.1 µm) and particle-bound polycyclic aromatic hydrocarbons from biomass combustion for source apportionment. *Chemosphere, 262*. https://doi-org.ezproxy.massey.ac.nz/10.1016/j.chemosphere.2020.127846

Sanders, E. B., Goldsmith, A. I., & Seeman, J. I. (2003). A model that distinguishes the pyrolysis of D-glucose, D-fructose, and sucrose from that of cellulose. Application to the understanding of cigarette smoke formation. *Journal of Analytical and Applied Pyrolysis, 66*(1-2), 29-50. https://doi-org.ezproxy.massey.ac.nz/10.1016/S0165-2370(02)00104-3

Sangthong, S., Suksabye, P., & Thiravetyan, P. (2016). Air-borne xylene degradation by *Bougainvillea buttiana* and the role of epiphytic bacteria in the degradation. *Ecotoxicology and Environmental Safety, 126*, 273-280. https://doi.org/10.1016/j.ecoenv.2015.12.017

Schaller, J., Pijnenburg, J. P. M., Ajithkumar, A., & Tricker, A. R. (2016). Evaluation of the Tobacco Heating System 2.2. Part 3: Influence of the tobacco blend on the formation of harmful and potentially harmful constituents of the Tobacco Heating System 2.2 aerosol. *Regulatory Toxicology and Pharmacology, 81*(2), S48-S58. https://doi.org/10.1016/j.yrtph.2016.10.016

Schick, S. F., Bloumt, B. C., Jacob, P., Saliba, N. A., Bernert, J. T., Hellani, A. E., Jatlow, P., Pappas, R. S., Wang, L., Foulds, J., Ghosh, A., Hecht, S. S., Gomez, J. C., Martin, J. R., Mesaros, C., Srivastava, S., St. Helen, G., Tarran, R., Lorkiewicz, P. K., … Bhatnagar, A. (2017). Biomarkers of exposure to new and emerging tobacco delivery products. *American Journal of Physiology – Lung Cellular and Molecular Physiology, 313*, 425-452. https://doi.org/10.1152/ajplung.00343.2016

Schmeltz, I., Chiong, K. G., Hoffmann, D. (1978). Formation and determination of ethyl carbamate in tobacco and tobacco smoke. *Journal of Analytical Toxicology, 2*(6), 265-268. https://doi.org/10.1093/jat/2.6.265

Schreiner, L., Bauer, P., & Buettner, A. (2018). Resolving the smell of wood – identification of odour-active compounds in Scots pine (*Pinus sylvestris* L.). *Scientific Reports, 8*(8294). https://doi.org/10.1038/s41598-018-26626-8

Sebio-Punal, T., Naya, S., Lopez-Beceiro, J., Tarrio-Saavedra, J. & Artiaga, R. (2012). Thermogravimetric analysis of wood, holocellulose, and lignin from five wood species. *Journal of Thermal Analysis and Calorimetry: An International Forum for Thermal Studies, 109*(3), 1163. https://doi.org/10.1007/s10973-011-2133-1

Senneca, O., Ciaravolo, S., & Nunziata, A. (2007). Composition of the gaseous products of pyrolysis of tobacco under inert and oxidative conditions. *Journal of Analytical and Applied Pyrolysis, 79*(1-2), 234-243. https://doi-org.ezproxy.massey.ac.nz/10.1016/j.jaap.2006.09.011

Senneca, O., Chirone, R., Salatino, P., & Nappi, L. (2007). Patterns and kinetics of pyrolysis of tobacco under inert and oxidative conditions. *Journal of Analytical and Applied Pyrolysis, 79*(1-2), 227-233. https://doi-org.ezproxy.massey.ac.nz/10.1016/j.jaap.2006.12.011

Sepetdjian, E., Halim, R. A., Salman, R., Jaroudi, E., Shihadeh, A., & Saliba, N. A. (2012). Phenolic compounds in particles of mainstream waterpipe smoke. *Nicotine & Tobacco Research, 15*(6), 1107-1112. https://dx.doi.org/10.1093%2Fntr%2Fnts255

Seraj, M., Chen, Q., & Jones, J. (2021). Food Smoke Generation by Frictional Heating. ***Not yet published.***

Sharma, P., & Diwan, P. K. (2017). Study of thermal decomposition process and the reaction mechanism of the eucalyptus wood. *Wood Science and Technology, 51*, 1081-1094. https://doi-org.ezproxy.massey.ac.nz/10.1007/s00226-017-0924-7

Severin, I., Dumont, C., Jondeau-Cabaton, A., Graillot, V., & Chagnon, M. (2010). Genotoxic activities of the food contaminant 5-hydroxymethylfurfural using different *in vitro* bioassays. *Toxicology Letters, 192*(2), 189-194. https://doi.org/10.1016/j.toxlet.2009.10.022

Shafizadeh, F., & Chin, P. P. S. (1977). Thermal Deterioration of Wood. In I. S. Goldstein (Ed.), *Wood Technology: Chemical Aspects* (pp. 57-81). American Chemical Society.

Shosha. (2020). *HEETS Amber Label.* https://www.shosha.co.nz/heets-amber-label

Shosha. (2020). *IQOS 3 DUO Kit.* https://www.shosha.co.nz/iqos-3-duo-kit

Shosha. (2020). *Smoka Kush Vaporizer.* https://www.shosha.co.nz/smoka-kush-vaporizer

Shotorban, B., Yashwanth, B. L., Mahalingam, S., & Haring, D. J. (2018). An investigation of pyrolysis and ignition of moist leaf-like fuel subject to convective heating. *Combustion and Flame, 190*, 25-35. https://doi.org/10.1016/j.toxlet.2009.10.022

Simon, B. F., Muino, I., & Cadahia, E. (2010). Characterization of volatile constituents in commercial oak wood chip. *Journal of Agricultural and Food Chemistry, 58*(17), 9587-9596. https://doi-org.ezproxy.massey.ac.nz/10.1021/jf101301a

Simonavicius, E., McNeil, A., Shahab, L., & Brose, L. S. (2018). Heat-not-burn tobacco products: a systematic literature review. *Tobacco Control, 28*(5), 582-594. https://doi.org/10.1136/tobaccocontrol-2018-054419

Singh, A., Bajpai, V., Kumar, S., Rawat, A., & Kumar, B. (2017). Analysis of isoquinoline alkaloids from *Mahonia leschenaultia* and *Mahonia napaulensis* roots using UHPLC-Orbitrap-MS^n and UHPLC-QqQ_{LIT}-MS/MS. *Journal of Pharmaceutical Analysis, 7*(2), 77-86. https://doi.org/10.1016/j.jpha.2016.10.002

Skrbic, B., Marinkovic, V., Spaic, S., Milanko, V., & Branovacki, S. (2018). Profiles of polycyclic aromatic hydrocarbons in smoke from combustion and thermal decomposition of poplar wood pellets and sawdust. *Microchemical Journal, 139*, 9-17. https://doi-org.ezproxy.massey.ac.nz/10.1016/j.microc.2018.02.007

Sleiman, M., Gundel, L. A., Pankow, J. F., Jacob, P., Singer, B. C., & Destaillats, H. (2010). Formation of carcinogens indoors by surface-mediated reactions of nicotine with nitrous acid, leading to potential thirdhand smoke hazards. *Proceedings of the National Academy of Science, 107*(15), 6576-6581. https://doi.org/10.1073/pnas.0912820107

Sleiman, M., Logue, J. M., & Montesions, V. N. (2016). Emissions from electronic cigarettes: Key parameters affecting the release of harmful chemicals. *Environmental Science & Technology, 50*(17). https://doi.org/10.1021/acs.est.6b01741

Sleiman, M., Maddalena, R. L., Gundel, L. A., & Destaillats, H. (2009). Rapid and sensitive gas chromatography ion-trap mass spectrometry method for the determination of tobacco specific N-nitrosamines in secondhand smoke. *Journal of Chromatography A*. https://doi.org/10.1016/j.chroma.2009.09.020

Smith, C. J., & Hansch, C. (2000). The relative toxicity of compounds in mainstream cigarette smoke condensate. *Food and Chemical Toxicology, 38*(7), 637-646. https://doi.org/10.1016/S0278-6915(00)00051-X

Smith, C. J., Perfetti, T. A., Morton, M. J., Rodgman, A., Garg, R., Selassie, C. D., & Hansch, C. (2002). The relative toxicity of substituted phenols reported in cigarette mainstream smoke. *Toxicological Sciences, 69*(1), 265-278. https://doi.org/10.1093/toxsci/69.1.265

Smith, C. J., Perfetti, T. A., Rumple, M. A., Rodgman, A., & Doolittle, D. J. (2000). "IARC Group 2A Carcinogens" reported in cigarette mainstream smoke. *Food and Chemical Toxicology, 38*(4), 371-383. https://doi-org.ezproxy.massey.ac.nz/10.1016/S0278-6915(99)00156-8

Smith, D. M., O'Connor, R. J., Wei, B., Travers, M., Hyland, A., Goniewicz, M. L. (2020). Nicotine and toxicant exposure among concurrent users (Co-Users) of tobacco and cannabis. *Nicotine & Tobacco Research, 22*(8), 1354-1363. https://doi-org.ezproxy.massey.ac.nz/10.1093/ntr/ntz122

Smoka Vape. (2019). *SMOKA Kush Vaporizer.* https://www.smokavape.com/vaporizer/kush-vaporizer/

Snehesh, A. S., Mukunda, H. S., Mahapatra, S., & Dasappa, S. (2017). Fischer-Tropsch route for the conversion of biomass to liquid fuels – Technical and economic analysis. *Energy, 130*, 183-191. https://doi-org.ezproxy.massey.ac.nz/10.1016/j.energy.2017.04.101

Soeteman-Hernandez, L. G., Bos, P. M. J., & Talhout, R. (2013). Tobacco smoke – related health effects induced by 1,3-butadiene and strategies for risk reduction. *Toxicological Sciences, 136*(2), 566-580. https://dx.doi.org/10.1093%2Ftoxsci%2Fkft194

Sonobe, T. & Worasuwannarak, N. (2008). Kinetic analyses of biomass pyrolysis using the distributed activation energy model. *Fuel, 87*(3), 414-421. https://doi-org.ezproxy.massey.ac.nz/10.1016/j.fuel.2007.05.004

Speight, J. G. (2011). *The Biofuels Handbook.* Royal Society of Chemistry. https://books.google.co.nz/books?id=pqVspazTrmsC&pg=PA307&lpg=PA307&dq=proximate+analysis+of+manuka+wood&source=bl&ots=cjLi2sIhX-&sig=ACfU3U274Jzle85-pMZylLfvtpWy8Pz1sQ&hl=en&sa=X&ved=2ahUKEwjP9t_Sh_3nAhXa6XMBHfWjDiEQ6AEwC3oECAkQAQ#v=onepage&q&f=false

St. Helen, G., Jacob III, P., Nardone, N., & Benowitz. (2018). IQOS: examination of Philip Morris International's claim of reduced exposure. *Tobacco Control, 27*(1), s30-s36. http://dx.doi.org.ezproxy.massey.ac.nz/10.1136/tobaccocontrol-2018-054321

Stabbert, R., Dempsey, R., Diekmann, J., Euchenhofer, C., Hagemeister, T., Haussmann, H., Knorr, A., Mueller, B. P., Pospisil, P., Reininghaus, W., Roemer, E., Tewes, F. J., & Detlef, J. V. (2017). Studies on the contributions of smoke constituents, individually and in mixtures, in a range of in vitro bioactivity assays. *Toxicology in Vitro, 42*, 222-246. https://doi.org/10.1016/j.tiv.2017.04.003

Stanfill, S. B., & Ashley, D. L. (2000). Quantitation of flavor-related alkenylbenzenes in tobacco smoke particulate by selected ion monitoring gas chromatography-mass spectrometry. *Journal of Agricultural and Food Chemistry, 48*(4), 1298-1306. https://doi-org.ezproxy.massey.ac.nz/10.1021/jf990772i

Staub, P. O., Schiestl, F. P., Leonti, M., & Weckerle, C. S. (2011). Chemical analysis of incense smokes used in Shaxi, Southwest Chine: A novel methodological approach in ethnobotany. *Journal of Ethnopharmacology, 138*(1), 212-218. https://doi-org.ezproxy.massey.ac.nz/10.1016/j.jep.2011.08.078

Stavanja, M. S., Curtin, G. M., Ayres, P. H., Bombick, E. R., Borgerding, M. F., Morgan, W. T., Garner, C. D., Pence, D. H., & Swauger, J. E. (2008). Safety assessment of diammonium phosphate and urea used in the manufacture of cigarettes. *Experimental and Toxicologic Pathology, 59*(6), 339-353. https://doi-org.ezproxy.massey.ac.nz/10.1016/j.etp.2007.11.015

Stevenson, T., & Proctor, R. N. (2008). The secret and soul of Marlboro. *American Journal of Public Health, 98*(7), 1184-1194. https://doi.org/10.2105/AJPH.2007.121657

Stockwell, C. E., Veres, P. R., Williams, J., & Yokelson, R. J. (2015). Characterization of biomass burning smoke from cooking fires, peat, crop residue and other fuels with high resolution proton-transfer-reaction time-of-flight mass spectrometry. *Atmospheric Chemistry and Physics, 15*, 845-865. https://acp.copernicus.org/preprints/14/22163/2014/acp-2014-584-manuscript-version2.pdf

Stotesbury, S. J., Willoughby, L. J., & Couch, A. (2000). Pyrolysis of cigarette ingredients labelled with stable isotopes. *Beitrage zur Tabakforschung International/ Contributions to Tobacco Research, 19*(2), 55-64. https://doi.org/10.2478/cttr-2013-0696

Streibel, T., Geibler, R., Saraji-Bozorgzad, M., Sklorz, M., Kaisersberger, E., Denner, T., & Zimmerman, R. (2009). Evolved gas analysis (EGA) in TG and DSC with single photon ionization mass spectrometry (SPI-MS): molecular organic signatures from pyrolysis of soft and hard wood, coal, crude oil and ABS polymer. *Journal of Thermal Analysis and Calorimetry: An International Forum for Thermal Studies, 93*(3), 795. https://doi.org/10.1007/s10973-009-0035-2

Sullards, M. C., Allegood, J. C., Kelly, S., Wang, E., Haynes, C. A., Park, H., Chen, Y., & Merrill, A. H. (2007). Structure-specific, quantitative methods for analysis of sphingolipids by liquid chromatography-tandem mass spectrometry: "Inside-out" sphingolipidomics. *Methods in Enzymology, 432*, 83-115. https://doi.org/10.1016/S0076-6879(07)32004-1

Sumayo, M. S., Son, J., & Ghim, S. (2018). Exogenous application of phenylacetic acid promotes root hair growth and induces the systemic resistance of tobacco against bacterial soft-rot pathogen *Pectobacterium carotovorum* subsp. *carotovorum. Functional Plant Biology, 45*, 1119-1127. https://doi.org/10.1071/FP17332

Sun, Y., Yang, G., & Wang, H. (2012). Structural features of Betula schmidtii Regel entitles as rigidy and heavy wood. *World Automation Congress 2012*, 1-5. https://ieeexplore-ieee-org.ezproxy.massey.ac.nz/document/6321384

Svoronos, P. D. N., & Bruno, T. J. (2002). Carbonyl Sulfide: A Review of Its Chemistry and Properties. *Industrial & Engineering Chemistry Research, 41*(22), 5321-5336. https://doi-org.ezproxy.massey.ac.nz/10.1021/ie020365n

Szramowiat-Sala, K., Korzeniewska, A., Sornek, K., Marczak, M., Wieronska, F., Berent, K., Goals, J., & Filipowicz, M. (2019). The properties of particulate matter generated during wood combustion in in-use-stoves. *Fuel, 253*, 792-801. https://doi-org.ezproxy.massey.ac.nz/10.1016/j.fuel.2019.05.026

Takada, D., Ehara, K., & Saka, S. (2004). Gas chromatographic and mass spectrometric (GC-MS) analysis of lignin-derived products from *Crytomeria japonica* treated in supercritical water. *The Japan Wood Research Society, 50*, 253-259. https://doi.org/10.1007/s10086-003-0562-6

Tanaka, S., Shiraga, K., Ogawa, Y., Fuji, Y., & Okumura, S. (2004). Effect of pore conformation on dielectric anisotropy of oven-dry wood evaluated using terahertz time-domain spectroscopy and eigenvalue problem for two-dimensional photonic crystals. *Journal of Wood Science, 60*, 194-200. https://doi-org.ezproxy.massey.ac.nz/10.1007/s10086-014-1390-6

TechInsights. (2017). *TechInsights iQOS Teardown.* https://www.documentcloud.org/documents/4457118-TechInsights-iQOS.html

Tekin, K., Karagoz, S., & Bektas, S. (2013). Effect of sodium perborate monohydrate concentrations on product distributions from the hydrothermal liquefaction of Scotch pine wood. *Fuel Processing Technology, 110*, 17-23. https://doi.org/10.1016/j.fuproc.2013.01.010

Theapparat, Y., Chandumpai, A., Leelasuphakul, W., & Laemsak, N. (2015). Pyroligenous acids from carbonisation of wood and bamboo: Their components and antifungal activity. *Journal of Tropical Forest Science, 27*(4), 517-526. http://search.ebscohost.com/login.aspx?direct=true&db=aph&AN=110262793&site=eds-live&scope=site

Tiwo, C. T., Tchoumbougnang, F., Nganou, E., Kumar, P., & Nayak, B. (2019). Effect of different smoking processes on the nutritional and polycyclic aromatic hydrocarbons composition of smoked *Clarias gariepinus* and *Cyprinus carpio*. *Food Science & Nutrition, 7*(7), 2412-2418. https://doi.org/10.1002/fsn3.1107

Tokareva, E. N., Pranovich, A. V., & Holmbom, B. R. (2011). Characteristic fragment ions from lignin and polysaccharides in ToF-SIMS. *Wood Science and Technology, 45*, 767-785. https://doi.org/10.1007/s00226-010-0392-9

Tongo, I., Ogbeide, O., & Ezemonye, L. (2016). Human health risk assessment of polycyclic aromatic hydrocarbons (PAHs) in smoked fish species from markets in Southern Nigeria. *Toxicology Reports, 4*, 55-61. https://dx.doi.org/10.1016%2Fj.toxrep.2016.12.006

Torikai, K., Yoshida, S., & Takahashi, H. (2004). Effects of temperature, atmosphere and pH on the generation of smoke compounds. *Food and Chemical Toxicology, 42*(9), 1409-1417. https://doi-org.ezproxy.massey.ac.nz/10.1016/j.fct.2004.04.002

Truong, H., Lomnicki, S., & Dellinger, B. (2008). Mechanisms of molecular product and persistent radical formation from the pyrolysis of hydroquinone. *Chemosphere, 71*(1), 107-113. https://doi-org.ezproxy.massey.ac.nz/10.1016/j.chemosphere.2007.10.007

Tsekos, C., Anastasakis, K., Schoenmakers, P. L., & de Jong, W. (2020). PAH sampling and quantification from woody biomass fast pyrolysis in a pyroprobe reactor with a modified tar sampling system. *Journal of Analytical and Applied Pyrolysis, 147*(104802). https://doi-org.ezproxy.massey.ac.nz/10.1016/j.jaap.2020.104802

Tshabalala, M. A., McSweeny, J. D., & Rowell, R. M. (2012). Heat treatment of wet wood fiber: A study of the effect of reaction conditions on the formation of furfurals. *Wood Material Science & Engineering, 7*(4), 202-208. https://doi.org/10.1080/17480272.2012.669406

Valin, S., Grateau, M., Thiery, S., Gauthier, G., Defoort, F. & Melkior, T. (2015). Influence of atmosphere (N_2/CO_2/H_2O) on wood centimetre-scale particle devolatilisation at 800^{o}C. *Fuel*, *139*, 584-593. https://doi-org.ezproxy.massey.ac.nz/10.1016/j.fuel.2014.09.043

VanderSchelden, G., de Foy, B., Herring, C., Kaspari, S., VanReken, T., & Jobson, B. (2017). Contributions of wood smoke and vehicle emissions to ambient concentrations of volatile organic compounds and

particulate matter during Yakima wintertime nitrate study. *Journal of Geophysical Research: Atmospheres, 122*. http://dx.doi.org/10.1002/2016JD025332

Varlet, V., Knockaert, C., Prost, C., & Serot, T. (2006). Comparison of odor-active volatile compounds of fresh and smoked salmon. *Journal of Agricultural and Food Chemistry, 54*(9), 3391-3401. https://doi-org.ezproxy.massey.ac.nz/10.1021/jf053001p

Varlet, V., Serot, T., Monteau, F., Bizec, B. L., & Prost, C. (2007). Determination of PAH profiles by GC-MS/MS in salmon processed by four cold-smoking techniques. *Food Additives and Contaminants, 24*(7), 744-757. https://doi.org/10.1080/02652030601139946

Vasiliou, A. K., Kim, J. H., Ormond, T. K., Piech, K. M., Urness, K. N., Scheer, A. M., Robichaud, D. J., Mukarakate, C., Nimlos, M. R., Daily, J. W., Guan, Q., Carstensen, H., & Ellison, G. B. (2013). Biomass pyrolysis: Thermal decomposition mechanisms of furfural and benzaldehyde. *Journal of Chemical Physics, 139*(10), 104310. https://doi-org.ezproxy.massey.ac.nz/10.1063/1.4819788

Vienneau, D. S., DeBoni, U., & Wells, P. G. (1995). Potential genoprotective role for UDP-glucuronosyltransferases. *Cancer Research, 55*(5), 1045-1051. https://cancerres.aacrjournals.org/content/55/5/1045.short

Vitasari, C. R. (2012). Extraction of bio-cased glycolaldehyde from wood-derived pyrolysis oils. *Technische Universiteit Eindhoven*. https://doi.org/10.6100/IR738958

Vu, A. T., Taylor, K. M., Holman, M. R., Ding, Y. S., Hearn, B., & Watson, C. H. (2015). Polycyclic aromatic hydrocarbons in the mainstream smoke of popular U.S. cigarettes. *Chemical Research in Toxicology, 28*(8), 1616-1626. https://doi-org.ezproxy.massey.ac.nz/10.1021/acs.chemrestox.5b00190

Wagner, A., Tobimatsu, Y., Phillips, L., Flint, H., Torr, K., Donaldson, L., Pears, L., & Ralph, J. (2011). CCoAOMT suppression modifies lignin composition in *Pinus radiata*. *The Plant Journal, 62*(1), 119-129. https://doi.org/10.1111/j.1365-313X.2011.04580.x

Wan, X., Kawamura, K., Ram, K., Kang, S., Loewen, M., Gao, S., Wu, G., Fu, P., Zhang, Y., Bhattarai, H., & Cong, Z. (2019). Aromatic acids as biomass-burning tracers in atmospheric aerosols and ice cores: A review. *Environmental Pollution, 247*, 216-228. https://doi.org/10.1016/j.envpol.2019.01.028

Wang, C., Li, L., Chen, R., Ma, X., Lu, M., Ma, W., & Peng, H. (2019). Thermal conversion of tobacco stem into gaseous products. *Journal of Thermal Analysis and Calorimetry*, 1-13. https://doi-org.ezproxy.massey.ac.nz/10.1007/s10973-019-08010-4

Wang, G., Fan, B., Chen, H., & Li, Y. (2020). Understanding the pyrolysis behavior of agriculture, forest and aquatic biomass: Products distribution and characterization. *Journal of the Energy Institute, 93*(5), 1892-1900. https://doi-org.ezproxy.massey.ac.nz/10.1016/j.joei.2020.04.004

Wang, H., Xin, H., Liao, Z., Li, J., Xie, W., Zeng, Q., Li, Y., Li, Q., & Chen, X. (2014). Study on the effect of cut tobacco drying on the pyrolysis and combustion properties. *Drying Technology, 32*, 130-134. http://eds.a.ebscohost.com.ezproxy.massey.ac.nz/eds/pdfviewer/pdfviewer?vid=1&sid=66639104-9588-4adf-b144-298931a92e23%40sdc-v-sessmgr04

Wang, J., Hu, Y., Xu, Y., Tian, Z., Pan, Y. (2017). On-line photoionization mass spectrometric study on the mouth retention of gaseous mainstream cigarette smoke. *Analytical Methods, 9*(24), 3653-3661. https://doi-org.ezproxy.massey.ac.nz/10.1039/C7AY00493A

Wang, K., Villano, S. M., & Dean, A. M. (2016). Experimental and kinetic modeling study of butene isomer pyrolysis: Part I. 1- and 2- Butene. *Combustion and Flame, 173*, 347-369. https://doi-org.ezproxy.massey.ac.nz/10.1016/j.combustflame.2016.07.037

Wang, L., Li, J., Chen, Y., Yang, H., Shao, J., Zhang, X. Yu, H., & Chen, H. (2019). Investigation of the pyrolysis characteristics of guiaicol lignin using combined Py-GC x GC/TOF-MS and in-situ FTIR. *Fuel, 251*, 496-505. https://doi-org.ezproxy.massey.ac.nz/10.1016/j.fuel.2019.04.061

Wang, L., Zhang, R., Li, J., Guo, L., Yang, H., Ma, F., & Yu, H. (2018). Comparative study of the fast pyrolysis behavior of ginkgo, poplar, and wheat straw lignin at different temperatures. *Industrial Crop and Products, 122*,465-472. https://doi-org.ezproxy.massey.ac.nz/10.1016/j.indcrop.2018.06.038

Wang, S., Guo, X., Wang, K., & Luo, Z. (2011). Influence of the interaction of components on the pyrolysis behaviour of biomass. *Journal or Analytical and Applied Pyrolysis, 91*(1), 183-189. https://doi.org/10.1016/j.jaap.2011.02.006

Wang, S., Liu, B., Sun, K., & Su, Q. (2004). Gas chromatographic – mass spectrometric determination of polycyclic aromatic hydrocarbons formed during the pyrolysis of phenylalanine. *Journal of Chromatography A, 1025*(2), 255-261. https://doi-org.ezproxy.massey.ac.nz/10.1016/j.chroma.2003.10.105

Wang, S., & Luo, Z. (2017). *Pyrolysis of Biomass*. De Gruyter. http://search.ebscohost.com/login.aspx?direct=true&db=nlebk&AN=1458970&site=eds-live&scope=site

Wang, S., Ru, B., Lin, H., Sun, W., & Luo, Z. (2015). Pyrolysis behaviours of four lignin polymers isolated from the same pine wood. *Bioresource, 182*, 120-127. https://doi.org/10.1016/j.biortech.2015.01.127

Wang, X., Conway, W., Burns R., McCann, N., & Maeder, M. (2010). Comprehensive study of the hydration and dehydration reactions of carbon dioxide in aqueous solution. *The Journal of Physical Chemistry, 114*(4), 1734-1740. https://doi-org.ezproxy.massey.ac.nz/10.1021/jp909019u

Wang, X., Wang, Z., Dai, Y., Ma, K., Zhu, L., & Tan, H. (2016). Thermogravimetric study on the flue-cured tobacco leaf pyrolysis and combustion using a distributed activation energy model. *Asia-Pacific Journal of Chemical Engineering, 12*(1), 75-84. https://doi-org.ezproxy.massey.ac.nz/10.1002/apj.2055

Wang, Z., Cao, J., & Wang, J. (2009). Pyrolytic characteristics of pine wood in a slowly heating and gas sweeping fixed-bed reactor. *Journal of Analytical and Applied Pyrolysis, 84*(2), 179-184. https://doi.org/10.1016/j.jaap.2009.02.001

Wenzl, T., & Zelinkova, Z. (2019). Polycyclic aromatic hydrocarbons in food and feed. In *Encyclopedia of Food Chemistry* (pp. 455-469). https://doi.org/10.1016/B978-0-08-100596-5.21805-2

White, J. L., Conner, B. T., Perfetti, T. A., Bombick, B. R., Avalos, J. T., Fowler, K. W., Smith, C. J., & Doolittle, D. J. (2001). Effect of pyrolysis temperature on the mutagenicity of tobacco smoke condensate. *Food and Chemical Toxicology, 39*(5), 499-505. https://doi-org.ezproxy.massey.ac.nz/10.1016/S0278-6915(00)00155-1

Wornat, M. J., Ledesma, E. B., & Marsh, N. D. (2001). Polycyclic aromatic hydrocarbons from the pyrolysis of catechol (ortho-dihydroxybenzene), a model fuel representative of entities in tobacco, coal, and lignin. *Fuel, 80*(12), 1711-1726. https://doi.org/10.1016/S0016-2361(01)00057-6

Wu, S., Shen, D., Hu, J., Zhang, H., & Xiao, R. (2016). Cellulose-lignin interactions during fast pyrolysis with different temperatures and mixing methods. *Biomass and Bioenergy, 90*, 209-217. https://doi-org.ezproxy.massey.ac.nz/10.1016/j.biombioe.2016.04.012

Xie, F., Yu, A., Cheng, Y., Qi, R., Li, Q., Liu, H., & Zhang, S. (2010). Rapid separation and determination of five phenolic acids in tobacco by CE. *Chromatographia, 72*, 1207-1212. https://doi.org/10.1365/s10337-010-1781-9

Xu, K., Feng, J., Zhong, T., Zheng, Z., & Chen, T. (2015). Effects of volatile chemical components of wood species on mould growth susceptibility and termite attack resistance of wood plastic composites. *International Biodeterioation & Biodegradation, 100*, 106-115. https://doi-org.ezproxy.massey.ac.nz/10.1016/j.ibiod.2015.02.002

Yamada, H., & Yatagai, M. (2007). The components of the smoke and headspace volatile from *Cryptomeria japonica* D. Don. *Journal of Essential Oil Research, 19*, 231-233. http://search.ebscohost.com/login.aspx?direct=true&db=edswsc&AN=000246865400009&site=eds-live&scope=site

Yan, B., Zhang, S., Chen, W., & Cai, Q. (2018). Pyrolysis of tobacco wastes for bio-oil with aroma compounds. *Journal of Analytical and Applied Pyrolysis, 136*, 248-254. https://doi.org/10.1016/j.jaap.2018.09.016

Yang, C., & Wender, S. H. (1964). Identification of aromatic aldehydes in cigarette smoke and in tobacco. *Phytochemistry, 3*(1), 17-22. https://doi-org.ezproxy.massey.ac.nz/10.1016/S0031-9422(00)83989-8

Yang, H., Yan, R., Chen, H., Lee, D. H., & Zheng, C. (2007). Characteristics of hemicellulose, cellulose and lignin pyrolysis. *Fuel, 86*(12-13), 1781-1788. https://doi-org.ezproxy.massey.ac.nz/10.1016/j.fuel.2006.12.013

Yang, H., Zhang, H., Pan, T., Wang, H., & Wang, Y. (2018). Benzo(a)pyrene promotes migration invasion and metastasis of lung adenocarcinoma cells by upregulating TGIF. *Toxicology Letter, 294*, 11-19. https://doi-org.ezproxy.massey.ac.nz/10.1016/j.toxlet.2018.05.005

Yang, W. (2012). I*nvestigation of Extractable Materials from Biochar* [Master's thesis, University of Waikato]. Research Commons at the University of Waikato. https://researchcommons.waikato.ac.nz/bitstream/handle/10289/6522/thesis.pdf?sequence=5&isAllowed=y

Yang, X., Felsmann, D., Kurimoto, N., Kruger, J., Wada, T., Tan, T., Carter, E. A., Kohse-Hoinghause, K., & Ju, Y. (2015). Kinetic studies of methyl acetate pyrolysis and oxidation in a flow reactor and a low-pressure flat flame using molecular-beam mass spectrometry. *Proceedings of the Combustion Institute, 35*(1), 491-498. https://doi-org.ezproxy.massey.ac.nz/10.1016/j.proci.2014.05.058

Yang, Y., Ma, Y., Yang, S., Yue, X., & Peng, W. (2020). Chemical components analysis of *Toona sinensis* bark and wood by pyrolysis-gas chromatography-mass spectrometry. *Asia-Pacific Journal of Chemical Engineering, 15*(S1), 2487. https://doi.org/10.1002/apj.2487

Yaylayan, V. A., & Haffenden, L. J. W. (2003). Mechanism of pyrazole formation in [13C-2] labelled glycine model systems: N-N bond formation during Maillard reaction. *Food Research International, 36*(6), 571-577. https://doi-org.ezproxy.massey.ac.nz/10.1016/S0963-9969(03)00003-6

Yershova, K., Yuan, J., Wang, R., Valentin, L., Watson, C., Gao, Y., Hecht, S. S., & Stepanov, I. Tobacco-specific N-nitrosamines and polycyclic aromatic hydrocarbons in cigarettes smoked by the participants of the Shanghai Cohort Study. *International Journal of Cancer, 139*(6), 1261-1269. https://doi-org.ezproxy.massey.ac.nz/10.1002/ijc.30178

Yildiz, Z., & Ceylan, S. (2019). Pyrolysis of tobacco waste biomass. *Journal of Thermal Analysis & Calorimetry, 136*(2), 783-794. https://doi.org/10.1007/s10973-018-7630-z

Yin, C., Xu, Z., Shu, J., Li, Y., Sun, W., Zhou, Z., Chen, M., & Zhong, F. (2015). Influence of physiochemical characteristics on the effective moisture diffusivity in tobacco. *International Journal of Food Properties, 18*(3), 690-698. https://doi.org/10.1080/10942912.2013.845785

Yin, F., Zhang, X., Song, S., Han, T., & Karangwa, E. (2015). Identification of aroma types and their characteristic volatile compounds of Chinese faint-scent cigarettes based on descriptive sensory analysis and GC-MS and partial least squares regression. *European Food Research and Technology, 242*, 869-880. https://doi-org.ezproxy.massey.ac.nz/10.1007/s00217-015-2593-9

Yokoi, M., & Shimod, M. (2017). Extraction of volatile flavor compounds from tobacco leaf through a low-density polyethylene membrane. *Journal of Chromatographic Science, 55*(3), 373-377. https://doi.org/10.1093/chromsci/bmw178

Yuan, Y., Xue, C., Guichuan, Z., & Fuzhang, D. (2007). Study on aroma components of tobacco leaves in Bijie area of Guizhou Province. *Anhui Agricultural Sciences, 35*(28), 8916-8918. https://en.cnki.com.cn/Article_en/CJFDTotal-AHNY200728074.htm

Yuan, Y., Zou, P., Zhou, J., Geng, Y., Fan, J., Clark, J., Li, Y., & Zhang, C. (2019). Microwave-assisted hydrothermal extraction of non-structural carbohydrates and hemicellulose from tobacco biomass. *Carbohydrate Polymers, 223*. https://doi-org.ezproxy.massey.ac.nz/10.1016/j.carbpol.2019.115043

Yusof, R., Khalid, M., & Khairuddin, S. M. (2013). Fuzzy data management on pores arrangement for tropical wood species recognition systems. *2013 Science and Information Conference*, 529-535. https://ieeexplore-ieee-org.ezproxy.massey.ac.nz/document/6661789

Zbancioc, G., Drochioiu, G., & Mangalagiu, I. I. (2012). Nicotine and tobacco alkaloids: A GC-MS analysis. Part 2: The tobacco and smoking. *International Journal of Criminal Investigation, 2*(4), 251-257. http://docs.manupatra.in/newsline/articles/Upload/208975F6-9C13-4787-9C69-A49CF7601001.pdf

Zeller, I., Malovichko, M. V., Hurst, H. E., Renaud, D. E., & Scott, D. A. (2019). Cigarette smoke reduces short chain fatty acid production by a *Porphyromonas gingivalis* clinical isolate. *Journal of Periodontal Research, 54*(5), 556-571. https://doi-org.ezproxy.massey.ac.nz/10.1111/jre.12660

Zellner, B. A., Presti, M. L., Barata, L. E. S., Dugo, P., Dugo, G., & Mondello, L. (2006). Evaluation of leaf-derived extracts as an environmentally sustainable source of essential oils by using gas chromatography-mass spectrometry and enantioselective gas chromatography-olfactometry. *Analytical Chemistry, 78*(3), 883-890. https://doi-org.ezproxy.massey.ac.nz/10.1021/ac051337s

Zha, Q., Qian, N. X., & Moldoveanu, S. C. (2002). Analysis of polycyclic aromatic hydrocarbons in a particulate phase of cigarette smoke using a gas chromatographic-high-resolution mass spectrometric technique. *Journal of Chromagraphic Science, 40*. https://doi.org/10.1093/chromsci/40.7.403

Zhai, K., Lai, M., Wu, Z., Zhao, M., Jing, Y., & Liu, P. (2018). Synthesis and initial thermal behaviour investigation of 2-alkenyl substituted pyrazine N-oxides. *Catalysis Communications, 116*, 20-26. https://doi-org.ezproxy.massey.ac.nz/10.1016/j.catcom.2018.07.017

Zhang, D., Tan, X., Ma, Q., Tian, H., Deng, S., Fan, S., Liu, Q., & Peng, W. (2008). Components determination of cold water extractive of *Eucalyptus tereticornis* wood chips by GC/MS. *2008 2nd International Conference on Bioinformatics and Biomedical Engineering* (pp.3210-3213). https://doi.org/10.1109/ICBBE.2008.1132

Zhang, J., & Shen, Q. (2019). Processing natural wood into bulk conducting materials. *SN Applied Sciences, 1*(1579). https://doi-org.ezproxy.massey.ac.nz/10.1007/s42452-019-1572-3

Zhang, X., Deng, H., Hou, X., Qiu, R., & Chen, Q. (2019). Pyrolytic behavior and kinetic of wood sawdust at isothermal and non-isothermal conditions. *Renewable Energy, 142*, 284-294. https://doi-org.ezproxy.massey.ac.nz/10.1016/j.renene.2019.04.115

Zhang, X., Zhang, Z., Ma, Q., Deng, H., & Zhang, M. (2009). Study on utilization value of pure natural medical resources of benzene/ethanol extractives of Chinese fir wood. *2009 Symposium on Photonics and Optoelectronics*, 1-3. https://doi.org/10.1109/SOPO.2009.5230145

Zhang, Y., Silcock, P., Jones, J. R., & Eyres, G. T. (2020). Changes in wood smoke volatile composition by manipulating the smoke generation conditions. *Journal of Analytical and Applied Pyrolysis, 148*, 104769. https://doi-org.ezproxy.massey.ac.nz/10.1016/j.jaap.2019.104769

Zhao, J., Xiuwen, W., Hu, J., Liu, Q., Shen, D., & Xiao, R. (2014). Thermal degradation of softwood lignin and hardwood lignin by TG-FTIR and Py-GC/MS. *Polymer Degradation and Stability, 108*, 133-138. https://doi-org.ezproxy.massey.ac.nz/10.1016/j.polymdegradstab.2014.06.006

Zhou, Z., Jin, H., Zhao, L., Wang, Y., Wen, W., Yang, J., Li, Y., Pan, Y., & Qi, F. (2017). A thermal decomposition study of pine wood under ambient pressure using thermogravimetry combined with synchrotron vacuum ultraviolet photoionization mass spectrometry. *Proceedings of the Combustion Institute, 36*(2), 2217-2224. https://doi-org.ezproxy.massey.ac.nz/10.1016/j.proci.2016.06.081

Zhu, L., Yan, J., Zhu, Z., Ouyang, Y., Zhang, X., Zhang, W., Dai, X., Luo, L., & Chen, H. (2013). Differential analysis of camphor wood products by desorption atmospheric pressure chemical ionization mass spectrometry. *Journal of Agricultural and Food Chemistry, 61*(3), 547-552. https://doi-org.ezproxy.massey.ac.nz/10.1021/jf303793t

Zi, W., Chen, Y., Pan, Y., Zhang, Y., He, Y., & Wang, Q. (2019). Pyrolysis, morphology and microwave absorption properties of tobacco stem materials. *Science of The Total Environment, 683*, 341-350. https://doi-org.ezproxy.massey.ac.nz/10.1016/j.scitotenv.2019.04.053

Zobel, N., Anca-Couce, A. (2015). Influence of intraparticle secondary heterogeneous reactions on the reaction enthalpy of wood pyrolysis. *Journal of Analytical and Applied Pyrolysis, 116*, 281-286. https://doi-org.ezproxy.massey.ac.nz/10.1016/j.jaap.2015.08.019

Appendices

Appendices A: Tobacco returns for Easy RYO Fine Cut tobacco and HEETS Amber Label from Ministry of Health (2019)

Ingredients	Quantity Not Exceeded (%)	
	Easy RYO Fine Cut tobacco	HEETS Amber Label
Tobacco	95.50	75.95
Water (in tobacco)	19.50	13.00
Glycerol	-	17.00

Propylene glycol	4.00	1.00
Cellulose	-	3.80
Guar gum	-	2.20
Potassium sorbate	0.25	-
Acetic acid	0.24	-
Cocoa extract (alcoholic)	0.0014	-
Sugar syrup inverted	0.0006	-
Flavourings	0.0006	0.05

Appendices B: Proximate analysis raw data

Table B1: Tobacco proximate analysis

Moisture	16.82%	17.27%	16.03%	17.30%
Volatiles	60.69%	60.51%	61.05%	60.97%
Ash	6.05%	6.54%	6.61%	6.01%
Fixed Carbon*	16.43%	15.68%	16.32%	15.72%

*Fixed carbon was calculated from the difference.

Table B2: HEETS proximate analysis

Moisture	14.26%	10.59%	16.38%
Volatiles	67.34%	68.63%	66.06%
Ash	6.74%	9.12%	6.69%
Fixed Carbon*	11.65%	11.65%	10.87%

*Fixed carbon was calculated from the difference.

Table B3: Kānuka proximate analysis

Moisture	7.91%	7.82%	6.99%
Volatiles	74.64%	74.69%	74.79%
Ash	0.73%	0.36%	1.05%
Fixed Carbon*	16.72%	17.13%	17.13%

*Fixed carbon was calculated from the difference.

Appendices C: Ultimate analysis raw data

Table C1: Tobacco ultimate analysis on a dry and ash free basis

N	2.04%	1.99%	2.08%	2.07%
C	37.70%	37.53%	38.00%	38.08%
H	5.38%	5.50%	5.70%	5.68%
S	0.25%	0.19%	0.18%	0.18%
O*	54.63%	54.79%	54.04%	53.99%

*Oxygen was calculated from the difference.

Table C2: HEETS ultimate analysis on a dry and ash free basis

N	1.86%	1.87%	1.99%	1.90%
C	38.20%	38.78%	41.13%	39.05%
H	7.07%	7.12%	7.60%	7.16%
S	0.10%	0.13%	0.10%	0.15%
O*	52.77%	52.10%	49.17%	51.74%

*Oxygen was calculated from the difference.

Table C3: Kānuka ultimate analysis on a dry and ash free basis

N	0.17%	0.22%	0.19%	0.17%
C	46.92%	46.93%	46.89%	46.18%
H	6.13%	6.92%	6.95%	6.92%
S	0.07%	0.00%	0.00%	0.00%
O*	46.72%	45.93%	45.97%	46.72%

*Oxygen was calculated from the difference.

Appendices D: Thermogravimetry (TG) and derived thermogravimetry results (DTG)

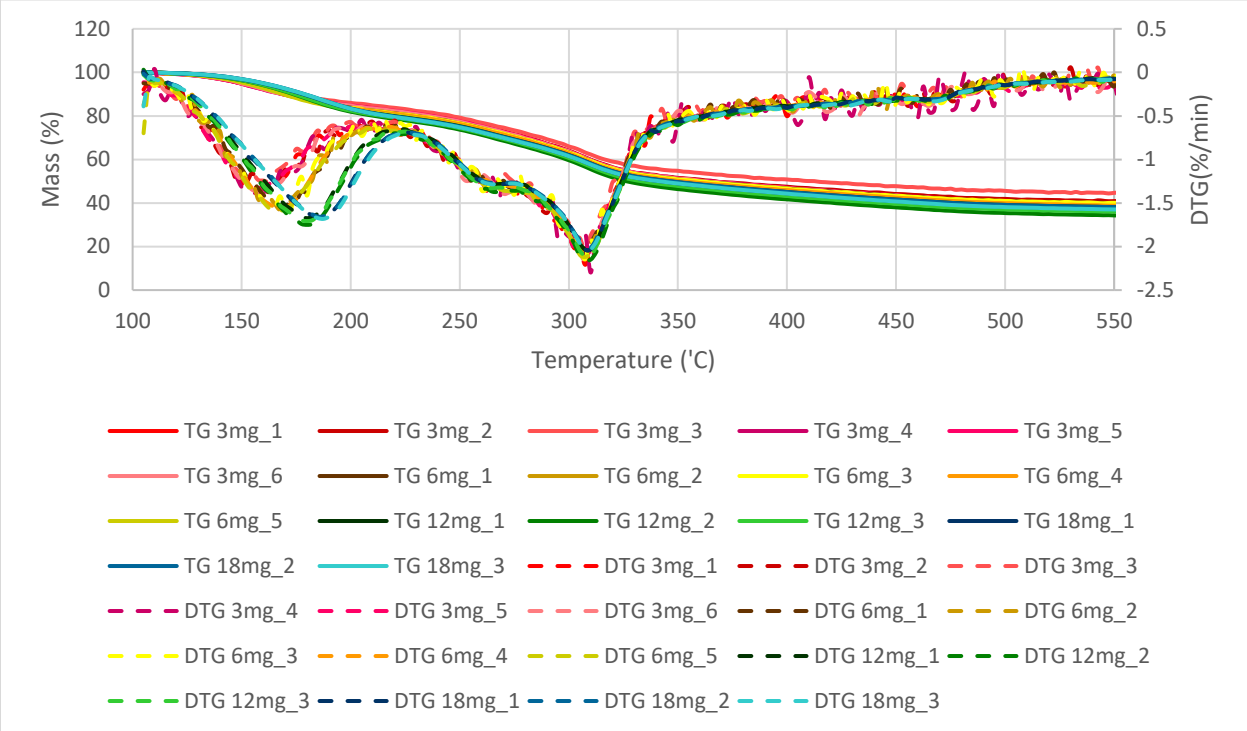

Figure D1: Graph of thermogravimetry (TG) and derivative thermogravimetry (DTG) versus temperature for HEETS samples heated at 5K/min after being held at 105°C for 45 minutes to remove moisture.

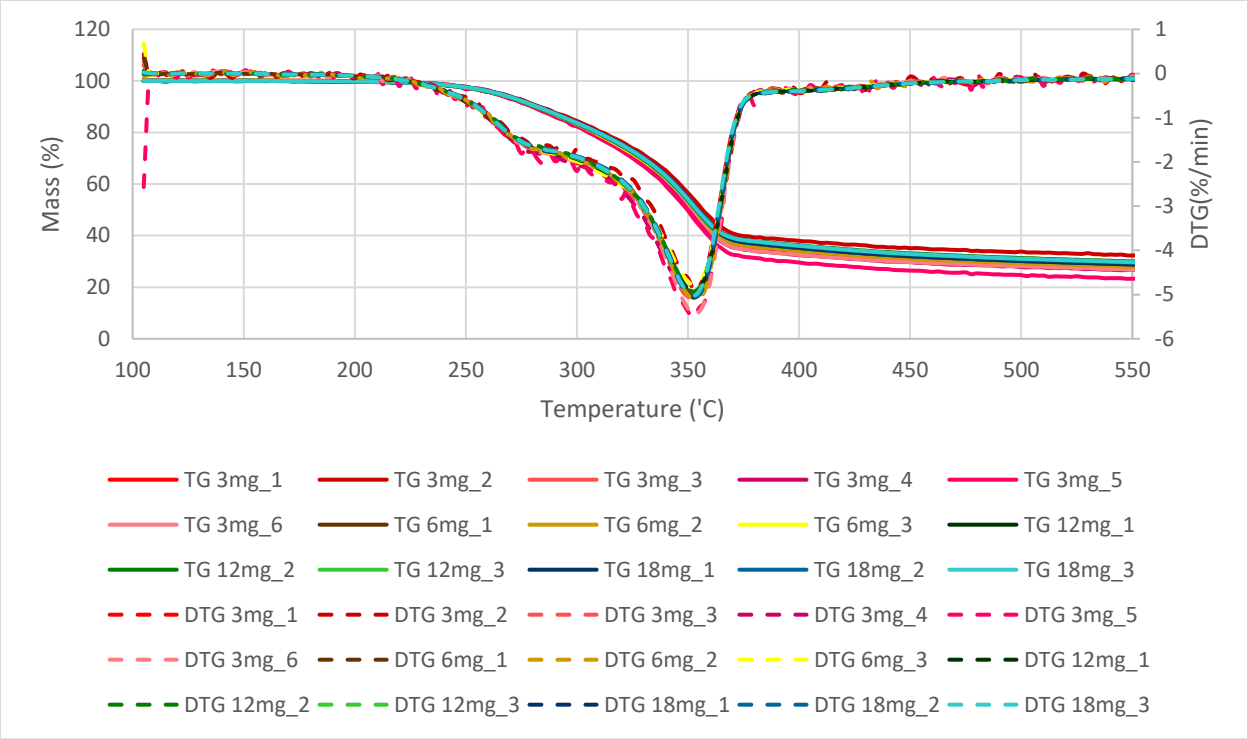

Figure D2: Graph of thermogravimetry (TG) and derivative thermogravimetry (DTG) versus temperature for kānuka samples heated at 5K/min after being held at 105^{o}C for 45 minutes to remove moisture.

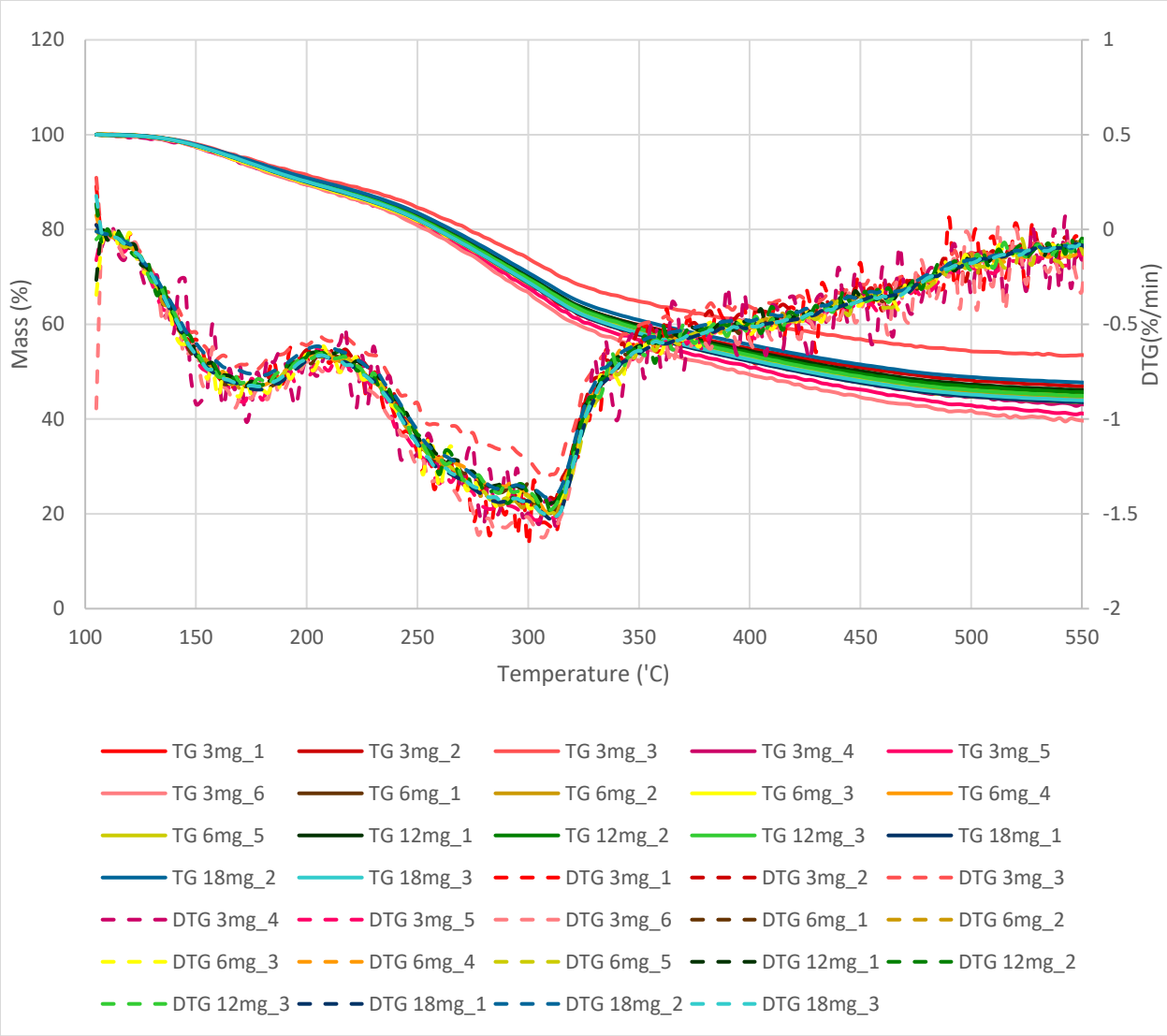

Figure D3: Graph of thermogravimetry (TG) and derivative thermogravimetry (DTG) versus temperature for tobacco samples heated at 5K/min after being held at 105^{o}C for 45 minutes to remove moisture.

Appendices E: Full size graphs comparing EGA/MS spectrum with the DTG curve

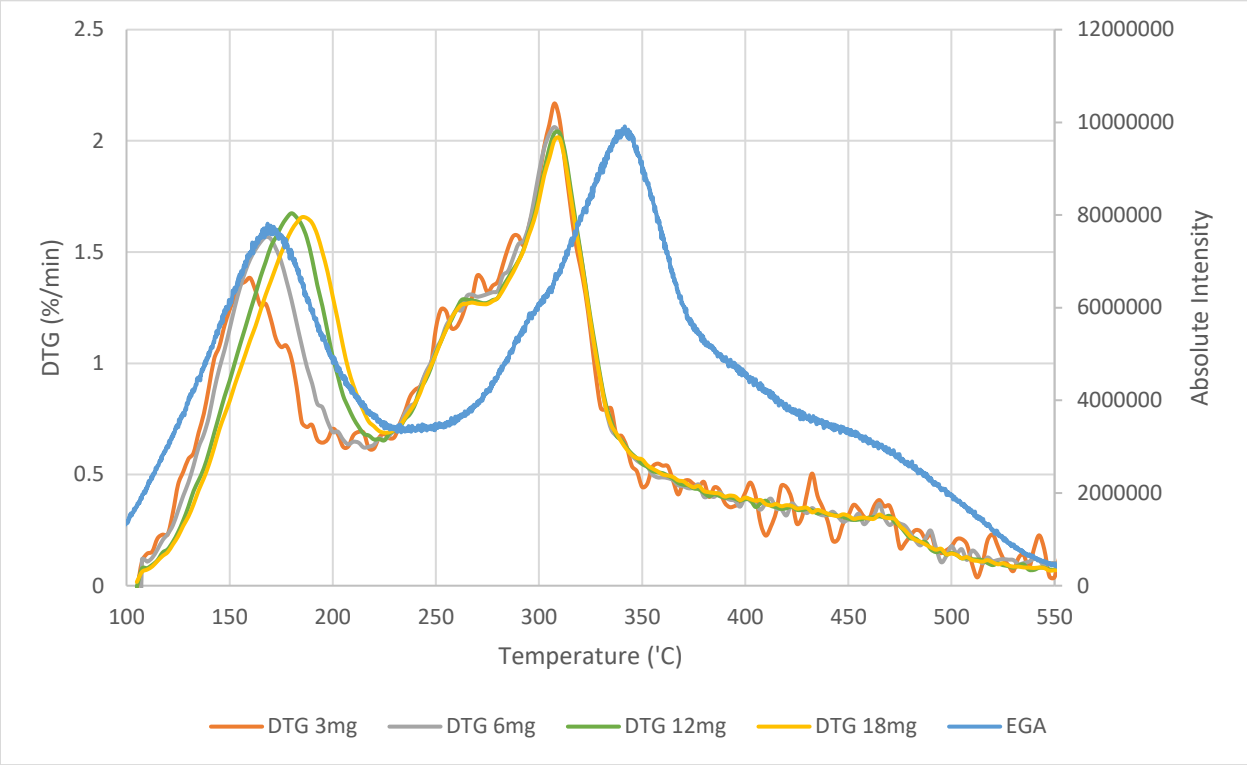

Figure E1: Curve comparing EGA/MS spectrum with the DTG curve for HEETS. One result for each different experiment is displayed, although a minimum of three replicates were completed for each.

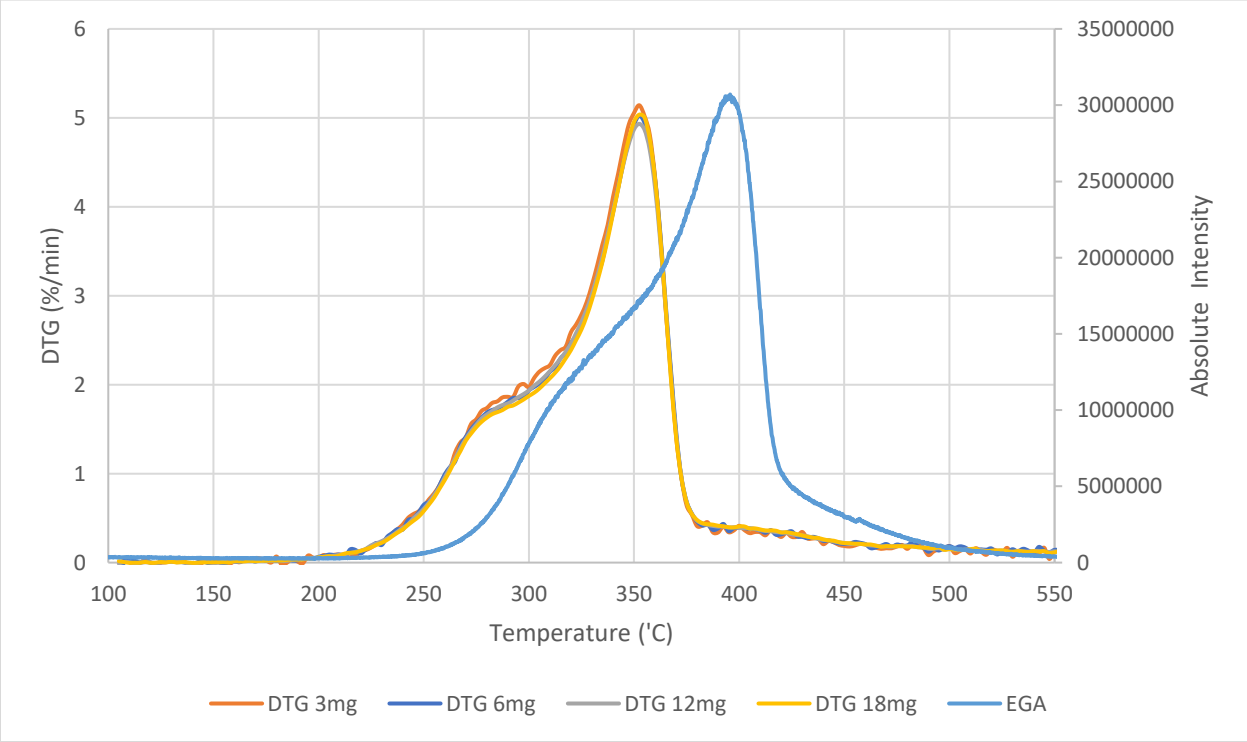

Figure E2: Curve comparing EGA/MS spectrum with the DTG curve for kānuka. One result for each different experiment is displayed, although a minimum of three replicates were completed for each.

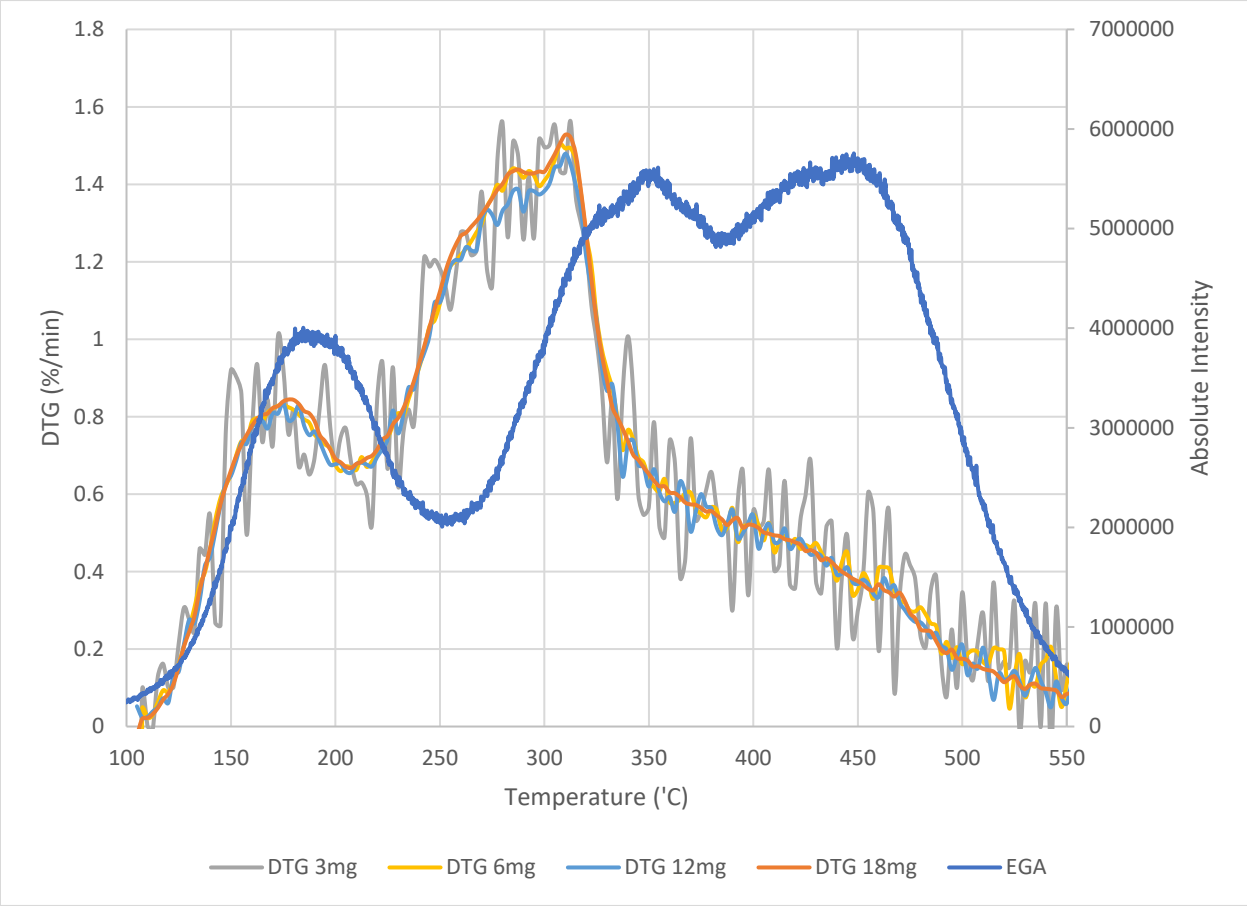

Figure E3: Curve comparing EGA/MS spectrum with the DTG curve for tobacco. One result for each different experiment is displayed, although a minimum of three replicates were completed for each.

Appendices F: EGA/MS spectrum for biomass

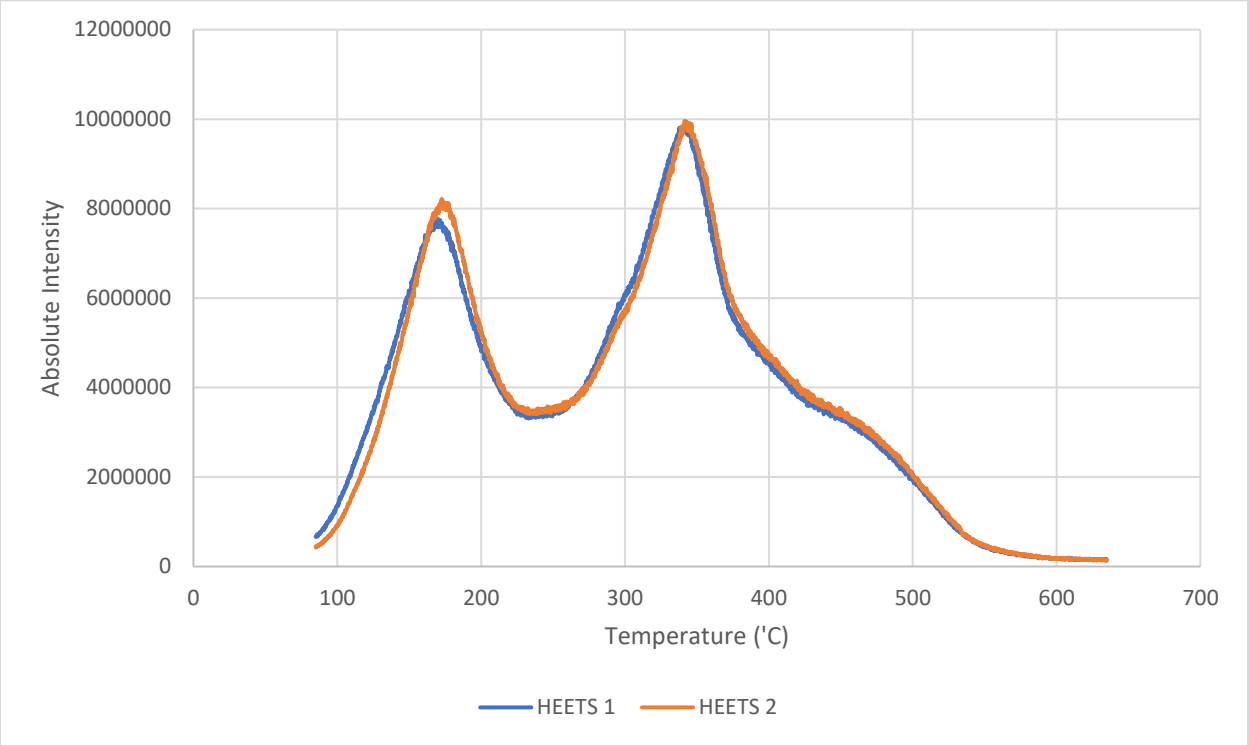

Figure F1: EGA/MS spectrum for a ~0.5mg sample of HEETS heated from 85°C to 630°C at 10 K/min. HEETS 1 and 2 represent 2 separate samples.

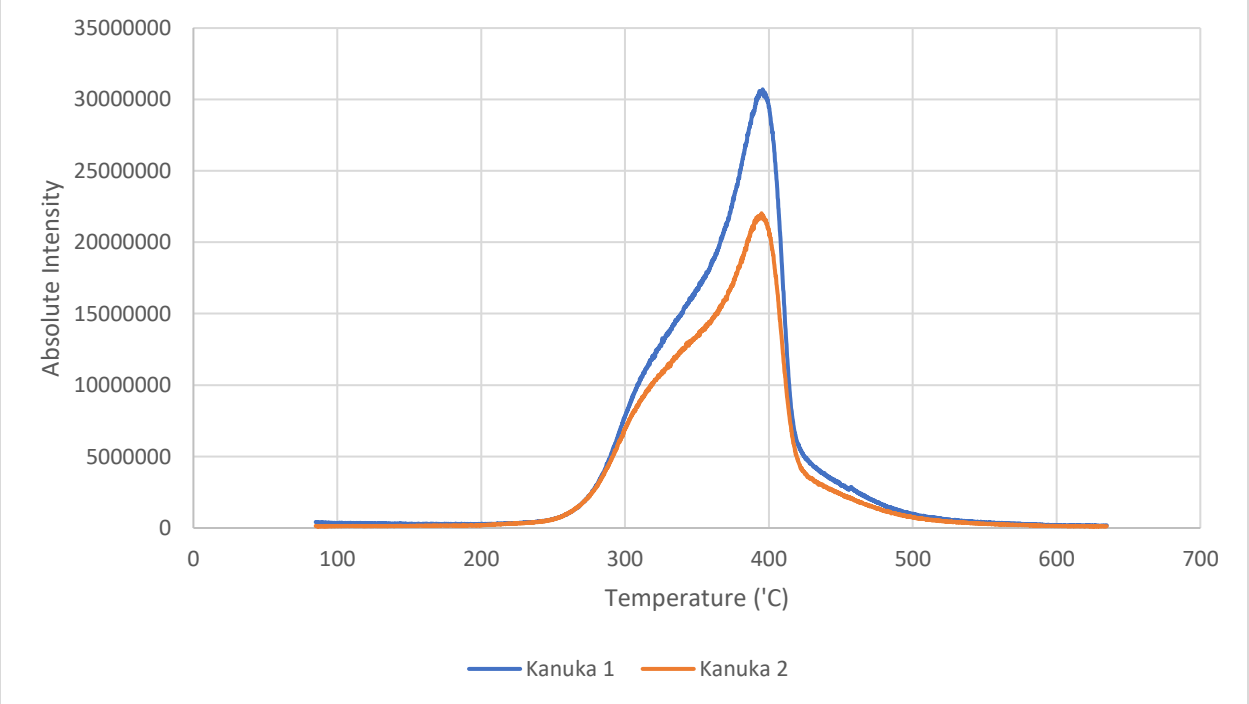

Figure F2: EGA/MS spectrum for a ~0.5mg sample of kānuka heated from 85°C to 630°C at 10 K/min. Kānuka 1 and 2 represent 2 separate samples.

Appendices G: Full size graphs comparing DTG curves with DSC curves for the biomass.

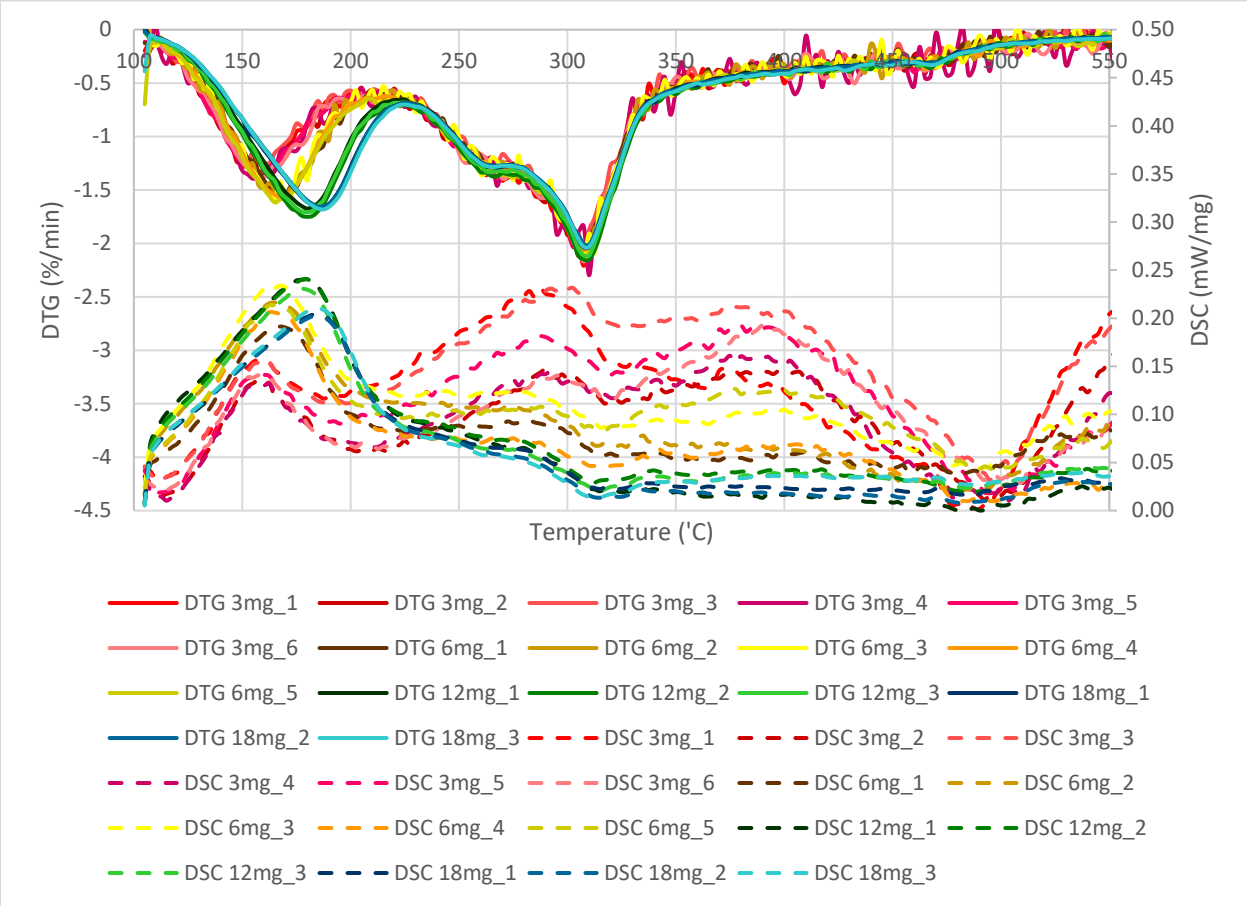

Figure G1: Comparison of DTG curves with DSC curves for HEETS.

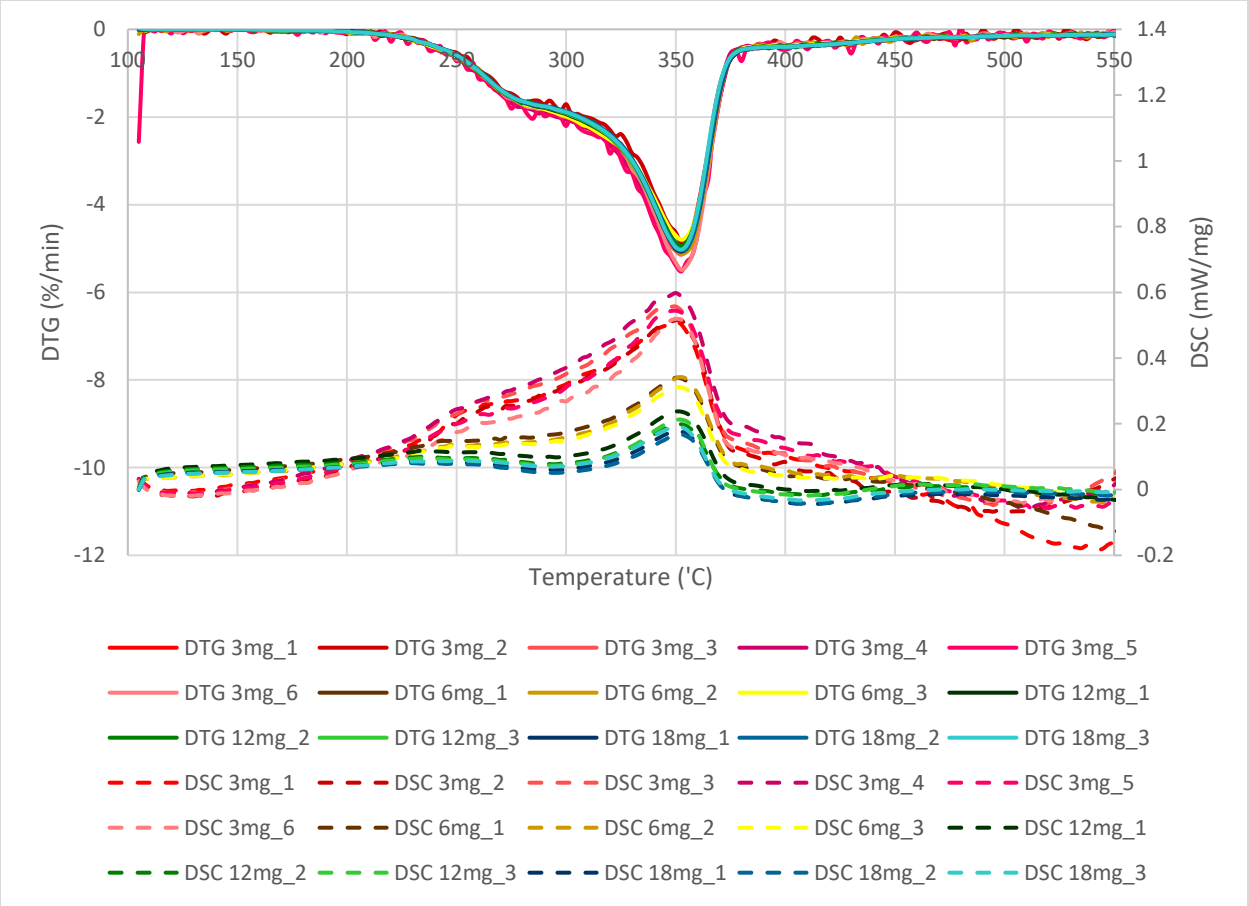

Figure G2: Comparison of DTG curves with DSC curves for kānuka.

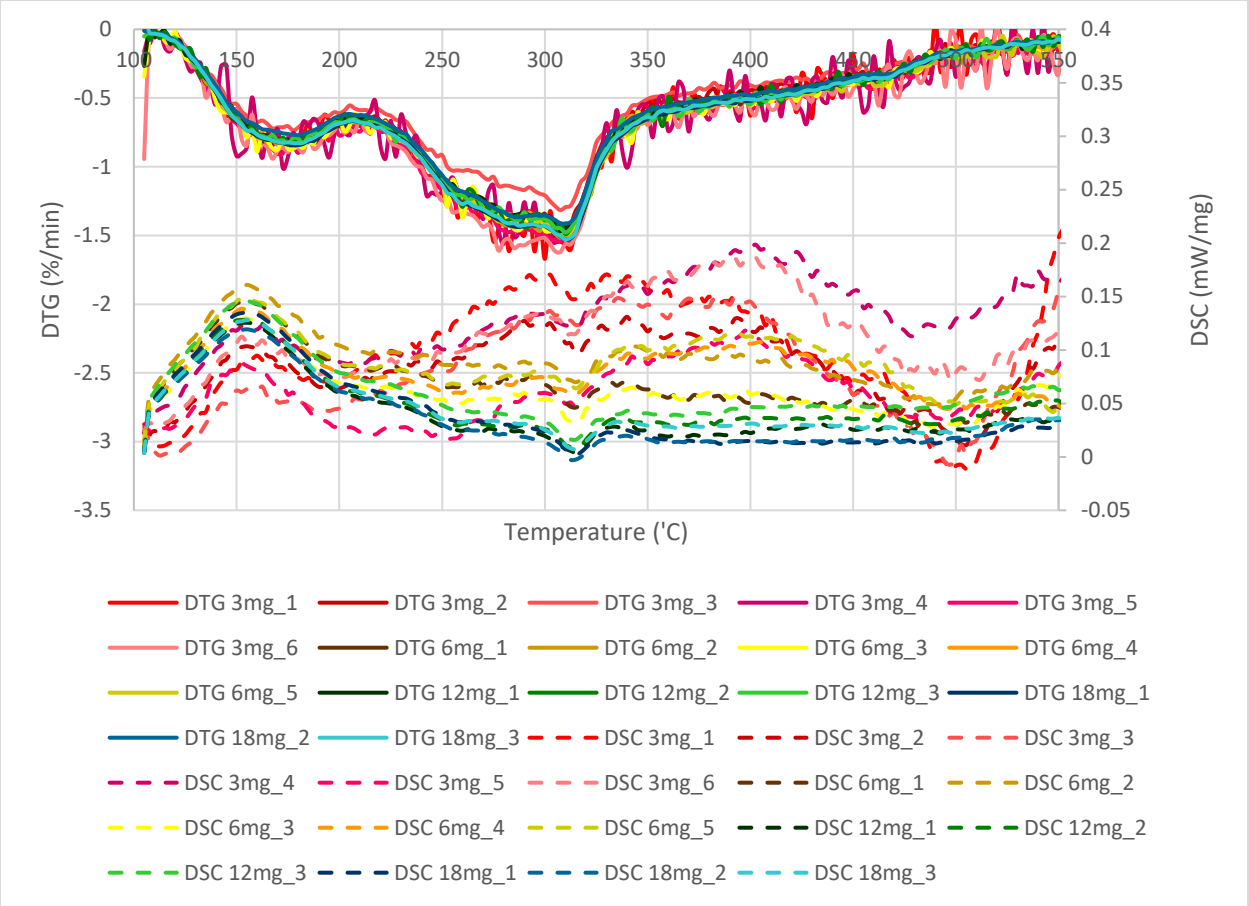

Figure G3: Comparison of DTG curves with DSC curves for tobacco.

Appendices H: Full sized graphs of absolute intensity over temperature for evolved gas analysis.

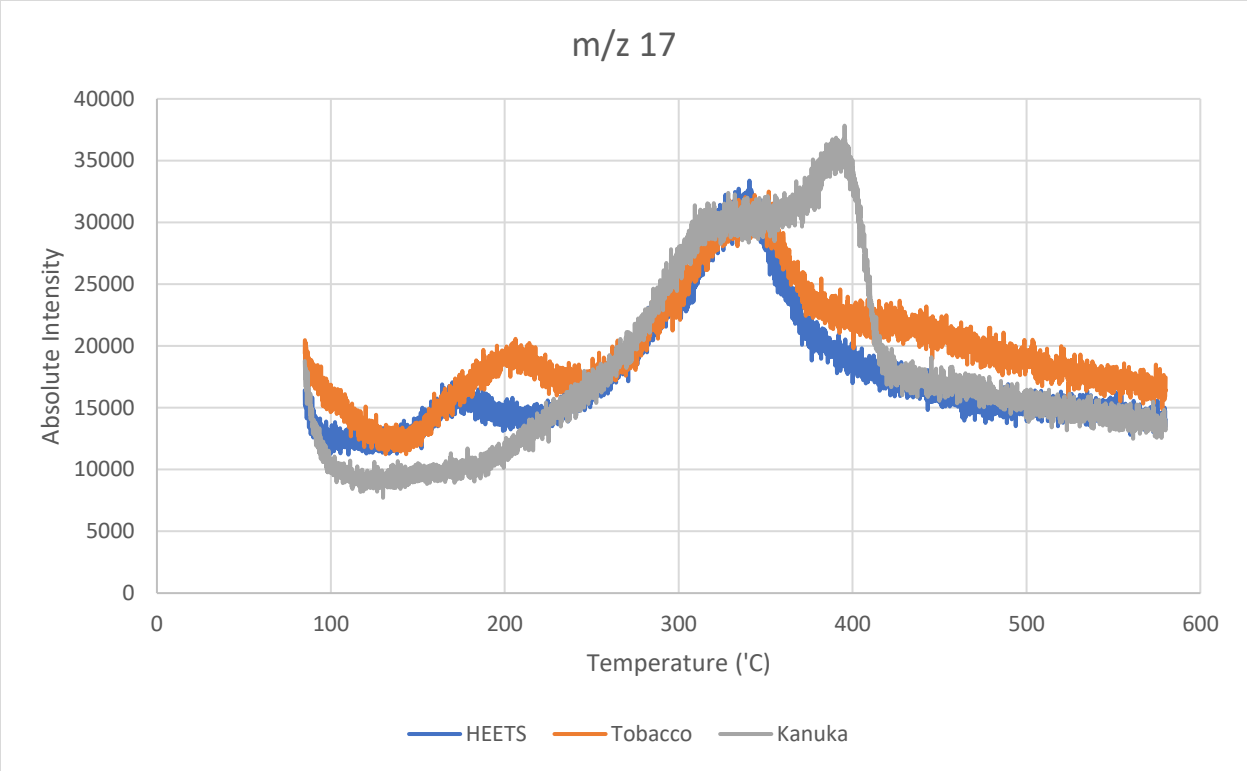

Figure H1: Graph of m/z 17 absolute intensity over temperature for evolved gas analysis of 0.5mg biomass samples for a range of molecular weights. Experiments involve a temp ramp of 10 K/min from 85°C to 580°C and a 20eV.

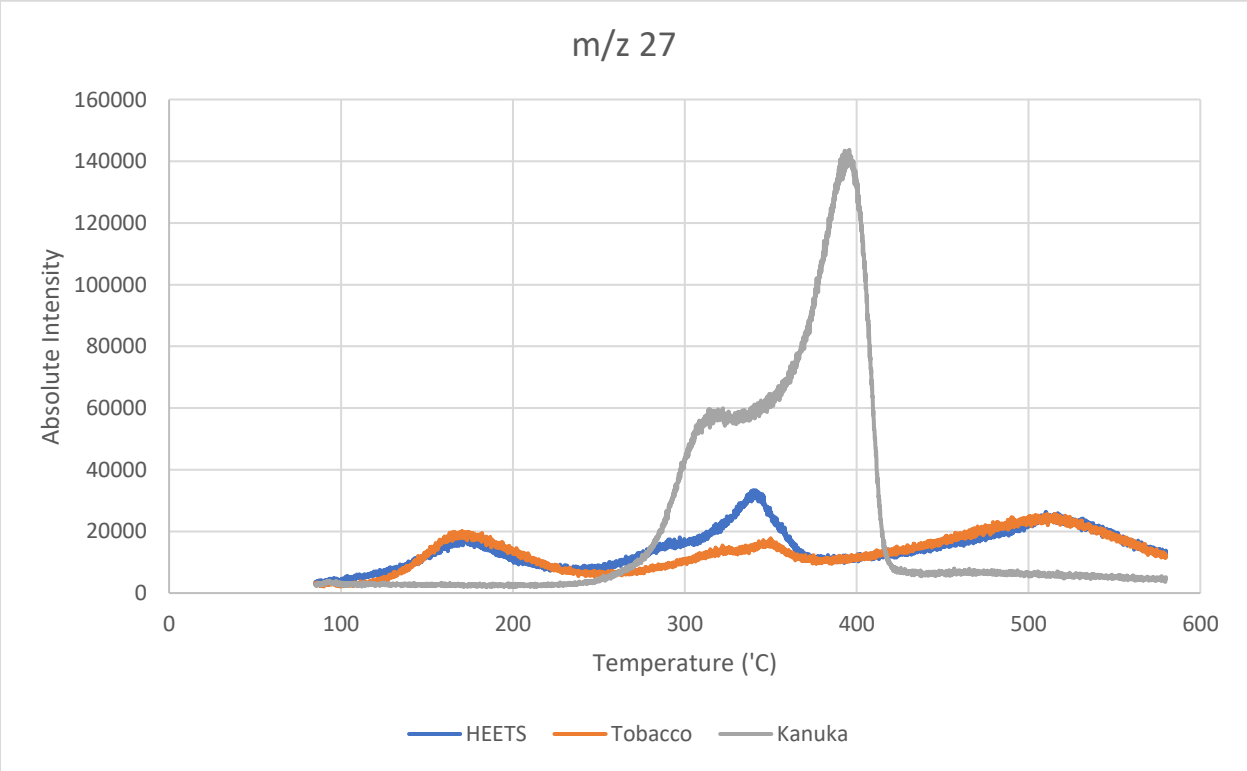

Figure H2: Graph of m/z 27 absolute intensity over temperature for evolved gas analysis of

0.5mg biomass samples for a range of molecular weights. Experiments involve a temp ramp of 10 K/min from 85°C to 580°C and a 20eV.

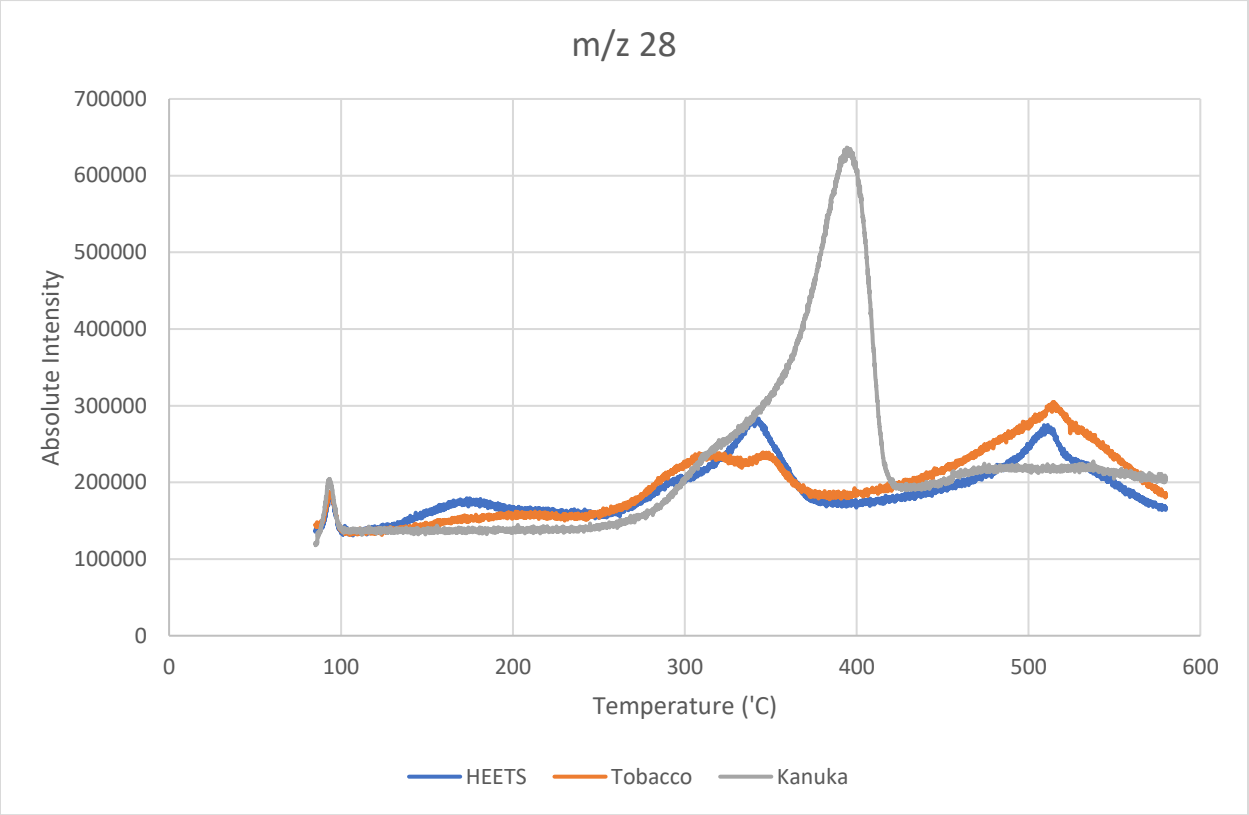

Figure H3: Graph of m/z 28 absolute intensity over temperature for evolved gas analysis of 0.5mg biomass samples for a range of molecular weights. Experiments involve a temp ramp of 10 K/min from 85°C to 580°C and a 20eV.

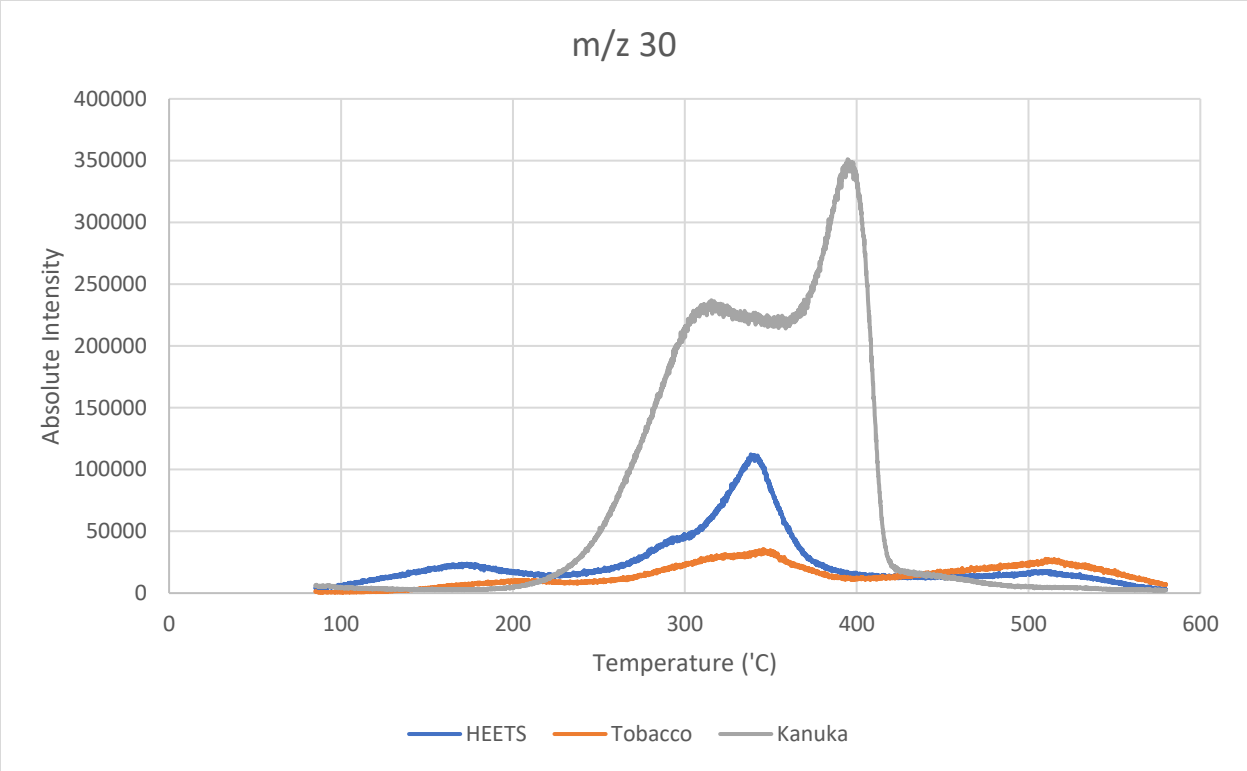

Figure H4: Graph of m/z 30 absolute intensity over temperature for evolved gas analysis of 0.5mg biomass samples for a range of molecular weights. Experiments involve a temp ramp of 10 K/min from 85°C to 580°C and a 20eV.

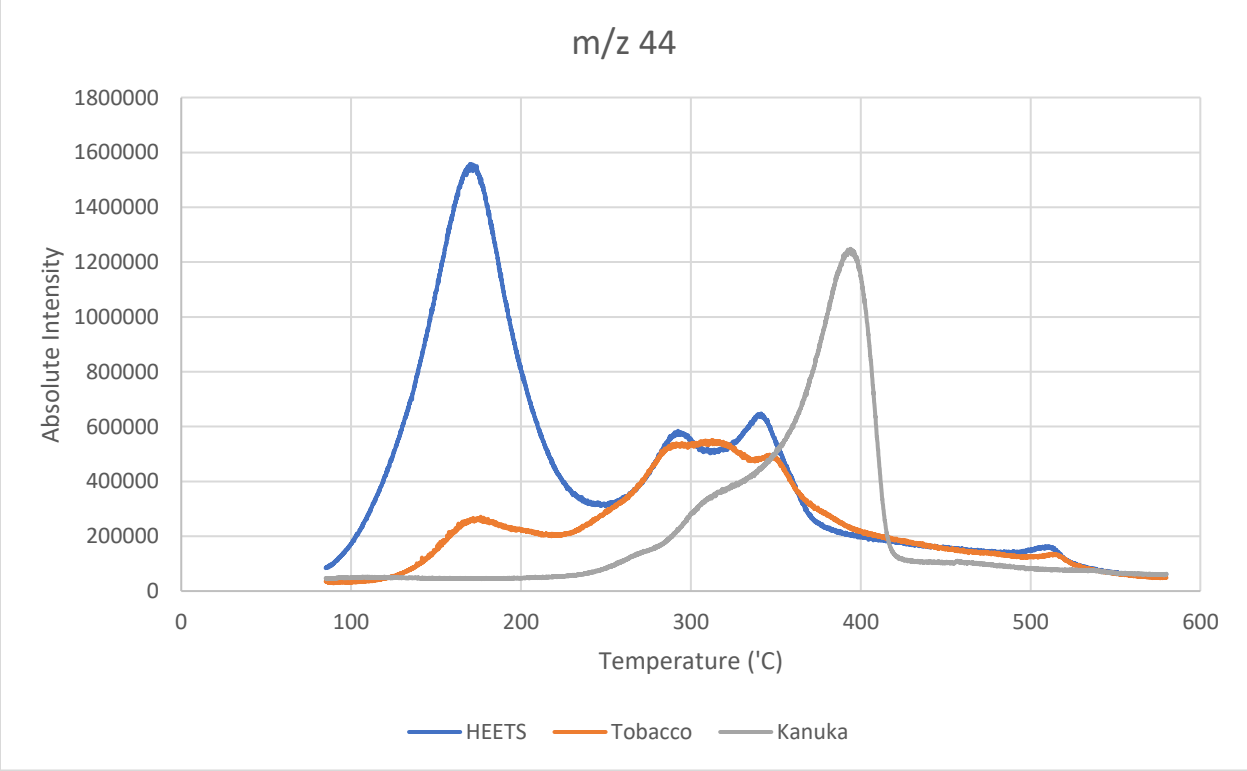

Figure H5: Graph of m/z 44 absolute intensity over temperature for evolved gas analysis of

0.5mg biomass samples for a range of molecular weights. Experiments involve a temp ramp of 10 K/min from 85°C to 580°C and a 20eV.

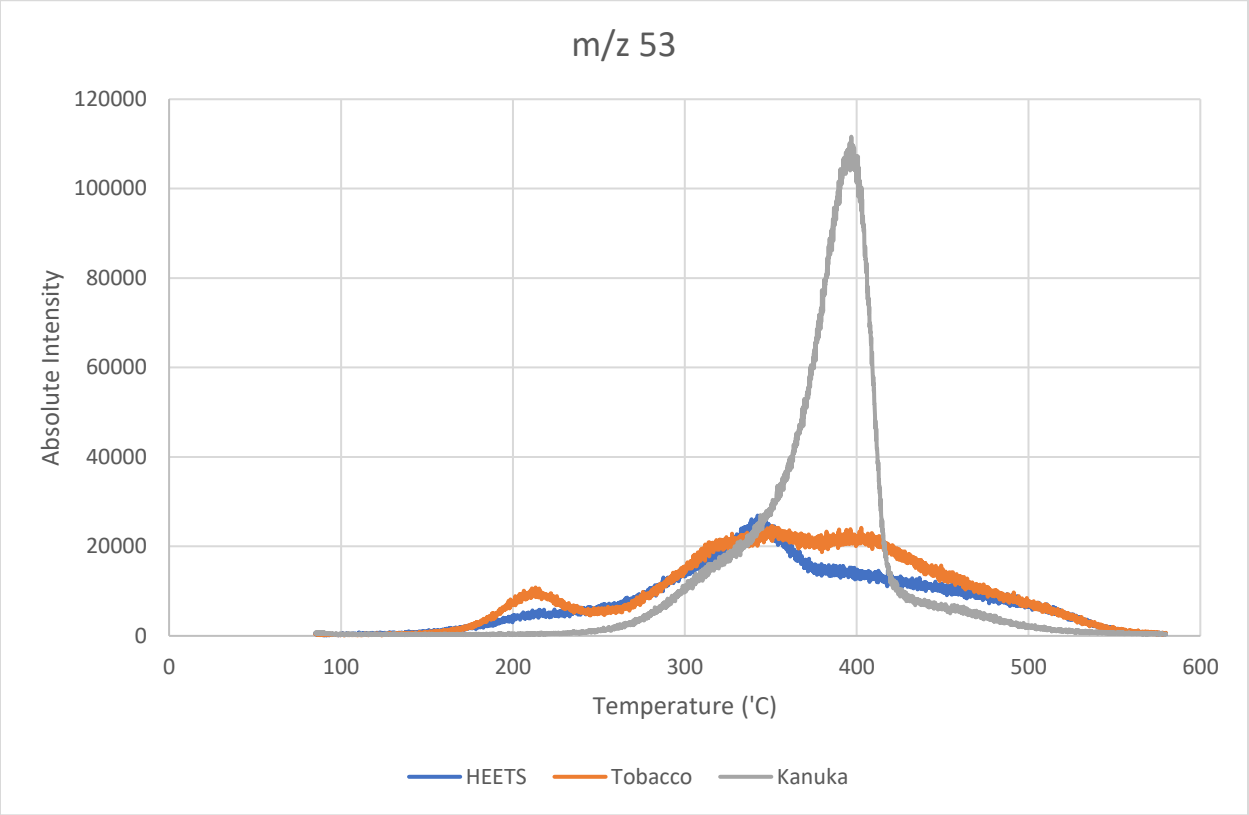

Figure H6: Graph of m/z 53 absolute intensity over temperature for evolved gas analysis of 0.5mg biomass samples for a range of molecular weights. Experiments involve a temp ramp of 10 K/min from 85°C to 580°C and a 20eV.

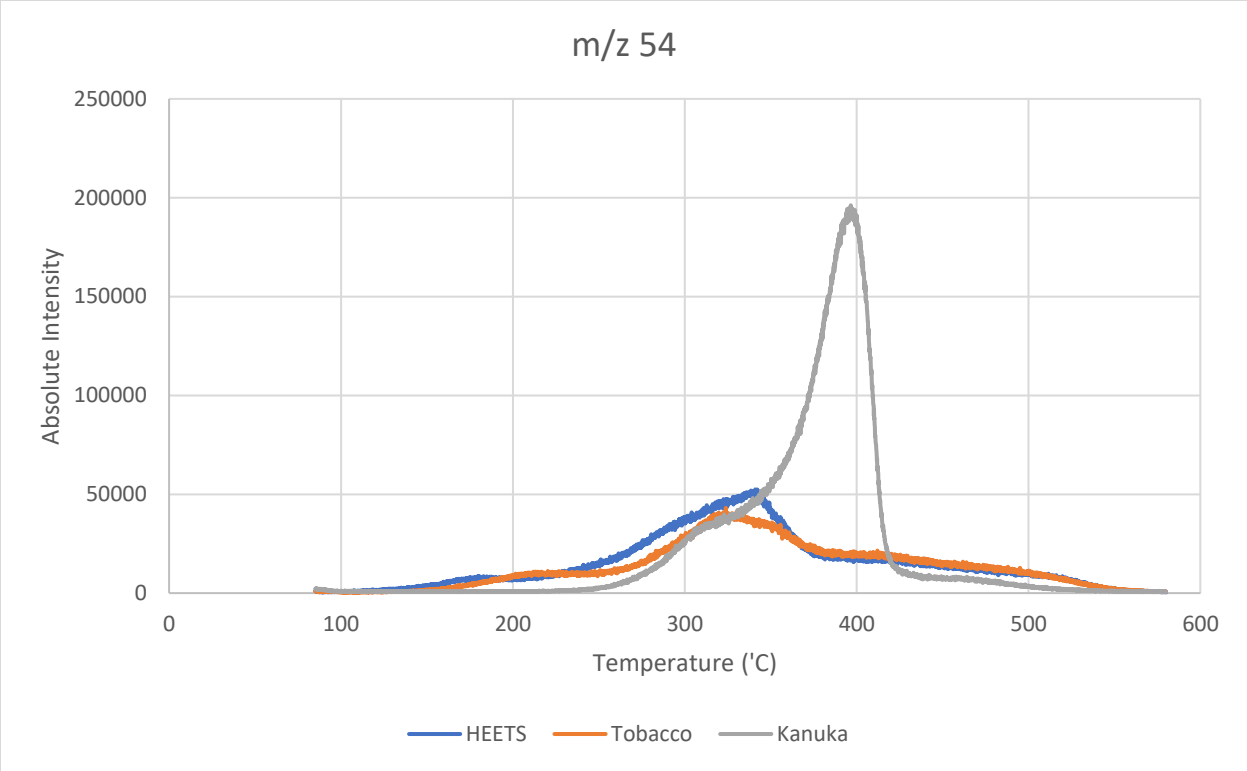

Figure H7: Graph of m/z 54 absolute intensity over temperature for evolved gas analysis of 0.5mg biomass samples for a range of molecular weights. Experiments involve a temp ramp of 10 K/min from 85°C to 580°C and a 20eV.

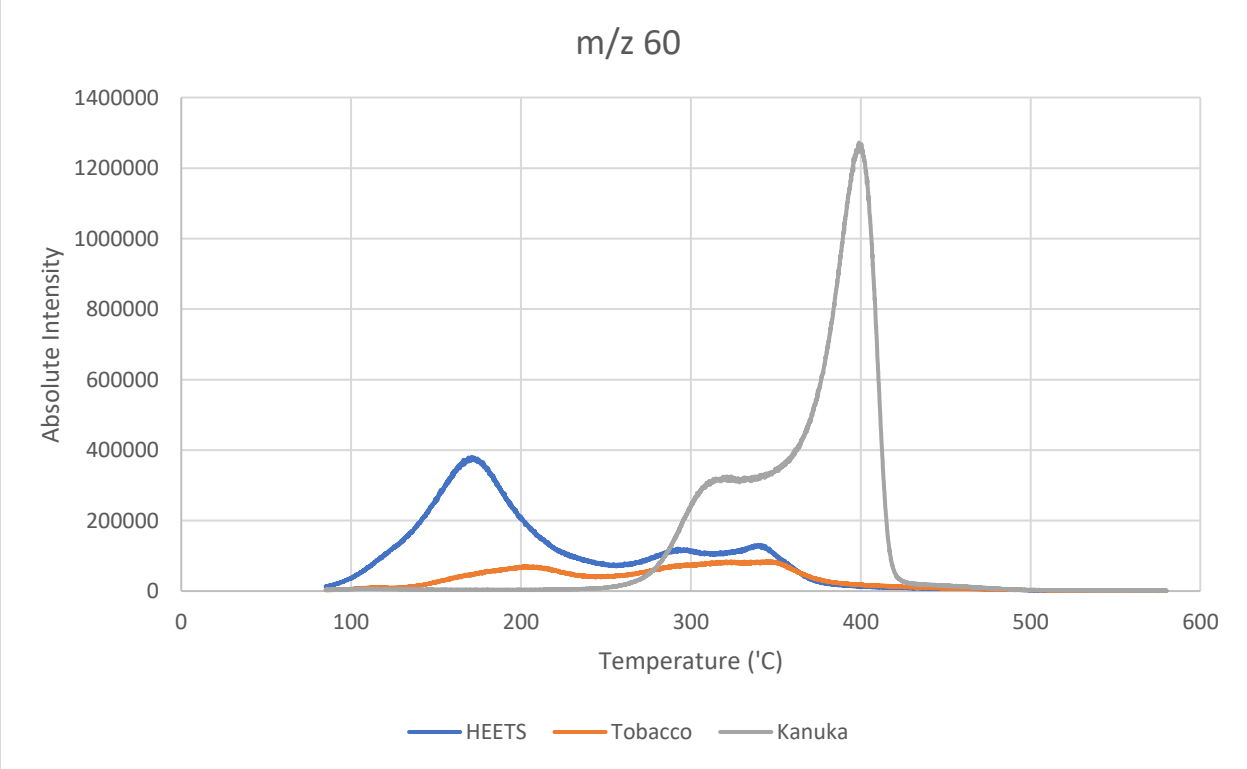

Figure H8: Graph of m/z 60 absolute intensity over temperature for evolved gas analysis of

0.5mg biomass samples for a range of molecular weights. Experiments involve a temp ramp of 10 K/min from 85°C to 580°C and a 20eV.

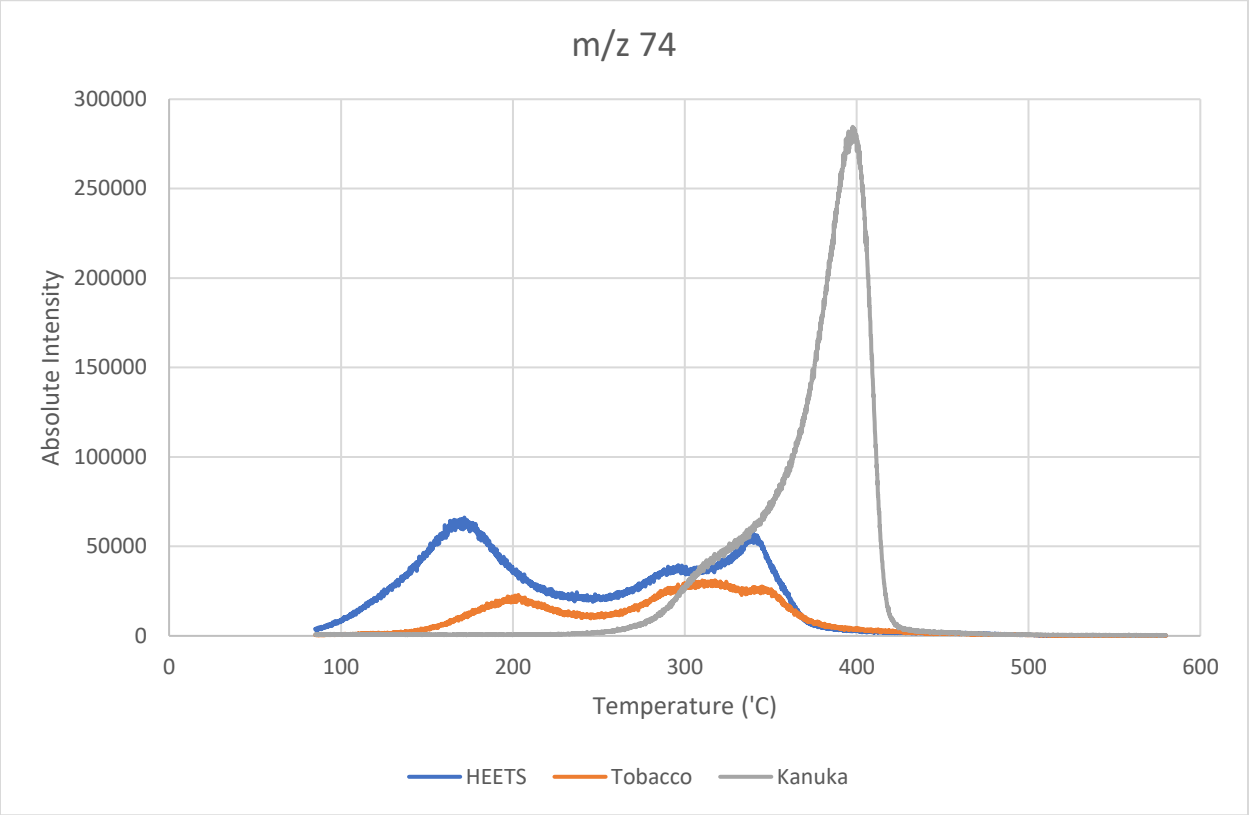

Figure H9: Graph of m/z 74 absolute intensity over temperature for evolved gas analysis of 0.5mg biomass samples for a range of molecular weights. Experiments involve a temp ramp of 10 K/min from 85°C to 580°C and a 20eV.

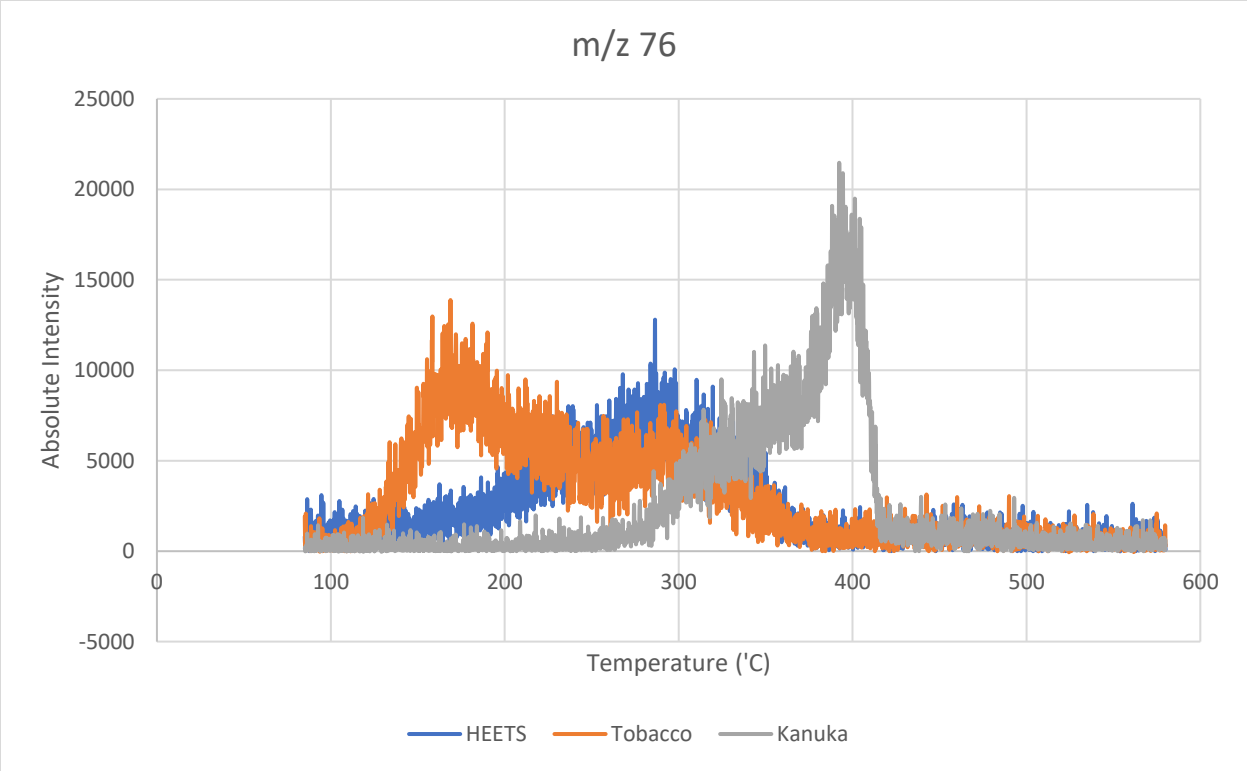

Figure H10: Graph of m/z 76 absolute intensity over temperature for evolved gas analysis of 0.5mg biomass samples for a range of molecular weights. Experiments involve a temp ramp of 10 K/min from 85°C to 580°C and a 20eV.

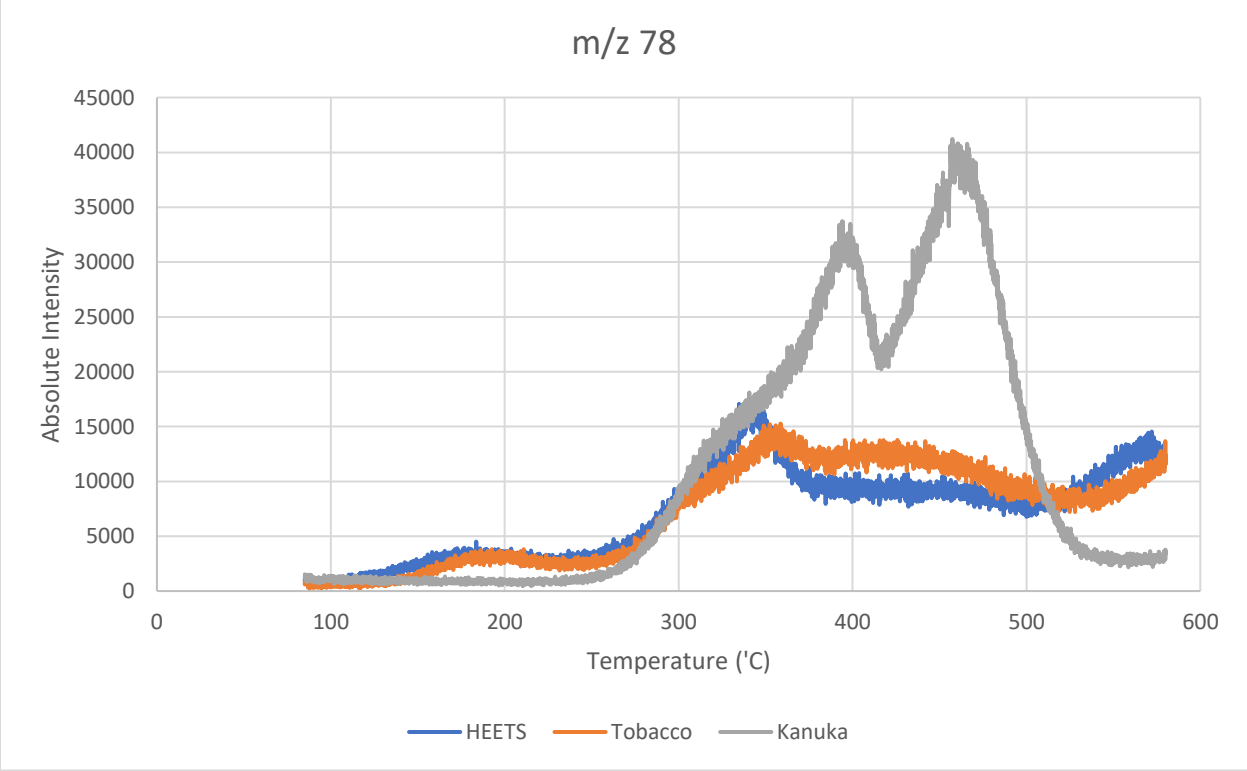

Figure H11: Graph of m/z 78 absolute intensity over temperature for evolved gas analysis of

0.5mg biomass samples for a range of molecular weights. Experiments involve a temp ramp of 10 K/min from 85°C to 580°C and a 20eV.

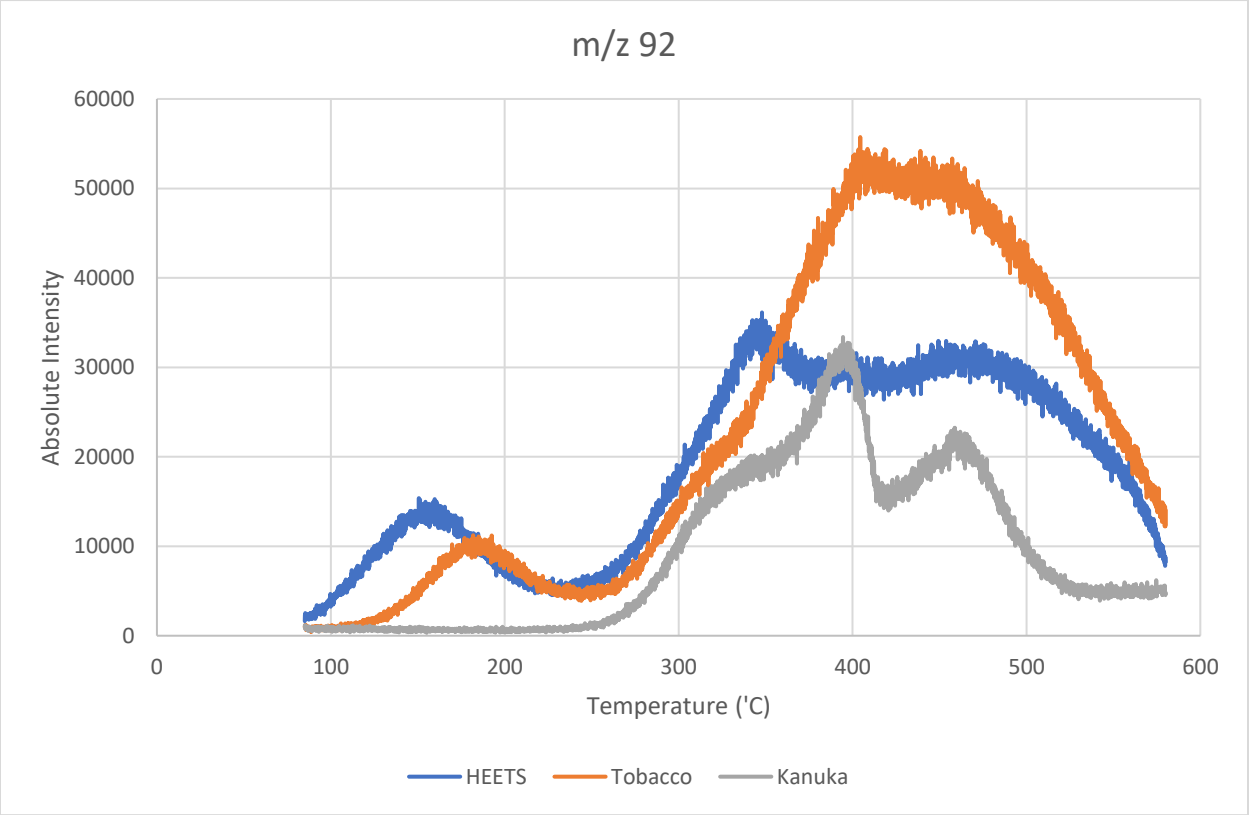

Figure H12: Graph of m/z 92 absolute intensity over temperature for evolved gas analysis of 0.5mg biomass samples for a range of molecular weights. Experiments involve a temp ramp of 10 K/min from 85°C to 580°C and a 20eV.

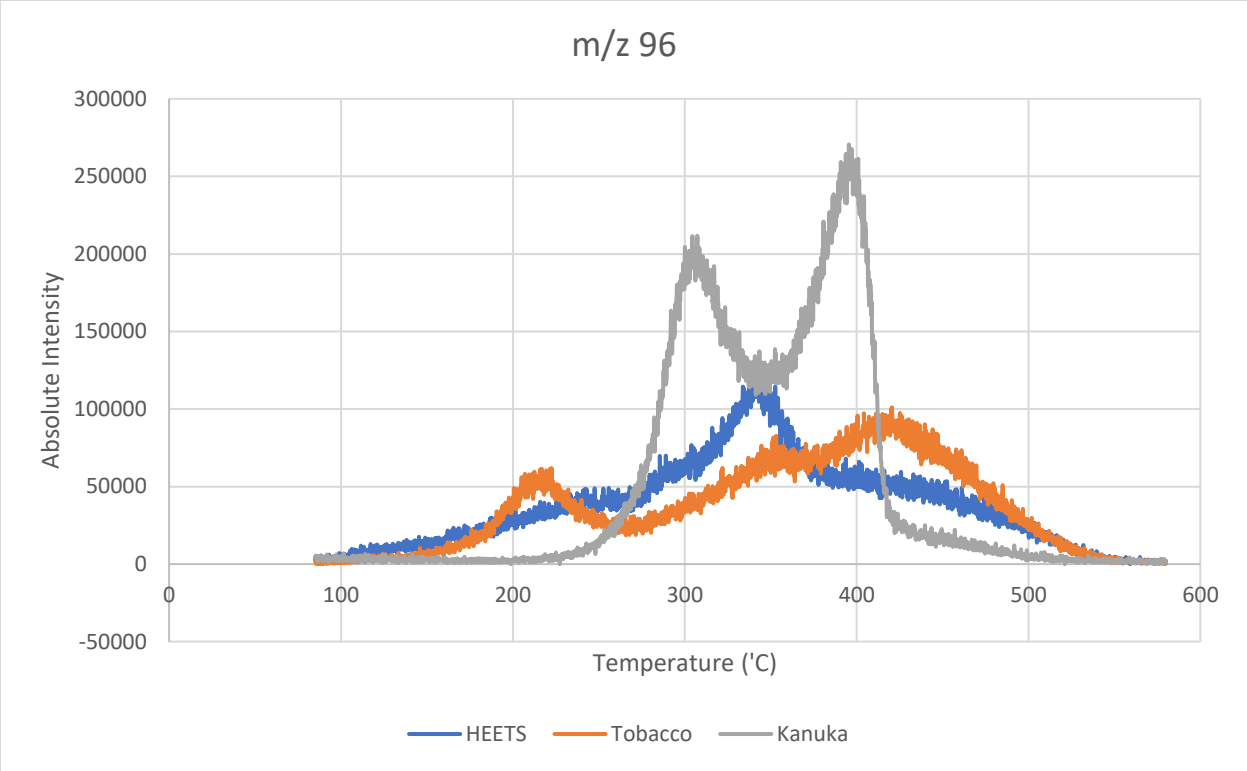

Figure H13: Graph of m/z 96 absolute intensity over temperature for evolved gas analysis of 0.5mg biomass samples for a range of molecular weights. Experiments involve a temp ramp of 10 K/min from 85°C to 580°C and a 20eV.

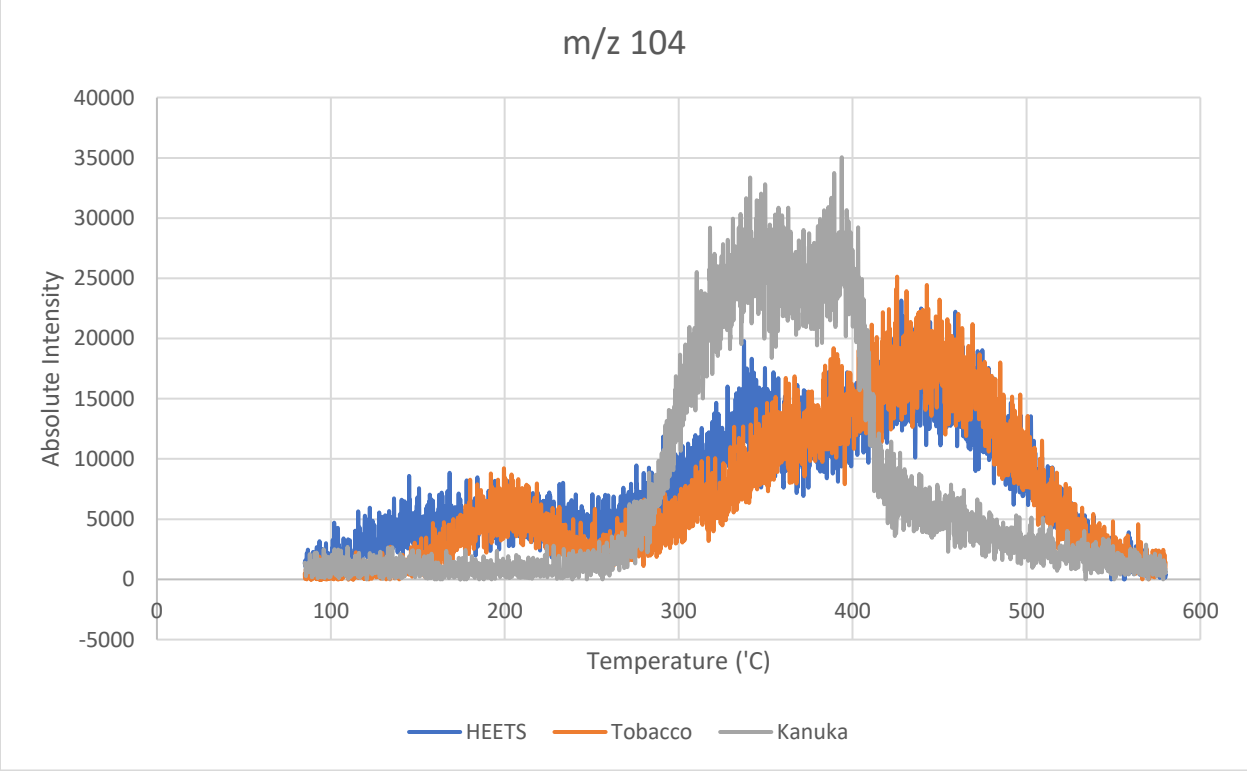

Figure H14: Graph of m/z 104 absolute intensity over temperature for evolved gas analysis of 0.5mg biomass samples for a range of molecular weights. Experiments involve a temp ramp of 10 K/min from 85°C to 580°C and a 20eV.

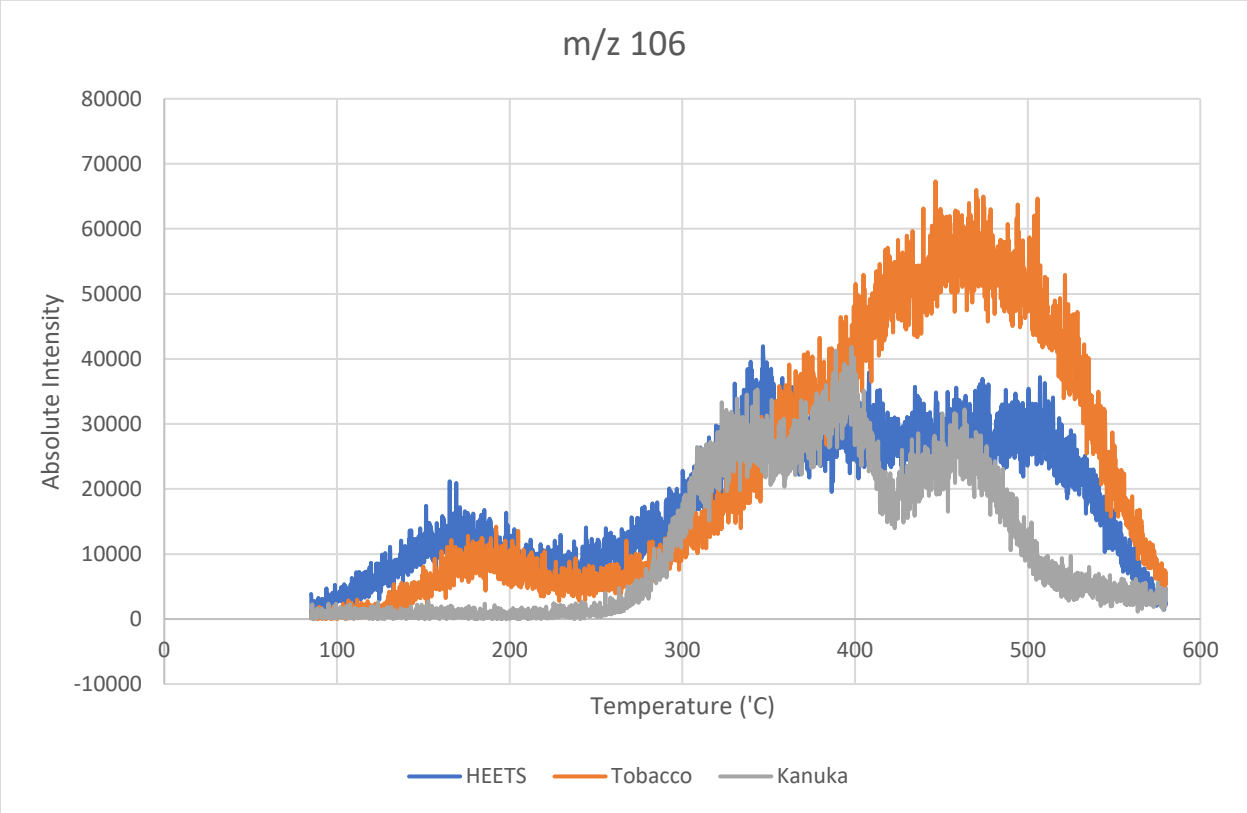

Figure H15: Graph of m/z 106 absolute intensity over temperature for evolved gas analysis of 0.5mg biomass samples for a range of molecular weights. Experiments involve a temp ramp of 10 K/min from 85°C to 580°C and a 20eV.

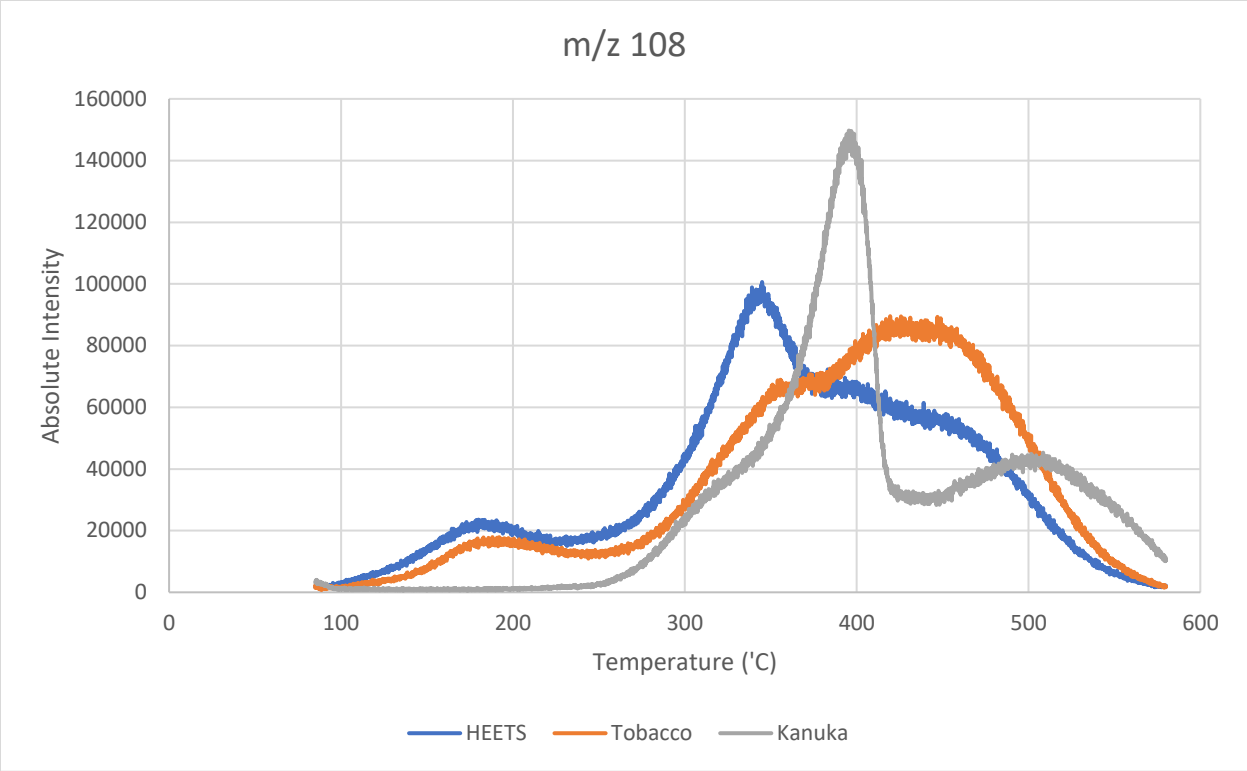

Figure H16: Graph of m/z 108 absolute intensity over temperature for evolved gas analysis of 0.5mg biomass samples for a range of molecular weights. Experiments involve a temp ramp of 10 K/min from 85°C to 580°C and a 20eV.

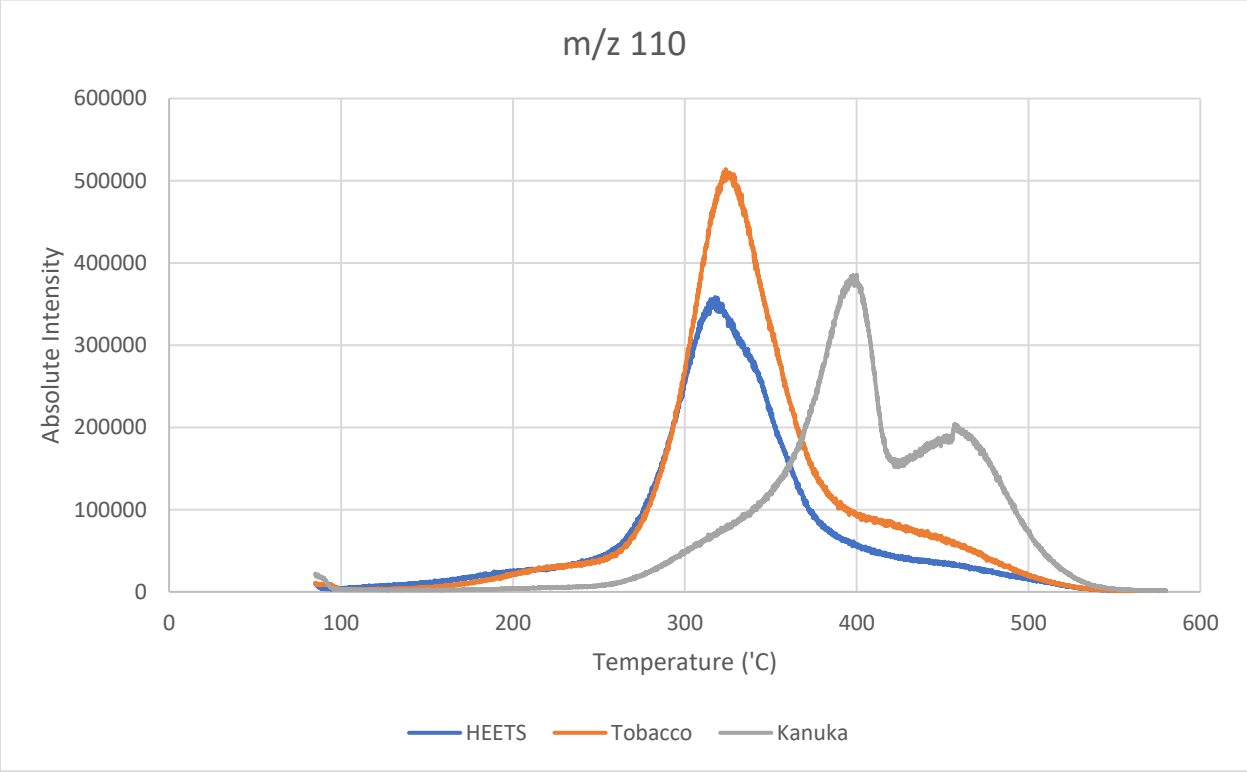

Figure H17: Graph of m/z 110 absolute intensity over temperature for evolved gas analysis of 0.5mg biomass samples for a range of molecular weights. Experiments involve a temp ramp of 10 K/min from 105°C to 580°C and a 20eV.

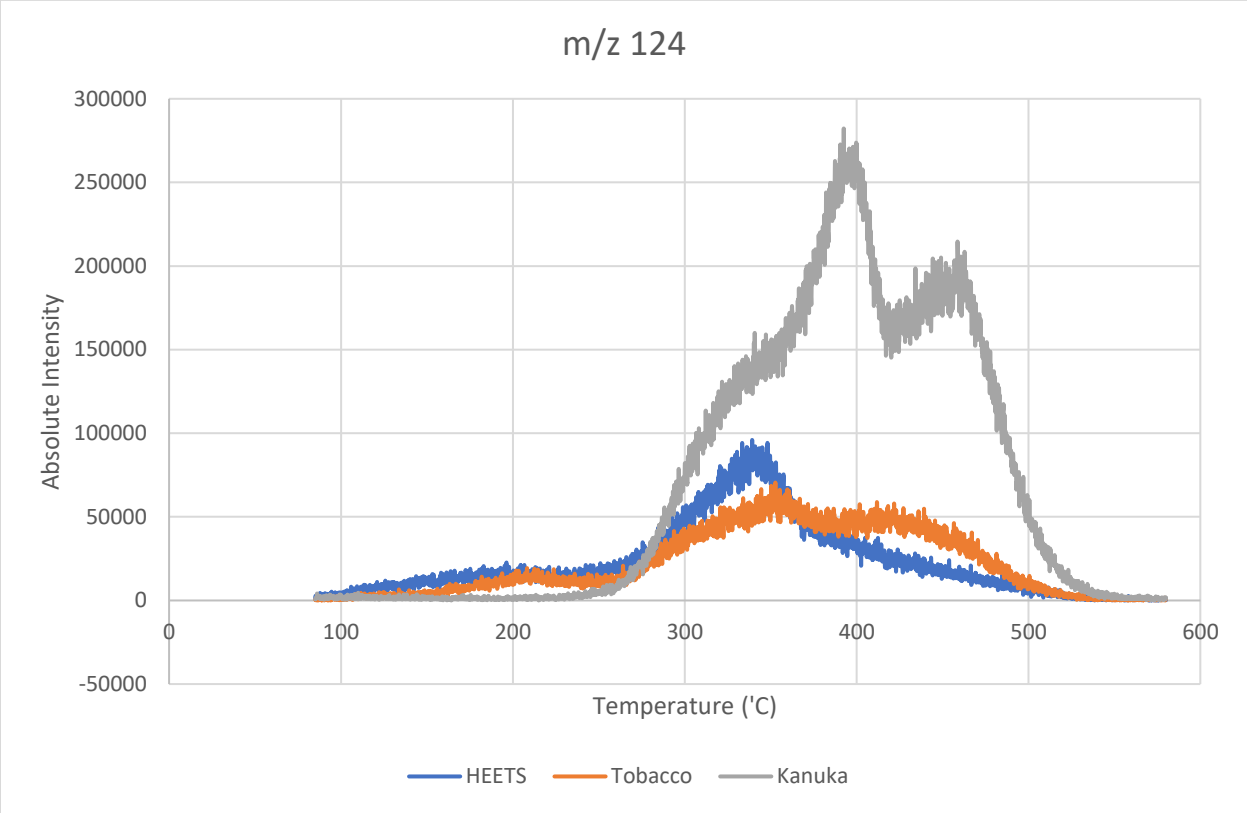

Figure H18: Graph of m/z 124 absolute intensity over temperature for evolved gas analysis of 0.5mg biomass samples for a range of molecular weights. Experiments involve a temp ramp of 10 K/min from 85°C to 580°C and a 20eV.

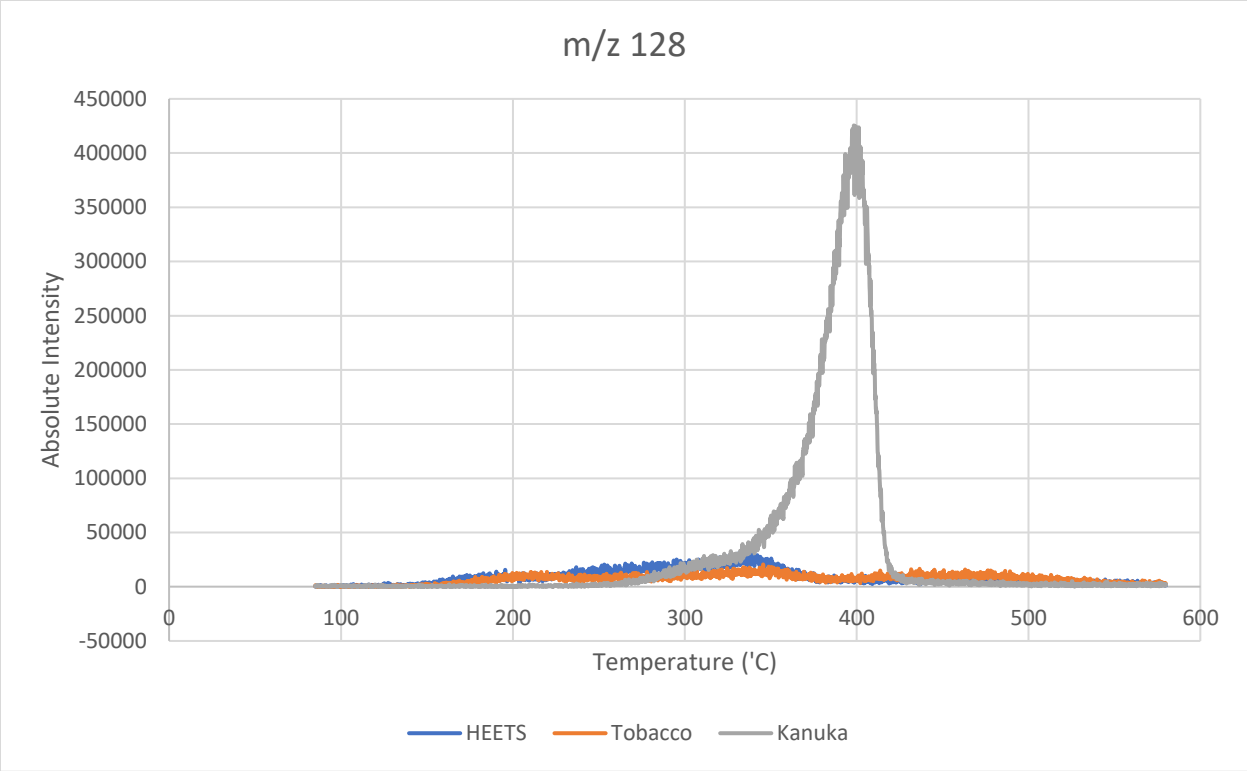

Figure H19: Graph of m/z 128 absolute intensity over temperature for evolved gas analysis of 0.5mg biomass samples for a range of molecular weights. Experiments involve a temp ramp of 10 K/min from 85^{o}C to 580^{o}C and a 20eV.

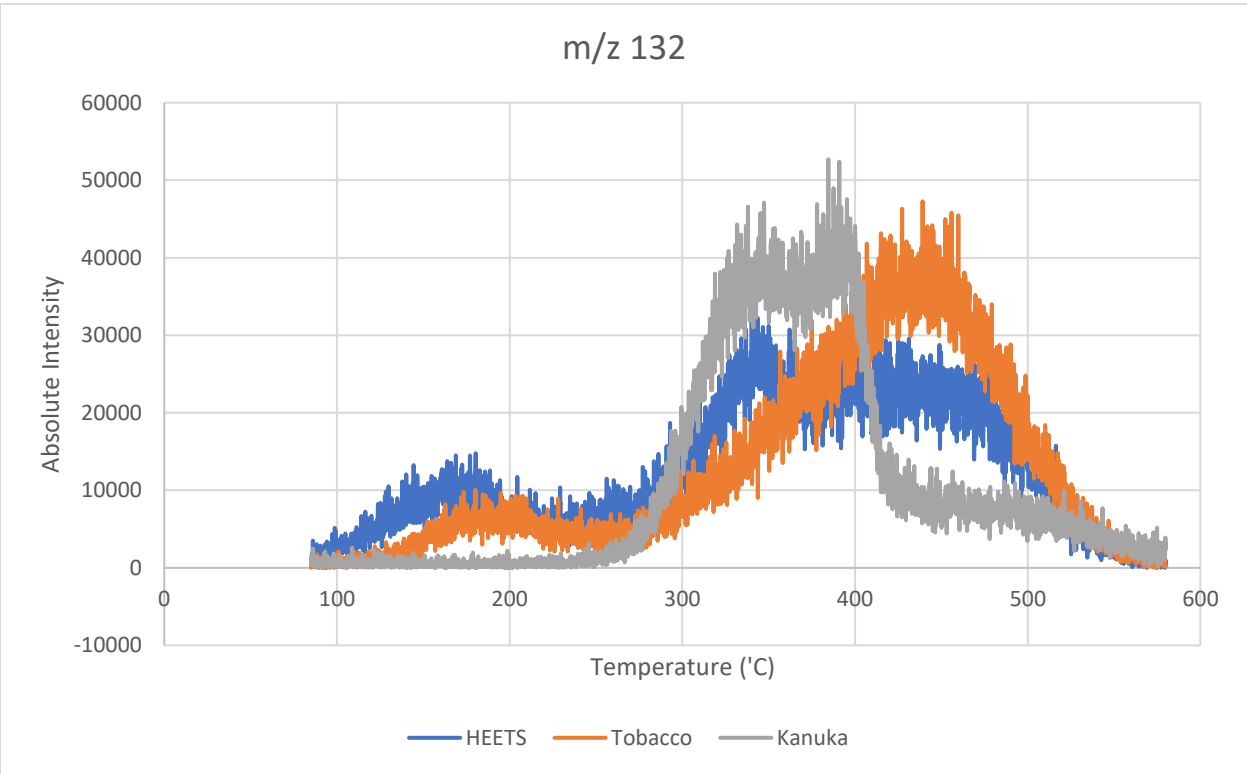

Figure H20: Graph of m/z 132 absolute intensity over temperature for evolved gas analysis of 0.5mg biomass samples for a range of molecular weights. Experiments involve a temp ramp of 10 K/min from 85°C to 580°C and a 20eV.

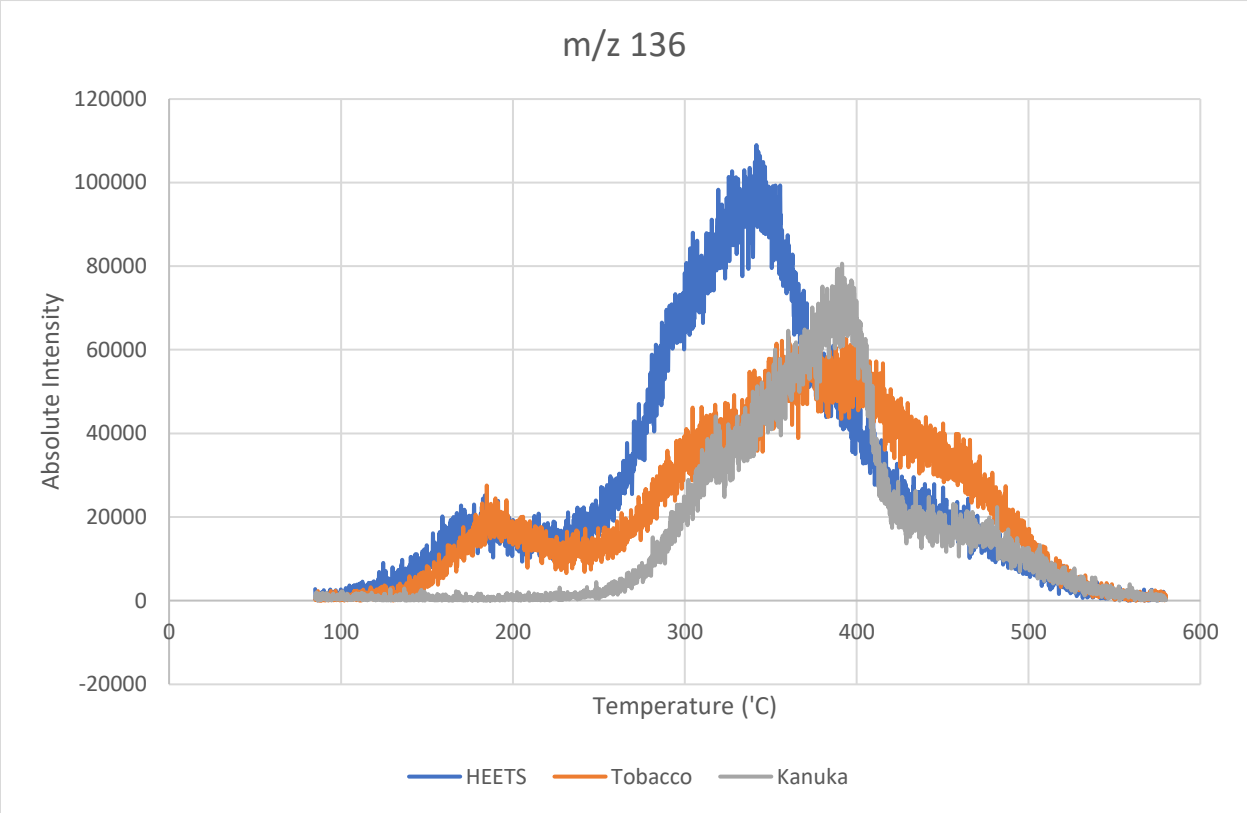

Figure H21: Graph of m/z 136 absolute intensity over temperature for evolved gas analysis of 0.5mg biomass samples for a range of molecular weights. Experiments involve a temp ramp of 10 K/min from 85°C to 580°C and a 20eV.

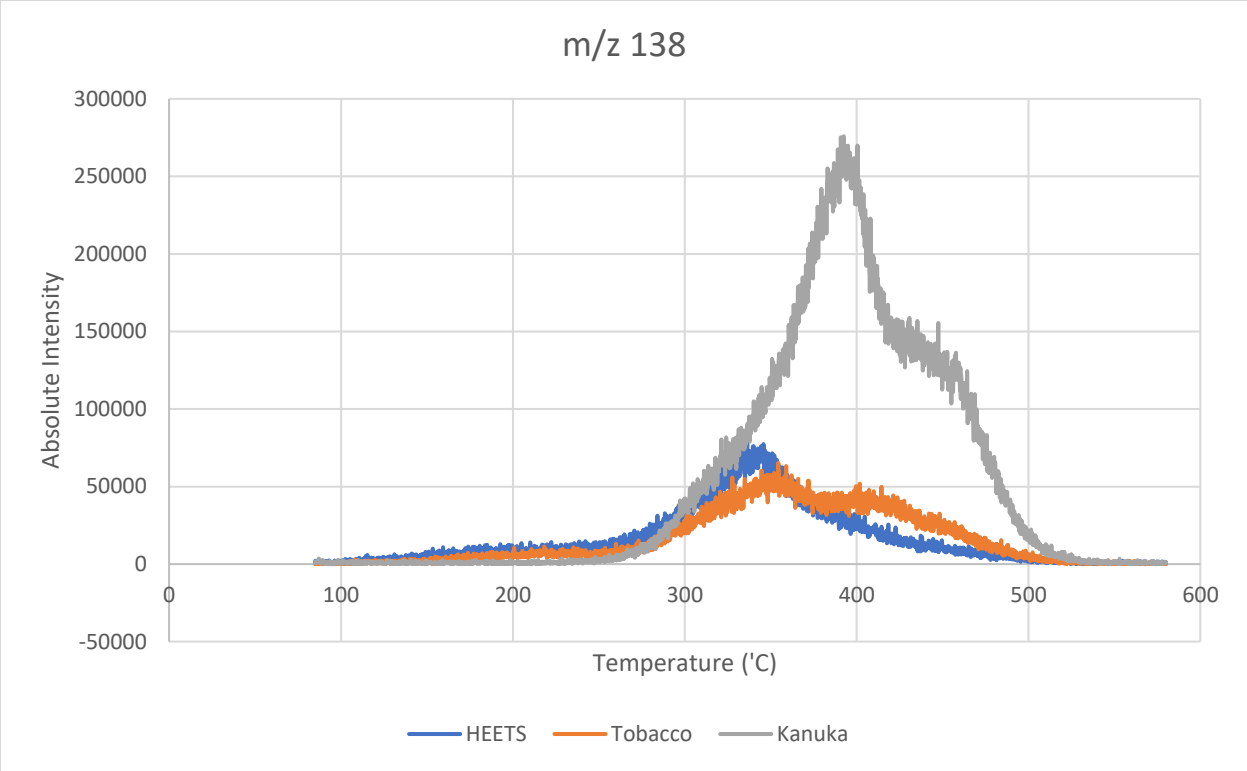

Figure H22: Graph of m/z 138 absolute intensity over temperature for evolved gas analysis of 0.5mg biomass samples for a range of molecular weights. Experiments involve a temp ramp of 10 K/min from 85°C to 580°C and a 20eV.

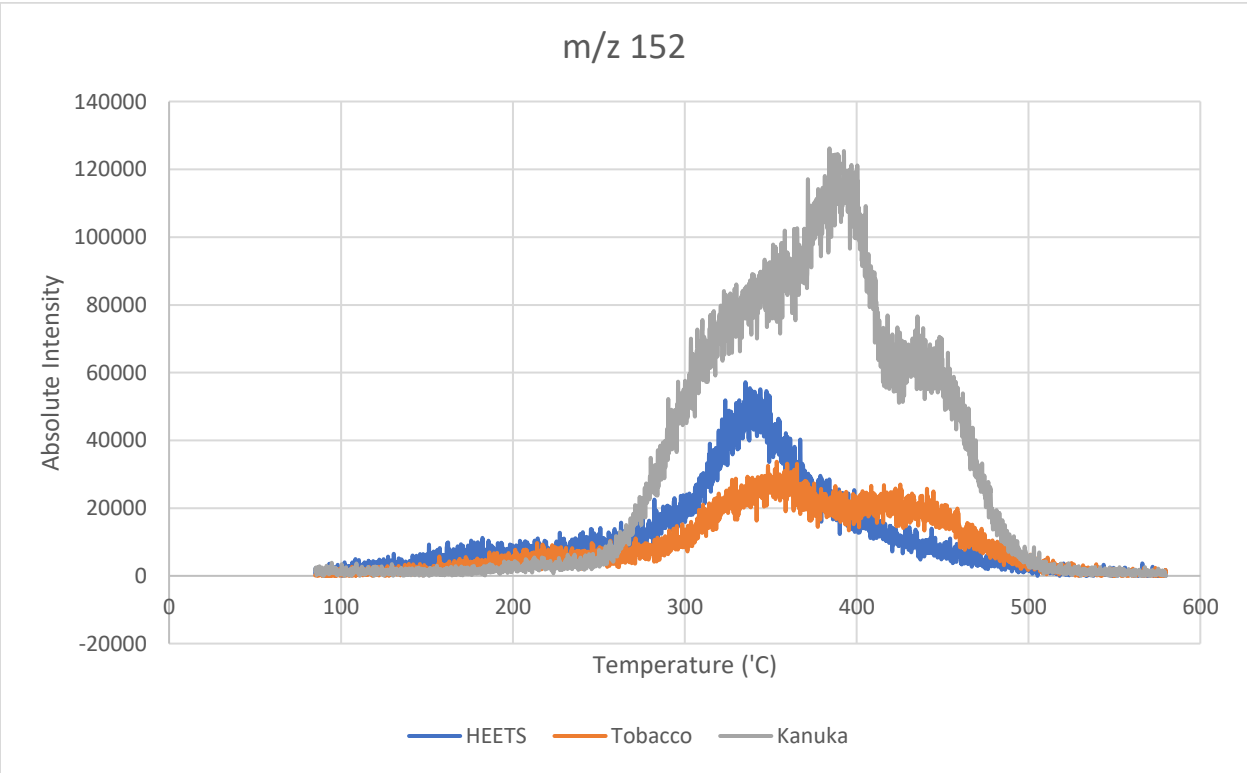

Figure H23: Graph of m/z 152 absolute intensity over temperature for evolved gas analysis of 0.5mg biomass samples for a range of molecular weights. Experiments involve a temp ramp of 10 K/min from 85°C to 580°C and a 20eV.

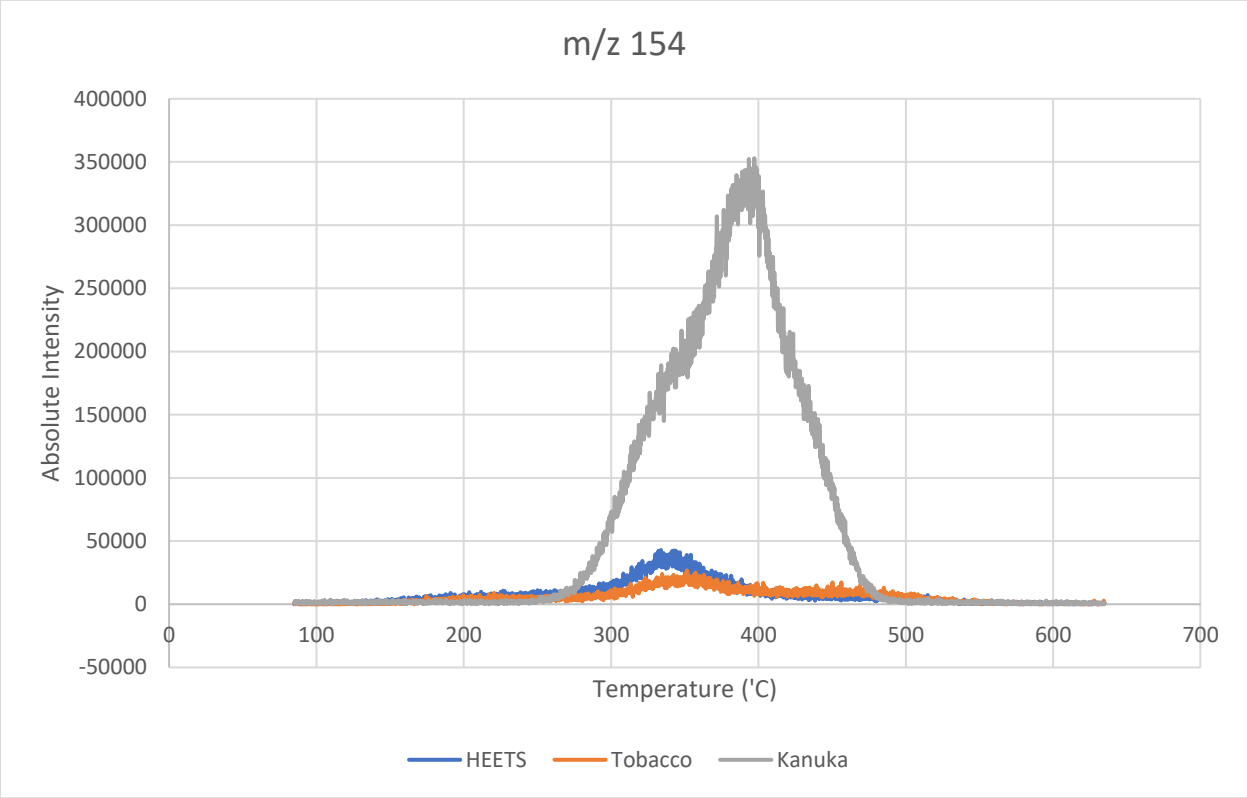

Figure H24: Graph of m/z 154 absolute intensity over temperature for evolved gas analysis of 0.5mg biomass samples for a range of molecular weights. Experiments involve a temp ramp of 10 K/min from 85°C to 580°C and a 20eV.

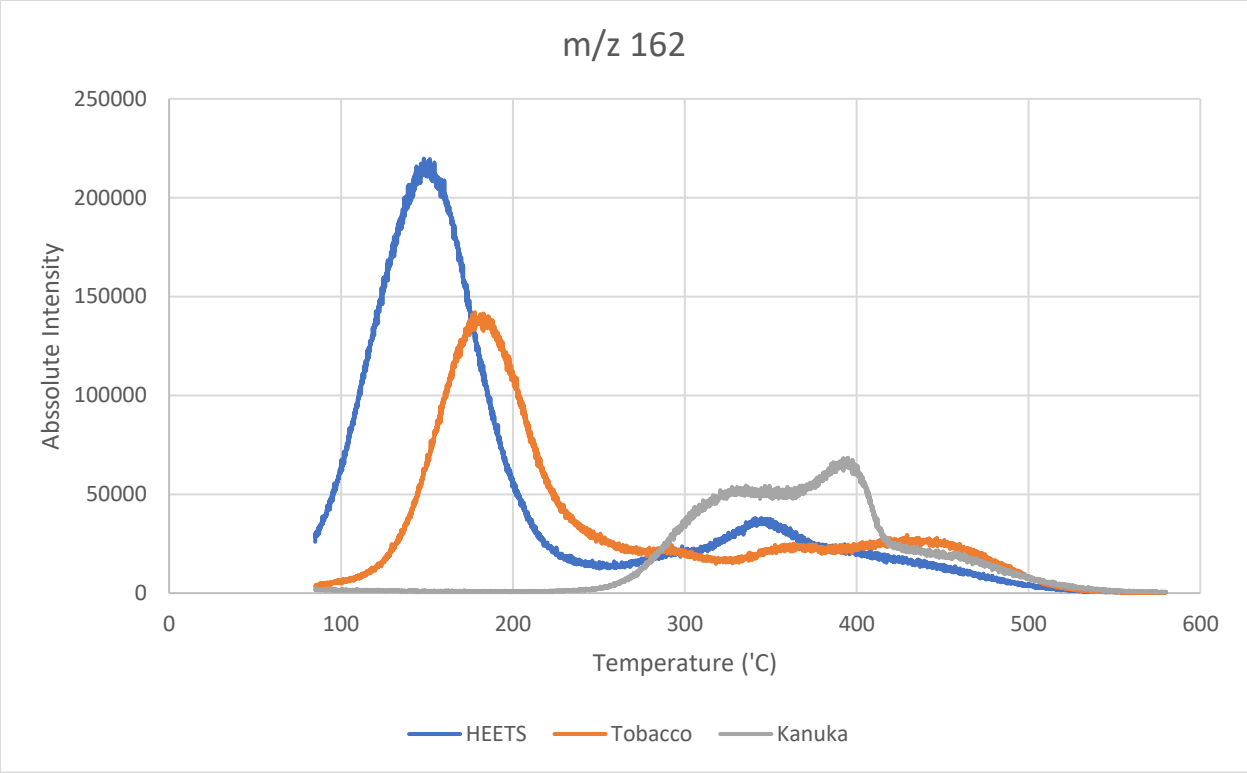

Figure H25: Graph of m/z 162 absolute intensity over temperature for evolved gas analysis of 0.5mg biomass samples for a range of molecular weights. Experiments involve a temp ramp of 10 K/min from 85^{o}C to 580^{o}C and a 20eV.

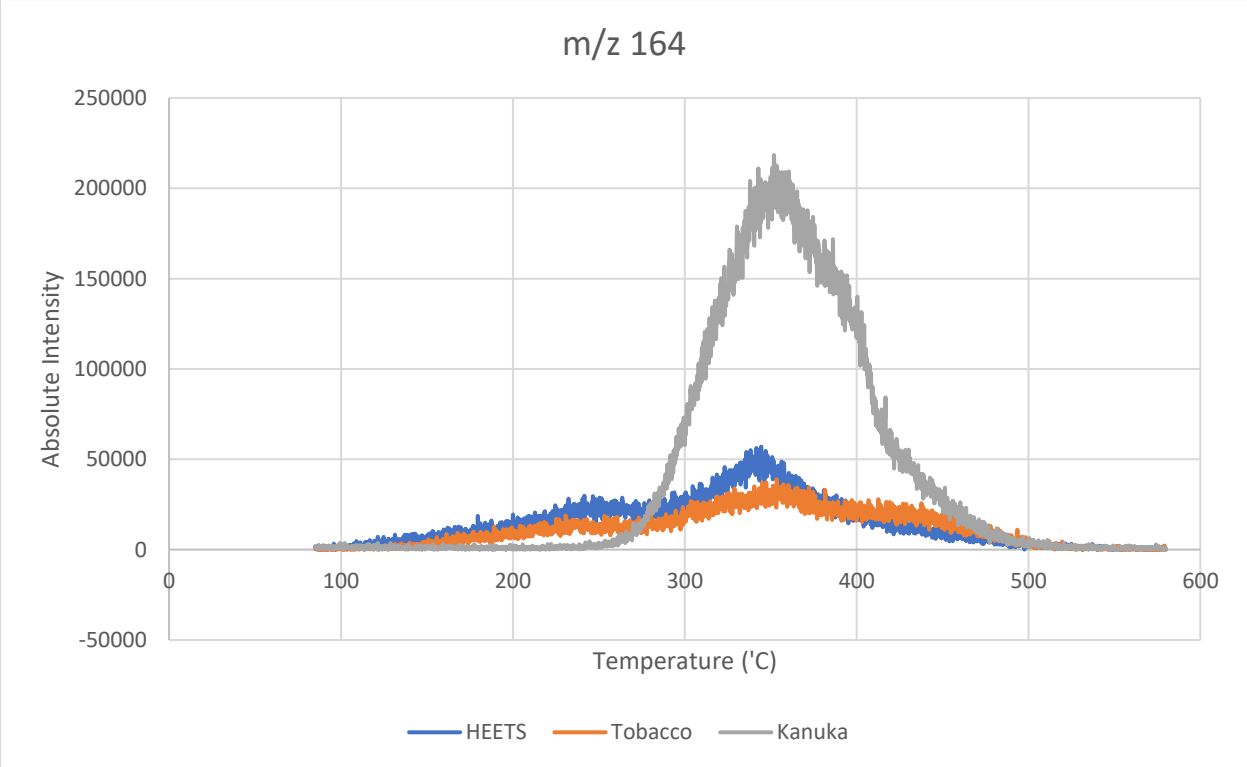

Figure H26: Graph of m/z 164 absolute intensity over temperature for evolved gas analysis of 0.5mg biomass samples for a range of molecular weights. Experiments involve a temp ramp of 10 K/min from 85°C to 580°C and a 20eV.

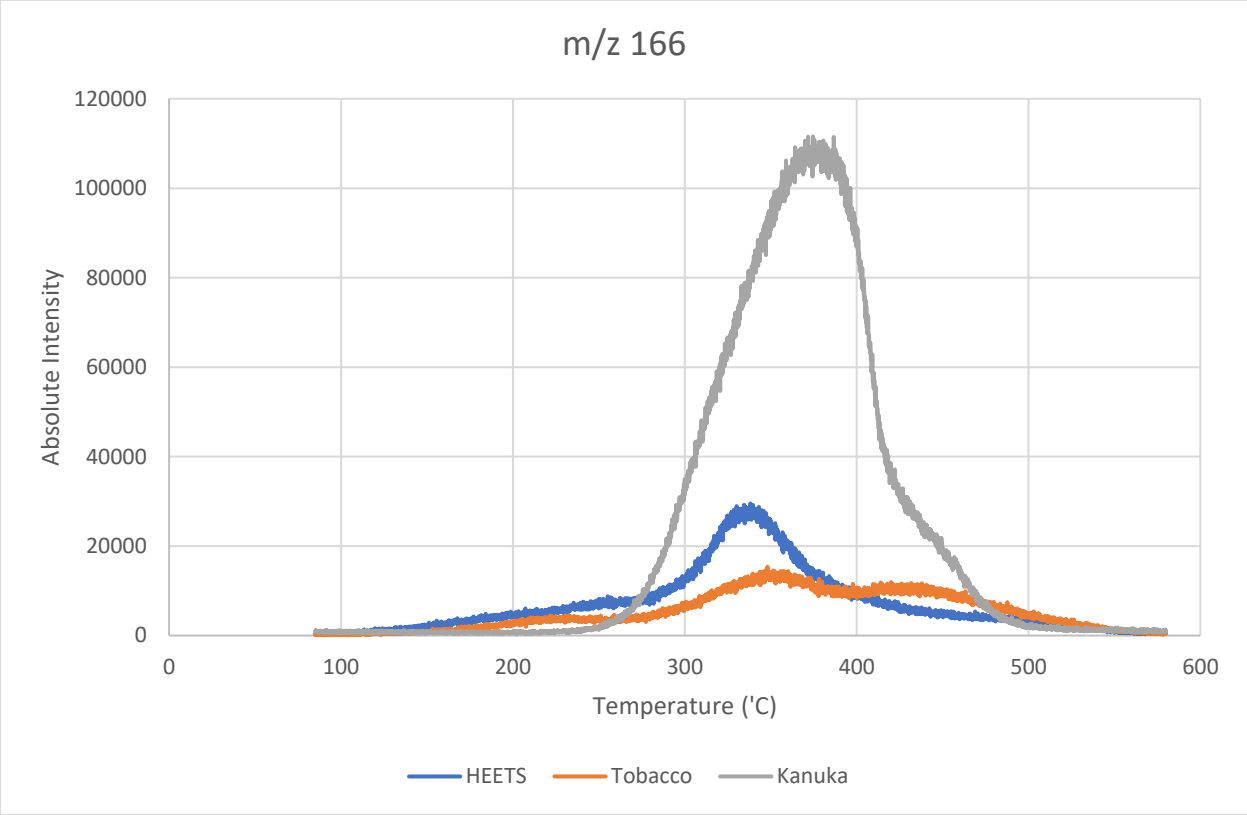

Figure H27: Graph of m/z 166 absolute intensity over temperature for evolved gas analysis of 0.5mg biomass samples for a range of molecular weights. Experiments involve a temp ramp of 10 K/min from 85°C to 580°C and a 20eV.

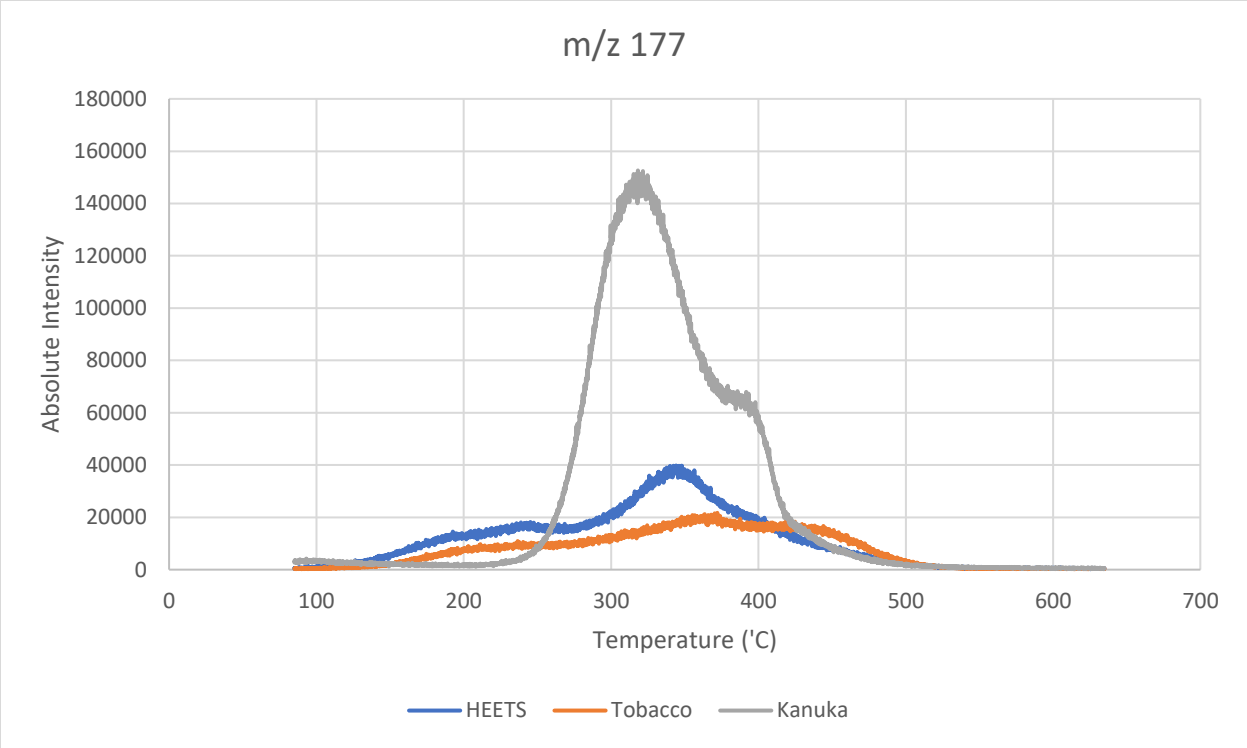

Figure H28: Graph of m/z 177 absolute intensity over temperature for evolved gas analysis of 0.5mg biomass samples for a range of molecular weights. Experiments involve a temp ramp of 10 K/min from 85°C to 580°C and a 20eV.

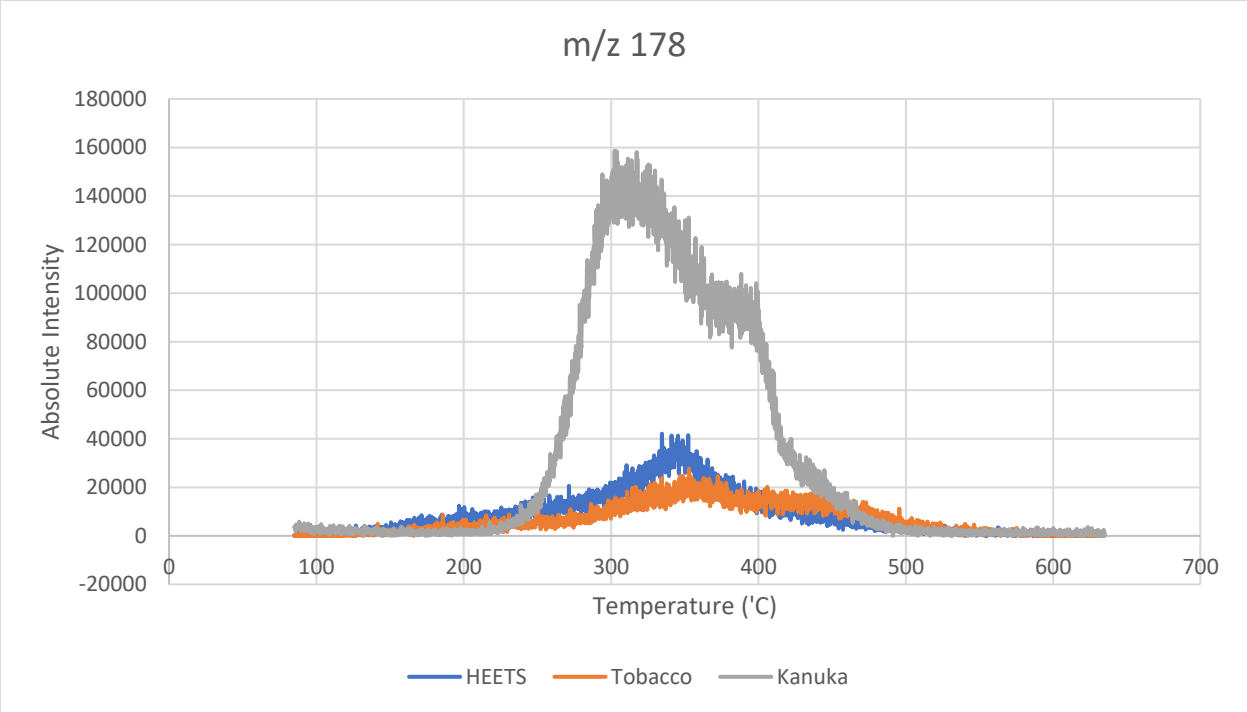

Figure H29: Graph of m/z 178 absolute intensity over temperature for evolved gas analysis of 0.5mg biomass samples for a range of molecular weights. Experiments involve a temp ramp of 10 K/min from 85°C to 580°C and a 20eV.

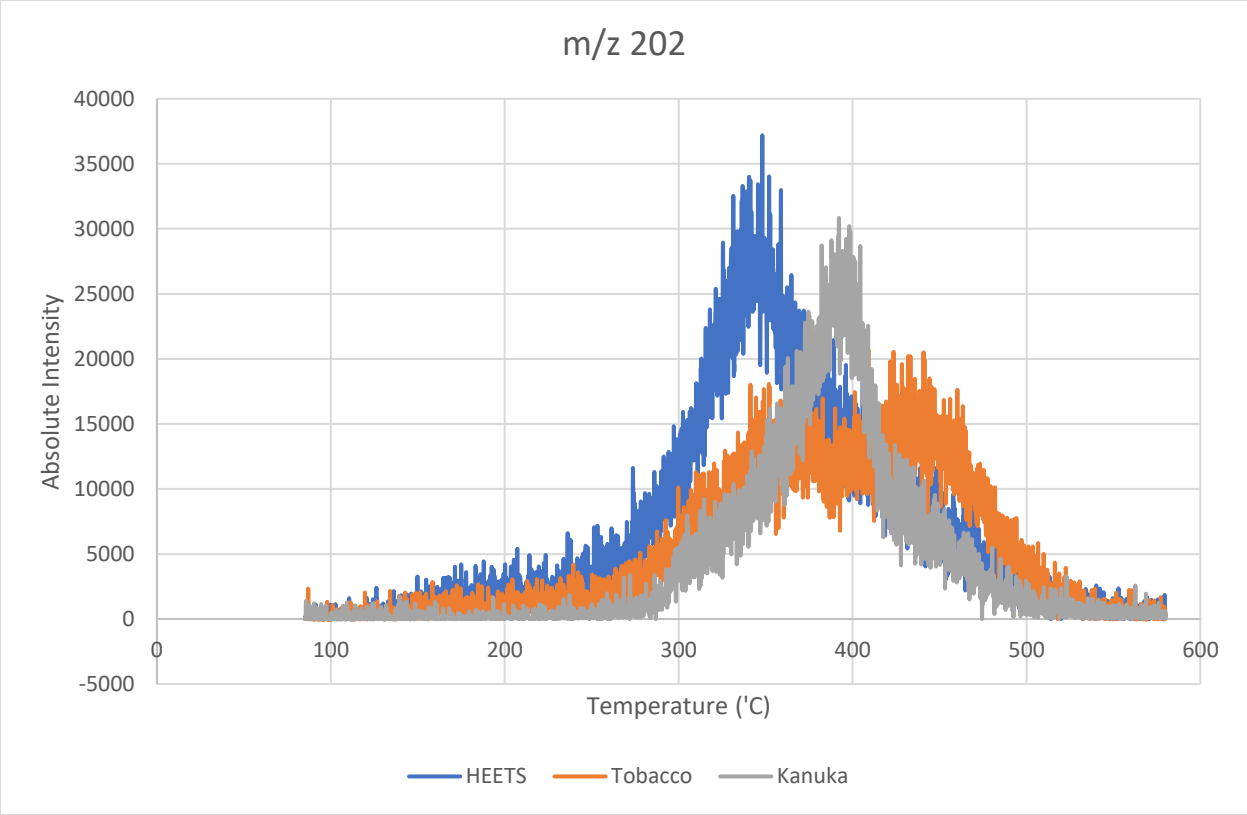

Figure H30: Graph of m/z 202 absolute intensity over temperature for evolved gas analysis of 0.5mg biomass samples for a range of molecular weights. Experiments involve a temp ramp of 10 K/min from 85°C to 580°C and a 20eV.

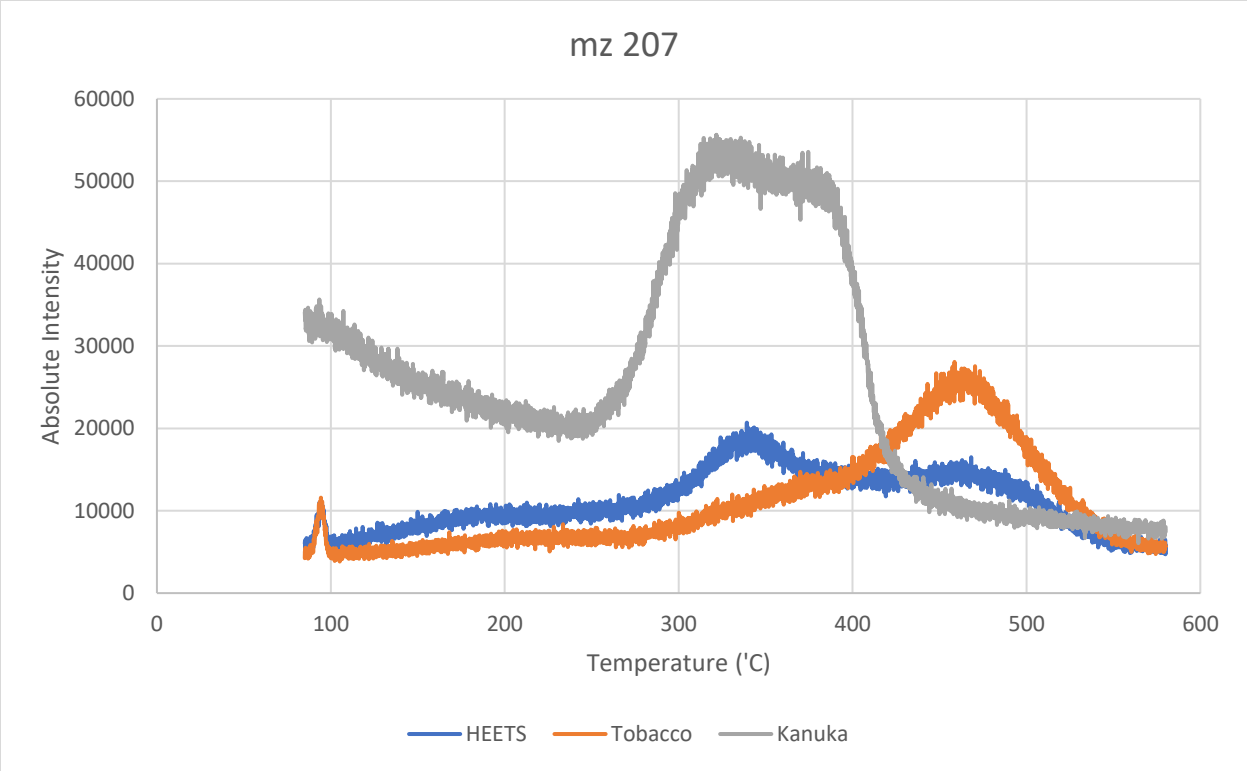

Figure H31: Graph of m/z 207 absolute intensity over temperature for evolved gas analysis of 0.5mg biomass samples for a range of molecular weights. Experiments involve a temp ramp of 10 K/min from 85°C to 580°C and a 20eV.

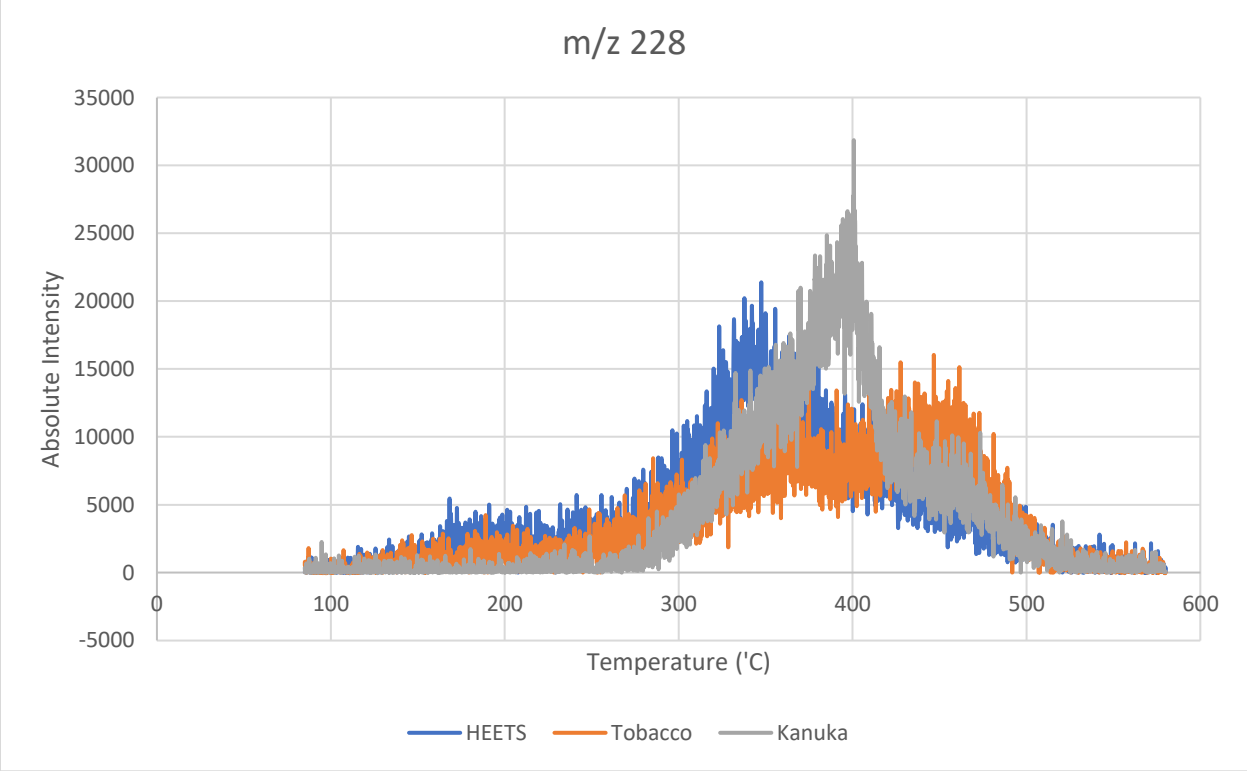

Figure H32: Graph of m/z 228 absolute intensity over temperature for evolved gas analysis of 0.5mg biomass samples for a range of molecular weights. Experiments involve a temp ramp of 10 K/min from 85°C to 580°C and a 20eV.

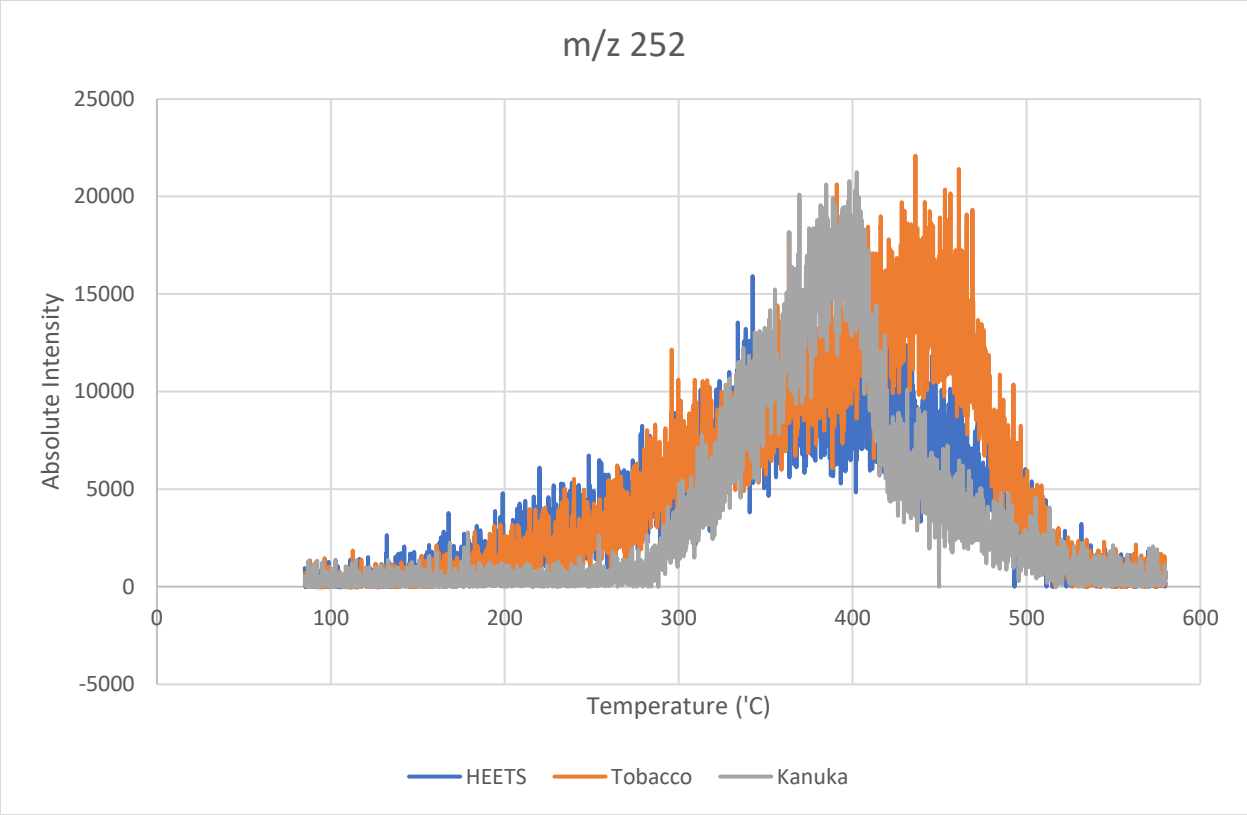

Figure H33: Graph of m/z 252 absolute intensity over temperature for evolved gas analysis of 0.5mg biomass samples for a range of molecular weights. Experiments involve a temp ramp of 10 K/min from 85°C to 580°C and a 20eV.

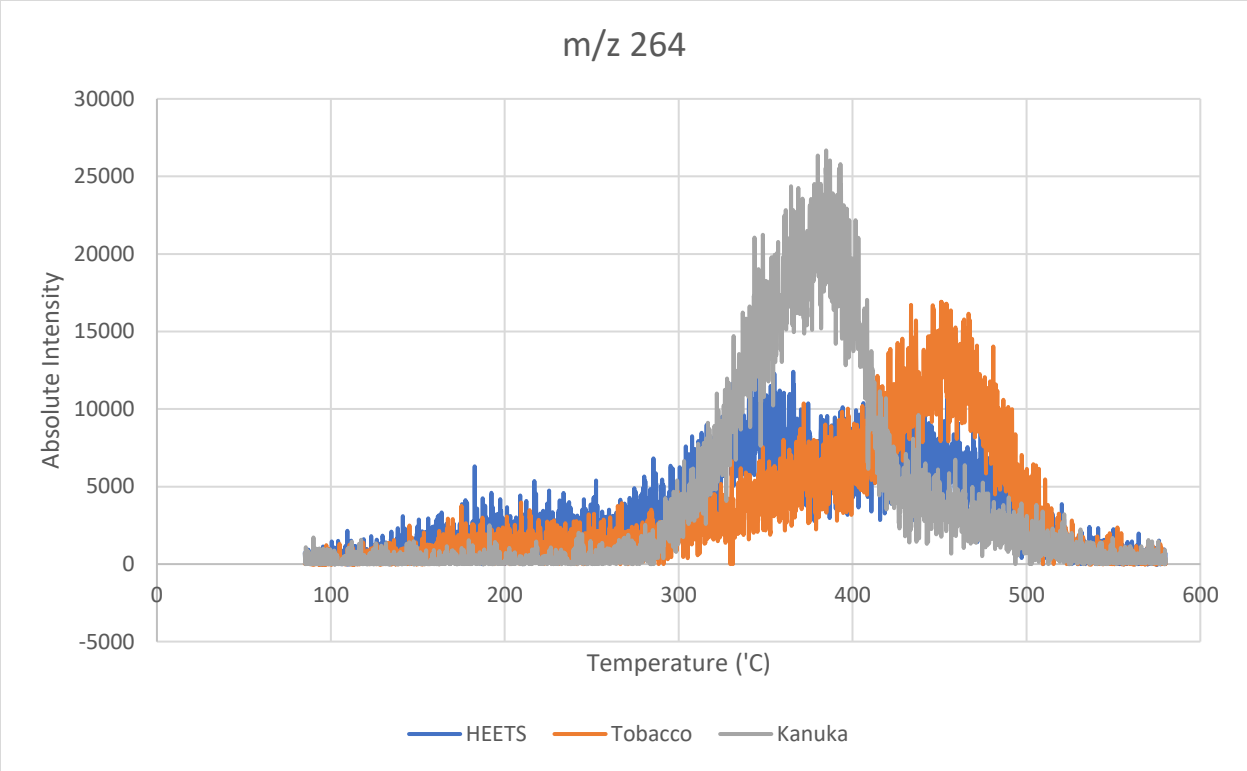

Figure H34: Graph of m/z 264 absolute intensity over temperature for evolved gas analysis of 0.5mg biomass samples for a range of molecular weights. Experiments involve a temp ramp of 10 K/min from 85^{o}C to 580^{o}C and a 20eV.

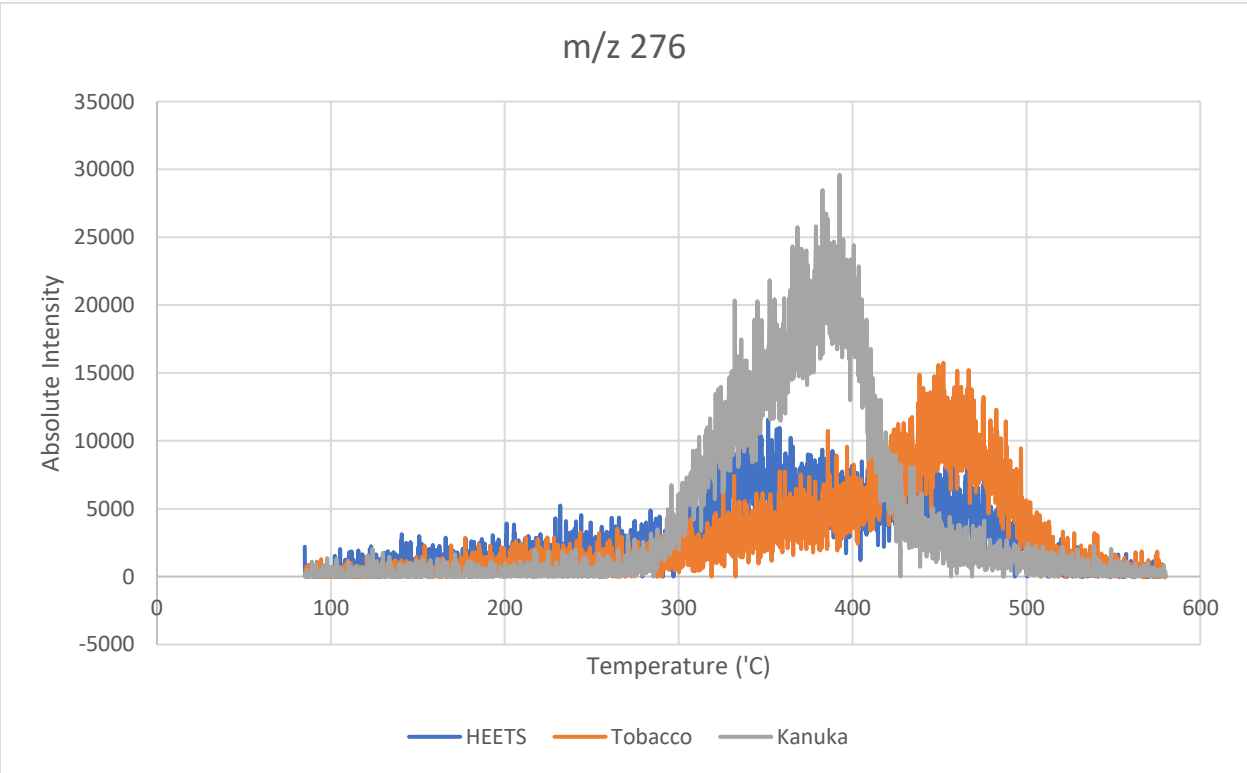

Figure H35: Graph of m/z 276 absolute intensity over temperature for evolved gas analysis of 0.5mg biomass samples for a range of molecular weights. Experiments involve a temp ramp of 10 K/min from 85°C to 580°C and a 20eV.

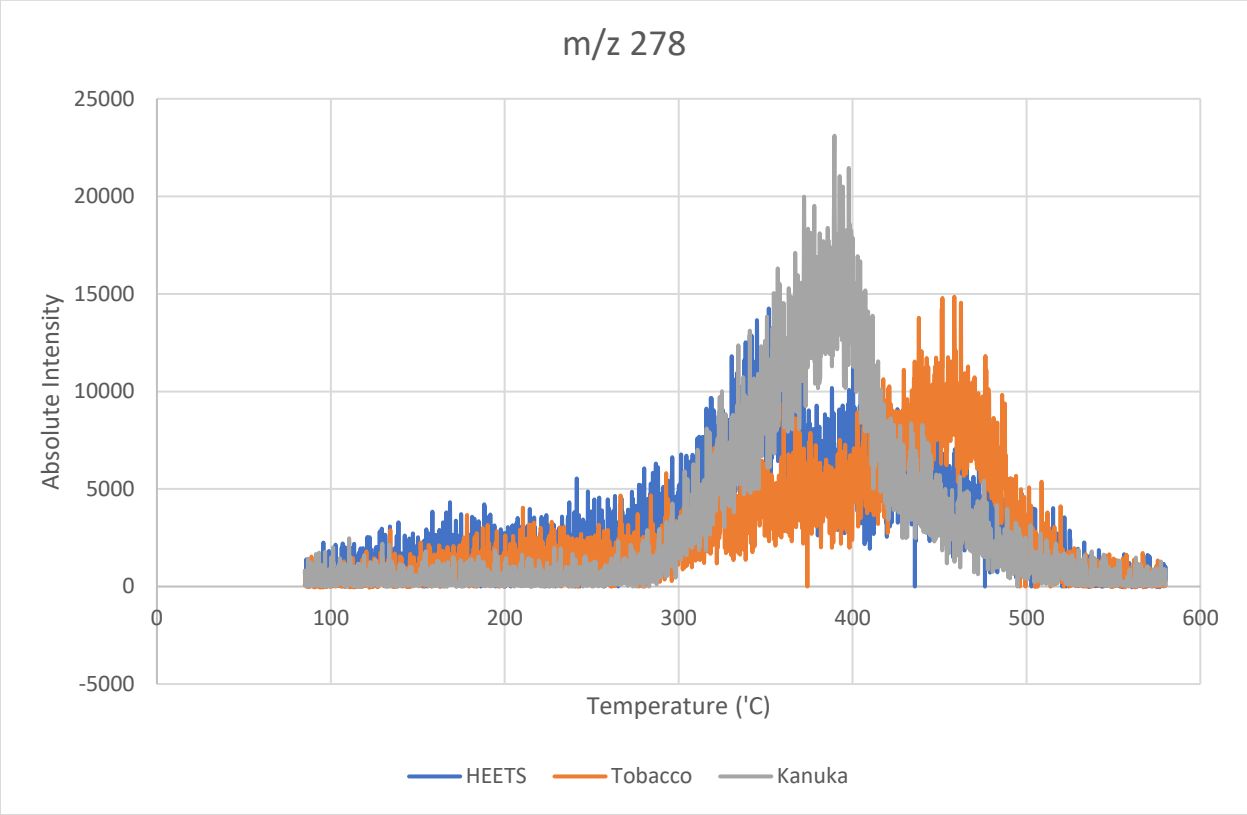

Figure H36: Graph of m/z 278 absolute intensity over temperature for evolved gas analysis of 0.5mg biomass samples for a range of molecular weights. Experiments involve a temp ramp of 10 K/min from 85°C to 580°C and a 20eV.

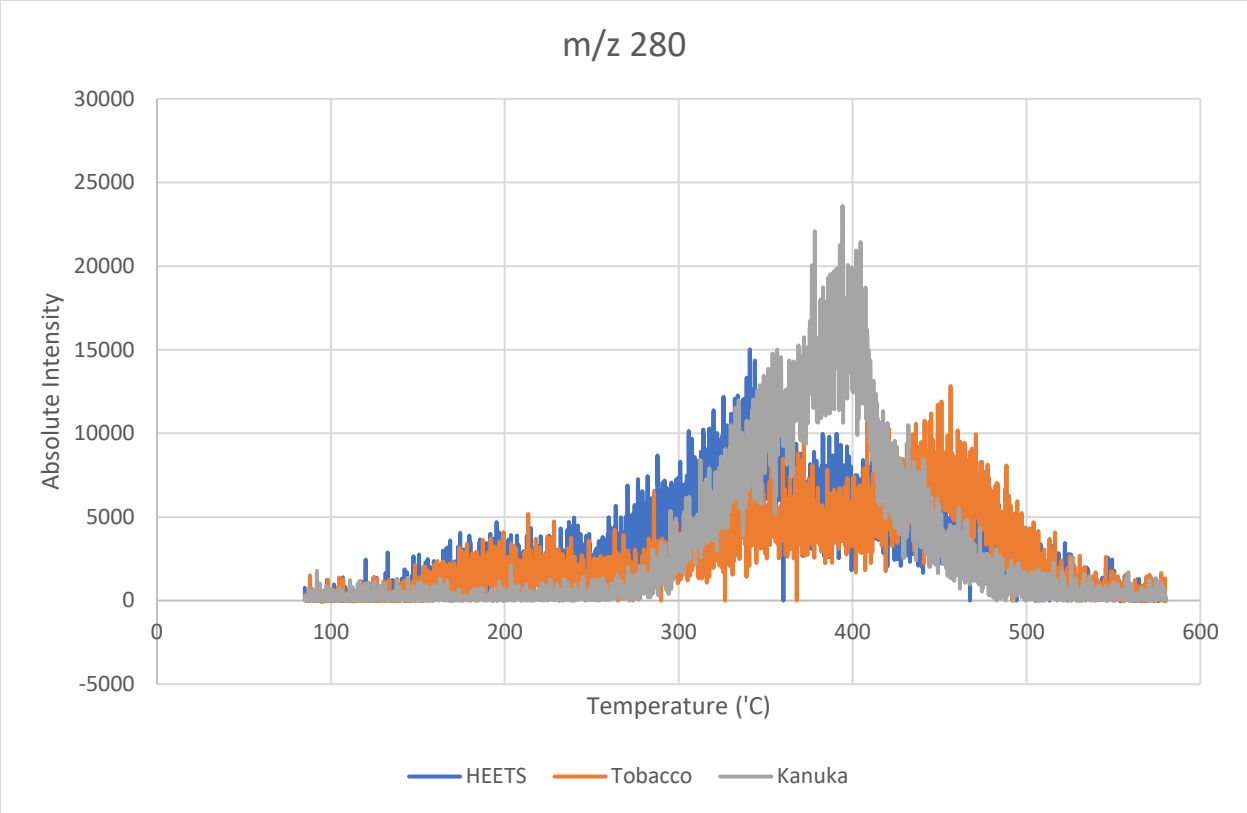

Figure H37: Graph of m/z 280 absolute intensity over temperature for evolved gas analysis of 0.5mg biomass samples for a range of molecular weights. Experiments involve a temp ramp of 10 K/min from 85^{o}C to 580^{o}C and a 20eV.

Appendices I: Py-GC/MS repeat at 390^{o}C

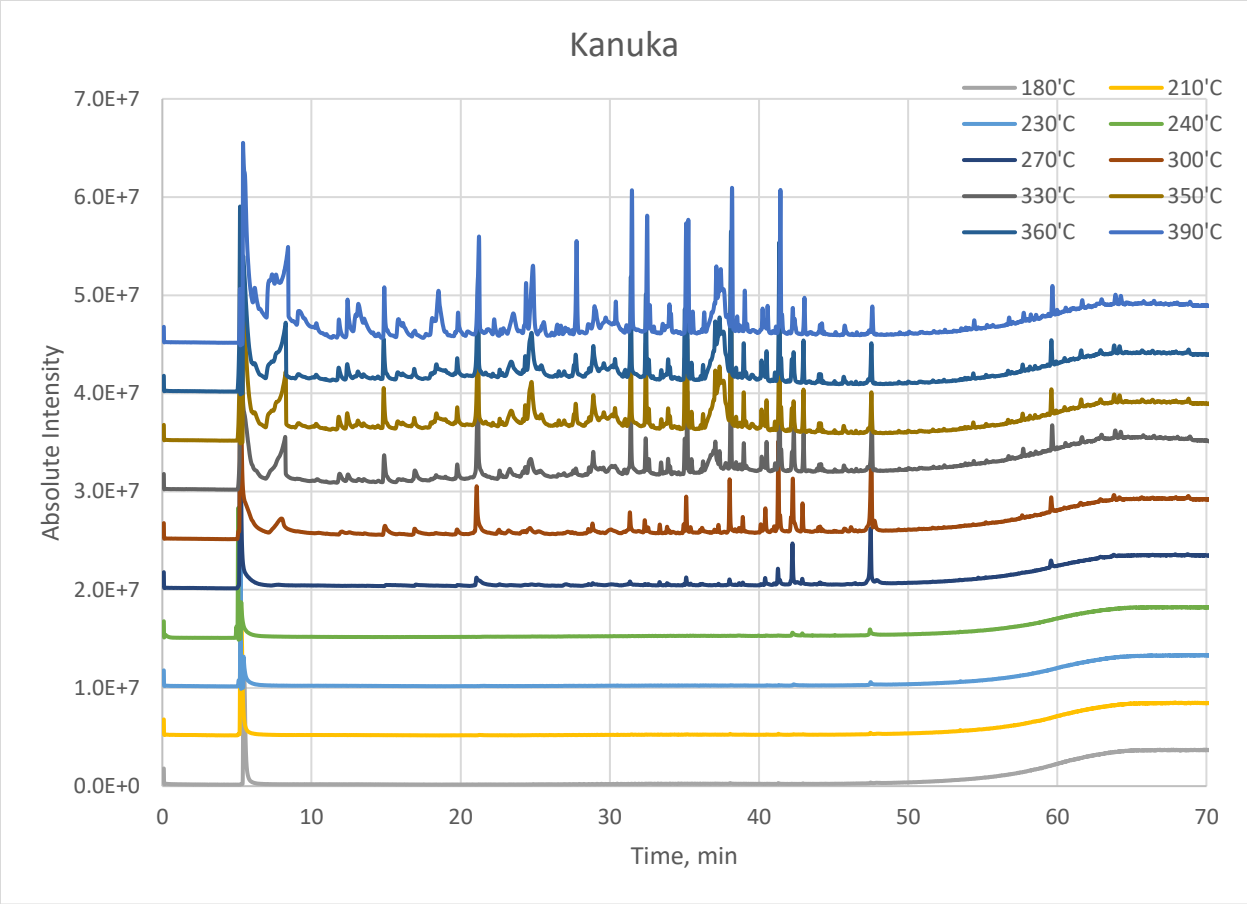

Figure I1: Graph of absolute intensity versus time for 2mg samples of kānuka heated to temperatures ranging from 180°C to 390°C. The different temperature runs have been separated by an absolute intensity of 5.0E+6 for visual display purposes.

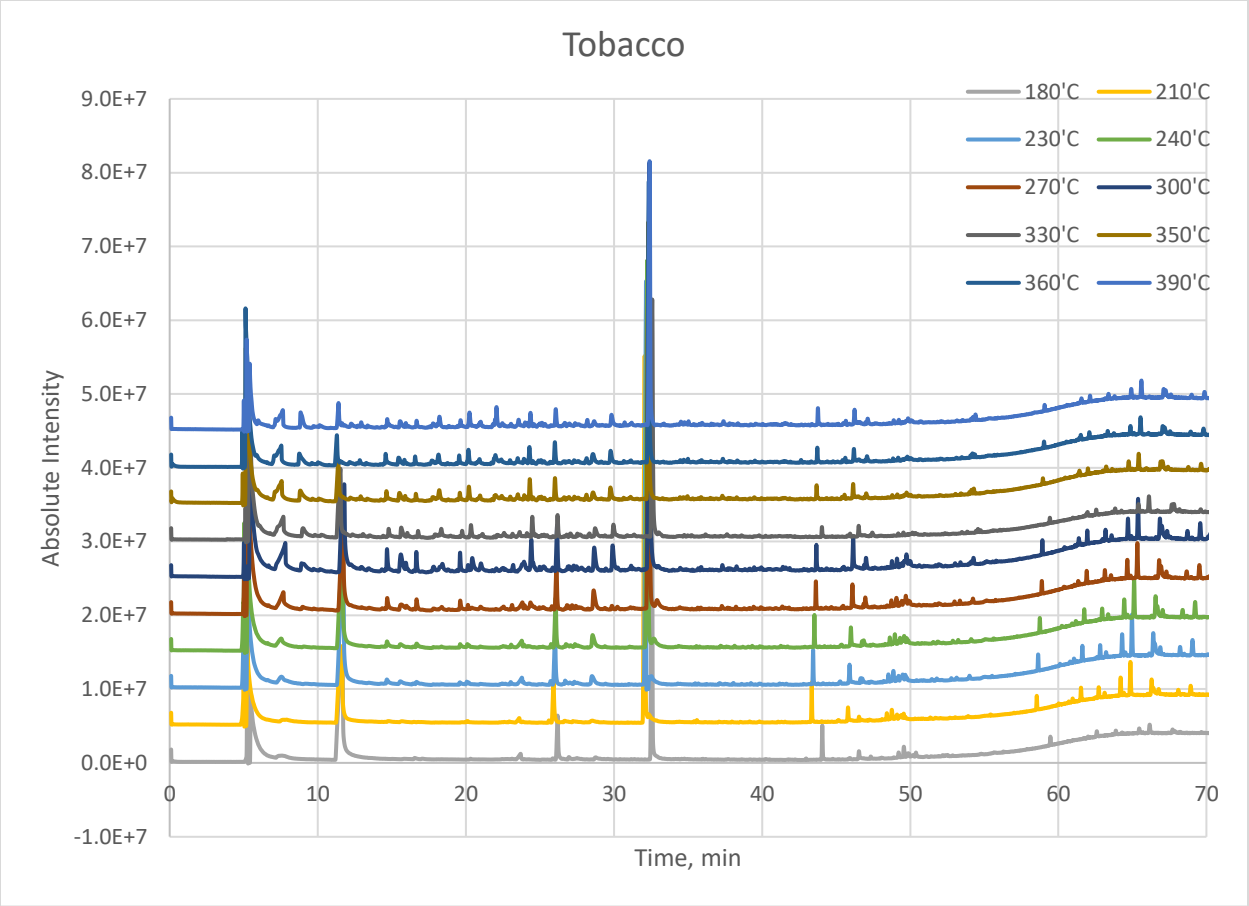

Figure I2: Graph of absolute intensity versus time for 2mg samples of tobacco heated to temperatures ranging from 180°C to 390°C. The different temperature runs have been separated by an absolute intensity of 5.0E+6 for visual display purposes.

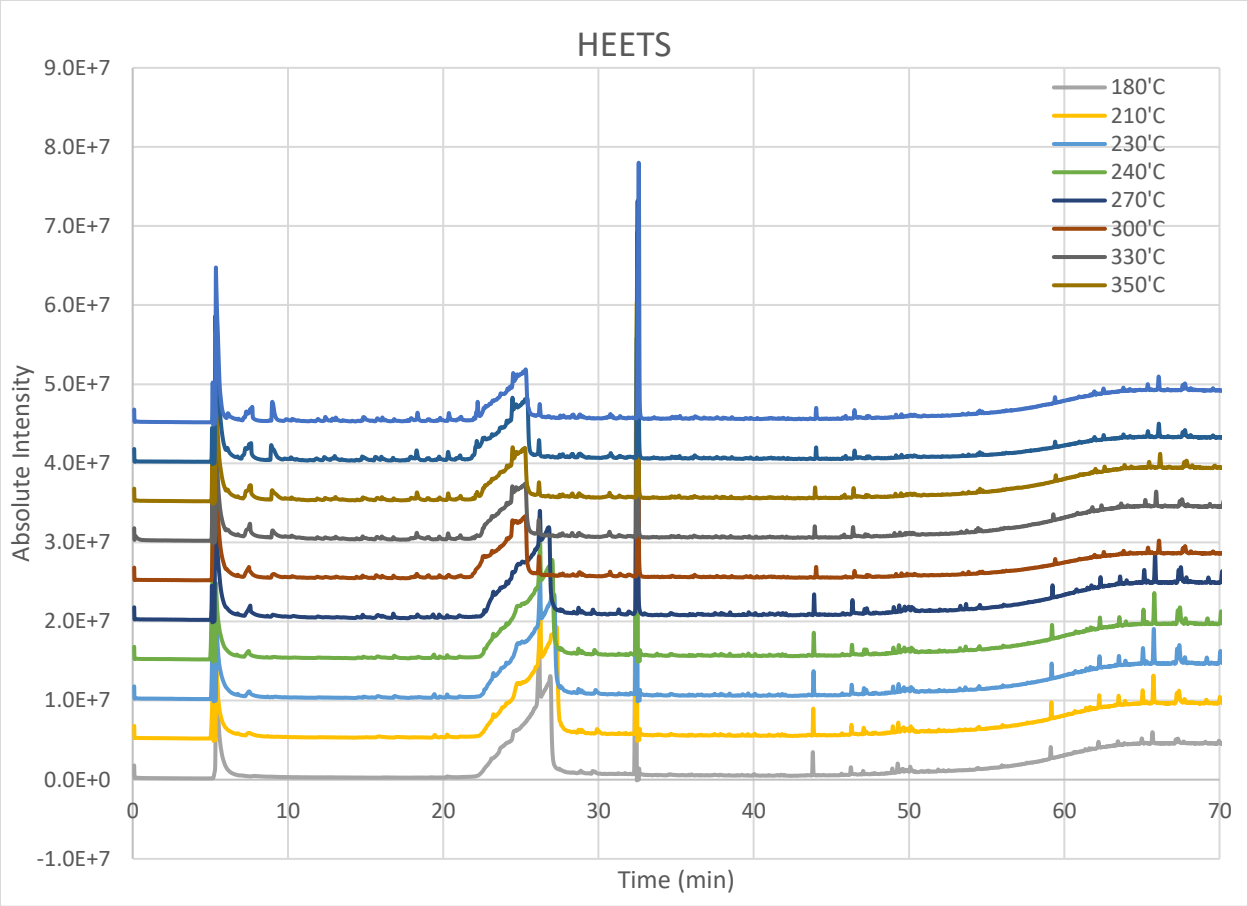

Figure I3: Graph of absolute intensity versus time for 2mg samples of HEETS heated to temperatures ranging from 180°C to 390°C. The different temperature runs have been separated by an absolute intensity of 5.0E+6 for visual display purposes.